

UC Berkeley

UC Berkeley Electronic Theses and Dissertations

Title

Cyclic di-AMP signaling in *Listeria monocytogenes*

Permalink

<https://escholarship.org/uc/item/7zz3w8gz>

Author

Whiteley, Aaron Thomas

Publication Date

2016

Peer reviewed|Thesis/dissertation

Cyclic di-AMP signaling in *Listeria monocytogenes*

By

Aaron Thomas Whiteley

A dissertation submitted in partial satisfaction of the

requirements for the degree of

Doctor of Philosophy

in

Infectious Diseases and Immunity

in the

Graduate Division

of the

University of California, Berkeley

Committee in charge:
Professor Daniel A. Portnoy, Chair
Professor Sarah A. Stanley
Professor Russell E. Vance
Professor Kathleen R. Ryan

Summer 2016

Abstract

Cyclic di-AMP signaling in *Listeria monocytogenes*

by

Aaron Thomas Whiteley

Doctor of Philosophy in Infectious Diseases and Immunity
University of California, Berkeley
Professor Daniel A. Portnoy, Chair

The Gram positive facultative intracellular pathogen *Listeria monocytogenes* is both ubiquitous in the environment and is a facultative intracellular pathogen. A high degree of adaptability to different growth niches is one reason for the success of this organism. In this dissertation, two facets of *L. monocytogenes*, growth and gene expression have been investigated. The first portion examines the function and necessity of the nucleotide second messenger c-di-AMP, and the second portion of this dissertation examines the signal transduction network required for virulence gene regulation.

Through previous genetic screens and biochemical analysis it was found that the nucleotide second messenger cyclic di-adenosine monophosphate (c-di-AMP) is secreted by the bacterium during intracellular and extracellular growth. Depletion of c-di-AMP levels in *L. monocytogenes* and related bacteria results in sensitivity to cell wall acting antibiotics such as cefuroxime, decreased growth rate, and decreased virulence. We devised a variety of bacterial genetic screens to identify the function of this molecule in bacterial physiology. The sole di-adenylate cyclase (encoded by *dacA*) responsible for catalyzing synthesis of c-di-AMP in *L. monocytogenes* could not be deleted by conventional methods. However, $\Delta dacA$ mutants could be obtained by flanking *dacA* with *loxP* sites and expressing the site-specific recombinase Cre. All of the $\Delta dacA$ mutants generated by this novel method on conventional medium harbored suppressor mutations that bypassed the essential functions of c-di-AMP in multiple ways. Characterization of $\Delta dacA$ suppressor mutations revealed cross-talk between c-di-AMP and (p)ppGpp, another nucleotide second messenger that slows growth in response to amino acid starvation as part of the stringent response. Depletion of c-di-AMP in rich media resulted in an increase in (p)ppGpp, which was toxic to the bacterium. Whereas (p)ppGpp is essential for growth in nutrient poor synthetic medium, c-di-AMP was found to be essential only in rich medium and genome sequencing of $\Delta dacA$ mutants constructed in synthetic medium revealed no suppressor mutations.

Synthetic medium thus provided a tool for generating $\Delta dacA$ mutants in combination with targeted mutations identified from our suppressor analysis. These mutants were further analyzed for growth in rich medium or resistance to cefuroxime. Suppressor mutations in the oligopeptide permease and glycine betaine osmolyte importer showed that peptides from rich medium were toxic to $\Delta dacA$ mutants due to a dysregulation of osmotic pressure. These defects in osmotic pressure could be overcome by addition of

salt to the medium, which allowed for recovery of $\Delta dacA$ on rich medium and ameliorated sensitivity of $\Delta dacA$ to cefuroxime. To identify how c-di-AMP regulated intracellular osmotic pressure, we screened for suppressor mutations that overcome growth on rich media and cefuroxime resistance. Suppressor mutations from this screen indicated that c-di-AMP inhibits pyruvate carboxylase in order to limit carbon flux into the TCA cycle when acetyl-CoA levels are high. Increased flux through the TCA cycle was only toxic when citrate synthase was present, implying that accumulation of citrate is toxic to $\Delta dacA$ mutants. These findings demonstrate a role of c-di-AMP in balancing central metabolism and TCA cycle intermediates for optimal growth on rich media, resistance to cefuroxime, and virulence.

Dedication

To my parents, Brian and Phyllis Whiteley
who gave me everything I ever needed
and then a lot more

Table of Contents

Chapter 1: Introduction	1
<i>Listeria monocytogenes</i>	2
Pathogenesis, innate immunity, and PAMPs.....	3
Cyclic dinucleotides and the immune response.....	4
Cyclic di-adenosine monophosphate (c-di-AMP) in bacterial physiology.....	4
Genetic screens for virulence genes.....	6
Virulence gene regulation in <i>L. monocytogenes</i>	7
Chapter 2: The PAMP c-di-AMP is essential for <i>Listeria monocytogenes</i> growth in rich but not minimal media due to a toxic increase in (p)ppGpp	8
Summary	9
Introduction	10
Results	12
Generation of <i>L. monocytogenes</i> Δ dacA mutants and identification of suppressor mutations.....	12
Development of a dacA essentiality assay.....	15
Suppressor mutations in relA decreased (p)ppGpp accumulation in response to starvation.....	15
Accumulation of (p)ppGpp is toxic to Δ dacA mutants.....	19
A screen for mutations that rescue the virulence defect of a Δ relAPQ mutant reveals a critical role for CodY.....	20
(p)ppGpp-dependent inactivation of CodY is necessary for the essentiality of dacA.....	23
dacA is not essential on minimal medium.....	24
Discussion	26
Experimental Procedures	29
Chapter 3: c-di-AMP Regulates Osmohomeostasis with Implications for Growth on Rich Medium, Antibiotic Resistance, and Virulence	37
Summary	38
Introduction	39
Results	41
Peptides in rich media are selectively toxic in the absence of c-di-AMP.....	41
c-di-AMP is essential for growth during osmotic stress.....	43
Characterizing Δ dacA suppressor mutations.....	45
PstA protein-protein interactions.....	47
Acetyl-CoA activation of PycA and is toxic to Δ dacA mutants.....	50
Toxicity of TCA cycle intermediates.....	53
Δ dacA virulence defects.....	54
Discussion	66
Chapter 4: Glutathione activates virulence gene expression of an intracellular pathogen	67
Summary	68
Introduction	69
Results	69
Genetic selection in macrophages.....	69

Glutathione is required for virulence	70
Isolation of suppressor mutations in vivo	72
PrfA binds glutathione allosterically	74
Discussion	77
Experimental Procedures	79
Chapter 5: An <i>in vivo</i> selection identifies <i>Listeria monocytogenes</i> genes required to sense the intracellular environment and activate virulence factor expression ...	83
Abstract.....	84
Author Summary	84
Introduction	85
Results	87
Genetic Selection in Macrophages	87
Virulence	89
In vivo suppressor analysis to dissect PrfA abundance versus activation	93
Vacuolar Escape and Cytosolic Growth.....	94
YjbH is necessary for ActA translation	97
Discussion	100
Experimental Procedures	104
Chapter 6: Concluding Thoughts and Unanswered Questions	112
c-di-AMP.....	113
Virulence Gene regulation.....	117
Chapter 7: Literature Cited	119

List of Figures

Figure 2.1 Graphical Abstract.....	9
Figure 2.2 Cre-lox deletion of <i>dacA</i> and Δ <i>dacA</i> suppressor mutations.	13
Figure 2.3 <i>dacA</i> essentiality assay.....	17
Figure 2.4 <i>dacA</i> essentiality assay validation using an alternative <i>ermR</i> gene location	18
Figure 2.5 Δ <i>dacA</i> suppressor mutations in <i>relA</i> affect starvation-induced (p)ppGpp.	18
Figure 2.6 (p)ppGpp accumulates during depletion of c-di-AMP leading to <i>dacA</i> essentiality and decreased growth rate.	21
Figure 2.7 A screen for suppressor mutations of the Δ <i>relAPQ</i> virulence defect reveals a critical role for inactivation of CodY.....	22
Figure 2.8 <i>dacA</i> is essential in rich medium due to CodY inactivation but <i>dacA</i> is not essential in minimal medium.....	25
Figure 3.1 Oligopeptides are toxic in the absence of c-di-AMP.....	42
Figure 3.2 Δ <i>dacA</i> mutants are defective for osmotic homeostasis.....	44
Figure 3.3 Mutations in <i>gbuC</i> are sufficient to suppress Δ <i>dacA</i> growth defects on rich media	45
Figure 3.4 Mutations in <i>pstA</i> suppress the sensitivity of Δ <i>dacA</i> to cefuroxime.....	46
Figure 3.5 Complementation of suppressor mutations.....	46
Figure 3.6 Pull-downs of PstA from <i>L. monocytogenes</i>	48
Figure 3.7 PstA protein-protein interactions	49
Figure 3.8 Suppressor analysis of cefuroxime resistance in Δ <i>dacA</i> <i>p-pstA</i>	51
Figure 3.9 Mutations eliminating acetyl-CoA activation of PycA suppress Δ <i>dacA</i> sensitivity of rich media and cefuroxime	52
Figure 3.10 TCA cycle intermediates are toxic in the absence of c-di-AMP.....	53
Figure 3.11 <i>pycA</i> mutations suppress the Δ <i>dacA</i> virulence defect.....	54
Figure 4.1 Forward genetic selection to identify factors required for virulence gene activation during infection.	70
Figure 4.2 <i>Listeria monocytogenes</i> Δ <i>gshF</i> is sensitive to hydrogen peroxide.....	71
Figure 4.3 <i>Listeria monocytogenes</i> Δ <i>gshF</i> is attenuated <i>in vivo</i>	71
Figure 4.4 BSO does not affect <i>L. monocytogenes</i> growth.	71
Figure 4.5 PrfA* bypasses the requirement for glutathione during infection.	73
Figure 4.6 The effect of Δ <i>gshF</i> is not specific to <i>actA</i> regulation.....	73
Figure 4.7 Glutathione-dependent PrfA activation is mediated by allosteric binding, not glutathionylation.	74
Figure 4.8 Fluorescence polarization binding isotherms.	75
Figure 4.9 PrfA(C/A) ₄ expression in <i>L. monocytogenes</i> grown in broth.	75
Figure 4.10 The PrfA(C/A) ₄ <i>gshF</i> ::Tn mutant exhibits a significant intracellular growth defect.	75
Figure 4.11 Model of glutathione-dependent PrfA activation.....	78
Figure 5.1 Schematic of genetic selection.....	88
Figure 5.2 Characterization of mutants identified in the genetic selection.	90
Figure 5.3 Analysis of <i>P-spxA1::Tn</i>	91
Figure 5.4 Complementation of transposon mutants.....	91
Figure 5.5 <i>In vivo</i> suppressor analysis.	93
Figure 5.6 Mutants impaired for vacuolar escape.	96

Figure 5.7 Growth curve in NOS2 ^{-/-} and NOX2 ^{-/-} BMMs.....	97
Figure 5.8 Post-transcriptional activation of ActA.....	99
Figure 5.9 Model of genes identified in this genetic selection and where in the <i>L. monocytogenes</i> life cycle they are required.....	101

List of Tables

Table 2.1 $\Delta dacA$ suppressor mutations.....	14
Table 2.2 Transposon mutations that suppress the $\Delta relAPQ$ plaque defect.....	23
Table 2.3 <i>L. monocytogenes</i> strains used in this study.....	35
Table 2.4 plasmids and <i>E. coli</i> strains used in this study.....	35
Table 2.5 Oligonucleotides used in this study.....	36
Table 3.1 Listeria Synthetic Media Recipe.....	55
Table 3.2 Tryptic Peptides identified by pull-down of PstA.....	59
Table 3.3 Orfs interacting with PstA by yeast 2-hybrid.....	61
Table 3.4 Proteins eluted with c-di-AMP from PstA-resin.....	62
Table 3.5 Suppressor mutations identified in $\Delta dacA$ <i>p-pstA</i> mutants capable of growing on rich media and resisting cefuroxime.....	65
Table 4.1 DNA-binding and glutathione-binding affinities of PrfA.....	75
Table 4.2 <i>L. monocytogenes</i> and <i>E. coli</i> strains used in this study.....	79
Table 4.3 Oligonucleotides used in this study.....	80
Table 5.1 Genes identified in the forward genetic selection.....	89
Table 5.2 <i>Escherichia coli</i> Strains.....	104
Table 5.3 <i>Listeria monocytogenes</i> Strains.....	105
Table 5.4 Oligonucleotide Primers Used in this Study.....	108

Acknowledgements

I would like to thank my mentor, Daniel A. Portnoy, who has nurtured my development as a scientist, a student, and a person throughout the course of graduate school. You taught me that scientists are humans, a collaboration is a relationship, and achievement isn't about the next paper or even your thesis, it's about getting it right and doing something that will matter. We have worked together when the lab was rich and poor, when I have had triumphant results and spectacular failures, and when our disagreements have been petty and seemingly insurmountable. Through it all, I wish I could do it again just for fun. Thanks Dan.

My lab mates are the other half of why graduate school was just so awesome. When I joined JD Sauer, Joshua Woodward, Nicole Meyer-Morse, Susannah McKay, Chris Rae, Benjamin Kline, Michelle Reniere, Matthieu Delincé, Chelsea Witte, Kristina Archer (my long time bay-mate), and Thomas Burke welcomed me, always provided advice, and supported my progress as a new member of the Portnoy family. Along the way still more great people joined including Jonathan Portman, Julia Durack, Paul Kennouche, Chen Chen, Gabriel Mitchell, and Qiongying Huang. Now the lab is totally different, though still filled with amazing people. Thanks to Eric Lee, Brittney Nguyen, Bret Peterson, Alfredo Chavez-Arroyo, and Alexander Louie the same family spirit lives on.

I have been trained by two incredible post-docs and gone on to train two talented undergrads myself, all of whom deserve special thanks. Joshua Woodward first trained me in the lab, introduced me to c-di-AMP, and has since remained one step ahead of me. I love our monthly phone calls. Without Michelle Reniere I never would have delved into virulence genes regulation where our skill sets truly synergized. Our work taught me how to be a collaborator and although I try to forget it, you showed me the importance of attention to detail. Alex Pollock and Nick Garelis catapulted my work forward and neither of them ever said no to staying late for that last piece of data. Both of you are exactly the kind of trainee every graduate student would kill for.

My projects would not be of the quality they are without rigorous scientific debate at the PO1 group, Tri-Lab, and countless Berkeley retreats. Thank you to the Barton and Vance labs, specifically Nicholas Arpaia (who I rotated with in the Barton lab), Kelsey Sivick, Meghan Koch, April Price, Dara Burdette, Kevin Barry, and Jeanette Tenthorey. Further scientific rigor was found in my dissertation committee thanks to Russell Vance, Sarah Stanley, and Kathleen Ryan. Thanks also to Aduro Biotech, Pete Lauer, and Bill Hanson-you guys are truly the capital of Listeria genetics.

I had the good fortune to end up in a special graduate group that formed a support network integral to my development at Berkeley. I learned about the strengths and challenges of a small program through Infectious Diseases and Immunity, with special help from Dr. Richard Stephens, Sarah Stanley, and Teresa Liu. All of the students in the graduate group helped create the memorable environment IDI became, especially Zoe Davis and Matthew Gardner.

Thank you to my family. I credit my parents Brian and Phyllis Whiteley with instilling in their three sons a good work ethic and a guiding interest in “being the change they wish to see in the world”. Although, my work ethic is also the result of lively and constructive competition between myself and my amazing brothers, Justin and Sam, whose talent and ingenuity inspire me. Finally, thank you to my fiancé Alexandra Greer, who once told me “The real knowledge is that which you find”. You always knew how to encourage me.

Curriculum Vitae

Education

2004-2008 B.S. Biochemistry and Molecular Biology
University of California, Davis – Davis, CA

Honors and Awards

- 2016 **Ridpath Memorial Award for the best oral presentation of dissertation research** – UC Berkeley, Infectious Diseases Division, School of Public Health
- 2015 **ASM Richard and Mary Finkelstein Travel Grant Award and Young Investigator Oral Presentation** – American Society of Microbiology
- 2014 **Irving H. Wiesenfeld Fellowship Awardee** – CEND at UC Berkeley
- 2014 **Student Leadership Award** – UC Berkeley, Infectious Disease and Immunity PhD Program, School of Public Health
- 2012-2015 **Graduate Research Fellowship Awardee** – NSF, Grant #DGE 1106400
- 2011 **Graduate Research Fellowship Honorable Mention** – NSF

Publications

- 2016 Reniere, M. L.*, **Whiteley, A. T.***, & Portnoy, D. A. An *In Vivo* Selection Identifies *Listeria monocytogenes* Genes Required to Sense the Intracellular Environment and Activate Virulence Factor Expression. *PLoS Pathogens* (2016) *Denotes co-first authorship
- 2015 **Whiteley, A.T.**, Pollock, A.J., and Portnoy, D.A. The PAMP c-di-AMP Is Essential for *Listeria monocytogenes* Growth in Rich but Not Minimal Media due to a Toxic Increase in (p)ppGpp, *Cell Host & Microbe* (2015)
- 2015 Kellenberger, C.A., Chen, C., **Whiteley, A.T.**, Portnoy, D.A., and Hammond, M.C. RNA-Based Fluorescent Biosensors for Live Cell Imaging of Second Messenger Cyclic di-AMP. *JACS* (2015)
- 2015 Reniere, M.L., **Whiteley, A.T.**, Hamilton, K.L., John, S.M., Lauer, P., Brennan, R.G., and Portnoy, D.A. Glutathione activates virulence gene expression of an intracellular pathogen. *Nature* (2015)
- 2013 Witte, C.E., **Whiteley, A.T.**, Burke, T.P., Sauer, J.D., Portnoy, D.A., and Woodward, J.J. Cyclic di-AMP Is Critical for *Listeria monocytogenes* Growth, Cell Wall Homeostasis, and Establishment of Infection. *MBio* (2013)

Chapter 1: Introduction

Listeria monocytogenes

In the simplest terms, the fitness of any organism is dependent on maximally using resources available to outcompete other organisms and proliferate. In the case of *Listeria monocytogenes*, the bacterium has evolved to thrive both in the environment as a saprophyte and within the mammalian host as an intracellular pathogen (Freitag et al., 2009). *L. monocytogenes* is a particularly successful saprophyte because it grows on diverse carbon sources, as a facultative anaerobe, at low temperatures, and at a variety of osmotic pressures. *L. monocytogenes* is also an impressive pathogen, displaying an unusually broad host range by using a seemingly impossibly small suite of virulence factors to proliferate in the cytosol of infected cells. These intracellular and extracellular lifestyles are also complementary: success in the environment allows *L. monocytogenes* to grow to sufficient densities to infect susceptible hosts, and success as a pathogen distributes *L. monocytogenes* to new environmental niches over a large area. A combination of environmental hardiness and severity of disease make *L. monocytogenes* a formidable bacterial threat to the food processing industry and to public health (Vázquez-Boland et al., 2001).

In addition to being a primary pathogen, *L. monocytogenes* is an ideal model pathogen for study due to its ease of genetic manipulation, a well-characterized lifecycle, and well-established infection models. *L. monocytogenes* is closely related to the model organism *Bacillus subtilis* and many of the genetic tools developed for this *B. subtilis* can be repurposed for *L. monocytogenes* (Camilli et al., 1993; Smith and Youngman, 1992). These tools have allowed molecular characterization of the mechanism by which *L. monocytogenes* infects a susceptible cell. The lifecycle starts upon encountering a host cell when *L. monocytogenes* is either actively phagocytosed (in the case of a macrophage) or otherwise becomes internalized (Miner et al., 2007). Escape from the confines of the host phagosome is mediated by listeriolysin O (LLO, encoded by *hly*), a cholesterol dependent cytolysin that oligomerizes in the phagosomal membrane to form large pores. Efficient escape from the phagosome also requires two phospholipases (PlcA and PlcB) and a metalloprotease (Mpl), which activates PlcB from an inactive pro-form (Portnoy et al., 1992). Once in the cytosol, *L. monocytogenes* synthesizes ActA, the WASP-mimic protein that nucleates actin via the Arp2/3 complex (Welch, 2007). The motility provided by polymerizing host actin propels *L. monocytogenes* into the next susceptible cell where the cycle can be repeated. All of the above described virulence factors are under the control of the master transcriptional regulator PrfA, which is absolutely required for expression of these and a few additional virulence genes. The sequential events of infection can be recapitulated in tissue culture and a mouse model of infection that recapitulates lethal disseminated disease.

L. monocytogenes readily infects a broad range of hosts, including the commonly utilized *Mus musculus* (Hamon et al., 2006). By using genetic modifications of both pathogen and host, *L. monocytogenes* infection models provide a unique window through which to probe host-pathogen interactions. The coevolution between *L. monocytogenes* and the mammalian host provides a unique opportunity to elucidate conserved aspects of bacterial pathogenesis, immunology, and host cell biology. The

following chapters of this thesis specifically explore different aspects of *L. monocytogenes* physiology and virulence gene regulation with implications for fitness in extracellular and intracellular growth niches in the context of pathogenic infection.

Pathogenesis, innate immunity, and PAMPs

It would appear that all forms of life are preyed upon by some sort of pathogen and defense against these parasites is paramount. Unicellular organisms like bacteria are constantly bombarded by viruses (phage) and even parasitized by other bacteria (e.g. *Bdellovibrio*). Indeed, pathogenesis is not restricted to the living; even viruses parasitize other viruses! (e.g. Hepatitis D and B). Fitness as an organism, therefore, requires the evolution of immunity to pathogens. This immunity can be subdivided into an innate component, which is encoded in the germline, and an adaptive component, which is acquired throughout the organism's lifetime as a result of exposure to specific pathogens. For bacteria, adaptive immunity is incorporated into the germline because there is no somatic tissue in a unicellular organism, but for metazoans adaptive immunity is not vertically transmitted. Metazoan germline encoded innate immune receptors are evolutionarily ancient and provide the capability to respond to a broad range of invading pathogens by recognizing conserved pathogen associated molecular patterns (PAMPs). In response, many bacterial pathogens have evolved to evade innate immune detection by the mammalian host in order to thrive (Vance et al., 2009). For example, *L. monocytogenes* has evolved to limit the release of PAMPs such as bacterial DNA and flagellin during infection, which would otherwise limit proliferation of the bacteria by activating the mammalian inflammasome and triggering host cell death via pyroptosis (Sauer et al., 2010). In some cases, though, pathogens have evolved to manipulate, and even selectively agonize host innate immune signaling in order to gain an advantage (Portnoy, 2005). For example, *Salmonella enterica* serotype typhimurium elicits inflammation in the intestine through expression of the type-3 secretion system, thereby generating an energy source that can only be used by the pathogen (Winter et al., 2013; 2010).

L. monocytogenes also appears to selectively trigger innate immune signaling to the detriment of the host, via type I interferon. In mice, type I interferon production or signaling leads to enhanced susceptibility during acute infection (Auerbuch et al., 2004), and dampens development of adaptive immunity (Archer et al., 2014). Forward genetic screens of bacterial mutants identified two independent type I interferon stimuli: bacterial DNA released during bacteriolysis and a substrate of multidrug resistance transporters (MDRs) (Crimmins et al., 2008; Sauer et al., 2010). During infection with wild-type *L. monocytogenes*, bacteriolysis is relatively infrequent (Sauer et al., 2010), but MDR expression increases (Kaplan Zeevi et al., 2013). Biochemical analysis of MDR mutants identified cyclic di-adenosine monophosphate (c-di-AMP) produced by *L. monocytogenes* as the stimulating ligand for the *L. monocytogenes* type I interferon response (Woodward et al., 2010).

Synthesis of c-di-AMP has only been identified in bacteria and some Archaea with no evidence for production by eukaryotes (Römling, 2008), suggesting the possibility that

c-di-AMP might represent a PAMP-like molecule that activates type I interferons in infected host cells. In parallel to identification of c-di-AMP secretion in *L. monocytogenes*, another forward genetic analysis identified the poorly understood host factor STimulator of INterferon Genes (STING) as necessary for induction of type I interferon during *L. monocytogenes* infection (Sauer et al., 2011). Subsequent biochemical analysis identified that STING was a host receptor for bacterial cyclic dinucleotides (Burdette et al., 2011). STING can detect both host- and bacterially-derived cyclic dinucleotides, although host-derived nucleotides are chemically distinct and more potent (Danilchanka and Mekalanos, 2013; Diner et al., 2013; Wu et al., 2012). With this, a pathway of host sensing emerged: c-di-AMP and STING appear to fall into a canonical PAMP::Pattern recognition receptor (PRR) relationship. Although *L. monocytogenes* benefits from interferon signaling downstream of detection of c-di-AMP, it remains to be determined if c-di-AMP is being secreted to manipulate the host, or as a happy (for *Listeria*) consequence of bacterial physiology.

Cyclic dinucleotides and the immune response

A common theme of intracellular bacterial pathogens is access to the host cytosol and induction of a type I interferon response (Vance et al., 2009). Despite this robust immune reaction, type I interferon receptor (IFNAR)-deficient mice are not universally immunocompromised (Trinchieri, 2010). Although it was originally thought that a singular ligand might be responsible for all type I interferon induced by bacterial pathogens, it is now appreciated that each bacterial pathogen appears to trigger type I interferon in slightly different manner. For example, *L. monocytogenes* activates type I interferon through secretion of c-di-AMP but *Mycobacterium tuberculosis* appears to release DNA into the cytoplasm of host cells (Manzanillo et al., 2012). Both of these cyclic dinucleotide ligands signal through STING, however DNA must first agonize cGAMP synthase (cGAS) which, upon DNA-binding, produces the noncanonical cyclic dinucleotide cyclic [guanosine(2'-5')p-adenosine(3'-5')p] (cGAMP) (Diner et al., 2013; Sun et al., 2012; Wu et al., 2012). The term "canonical" and "noncanonical" dinucleotide linkages refer to the canonical 3'-5' linkages found between bacterial cyclic dinucleotides c-di-AMP and c-di-GMP, and the noncanonical 2'-5'/3'-5' mixed linkage found in cGAMP. Although these nucleotides all bind STING, the affinity of the interaction and structural rearrangements upon nucleotide binding differ (Kranzusch et al., 2015). Further, human alleles of STING have been identified that discriminate between bacterial cyclic dinucleotides and cGAMP (Diner et al., 2013). The consequences of different nucleotides signaling through STING remains an active area of investigation.

Cyclic di-adenosine monophosphate (c-di-AMP) in bacterial physiology

The molecule c-di-AMP is a nucleotide second messenger, a family of small molecules that signal through allosteric interactions with proteins and riboswitches in response to environmental stimulus. Nucleotide second messengers are found ubiquitously among all forms of life. Three analogous and well-studied nucleotide second messengers are

cAMP, pppGpp/ppGpp (collectively referred to here as (p)ppGpp), and cyclic-di-GMP. Each of these nucleotides carry out core functions that are conserved among bacteria. However, it is not uncommon to find novel receptors, synthases, and functions for second messengers that are organism specific. For example, the cyclic di-purine c-di-GMP generally modulates the transition between motile and sessile behaviors to affect bacterial biofilm formation and virulence (Hengge, 2009). The molecule c-di-AMP is analogous to c-di-GMP but is functionally distinct and there is no unified hypothesis of the core function for this molecule (Corrigan and Gründling, 2013).

Cyclic-di-AMP was first discovered in the crystal structure of the DisA protein of *B. subtilis*, which is involved in sporulation and, although unknown at the time, is one of the three di-adenylate cyclases (DACs) encoded by its genome. The portion of DisA crystalized was a domain of unknown function (formerly DUF147, now DisA_N PF02457). It was immediately appreciated that the distribution of similar di-adenylate cyclases based on protein domain analysis stretched from virtually all Gram positive bacteria, to certain Gram negative bacteria, and some Archaea (Römling, 2008). However, the signaling consequences of the nucleotide were not realized until identification of a c-di-AMP-degrading phosphodiesterase was identified (Rao et al., 2010). In multiple species, inactivating mutations in the c-di-AMP specific phosphodiesterase, represented by the *B. subtilis* homolog *gdpP* (formerly *yybT* and *pdeA* in *L. monocytogenes*), increase intracellular c-di-AMP, resistance to β -lactam antibiotics, and resistance to acid stress (Corrigan et al., 2011; Rallu et al., 2000; Rao et al., 2010; Witte et al., 2013). Recently, PgpH was identified as an additional broadly-conserved c-di-AMP phosphodiesterase with seven transmembrane domains and a large extracellular domain that undoubtedly participates as a sensor for an unknown stimulus (Huynh et al., 2015). c-di-AMP signaling appeared to extend far beyond just sporulating organisms and a general role for c-di-AMP appears to be coordinating cell wall homeostasis, growth/central metabolism, osmoregulation/potassium homeostasis, and virulence (Corrigan and Gründling, 2013). Either too little or too much c-di-AMP is deleterious to growth and an imbalance of c-di-AMP can result in accumulation of (p)ppGpp (Corrigan et al., 2015; Mehne et al., 2013; Whiteley et al., 2015; Witte et al., 2013; Zhu et al., 2016). Regulation of c-di-AMP levels is thus extremely important to the health of the organism.

Regulation of c-di-AMP concentration occurs at three levels: synthesis by DACs, degradation by phosphodiesterases, and potentially by export from the bacterium. GdpP may serve to integrate multiple signals into c-di-AMP levels as it is inhibited by nitric oxide and the nucleotide (p)ppGpp, an additional basis for cross-talk between these secondary messengers (Rao et al., 2010). However, whereas multiple small molecule interactions alter GdpP phosphodiesterase catalytic capabilities, only protein-protein interactions have been identified to modulate DAC activity (Mehne et al., 2013; Rao et al., 2010; 2011; Zhang and He, 2013). The DAC-protein regulation likely corresponds to a sensory function of the cognate protein interactor, but the few interactions documented require further characterization (See Chapter 7 for greater discussion). Finally, in *L. monocytogenes*, c-di-AMP can be secreted via multiple transporters (Crimmins et al., 2008; Woodward et al., 2010). It is unclear if secretion alters

intracellular nucleotide concentrations and may be an unprecedented mode of controlling intracellular nucleotide signaling.

Previous high-throughput studies identified DAC-encoding genes as essential in Firmicutes (Chaudhuri et al., 2009; French et al., 2008; Glass et al., 2006; Song et al., 2005). For example, in *B. subtilis* it is possible to obtain mutations in two but not all three DAC-encoding genes (Mehne et al., 2013). Attempts to delete the solitary DAC in *L. monocytogenes* and *Streptococcus pyogenes* by conventional methods have also been unsuccessful (Kamegaya et al., 2011; Witte et al., 2013; Woodward et al., 2010). So far, *Streptococcus mutans* appears to be the only Firmicute in which DACs are not essential (Cheng et al., 2016), though this strain was made by selecting a marked deletion and may harbor suppressor mutations. In Actinobacteria there is no evidence for c-di-AMP essentiality: the sole di-adenylate cyclases in *M. tuberculosis* and *M. smegmatis* have been successfully deleted (Tang et al., 2015; Yang et al., 2014).

Genetic screens for virulence genes

Virulence genes have traditionally been defined as accessory genetic elements required for efficient host colonization that are upregulated during pathogenesis. These genes encode proteins that are often extracellular, such that they can readily interact with the host. Investigators first used these criteria to identify mutations in genes encoding virulence factors with overt phenotypes, such as secreted hemolysins visible on blood-agar. Later, transposons were engineered to create PhoA fusion proteins to isolate mutations that only disrupted secreted proteins, which could be interrogated for defects in pathogenesis (Taylor et al., 1987). As molecular techniques improved, researchers next used a variety of signature-tagged mutagenesis (Hensel et al., 1995) techniques including TRASH screens (Sasseti et al., 2001) and Tn-seq methods to globally identify genes specifically required for growth *in vivo* (Gawronski et al., 2009; Goodman et al., 2009; Langridge et al., 2009; van Opijnen et al., 2009). These findings proved powerful for understanding virulence determinants, but often also identified genes indirectly required for virulence, such as biosynthetic genes (Chiang et al., 1999).

In an effort to identify virulence genes specifically required for host colonization and not just growth, many groups have focused on genes upregulated during infection. Prior to micro-arrays and RNA-seq quantifications of gene expression, transposons were engineered to generate beta-galactosidase transcriptional fusions upon interruption of genes (Klarsfeld et al., 1994). In such “brut force” methods *lacZ* expression, the proxy for the disrupted gene, could be quantified both *in vitro* and intracellularly. In order to capture genes upregulated during infection in an animal model, “*in vivo* expression technology” or IVET was next developed. Here transposons were equipped to create transcriptional fusions of both auxotrophic and antibiotic resistance markers to select for genes induced *in vivo* (Chiang et al., 1999). However, these IVET systems often biased findings towards highly and constitutively expressed genes. These limitations were overcome with resolvase IVET, where transposon borne transcriptional fusions of the DNA-recombinase resolvase determined the terminal excision of an antibiotic resistance

gene via DNA recombination (Camilli et al., 1994). In addition to those listed here there have been many different approaches to identifying and characterizing novel virulence genes in a wide variety of pathogens. However, a relatively unexplored facet of pathogen biology that has been difficult to study is the regulation of virulence gene expression. Specifically, how does a bacterial pathogen know when to turn on virulence genes?

Virulence gene regulation in *L. monocytogenes*

Upon access to the host cytosol *L. monocytogenes* remodels its proteome by transcriptionally upregulating a suite of virulence genes that are regulated by the transcriptional regulator PrfA (las Heras et al., 2011). The most highly expressed protein is ActA, which is virtually undetectable during growth in the lab and the most abundant protein made by *Listeria* during intracellular growth (D. Portnoy personal communication). PrfA is a CRP-family transcriptional regulator that binds to PrfA boxes, which are specific palindromic DNA sequences that precede the virulence genes *hly/plcA*, *mpl*, *actA-plcB-orfXYZ*, *bsh*, *hpt*, *inlAB*, and *inlC*. The highest affinity PrfA boxes drive transcription of so called “early” genes like *hly/plcA*, which are divergently transcribed from the same PrfA-box, and feeds forward by driving distal expression of *prfA* via read-through transcription. Low affinity PrfA boxes such as the sequence driving *actA/plcB/orfXYZ* have been hypothesized to be important for “late” genes. The temporal descriptions of early and late correspond to the life cycle of *L. monocytogenes* where early events involve exiting the vacuole and late events include spreading cell-to-cell. The transition in gene expression thus implies a shift in activation state of PrfA during infection, however, the precise molecular details of how PrfA is activated is an ongoing area of research.

Chapter 2: The PAMP c-di-AMP is essential for *Listeria monocytogenes* growth in rich but not minimal media due to a toxic increase in (p)ppGpp

The majority of this chapter was published in:

Whiteley, A. T., Pollock, A. J. & Portnoy, D. A. The PAMP c-di-AMP Is Essential for *Listeria monocytogenes* Growth in Rich but Not Minimal Media due to a Toxic Increase in (p)ppGpp. *Cell Host Microbe* **17**, 788–798 (2015).

Summary

Cyclic di-adenosine monophosphate (c-di-AMP) is a widely distributed second messenger that appears to be essential in multiple bacterial species, including the Gram-positive facultative intracellular pathogen *Listeria monocytogenes*. In this study, the only *L. monocytogenes* diadenylate cyclase gene, *dacA*, was deleted using a Cre-lox system activated during infection of cultured macrophages. All $\Delta dacA$ strains recovered from infected cells harbored one or more suppressor mutations that allowed growth in the absence of c-di-AMP. Suppressor mutations in the synthase domain of the bi-functional (p)ppGpp synthase/hydrolase led to reduced (p)ppGpp levels. A genetic assay confirmed that *dacA* was essential in wild-type but not strains lacking all three (p)ppGpp synthases. Further genetic analysis suggested that c-di-AMP was essential because accumulated (p)ppGpp altered GTP concentrations, thereby inactivating the pleiotropic transcriptional regulator CodY. We propose that c-di-AMP is conditionally essential for metabolic changes that occur in growth in rich medium and host cells but not minimal medium.

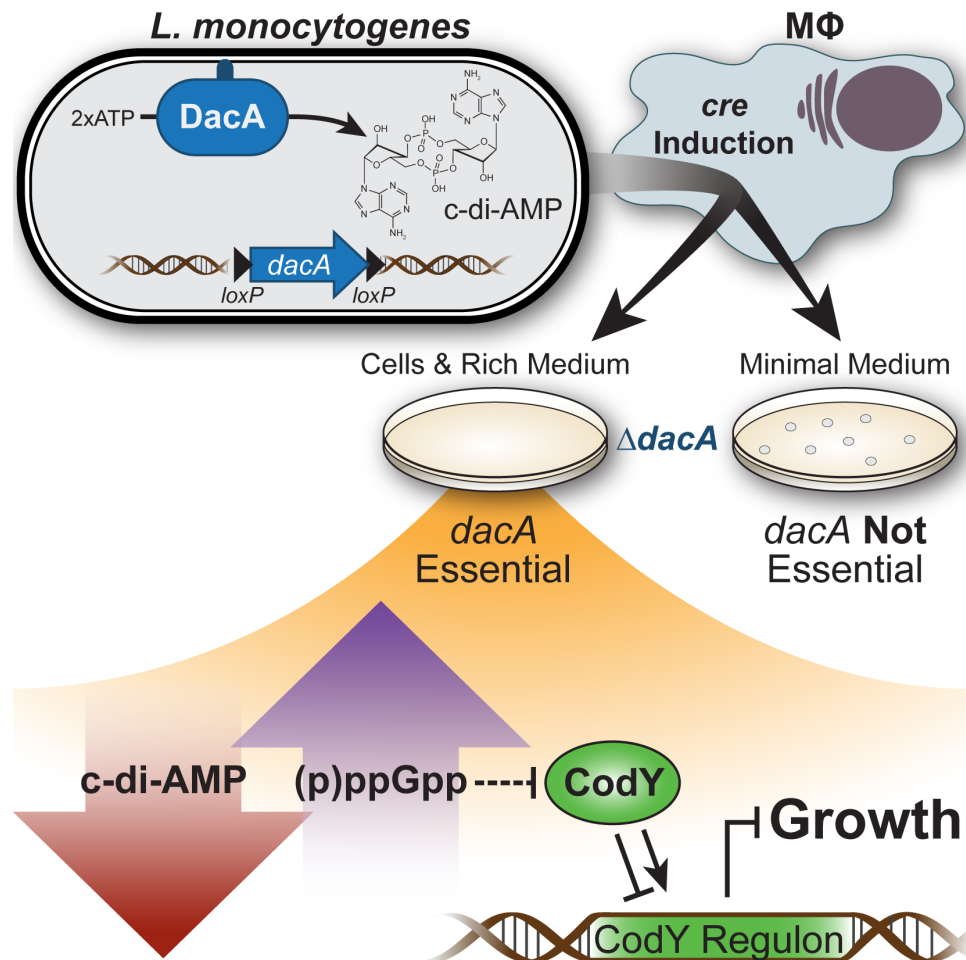


Figure 2.1 Graphical Abstract

Introduction

Listeria monocytogenes is a hardy and ubiquitous Gram-positive, facultative intracellular, foodborne pathogen that thrives as an environmental saprophyte, yet is capable of causing serious, often fatal, disease in a wide range of animals including humans (Cossart, 2011). Its broad growth range is accompanied by a largely prototrophic metabolism, capable of utilizing an array of carbon and nitrogen sources and requiring only a few essential vitamins and amino acids (Tsai and Hodgson, 2003). Remarkably, *L. monocytogenes* grows in the cytosol of host cells at a similar rate to rich medium (doubling in approximately 40 minutes) (Joseph and Goebel, 2007). To accomplish such efficient intracellular growth, *L. monocytogenes* remodels its transcriptional program upon entering host cells by activation of the master virulence regulator PrfA (Freitag et al., 2009). PrfA is required for the expression of many determinants of pathogenesis, but it also contributes to metabolic adaptations. For instance, transcription of *hpt*, encoding a hexose phosphate transporter, is PrfA-regulated, allowing growth on glucose-1-phosphate in the host cell cytosol (Chico-Calero et al., 2002). *L. monocytogenes* also uses non-PrfA mediated mechanisms for remodeling its metabolism. For example, pyruvate carboxylase (PycA) is dispensable in rich medium but required for pathogenesis and is regulated allosterically by cyclic diadenosine monophosphate (c-di-AMP) (Schär et al., 2010; Sureka et al., 2014).

c-di-AMP is member of the cyclic-di-nucleotide family of second messengers that includes cyclic di-guanosine monophosphate (c-di-GMP) and cyclic-AMP-GMP produced by bacteria and cyclic[G(2' -5')pA(3' -5')p] (cGAMP) produced by some metazoans (Danilchanka and Mekalanos, 2013). The role of c-di-AMP during infection was identified as a result of biochemical characterization of *L. monocytogenes* mutants that triggered diminished or enhanced activation of the cytosolic surveillance pathway (CSP) (Crimmins et al., 2008; Woodward et al., 2010). The CSP is characterized by the robust induction of host type I interferon and has implications for both innate and adaptive immunity (Archer et al., 2014; O'Riordan et al., 2002). *L. monocytogenes* secretes c-di-AMP through multidrug efflux pumps, however, the affect of secreted c-di-AMP on the bacterium is not known and remains an active area of investigation (Kaplan Zeevi et al., 2013; Tadmor et al., 2014). c-di-AMP differs from c-di-GMP, the most extensively characterized bacterial cyclic di-nucleotide, in that bacteria usually encode a single diadenylate cyclase that is often essential (Corrigan and Gründling, 2013). The DAC protein domain (Pfam: DisA_N, PF02457) is the only identified protein domain capable of c-di-AMP synthesis *in vivo* and is widely distributed among archaea, Gram-positive bacteria, and some Gram-negative bacteria (Witte et al., 2008). *L. monocytogenes* encodes only one DAC, *dacA*, which cannot be deleted by conventional methods and is therefore also predicted to be essential (Witte et al., 2013). In addition, high-throughput and targeted studies have identified c-di-AMP as essential in *Bacillus subtilis*, *Staphylococcus aureus*, *Streptococcus pyogenes*, *Streptococcus pneumoniae*, *Mycoplasma genitalium*, and *Mycoplasma pulmonis* (Corrigan and Gründling, 2013).

Many c-di-AMP-associated phenotypes have been observed in bacterial mutants containing inactivating mutations in c-di-AMP-degrading phosphodiesterases. Genetic

screens in multiple organisms established that inactivating mutations in homologs of the conserved phosphodiesterase GdpP increase intracellular c-di-AMP levels, increase resistance to acid-stress, suppress mutations in lipoteichoic acid biosynthesis, and increase resistance to β -lactam antibiotics (Corrigan et al., 2011; Luo and Helmann, 2012; Rallu et al., 2000; Witte et al., 2013). Likewise, bacterial mutants depleted for DAC expression exhibit increased sensitivity to β -lactam antibiotics (Mehne et al., 2013; Witte et al., 2013). A diverse set of proteins interact with c-di-AMP, and a conserved c-di-AMP interacting riboswitch regulates translation of a wide array of genes in many organisms (Corrigan et al., 2013; Nelson et al., 2013; Sureka et al., 2014). However, none of the identified c-di-AMP receptors are conserved among all c-di-AMP-producing organisms, despite conservation of many c-di-AMP-related phenotypes (Corrigan and Gründling, 2013). Here we report the isolation and characterization of suppressor mutations that allow *L. monocytogenes* to grow in the absence of c-di-AMP. Our findings may help unify divergent c-di-AMP-related phenotypes and support a model in which *L. monocytogenes* requires intracellular c-di-AMP for metabolic adaptations during growth in rich medium and in host cells.

Results

Generation of L. monocytogenes ΔdacA mutants and identification of suppressor mutations

There is mounting evidence that c-di-AMP is an essential molecule in many Firmicutes, including *L. monocytogenes* (Corrigan and Gründling, 2013). Accordingly, we were unable to generate $\Delta dacA$ mutants in wild-type *L. monocytogenes*, but were successful in generating a $dacA$ deletion in a strain that contained a second copy of $dacA$ expressed from an inducible promoter (Witte et al., 2013; Woodward et al., 2010). We sought an alternative method to delete $dacA$ based on an inducible Cre-lox system (Reniere et al., 2015). loxP sites were inserted into the *L. monocytogenes* chromosome flanking $dacA$ ($dacA^{fl}$). Codon-optimized cre recombinase was expressed from the $actA$ promoter ($P_{actA-cre}$) and cloned into a temperature-sensitive plasmid. The $actA$ promoter was chosen because it is not expressed in broth but highly active during growth inside mammalian cells (Shetron-Rama et al., 2002). The $dacA^{fl} P_{actA-cre}$ strain grew normally in broth but resulted in deletion of $dacA$ upon infection of cultured macrophages (Figure 2.2A). Wild-type bacteria from infected macrophages formed colonies on rich medium agar in approximately 14 hours, whereas $\Delta dacA$ mutants formed visible colonies between days 2-5. The $\Delta dacA$ mutants, cured of the cre expressing plasmid, were verified by PCR using primers internal to the $dacA$ gene and external to the $dacA$ -locus.

Five mutants, numbered $\Delta dacA.1$ - $\Delta dacA.5$, were chosen for initial characterization. As expected these mutants grew poorly in brain-heart infusion (BHI) broth, a rich medium commonly used for cultivating *L. monocytogenes* (Figure 2.2B). We hypothesized that $dacA$ was essential but that these $\Delta dacA$ strains contained suppressor mutations that bypassed the essential functions of c-di-AMP. Genome sequencing of strains $\Delta dacA.1$ - $\Delta dacA.5$ and the parent $dacA^{fl}$ confirmed that $dacA$ was absent and revealed two groups of mutations not found in the parent strain (Table 2.1). Four strains contained mutations in the 5-gene operon *oppABCDF* encoding a previously identified oligopeptide permease (Opp)(Borezee et al., 2000b). These four mutants displayed decreased sensitivity to killing by the toxic tri-peptide bialaphos that is transported exclusively by the Opp (Figure 2.2C)(Borezee et al., 2000b). The only strain without an *opp* mutation ($\Delta dacA.3$) encoded a point mutation (R295S) in the synthase domain of the previously identified bi-functional guanosine penta- and tetraphosphate ((p)ppGpp) synthase/hydrolase *relA* (Bennett et al., 2007; Taylor et al., 2002) and remained bialaphos-sensitive (Figure 2.2C and Figure 2.2E). These data indicated that the *opp* nucleotide changes were loss-of-function mutations, consistent with the disruptive nature of these polymorphisms (frame-shifts and a premature stop codon) and that the *relA* mutation in the $\Delta dacA.3$ strain did not affect Opp activity.

To further investigate $dacA$ essentiality an additional 284 $\Delta dacA$ mutants were selected for characterization. All of the $\Delta dacA$ strains isolated encoded mutations. Of these mutants, 94.37% were resistant to bialaphos, suggesting mutations in *opp* genes, and 1.76% harbored *relA* mutations as determined by Sanger sequencing of the synthase

domain of the *relA* gene (Figure 2.2D). The additional *relA* alleles identified are depicted in Figure 2.2E. Genome sequencing of the remaining 11 mutants $\Delta dacA.6$ - $\Delta dacA.17$ that were sensitive to bialaphos and did not harbor *relA* synthase domain mutations revealed that each strain contained more than one mutation (Table 2.1). These additional mutations often recurred in the same genes (three of which share cystathionine- β -synthase (CBS) domains), appeared in genes encoding identified c-di-AMP binding proteins (Sureka et al., 2014), and included *opp* and *relA* mutations that escaped detection (Table 2.1). Characterization of *opp* and other suppressor mutations will be the subject of future studies.

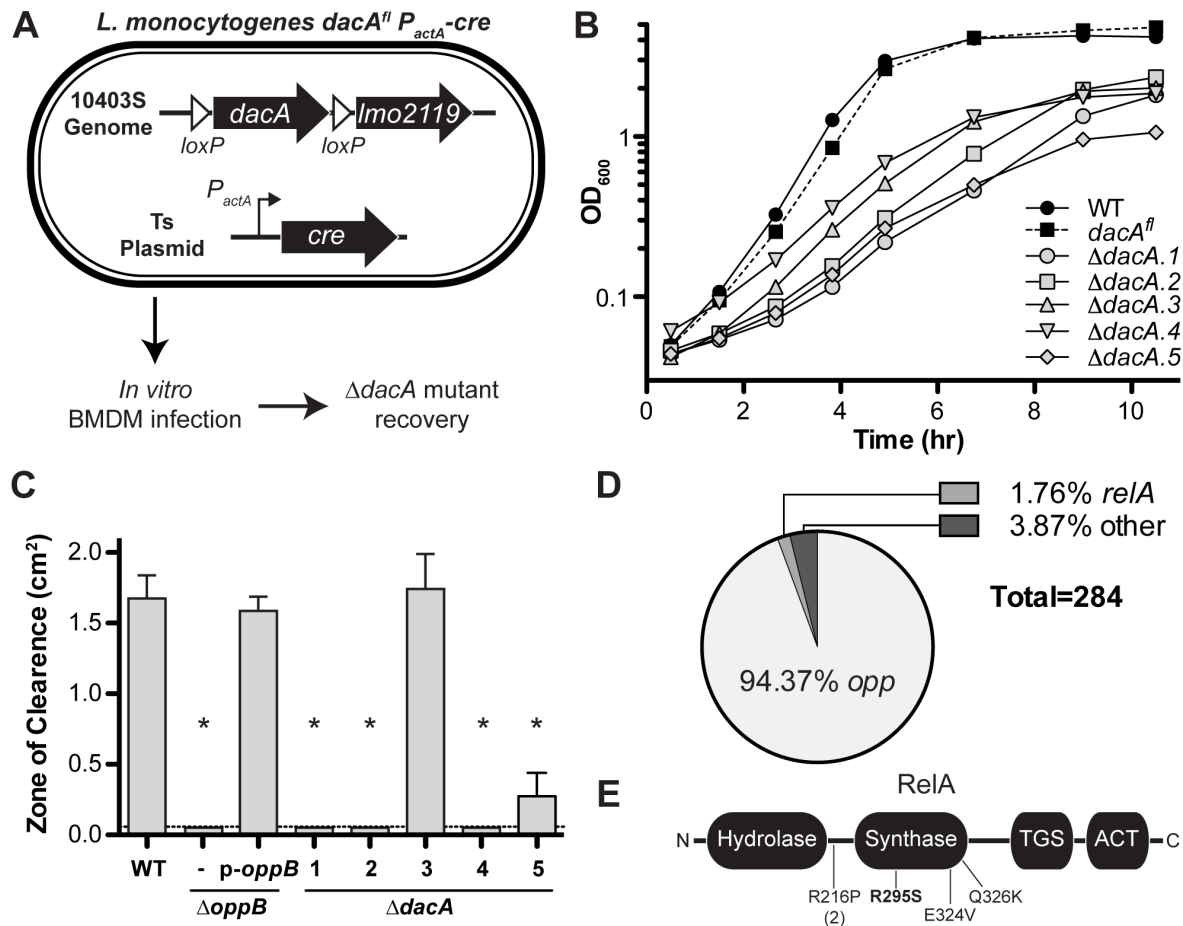


Figure 2.2 Cre-lox deletion of *dacA* and $\Delta dacA$ suppressor mutations.

(A) Schematic representation of the *L. monocytogenes* strain used to delete *dacA*. The $\Delta dacA$ mutants were recovered after *cre* was induced during infection of bone marrow-derived macrophages (BMDMs) from a temperature sensitive (Ts) plasmid that could be cured from $\Delta dacA$ mutants. (B) BHI broth growth curve of wild-type (WT), floxed-*dacA* (*dacA^{fl}*), and $\Delta dacA$ mutants (for genotypes see Table 2.1) Data are representative of three independent experiments. (C) Sensitivity to the toxic tripeptide bialaphos as measured by disk diffusion. Data are mean \pm standard error of the mean (s.e.m) of three independent experiments. *p-oppB* represents *oppB* complemented under its native promoters. The dotted line represents the limit of detection (L.o.D.) and **p* \leq 0.01 by two-tailed Student's t-test as compared to WT. (D) Frequency of *opp* and *relA* suppressor mutations within a collection of 284 $\Delta dacA$ mutants. (E) Depiction of RelA protein with conserved hydrolase, synthase, ThrRS-GTPase-SpoT (TGS), and Aspartokinase-Chorismate-mutase-TyrA (ACT) domains. Annotation of specific amino acid changes as a result of suppressor mutations: R295S was the first identified in $\Delta dacA.3$ and R216P was identified twice.

Strain	<i>oppA</i> ^a BCDF (<i>Imo2196-2192</i>)	<i>relA</i> (<i>Imo1523</i>)	<i>gbuA</i> ^b BC (<i>Imo1014-1016</i>)	<i>pycA</i> ^a (<i>Imo1072</i>)	<i>cbpB</i> ^{ab} (<i>Imo1009</i>)	<i>pstA</i> ^a (<i>Imo2692</i>)	Other mutations	Gene description
Δ <i>dacA.1</i>	<i>oppA</i> K534fs						<i>Imo0241</i> (R171L)	TrmH/SpoU family RNA methyltransferase similar to <i>yacO</i>
Δ <i>dacA.2</i>	<i>oppC</i> V297fs							
Δ <i>dacA.3</i>		R295S						
Δ <i>dacA.4</i>	<i>oppA</i> Q417*						<i>Imo1718</i> (T196A)	Conserved hypothetical protein, DUF871
Δ <i>dacA.5</i>	<i>oppD</i> T328fs							
Δ <i>dacA.6</i>			<i>gbuB</i> M213fs <i>gbuC</i> A250V	I725N			<i>polC</i> (<i>Imo1320</i> , V1141F) <i>guaB2</i> ^b (<i>Imo2758</i> , P211S)	DNA polymerase III subunit alpha IMP dehydrogenase
Δ <i>dacA.7</i>	<i>oppB</i> A185E		<i>gbuA</i> V151F		H26P			
Δ <i>dacA.8</i>	<i>oppB</i> F261S			N380K			<i>Imo2581</i> (I268fs)	Similar to heme efflux pump
Δ <i>dacA.9</i>	<i>oppA</i> LMRG_01636: 1001ins39nt in 42% of DNA			G1032D			<i>Imo0284</i> (LMRG_02587:942C>T) <i>Imo1632</i> (LMRG_01334:408G>A) <i>Imo2353</i> (LMRG_01490:1776G>A)	Methionine import ATP-binding subunit, metN Anthranilate synthase component II Hypothetical protein
Δ <i>dacA.10</i>			<i>gbuA</i> R314fs		G72E		<i>citZ</i> (<i>Imo1567</i> , E14*)	Citrate synthase
Δ <i>dacA.11</i>	<i>oppA/B</i> LMRG_01637: -218G>A			L1018P				
Δ <i>dacA.12</i>			<i>gbuC</i> E190fs		E34*			
Δ <i>dacA.13</i>					V118* (151nt del.)	I60N	<i>mazE</i> (<i>Imo0887</i> , A82fs) <i>ktrD</i> (<i>Imo0993</i> , V334_G335delG)	Toxin-anti-toxin transcriptional regulator TrkH family low affinity K ⁺ transporter
Δ <i>dacA.14</i>		G109C	<i>gbuB</i> LMRG_02115: 508ins9nt			Q69*	<i>menH</i> (<i>Imo1931</i> , E3K)	2-heptaprenyl-1,4-naphthoquinone methyltransferase
Δ <i>dacA.15</i>	<i>oppD</i> T184P		<i>gbuA</i> K214fs	G714fs in 6% of DNA	K42fs	L20R	<i>Imo1799</i> (LMRG_02823:1452T>G)	LPXTG motif containing hypothetical protein
Δ <i>dacA.16</i>		T445K	<i>gbuA</i> G42D	LMRG_00534: -36G>A			Intergenic <i>Imo2714/2715</i> (LMRG_01982:-109C>A)	Terminator of <i>cydD</i> (cytochrome BD transporter)

Table 2.1 Δ *dacA* suppressor mutations

Nonsynonymous mutations resulting in amino acid changes are annotated using EGD-e ordered locus. Synonymous mutations are annotated using 10403S LMRG locus:nucleotide 3' of ORF start codon. Unless otherwise stated all mutations were found in >80% of sequenced DNA. Abbreviations/annotations: *oppABCDF*, oligopeptide transporter operon; *relA*, bi-functional (p)ppGpp synthase/hydrolase; *gbuABC*, glycine/betaine ABC family transporter; *pycA*, pyruvate carboxylase; *cbpB*, c-di-AMP binding protein B; *pstA*, PII-like signal transduction protein; fs, frame-shift mutation; *, premature stop codon.

^a Identified as interacting with c-di-AMP or enriched on c-di-AMP conjugated sepharose beads (Sureka et al., 2014)

^b CBS domain containing protein.

Development of a dacA essentiality assay

The above results suggested that *dacA* was essential and that each of the $\Delta dacA$ mutants had accumulated one or more suppressor mutations. To expand upon these studies we developed a rapid essentiality assay based on the method of co-transduction of linked genetic markers used to show gene essentiality in *Escherichia coli* (Las Peñas et al., 1997). Two donor *L. monocytogenes* strains were constructed, *dacA* and $\Delta dacA$ using Cre-lox, in which the *dacA* locus was marked by a kanamycin resistance gene (*kanR*) 3' to the *dacA* locus. A *himar1* transposon (*ermR*) encoding an erythromycin resistance gene was present 16.6 kb 5' of the *dacA* locus (Figure 2.3A). The assay was performed by: 1) lysogenizing recipient *L. monocytogenes* strains with phage derived from either of the two drug-resistant donor strains, 2) selecting for transduction on erythromycin, and 3) analyzing genetic linkage by scoring transductants for kanamycin resistance (Figure 2.3A). In a wild-type recipient, the *dacA-kanR* allele displayed approximately 35% linkage with the *ermR* gene, while co-transduction of the $\Delta dacA-kanR$ allele was below the limit of detection (Figure 2.3B). This linkage disequilibrium was ameliorated in recipients merodiploid for *dacA* (WT p-*dacA*), indicating the difference in linkage between *dacA-kanR* and $\Delta dacA-kanR$ alleles was specific to deletion of the *dacA* gene (Figure 2.3B). Moreover, the genetic linkage analysis produced similar results when performed with an alternative *himar1* transposon 10 kb 5' of the *dacA* locus, demonstrating that the location of the *himar1* transposon had no affect on the results (Figure 2.4).

The $\Delta dacA$ phage lysate used for the essentiality assay was derived from a strain that presumably harbors suppressor mutations as a result of the Cre-lox mediated deletion of *dacA*. Given the results of the linkage experiments, these suppressor mutations were not linked to the *dacA* locus. To further assess the impact of suppressor mutations, $\Delta dacA.1-5$ mutants generated through Cre-lox recombination were subjected to the identical linkage analysis described above (Figure 2.3A). Linkage was unaffected in $\Delta dacA.1,2,4,$ and 5 , verifying the existence of suppressor mutations and that the *dacA* gene was no longer essential in these strains (Figure 2.3C). Linkage analysis was not determined for $\Delta dacA.3$ (encoding a *relA*^{R295S} mutation) owing to an inability to obtain erythromycin-resistant transductants in this background for an unknown reason. This limitation was overcome by reconstructing the *relA*^{R295S} mutation in a wild-type background. *dacA* was also not essential in this background, confirming the *relA*^{R295S} mutation suppresses *dacA* essentiality (Figure 2.3C). These data were consistent with *dacA* being essential to wild-type *L. monocytogenes* and established an assay whereby comparison of *dacA* and $\Delta dacA$ genetic linkage is a measure of *dacA* essentiality.

Suppressor mutations in relA decreased (p)ppGpp accumulation in response to starvation

We chose to characterize the suppressor mutations in *relA* because these mutations appeared sufficient to ablate *dacA* essentiality and because of the previously documented nucleotide cross-talk between c-di-AMP and (p)ppGpp (Corrigan et al., 2015; Rao et al., 2010; Sureka et al., 2014). The $\Delta dacA$ suppressor mutations in *relA*

clustered within or near the synthase domain of the RelA protein (Figure 2.2E). RelA (encoded by a homologue of the *E. coli relA/spoT* gene) synthesizes (p)ppGpp in response to starvation during the “stringent response” by transferring two phosphates from ATP to either GTP or GDP to produce pppGpp or ppGpp, respectively (collectively referred to as (p)ppGpp). In Firmicutes, RelA is also a hydrolase that degrades (p)ppGpp when nutrients are abundant (Mechold et al., 1996). The hydrolase and synthase enzymatic activities can be separated by point mutations in their respective domains (Hogg et al., 2004). The impact of the *relA*^{R295S} suppressor mutation was interrogated by reconstructing the mutation in the chromosome of wild-type *L. monocytogenes* and measuring ³²P-labeled intracellular nucleotides by thin layer chromatography (TLC). These experiments were performed in low-phosphate defined medium supplemented with tryptone, which mimicked rich medium and stimulated uptake of added ³²P (Taylor et al., 2002). Amino acid starvation was simulated using serine hydroxamate (SHX) and (p)ppGpp was quantified as a proportion of (p)ppGpp + GTP levels. Control experiments demonstrated that wild-type *E. coli* (CF1943) accumulated (p)ppGpp in response to starvation while *E. coli* carrying a disrupted *relA* gene (CF1944) did not (Figure 3A and 3B). Wild-type *L. monocytogenes* also accumulated (p)ppGpp in response to starvation, however, mutants expressing *relA*^{R295S} did not (Figure 2.5A and C), supporting the supposition that this mutation disrupted RelA synthase activity.

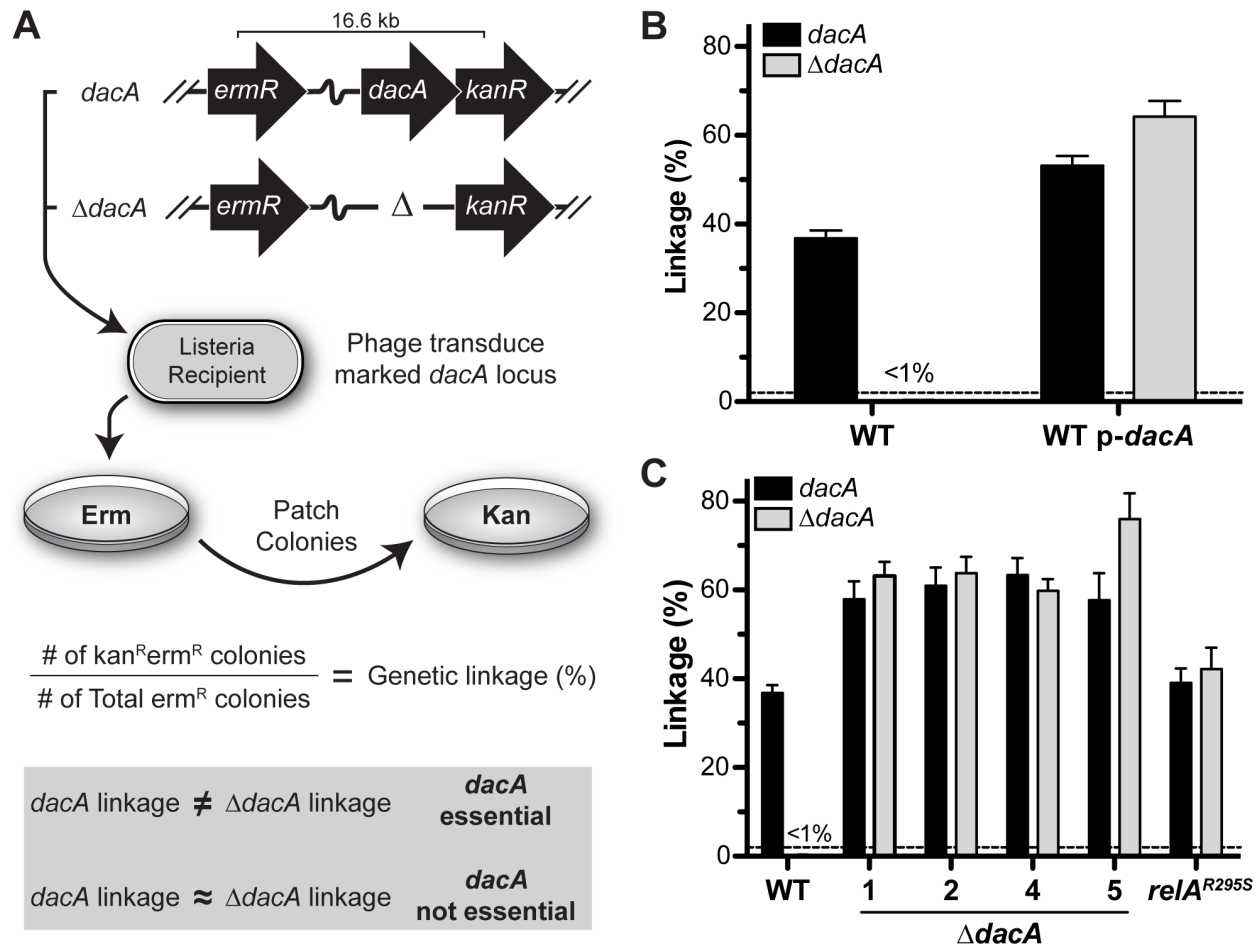


Figure 2.3 *dacA* essentiality assay.

(A) Schematic of *dacA* essentiality assay depicting erythromycin resistance genes (*ermR*), kanamycin resistance genes (*kanR*) 3' of *dacA* and Δ *dacA*, erythromycin (Erm)/kanamycin (Kan) containing medium-agar, and resistant transductants (*ermR/kanR*). See text for description. (B) Genetic linkage of *dacA* or Δ *dacA* with co-transduced antibiotic resistance marker in wild-type or mutants merodiploid for *dacA* (p-*dacA*). (C) *dacA* essentiality assay of Δ *dacA* suppressor mutants, Δ *dacA*.3 (encoding a *relA*^{R295S} mutation) was not determined due to an inability to obtain *ermR* transductants in this background. The *relA*^{R295S} mutation was interrogated instead by reconstructing the mutation in a wild-type background. Dotted line indicates L.o.D. and all data are mean \pm s.e.m of at least three independent experiments.

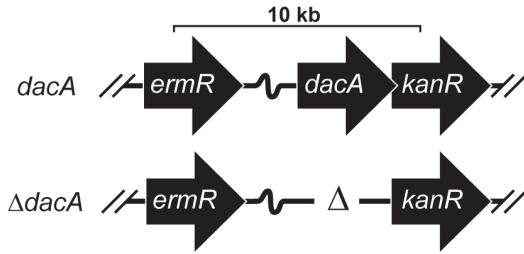


Figure 2.4 *dacA* essentiality assay validation using an alternative *ermR* gene location

dacA essentiality assay performed using an alternative *himar1* transposon in *lmo2110*, 10 kb from the *dacA* locus. Dotted line indicates L.o.D., data are mean \pm s.e.m of two independent experiments.

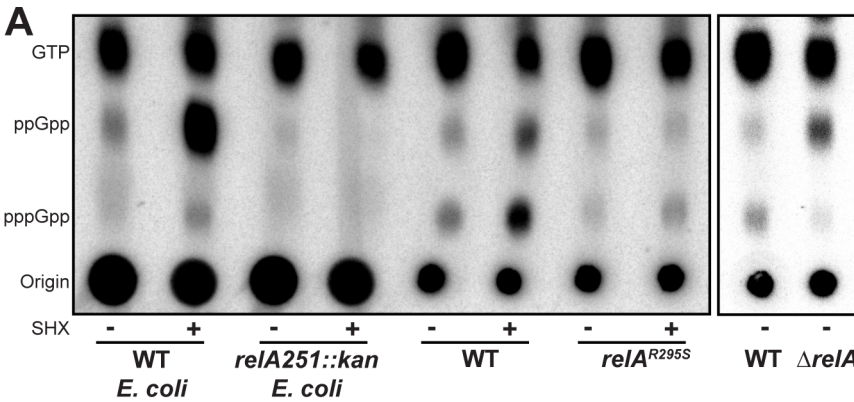
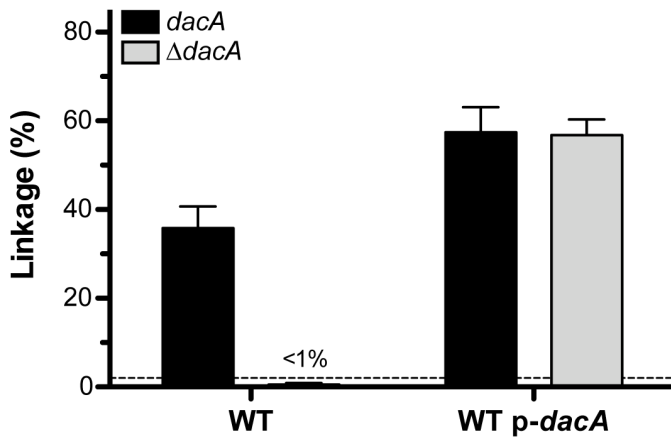
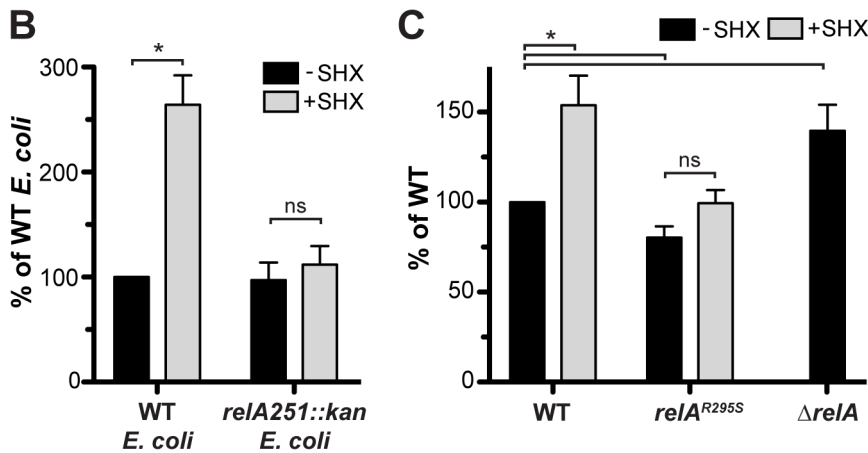


Figure 2.5 Δ *dacA* suppressor mutations in *relA* affect starvation-induced (p)ppGpp.

Thin layer chromatography (TLC) of 32 P-labeled intracellular nucleotides from bacterial mutants. Bacteria were grown in low-phosphate defined medium plus tryptone and, where indicated, starvation was induced using serine hydroxamate (SHX). Wild-type *E. coli* (CF1943) and *relA251::kan E. coli* (CF1944) are included as controls; all other strain are *L. monocytogenes*.

A representative TLC is shown (A), and quantification of the ratio $(pppGpp+ppGpp) / (pppGpp+ppGpp+GTP)$ as a percent of wild-type is shown for *E. coli* (B) and *L. monocytogenes* (C). All data are representative of $n=10$ independent experiments, graphed data are mean \pm s.e.m. of pooled data, * $p \leq 0.05$ by two-tailed Student's *t*-test, and ns denotes not significant ($p > 0.05$).



In related Firmicutes, two proteins (RelP and RelQ) in addition to RelA are capable of synthesizing (p)ppGpp, although RelA is the only synthase predicted to respond to starvation (Nanamiya et al., 2008). The other two small alarmone synthases, identified here as *relP* (*Imo0802*) and *relQ* (*Imo0967*) based on their homology to *B. subtilis*, *S. aureus*, and *Streptococcus mutans* (Geiger et al., 2014; Lemos et al., 2007; Nanamiya et al., 2008) were likely responsible for the basal levels of (p)ppGpp observed in the untreated condition (Figure 2.5A and C). RelA is unique because it is the only identified (p)ppGpp hydrolase in *L. monocytogenes*. The hydrolase function of RelA was revealed by increased (p)ppGpp levels in a $\Delta relA$ mutant as compared to wild-type (Figure 2.5A and C). The difference between the levels of (p)ppGpp in the untreated $\Delta relA$ and *relA*^{R295S} strains was therefore due to the functional hydrolase component of the RelA^{R295S} protein which can degrade (p)ppGpp synthesized by RelP and RelQ. These data demonstrated that the suppressor mutation in RelA encoded a hydrolase-only form of the protein.

Accumulation of (p)ppGpp is toxic to $\Delta dacA$ mutants

In Firmicutes, (p)ppGpp inhibits DNA primase and enzymes that catalyze GTP synthesis (Kriel et al., 2012; Wang et al., 2007). The net effect of increased (p)ppGpp is both a transcriptional and translational response that results in a decreased growth rate (Dalebroux and Swanson, 2012). We hypothesized that the *relA*^{R295S} mutation suppressed *dacA* essentiality by decreasing (p)ppGpp that may have accumulated as a consequence of deletion of *dacA*. We tested the first part of this hypothesis by measuring (p)ppGpp under non-starvation conditions in a *dacA* conditional depletion strain ($c\Delta dacA$) which expressed *dacA* under the control of an IPTG inducible promoter (Witte et al., 2013). In comparison to wild-type, conditional depletion of *dacA* led to an increase in (p)ppGpp levels in non-starvation conditions (Figure 2.6A and B).

To further evaluate the role of increased (p)ppGpp in *dacA* essentiality we constructed a *L. monocytogenes* strain lacking (p)ppGpp by sequentially deleting the *relP*, *relQ*, and *relA* genes ($\Delta relAPQ$), and subjected this strain to the *dacA* essentiality assay in BHI (Figure 2A). The *dacA* gene was no longer essential in the $\Delta relAPQ$ background (Figure 2.6C). Complementation of $\Delta relAPQ$ with any of the three (p)ppGpp synthases using their native promoters restored the essentiality of the *dacA* gene (Figure 2.6C). These data indicated that *dacA* was essential due to accumulation of the nucleotide (p)ppGpp rather than an interaction with any single (p)ppGpp synthase. Additionally, *relA* was sufficient to render *dacA* essential, which suggested that although RelA is a bifunctional synthase/hydrolase, in the absence of c-di-AMP RelA functioned as a synthase.

The *dacA* gene was not essential in a $\Delta relAPQ$ background, although the $\Delta dacA\Delta relAPQ$ mutant grew slowly compared to wild-type (Figure 2.6D). These data established a role for (p)ppGpp in *dacA* essentiality. Additionally, we hypothesized that the accumulation of (p)ppGpp observed after depletion of *dacA* (Figure 4A and 4B) might be partially responsible for the growth defect of the $c\Delta dacA$ strain (Witte et al., 2013). This hypothesis was tested by measuring growth rate of a conditional *dacA*

depletion strain constructed in a wild-type or $\Delta relAPQ$ background ($c\Delta dacA\Delta relAPQ$) in BHI. In the presence of IPTG the conditional *dacA* depletion strains $c\Delta dacA\Delta relAPQ$ and $c\Delta dacA$ grew similarly to wild-type. In the absence of IPTG (when *dacA* is depleted) the $c\Delta dacA\Delta relAPQ$ strain displayed an increased growth rate compared to the $c\Delta dacA$ strain (Figure 2.6E). These data are consistent with a role for c-di-AMP in maintaining low (p)ppGpp levels that are otherwise detrimental for growth.

A screen for mutations that rescue the virulence defect of a $\Delta relAPQ$ mutant reveals a critical role for CodY

We next sought to understand the function(s) of (p)ppGpp in *L. monocytogenes*. *relA* mutants are attenuated for pathogenesis (Bennett et al., 2007), although the role of (p)ppGpp in infection is still unclear since our data indicated that *relA* mutants have elevated levels of (p)ppGpp (Figure 2.5A and C). The $\Delta relAPQ$ mutant grew similarly to wild-type in rich medium, despite lacking all sources of (p)ppGpp (Figure 2.6D), however, it was severely attenuated in a plaque assay, an *in vitro* infection model that serves as a surrogate for virulence (Figure 5A). In this assay, confluent mammalian fibroblasts are infected with *L. monocytogenes* and intracellular growth and cell-to-cell spread of the bacteria produce a zone of clearance (plaque) that is quantifiable and high-throughput (Sun et al., 1990). Small plaques often correlate to virulence defects *in vivo* and the $\Delta relAPQ$ strain produced small plaques that were 32% the area of wild-type plaques (Figure 2.7A).

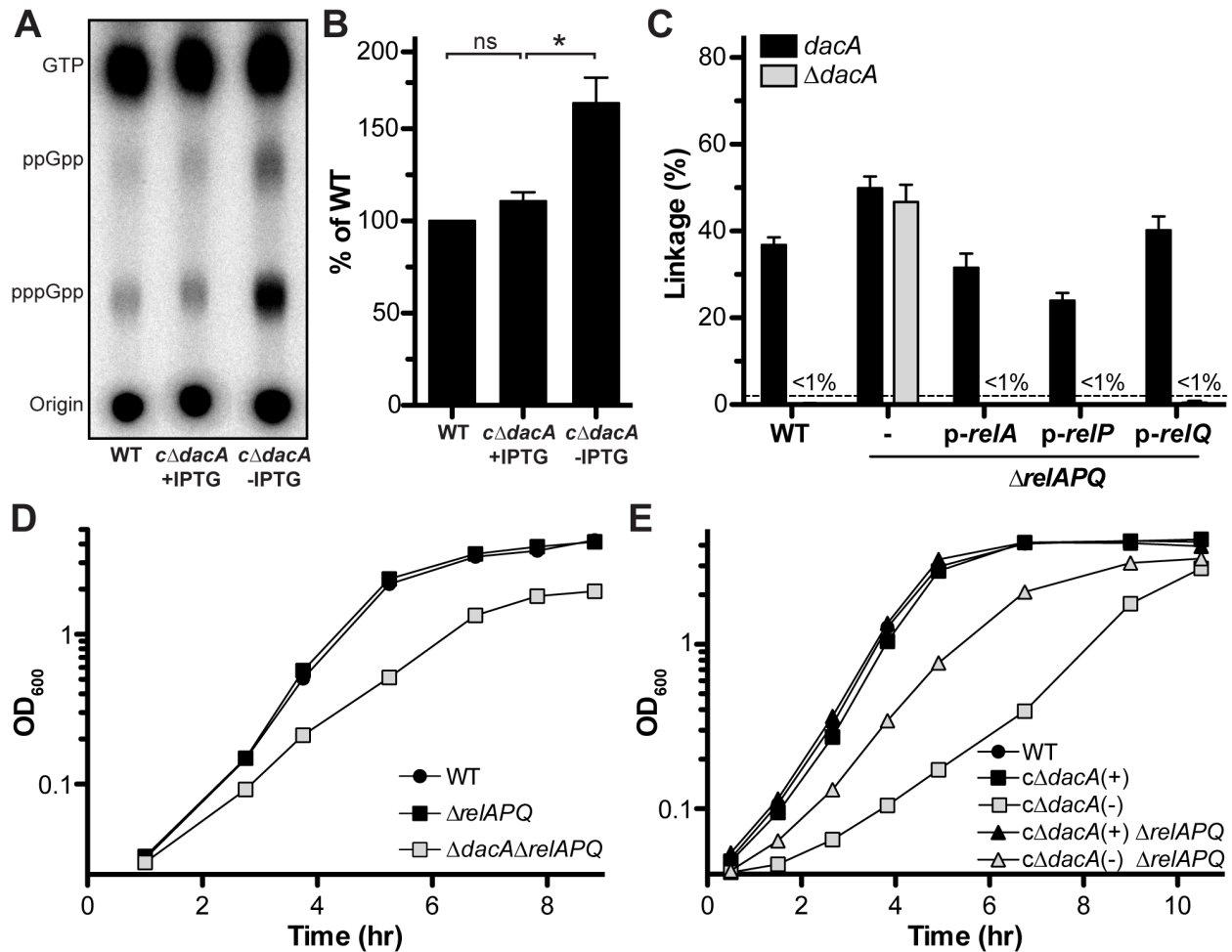


Figure 2.6 (p)ppGpp accumulates during depletion of c-di-AMP leading to *dacA* essentiality and decreased growth rate.

(A and B) TLC analysis of ^{32}P -labeled intracellular nucleotides from bacteria grown in low-phosphate defined medium plus tryptone without starvation. Chromosomal *dacA* was deleted in a strain harboring an IPTG-inducible *dacA* gene to construct a conditional *dacA* depletion strain (*cΔdacA*) (Witte et al., 2013). A representative TLC is shown (A), and quantification of the ratio $(\text{pppGpp} + \text{ppGpp}) / (\text{pppGpp} + \text{ppGpp} + \text{GTP})$ is shown as a percent of WT (B). Data are representative of $n=11$ independent experiments, graphed data are mean \pm s.e.m. of pooled data, $*p \leq 0.05$ by two-tailed Student's *t*-test, and ns denotes not significant. (C) *dacA* essentiality assay. Complemented genes indicated by (p-) were introduced at a neutral site using their native promoter. Dotted line indicates L.o.D., data are mean \pm s.e.m. of at least three independent experiments. (D and E) BHI broth growth curves, with or without (+/-) IPTG in panel E. Data are representative of three independent experiments.

These results suggested that (p)ppGpp was necessary for a productive infection. We speculated that the contribution of (p)ppGpp to virulence and toxicity to Δ *dacA* mutants were related and performed a transposon mutagenesis screen for mutations that rescued the small plaque phenotype of the Δ *relAPQ* mutant. We identified 98 mutants from over 10,000-screened that displayed increased plaque size. DNA sequencing of the region adjacent to the transposon insertions and phage transduction led to the identification of 14 genes, that when disrupted, significantly increased the Δ *relAPQ* plaque size (Figure 2.7A and Table 2.2).

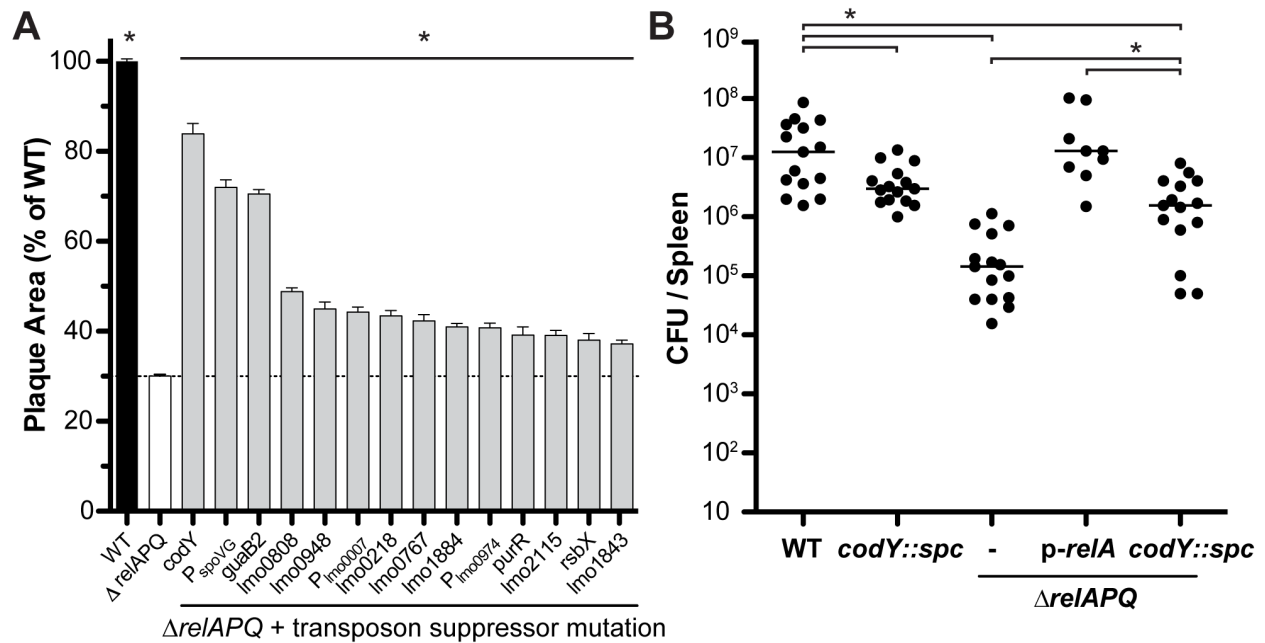


Figure 2.7 A screen for suppressor mutations of the $\Delta relAPQ$ virulence defect reveals a critical role for inactivation of CodY.

(A) A murine fibroblast (L2 cell) monolayer was infected with *L. monocytogenes* mutants from Table 2.2, producing plaques. The reduced plaque area correlates with reduction in virulence. Data are mean \pm s.e.m of pooled data from least three independent experiments, P preceding a gene name indicates the transposon is in the promoter, $*p \leq 0.05$ by one-way ANOVA compared with $\Delta relAPQ$. (B) Recovered CFU at 48 hours post-infection from CD-1 mice intravenously infected via tail-vein with 10^5 CFU of each indicated strain. Data are pooled results from at least two independent experiments, bars indicate median value, *p-relA* represents *relA* complemented under its native promoter, $*p \leq 0.05$ using two-tailed Student's *t*-test.

Transposon insertions in *codY* produced the most significant increase in the $\Delta relAPQ$ plaque size (Figure 2.7A and Table 2.2). CodY is activated by high GTP levels and branch chain amino acids to promote DNA binding that transcriptionally represses a large regulon of genes, but also is capable of transcriptional activation of a few genes (Geiger and Wolz, 2013). In *B. subtilis*, (p)ppGpp inhibits GTP synthesis at multiple enzymatic steps and the subsequent decrease in GTP leads to CodY deactivation (Kriel et al., 2012). The $\Delta relAPQ$ mutant is incapable of modulating GTP levels via (p)ppGpp, and thus CodY remains constitutively activated. In *L. monocytogenes*, *codY* mutations likely rescue the plaque defect of the $\Delta relAPQ$ mutant by phenocopying (p)ppGpp-dependent inhibition of GTP synthesis that takes place in wild-type bacteria, and demonstrates a critical role for CodY deactivation during infection. Other identified suppressor mutations (such as *guaB2*, *Imo1884*, and *purR*) in purine nucleotide synthesis/acquisition might have affected CodY activity by modulating intracellular GTP levels. We confirmed that these mutations were epistatic to mutations in *codY* by constructing a marked deletion in *codY* (*codY::spc*) and transducing the isolated transposons into the $\Delta relAPQ$ *codY::spc* background (Table 2.2). Only mutations in the promoter of *spoVG* and *Imo0948* further increased the $\Delta relAPQ$ *codY::spc* plaque size. However, *Imo0948::himar1* also increased the plaque area of wild-type and thus was likely not specific to (p)ppGpp (Table 2.2). Although *spoVG* is regulated by (p)ppGpp in *B. subtilis* (Tagami et al., 2012) and has been identified with divergent phenotypes in

multiple organisms (Jutras et al., 2013; Matsuno and Sonenshein, 1999; Meier et al., 2007), it is unclear how this mutation contributed to the virulence of the $\Delta reIAPQ$ mutant.

Gene Name ^a	Annotation ^b	himar1 Location ^c	Plaque Area (%WT \pm s.e.m.)		
			$\Delta reIAPQ$ ^d	$\Delta reIAPQ$ <i>codY::spc</i> ^d	wild-type ^d
<i>codY</i> (<i>Imo1280</i>)	GTP-responsive transcriptional regulator	LMRG_00730:: 119	84 \pm 2.3	N/A	89 \pm 1.2
<i>P_{spoVG}</i> (<i>P_{Imo0196}</i>)	Promoter of genes similar to <i>spoVG</i>	LMRG_02618:: -144	72 \pm 1.6	89 \pm 1.6	105 \pm 1.6
<i>guaB2</i> (<i>Imo2758</i>)	Inosine-5'-monophosphate (IMP) dehydrogenase	LMRG_01938:: 220	71 \pm 1.0	77 \pm 1.0	93 \pm 1.4
<i>Imo0808</i>	Spermidine/putrescine ABC transporter	LMRG_02789:: 1593	49 \pm 0.9	83 \pm 2.3	108 \pm 1.6
<i>Imo0948</i>	GntR family transcriptional regulator	LMRG_02047:: 494	45 \pm 1.5	84 \pm 1.2	111 \pm 2.4
<i>Imo0006/7</i>	Between DNA Gyrase subunits B/A	LMRG_02435:: -26	44 \pm 1.2	70 \pm 1.1	99 \pm 1.3
<i>Imo0218</i>	S1 RNA binding domain protein similar to <i>yabR</i>	LMRG_02640:: 121	43 \pm 1.2	72 \pm 2.6	102 \pm 2.7
<i>Imo0767</i>	Sugar ABC transporter permease	LMRG_00455:: 222	42 \pm 1.4	80 \pm 0.9	100 \pm 1.3
<i>Imo1884</i>	Xanthine uptake transporter similar to <i>pbuX</i>	LMRG_01031:: 319	41 \pm 0.7	77 \pm 1.5	107 \pm 2.9
<i>P_{Imo0974}</i>	Promoter of D-alanine-poly(phosphoribitol) ligase (<i>dlt</i>) operon	LMRG_02073:: -223	41 \pm 1.1	77 \pm 1.6	100 \pm 1.9
<i>purR</i> (<i>Imo0192</i>)	Purine associated transcriptional repressor	LMRG_02614:: 471	39 \pm 1.8	70 \pm 1.5	93 \pm 1.6
<i>anrB</i> (<i>Imo2115</i>)	FtsX family ABC transporter permease associated with nisin resistance	LMRG_01269:: 1842	39 \pm 1.1	80 \pm 1.9	104 \pm 2.4
<i>rsbX</i> (<i>Imo0896</i>)	Negative regulator of sigma-B (serine phosphatase)	LMRG_02320:: 2103	38 \pm 1.5	59 \pm 0.9	72 \pm 1.2
<i>Imo1843</i>	RluA family 23S pseudouridylate synthase	LMRG_00990:: 876	37 \pm 0.9	80 \pm 1.1	96 \pm 2.0

Table 2.2 Transposon mutations that suppress the $\Delta reIAPQ$ plaque defect.

^a Annotated using EGD-e ordered loci and previously published name where appropriate. P indicates the transposon location is within a predicted promoter of the annotated gene.

^b Gene similarity based on *Bacillus subtilis* genome annotation

^c Sequence-mapped transposon insertion site (10403S ordered genetic locus::nucleotides 3' of ORF start codon)

^d Genetic background of the transposon mutant, data represent the mean \pm s.e.m. for at least 3 independent experiments, bold-face numbers indicate plaque area was significantly different from background strain ($p \leq 0.05$ by one-way ANOVA, Tukey test)

In a mouse model of infection, the $\Delta reIAPQ$ mutant was approximately 100-fold less virulent compared to wild-type or the $\Delta reIAPQ$ strain complemented with *reIA* under its native promoter (Figure 2.7B). The *codY::spc* mutation suppressed the virulence defect of the $\Delta reIAPQ$ strain to the level of a *codY::spc* mutation alone, approximately 10-fold less virulent than wild-type (Figure 2.7B). The virulence defect of the *codY::spc* mutant is consistent with previous reports demonstrating a virulence defect for a *codY* mutant (Lobel et al., 2015; 2012), and mutations in *codY* suppress the virulence defect of other pathogenic Firmicutes with decreased (p)ppGpp (Geiger and Wolz, 2013). Our data suggested that the principle role of (p)ppGpp during infection was the inhibition of GTP synthesis leading to inactivation of CodY.

(p)ppGpp-dependent inactivation of CodY is necessary for the essentiality of dacA

We speculated that the function of (p)ppGpp during infection overlaps with the role of (p)ppGpp in *dacA* essentiality. Accordingly, *dacA* may not be essential in the $\Delta reIAPQ$ mutant because in the absence of (p)ppGpp, GTP remains elevated, and CodY is highly active. We examined the role of CodY in the essentiality of *dacA* by comparing the $\Delta reIAPQ$ and $\Delta reIAPQ\ codY::spc$ mutants in the genetic assay for *dacA* essentiality (Figure 2.3A). While *dacA* was not essential in the $\Delta reIAPQ$ mutant, addition of a *codY* mutation returned *dacA* to its original essential phenotype (Figure 2.8A). Addition of the *spoVG* mutation to the $\Delta reIAPQ$ mutant strain did not alter *dacA* essentiality (Figure 2.8A). These results suggested that among the diverse functions of (p)ppGpp, inactivation of GTP synthesis and thus inactivation of CodY was selectively toxic to $\Delta dacA$ mutants. Further, these findings imply that elements of the CodY regulon, which are necessary for infection, may be toxic in the absence of c-di-AMP.

dacA is not essential on minimal medium

We hypothesized that *dacA* might no longer be essential in growth conditions that favored inactivation of CodY. The best example of such a condition is in minimal medium, where a *B. subtilis* strain unable to produce (p)ppGpp cannot grow without a *codY* mutation (Kriel et al., 2012; 2014). Similarly in *L. monocytogenes*, the $\Delta reIAPQ$ mutant does not grow on minimal medium (data not shown), prompting us to examine these growth conditions. Unlike rich medium, *dacA* was no longer essential in a defined minimal medium (Figure 2.8B)(Phan-Thanh and Gormon, 1997). Remarkably, in-frame $\Delta dacA$ deletions were readily obtainable by allelic exchange when bacteria were cultivated in minimal medium. Genome sequencing of $\Delta dacA$ mutants constructed on minimal medium using a marked *dacA* deletion confirmed the absence of suppressor mutations. These data suggested a model in which c-di-AMP is essential for growth in rich medium because in the absence of c-di-AMP (p)ppGpp accumulated and indirectly inactivated CodY, which facilitated transcriptional changes selectively toxic to $\Delta dacA$ mutants. This work identified that mutations which decreased (p)ppGpp or replacement with a medium favoring CodY inactivation were sufficient to reverse the essentiality of *dacA*.

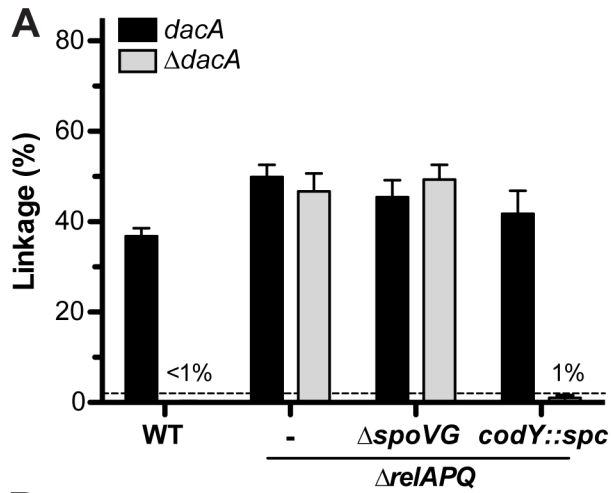
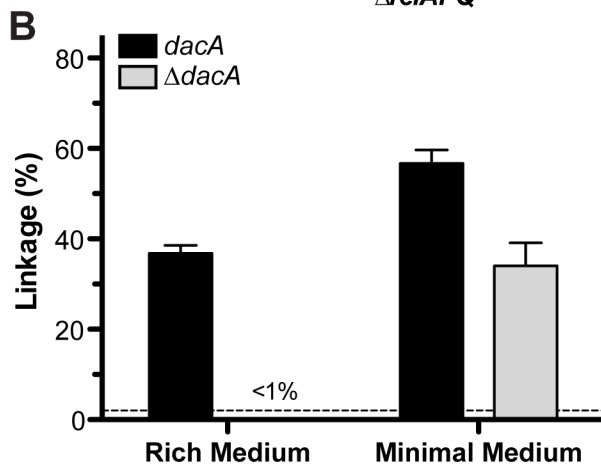


Figure 2.8 *dacA* is essential in rich medium due to CodY inactivation but *dacA* is not essential in minimal medium.

(A and B) *dacA* essentiality assay. (B) The commonly used rich medium is BHI and minimal medium for *L. monocytogenes* is detailed in the supplemental experimental procedures. Dotted line indicates L.o.D., data are mean \pm s.e.m of at least three independent experiments.



Discussion

There is an emerging consensus that c-di-AMP is an essential molecule in Firmicutes (Corrigan and Gründling, 2013). However, here we report the isolation of *L. monocytogenes* *dacA* deletion mutants that lack c-di-AMP. As conventional approaches of isolating mutations were unsuccessful, a strain was constructed in which *loxP* sites were introduced into the *L. monocytogenes* chromosome flanking the *dacA* gene, and Cre recombinase was expressed from the PrfA-regulated *actA* promoter that is induced in host cells (Reniere et al., 2015). Upon infection of macrophages, Cre was expressed leading to deletion of *dacA*, thereby providing an unbiased selection for *L. monocytogenes* mutants able to grow in the absence of the c-di-AMP. All Δ *dacA* mutants isolated from the infected cells contained one or more suppressor mutations that promoted bacterial growth in rich medium. Mutations in the synthase domain of the bi-functional RelA/SpoT homolog *relA* that retained (p)ppGpp hydrolase activity, or deletion of all three *L. monocytogenes* (p)ppGpp synthase genes (Δ *relAPQ*) suppressed *dacA* essentiality. Although the growth defect of the Δ *dacA* Δ *relAPQ* strain implies additional roles for c-di-AMP in bacterial physiology, these data suggested that Δ *dacA* mutants failed to grow in rich medium and in cells because (p)ppGpp levels were elevated, a condition known to inhibit bacterial growth (Dalebroux and Swanson, 2012).

We reasoned that there might be an overlap between the (p)ppGpp-regulated genes required for pathogenesis and those that suppressed *dacA* essentiality. Therefore, we screened for transposon mutations that suppressed the plaque defect of a strain lacking (p)ppGpp (Δ *relAPQ*), which was nearly 100-fold less virulent in mice. Fourteen loci were identified and transposon mutations disrupting *codY* produced the largest plaque. Mutations in *codY* restored the virulence of *L. monocytogenes* strains lacking (p)ppGpp to that of the *codY* mutant alone. CodY is a GTP-responsive transcriptional regulator whose function is inextricably linked with (p)ppGpp levels (Geiger and Wolz, 2013). During exponential growth in rich medium, CodY is GTP-bound and represses dozens of biosynthetic operons (Sonenshein, 2007). CodY also enhances transcription of genes involved in GTP synthesis, most notably *guaB*, causing a feed-forward regulatory loop that maintains CodY activation (Bennett et al., 2007). During starvation, (p)ppGpp interrupts this feed-forward loop through allosteric inhibition of GTP-synthesis enzymes, thereby allowing for the expression of many biosynthetic operons (Kriel et al., 2012). Other mutations that suppressed virulence defects of the Δ *relAPQ* mutant, such as *guaB2*, *Imo1884*, and *purR*, were epistatic to *codY* because they likely recapitulate the role of (p)ppGpp, decreasing GTP abundance and therefore the activity of CodY. Most importantly however, the *codY* mutation restored the essentiality of *dacA* in a Δ *relAPQ* mutant. Therefore, c-di-AMP essentiality is likely caused by one or more CodY-regulated genes that are inappropriately expressed in rich medium due to elevated levels of (p)ppGpp. If this were correct, one would predict that *dacA* might not be essential in conditions favoring expression of CodY-regulated genes, such as minimal medium where CodY repressed genes are essential for growth (Kriel et al., 2014). Indeed, we were able to construct suppressorless Δ *dacA* mutants in minimal medium using conventional methods of allelic exchange.

It is not clear why c-di-AMP is essential in rich but not minimal media. However, c-di-AMP is an allosteric inhibitor of *L. monocytogenes* pyruvate carboxylase (PycA), an enzyme that catalyzes the conversion of pyruvate to oxaloacetate, entry of carbon into the TCA cycle, and is essential for growth in minimal medium (Schär et al., 2010; Sureka et al., 2014). Depletion of c-di-AMP leads to over-activity of PycA and thus increased levels of TCA cycle intermediates, such as glutamate/glutamine, primarily because *L. monocytogenes* has an incomplete TCA cycle and lacks α -ketoglutarate dehydrogenase. Consequently, mutations in citrate synthase (*citZ*), the first step of the TCA cycle, relieve the buildup of glutamate/glutamine and suppress the virulence defect of a conditional *dacA* depletion strain (Sureka et al., 2014). Interestingly, among our Δ *dacA* suppressor mutants that contained multiple mutations, we identified missense and promoter mutations in *pycA* and a premature stop codon in *citZ*, suggesting that mutations which lower potentially toxic concentrations of glutamate/glutamine counter *dacA* essentiality. Although it is not clear how increased glutamate/glutamine levels might result in toxicity, it may be noteworthy that in *E. coli*, glutamate functions as the principle counter-ion to K⁺ (McLaggan et al., 1990; 1994), which is an indispensable cation for balancing osmotic stress in bacteria (Epstein, 2003). In *S. aureus*, three of the four identified c-di-AMP-binding proteins modulate intracellular potassium levels (Corrigan et al., 2013), and in a diverse set of organisms the c-di-AMP binding *ydaO-yuaA* riboswitch regulates potassium transporters and osmoprotection genes (Nelson et al., 2013). We hypothesize that bacteria lacking c-di-AMP accumulate both K⁺ and glutamate and are unable to regulate a subsequent lethal change in internal osmotic pressure. In support of this, we identified mutations in the glycine betaine/proline osmoprotection transporter in some of our Δ *dacA* suppressors mutants that contained multiple mutations, although we were unable to rescue Δ *dacA* essentiality by adding osmoprotectants or altering salt concentrations (data not shown). In minimal medium *dacA* may not be essential because glutamate is required for synthesis of many additional metabolites made under nutrient stress (Sonenshein, 2007). In addition, CodY over-activation (in the absence of (p)ppGpp) could remedy *dacA* essentiality by repressing glutamate synthase or altering *L. monocytogenes* metabolism to provide decreased PycA precursors (Brinsmade et al., 2014; Sonenshein, 2007).

The results of this study suggest that there is a signaling loop between (p)ppGpp and c-di-AMP, which is not surprising since c-di-AMP-specific phosphodiesterases are inhibited by (p)ppGpp (Corrigan et al., 2015; Huynh et al., 2015; Rao et al., 2010). What is surprising is that deletion of c-di-AMP phosphodiesterases *pgpH* and *gdpP* in *L. monocytogenes* and *S. aureus* respectively led to increased (p)ppGpp during stress despite containing elevated levels of c-di-AMP (Corrigan et al., 2015; Liu et al., 2006), the opposite of the phenotype predicted by work presented here. We hypothesize that both high and low c-di-AMP can contribute to increased (p)ppGpp by altering central metabolism and amino acid biosynthesis, specifically the levels of the branch-chain amino acids (BCAAs) valine, leucine, and isoleucine. (p)ppGpp production is stimulated by low BCAA levels which are uniquely poised as sensors of nutrient stress because they require precursors from carbon, nitrogen, and sulfur metabolism for their synthesis (Somerville and Proctor, 2009). Valine and leucine are derived from pyruvate whereas

isoleucine is derived from oxaloacetate (Sonenshein, 2007). In *L. monocytogenes*, c-di-AMP may affect the abundance of these precursors by regulating PycA activity (Schär et al., 2010; Sureka et al., 2014). When over-active (low c-di-AMP), PycA activity leads to pyruvate depletion and potentially low levels of valine and leucine. When under-active (high c-di-AMP), the bacterium is depleted of oxaloacetate. This hypothesis is consistent with the demonstrated toxicity of excess c-di-AMP (Huynh et al., 2015; Mehne et al., 2013) and places c-di-AMP as a key regulator of metabolic homeostasis.

Both c-di-AMP and (p)ppGpp contribute to bacterial stress responses; for example, in related Firmicutes, mutations in *relP* and *relQ* increase antibiotic sensitivity while mutations in c-di-AMP-dependent phosphodiesterases lead to increased antibiotic resistance (Abranches et al., 2009; Corrigan and Gründling, 2013; Geiger et al., 2014). Importantly, there are fundamental differences between (p)ppGpp and c-di-AMP: whereas the former is only made during acute stress, the latter appears to be present during all growth conditions (Corrigan and Gründling, 2013). Even in minimal medium, where c-di-AMP is not essential, $\Delta dacA$ mutants grew slowly compared to wild-type (data not shown). Another fundamental difference is that c-di-AMP is secreted by *L. monocytogenes* during growth in media and in cells, perhaps altering intracellular nucleotide concentrations or regulating extracellular processes (Woodward et al., 2010). There is also evidence that *Chlamydia trachomatis* and *Mycobacterium tuberculosis* are capable of secreting c-di-AMP during infection (Barker et al., 2013; Yang et al., 2014). Collectively, these properties make c-di-AMP an ideal pathogen-associated molecular pattern (PAMP); i.e., it is highly expressed, conserved, essential for virulence, and secreted, thereby triggering STING a central hub of host innate immunity (Danilchanka and Mekalanos, 2013; Vance et al., 2009).

Experimental Procedures

Generation of $\Delta dacA$ suppressor mutants by Cre-lox

The *dacA^{fl} P_{actA}-cre* strain was grown at 30°C overnight without agitation and bone marrow-derived macrophages (BMDMs) were infected as previously described using gentamicin to kill extracellular bacteria (Witte et al., 2013). After infection, bacteria were grown intracellularly for four hours to allow for adequate cytosolic access and *actA* induction. Infected BMDMs were then washed three times with sterile PBS, lysed with 0.1% NP-40, and plated on media-agar at 37°C, curing the *cre*-containing plasmid. $\Delta dacA$ mutants were verified by PCR using primers internal to *dacA* and primers external to the *dacA* locus. In some cases, BMDM lysates were initially plated at 30°C on selective BHI-agar to enrich for bacteria that retained the *P_{actA}-cre* plasmid, prior to plasmid-curing at 37°C. For generating 284 additional $\Delta dacA$ suppressor mutants: 24 independent infections with *dacA^{fl} P_{actA}-cre* were used, *dacA* deletion was confirmed by PCR, bacteria were grown in minimal medium with bialaphos to analyze Opp activity, the synthase domain of *relA* was sequenced with primers *relA*-syn-F/R, and Opp activity was reanalyzed by disk diffusion.

dacA essentiality assay

The *dacA* essentiality assay was performed by adapting previously described methods (Las Peñas et al., 1997). Three transducing lysates were constructed from *dacA^{fl}-kanR Imo2103/2104::himar1* (*dacA* lysate) and three transducing lysates were constructed from $\Delta dacA$ -*kanR Imo2103/2104::himar1* ($\Delta dacA$ lysate) produced by Cre-lox deletion of *dacA*. *dacA* essentiality in a recipient strain was analyzed by transducing with each of the six lysates and selecting for erythromycin-resistant (*erm^R*) transductants on the indicated media. At 48 hours, 50 transductants were patched from each transduction onto appropriate media-agar containing either erythromycin or kanamycin. The proportion of kanamycin resistant colonies is a measure of genetic linkage and one out of 50 colonies defined the limit of detection at 2%. As a control, the essentiality assay was also performed with a *Imo2110::himar1* transposon insertion instead of *Imo2103/2104::himar1*. The mean genetic linkage from the three transducing lysates per genotype constituted one experiment, data represent the mean \pm s.e.m. for at least three independent experiments. For wild-type merodiploid for *dacA*, an IPTG inducible *dacA* was introduced into wild-type and the experiment was performed in the presence of IPTG.

Virulence Analysis

In vivo virulence analysis was performed as previously described (Reniere et al., 2015) with the following changes: female, 8-12 week old CD-1 mice (Charles River) were injected via tail-vein with 200 μ L of PBS containing 10⁵ CFU of *L. monocytogenes*. Mice were euthanized 48 hours post infection, liver and spleen removed, organs homogenized in filter-sterilized 0.1% NP40, and the CFU of the liver and spleen enumerated by plating serial dilutions on LB-Agar containing streptomycin. Statistical significance was determined by a two-tailed heteroscedastic Student's *t*-test. This study was carried out in strict accordance with the recommendations in the Guide for the Care and Use of Laboratory Animals of the National Institutes of Health. All protocols were

reviewed and approved by the Animal Care and Use Committee at the University of California, Berkeley (MAUP# R235-0813B).

Bacterial strains and culture conditions

All *Listeria monocytogenes* strains were derivatives of 10403S (Bécavin et al., 2014; Bishop and Hinrichs, 1987) cultured in Difco brain-heart infusion (BHI, BD Biosciences) at 37°C, with shaking, and without antibiotics unless otherwise stated. Growth was measured by the optical density at a wavelength of 600 nm (OD₆₀₀) using a spectrophotometer. Frozen bacterial stocks were stored at -80°C in BHI + 40% glycerol. All chemicals were purchased from Sigma-Aldrich unless otherwise stated. Antibiotics were used at the following concentrations unless otherwise stated: streptomycin (200 µg/mL), carbenicillin (100 µg/mL), kanamycin (15 µg/mL in BHI, 50 µg/mL in minimal medium), chloramphenicol (7.5 µg/mL for *L. monocytogenes*, 10 µg/mL for *E. coli*), erythromycin (1 µg/mL), spectinomycin (100 µg/mL), tetracycline (2 µg/mL), and bialaphos (10 µg/mL, Gold Biotechnology, St. Louis, MO). Isopropyl β-D-1-thiogalactopyranoside (IPTG) was used at 1 mM. Overnight cultures of *cΔdacA* strains were grown in the same medium they would be diluted into for the subsequent experiment such that conditions lacking IPTG were inoculated from overnight cultures lacking IPTG, as previously described (Witte et al., 2013). Previously described chemically defined minimal medium (Phan-Thanh and Gormon, 1997) was used with double the iron (III) citrate, which improved growth of wild-type *L. monocytogenes*. The final concentrations of ingredients are as follows: glucose, 55.5 mM (1%); KH₂PO₄, 48.2 mM; Na₂HPO₄ · 7H₂O, 115.5 mM; MgSO₄ · 7H₂O, 1.7 mM; biotin, 2.05 µM; riboflavin, 1.33 µM; p-aminobenzoic acid, 7.29 µM; lipoic acid, 0.02 µM; L-arginine · HCl, L-histidine · HCl · 2H₂O, DL-isoleucine, L-leucine, DL-methionine, L-phenylalanine, L-tryptophan, and DL-valine were all used at 0.1 g/L; nicotinamide, 8.19 µM; D-pantothenic acid hemicalcium, 4.2 µM; pyrodoxal · HCl 4.91 µM; thiamine · HCl, 2.96 µM; adenine, 18.5 µM; iron (III) citrate, 0.72 mM; L-cysteine · 2HCl, 634 µM; L-glutamine, 4.1 mM. Minimal medium agar plates were prepared by combining autoclaved 2x agarose (10 g/L final conc., U.S. Biotech Sources) with 2x filter-sterilized minimal medium.

DNA manipulations and strain construction

All enzymes and kits for vector construction were purchased from New England BioLabs Inc. and were used according to the manufacturers instructions. DNA inserts for vectors were amplified from *L. monocytogenes* genomic DNA, restriction digested with indicated enzymes (see Table 2.5), ligated with Quick Ligation Kit, and transformed into chemically competent XL1-Blue *E. coli*. Vectors were introduced into *L. monocytogenes* via conjugation with transformed SM10 *E. coli* (Shanker and Atkins, 1996). Allelic exchange was performed as previously described (Camilli et al., 1993) using a conjugation-proficient version of *pKSV7* (*pKSV7-oriT*) (Kline et al., 2015; Sauer et al., 2010). DNA inserts were constructed and inserted into this vector. Briefly, for in-frame deletions, 1-0.75 kb 5' of the target gene was amplified (primers A & B) and joined to an equivalently sized DNA fragment 3' of the target gene (primer C & D) by sequence overlap exchange (SOE) PCR, leaving an ORF encoding only the first and last six amino acids of the target gene. For marked deletions, an antibiotic resistance

gene was inserted in-frame in place of the target gene, introduced into the chromosome by allelic exchange, and introduced into new recipients by phage-transduction. For addition of *loxP* sites by allelic exchange, three DNA fragments were inserted into pKSV7 sequentially, two of which were amplified with primers that added *loxP* sites. For complementation, pPL2 and derivatives therein (including pPL2t, a version of pPL2 that is tetracycline resistant in *L. monocytogenes*) were used as previously described (Lauer et al., 2002). In some cases, transcriptional terminators (term) were added to complementation constructs. Target genes were amplified with their native promoter, which was sometimes added by SOE PCR. The kanamycin resistance gene was amplified from pMK (Monk et al., 2008) and spectinomycin resistance gene was amplified from pTEX5235 (Teng et al., 1998). Strains constructed with spectinomycin resistance were verified by PCR due to appearance of spontaneous resistance. For construction of *dacA^{fl} P_{actA}-cre*: The *loxP* sites flanking the *dacA* gene were inserted into the chromosome of 10403S via allelic exchange to generate the *dacA^{fl}* strain. The mutant *lox66* and *lox71* (derivatives of *loxP*) were used to ensure unidirectional DNA-recombination (Oberdoerffer et al., 2003; Sternberg and Hamilton, 1981). A codon-optimized *cre* (Reniere et al., 2015) was constructed under the *actA* promoter, expressed from the temperature-sensitive vector pKSV7-oriT, and introduced to *dacA^{fl}* via conjugation.

Ordered Loci for genes are as follows: [gene name (EGDe ordered locus using GenBank: GCA_000196035.1, 10403S ordered locus using GenBank: GCA_000168695.2)] *dacA* (*Imo2120*, *LMRG_01274*), *oppB* (*Imo2195*, *LMRG_01637*), *relA* (*Imo1523*, *LMRG_01547*), *relP* (*Imo0802*, *LMRG_02795*), *relQ* (*Imo0967*, *LMRG_02066*), *codY* (*Imo1280*, *LMRG_00730*), *guaB2* (the second of two possible IMP dehydrogenases, *Imo2758*, *LMRG_01938*), and *spoVG* (two paralogs which were both deleted, *Imo0196-Imo0197*, *LMRG_02618-LMRG_02619*).

Genome Sequencing

Genome sequencing was performed as previously described (Burke et al., 2014). Briefly, strains were grown overnight in 5 mL of medium and genomic DNA was extracted using the MasterPure Gram Positive DNA Purification Kit (Epicentre, Madison, WI) according to the manufacturers instructions. DNA was then submitted for library preparation and genome sequencing in three independent batches. *dacA^{fl}* and Δ *dacA*.1- Δ *dacA*.5 were prepared and sequenced at the Tufts University Core Facility for Genomics using paired end 50 Illumina sequencing. Δ *dacA*.6- Δ *dacA*.16 and Δ *dacA-kanR*.MM1-2 were prepared and sequenced at the UC Berkeley QB3 Genomics Sequencing Laboratory using single read 50 Illumina sequencing. Data was assembled and aligned to the 10403S reference genome (GenBank: GCA_000168695.2) demonstrating >50x coverage. SNP/InDel/structural variation from the *dacA^{fl}* strain was determined (CLC Genomics Workbench, CLC bio).

Disk diffusions

Antibiotic susceptibility was determined as previously described (Rae et al., 2011; Reniere et al., 2015). Briefly, 10⁷ bacteria were immobilized in 4 mL of top-agar (0.8% agar and 0.8% NaCl) and evenly distributed on 15 mL minimal medium-agar plate. 8

mm sterile filter-paper disks were soaked in the appropriate drug, placed in the center of the agar plate, and incubated overnight at 37°C. Bialaphos susceptibility was measured using disks soaked with 100 µg of drug in sterile water. Statistical significance was determined by a two-tailed heteroscedastic Student's *t*-test.

Phage transduction

Generalized transduction was performed as previously described (Zemansky et al., 2009) using the U153 phage (Hodgson, 2000). Briefly, phage were propagated in *L. monocytogenes* SLCC-5764 at 30°C. To generate a transducing lysate approximately 10⁹ colony forming units (CFU) of donor strain was combined with ≈10⁷ plaque forming units (PFU) of U153 and immobilized in 0.7% LB-agar with 10mM MgSO₄ and 10mM CaCl₂ overnight at 30°C. Recovered phage could be used for generalized transduction by lysogenizing 10⁸ CFU of recipient *L. monocytogenes* with ≈10⁷ PFU of transducing lysate in LB broth with 10mM MgSO₄ and 10mM CaCl₂, incubating for 30 minutes at 30°C, and selecting for the appropriate antibiotic resistance gene on selective BHI-agar at 37°C.

(p)ppGpp quantification

(p)ppGpp was measured as previously described with only minor changes (Taylor et al., 2002). Briefly, bacteria were grown in low-phosphate defined medium plus tryptone (LPDMT): minimal medium (Phan-Thanh and Gormon, 1997) modified with 100 mM morpholinepropanesulfonic acid (MOPS) buffer and 1000-fold decreased phosphate plus 0.4% w/v Bacto-Tryptone (BD Biosciences) to support growth of (p)ppGpp mutants and mimic rich medium. Overnight LPDMT cultures were sub-cultured in LPDMT and grown until mid-log before further sub-culturing of 5 X 10⁸ CFU in LPDM in 20 µCi/mL of carrier-free H₃³²PO₄. After 60-120 minutes at 37°C bacteria were washed in fresh LPDM, extracted with 13M formic acid, and freeze-thawed three times in dry ice-ethanol bath to disrupt cells. Where appropriate serine hydroxamate was added at a final concentration of 2 mg/mL, 10 minutes before harvest. Cell debris was removed by centrifugation, extracts were spotted on PEI Cellulose TLC plates (EMD Millipore), and developed in 1.5 M KH₂PO₄ pH 3.4. Dried TLC plates were exposed to phosphor-storage screen (Kodak) for >4 hours before imaging on a Typhoon scanner (GE Healthcare). Nucleotides were identified using GTP[γ-³²P] and *E. coli* mutant standards CF1943 and CF1944, which were generously provided by Michael Cashel (National Institutes of Health). Phosphor-storage screen scans were quantified using ImageQuant software (GE Healthcare) without background subtraction. The volume of intensity (without background correction) for identified nucleotide spots was used for calculation of (pppGpp + ppGpp) / (pppGpp + ppGpp + GTP) levels. Statistical significance was determined by a two-tailed heteroscedastic Student's *t*-test.

Plaque Assay

Plaque assays were performed as previously described (Sun et al., 1990). Briefly, L2 murine fibroblasts propagated in DMEM plus 10% fetal bovine serum (HyClone), 1 mM sodium pyruvate, and 2 mM L-glutamine were plated 1.2 X 10⁶ cells/well in a 6-well plate and infected at a multiplicity of infection (MOI) of approximately 300 with overnight cultures of *L. monocytogenes* grown at 30°C without agitation. After one hour the cells

were washed with PBS three times and over-layered with medium plus 0.7% agarose and gentamicin at 10 µg/mL. Cells were stained with Neutral Red 12-24 hours prior to imaging at 72 hours post infection and cell-to-cell spread (Tilney and Portnoy, 1989) forms a zone of clearance called a “plaque”. Plaque area was measured using ImageJ software (Schneider et al., 2012), collecting >5 plaques per strain per experiment. Statistical significance was determined by a two-tailed heteroscedastic Student’s *t*-test.

ΔrelAPQ Virulence Suppressor Screen

The *ΔrelAPQ* strain was mutagenized with *himar1* transposons as previously described (Zemansky et al., 2009) and the pooled mutant libraries were stored at -80°C. These libraries were diluted into BHI and cultured for 2-4 hours before being used for the plaque assay. Plaques visibly larger than the *ΔrelAPQ* strain were picked using a sterile pipet tip and recovered on selective BHI-agar plates. Chromosomal insertions of *himar1* were transduced back into the unmutagenized *ΔrelAPQ* parent and the plaque assay repeated to verify a single *himar1* insertion was capable of recapitulating the increased plaque size. Mutations were determined to suppress the *ΔrelAPQ* virulence defect if plaque area was significantly increased based on the stringent one-way ANOVA and subsequent Tukey test with 95% confidence interval. Transducing lysates could then also be used for analysis of mutation in alternative genetic backgrounds.

Transposon locations were determined using arbitrarily primed PCR with Hot-Start TaKaRa Taq (Takara Bio): Round 1 TN1 and ARB1 annealed at 42°C for 30 cycles, Round 2 TN2 and ARB2 annealed at 61°C for 40 cycles. PCR product was prepared using Exo-SAP and sequenced (Elim BioPharma) using primer TNSEQ (see Table 2.5).

Table 2.3 *L. monocytogenes* strains used in this study

Strain #	Strain	Description	Reference
	10403S	Wild-type	(Bécavin et al., 2014)
DP-L6254	<i>lox66-dacA-lox71 (dacA^{fl})</i>	Chromosomally floxed <i>dacA</i> (<i>Imo2120</i>)	This study
DP-L6255	<i>dacA^{fl} pKSV7-oriT-P_{actA}-Cre</i>	Parent strain for <i>dacA</i> deletion by Cre/lox	This study
DP-L6256	Δ <i>dacA.1</i>	Suppressor strain	This study
DP-L6257	Δ <i>dacA.2</i>	Suppressor strain	This study
DP-L6258	Δ <i>dacA.3</i>	Suppressor strain	This study
DP-L6259	Δ <i>dacA.4</i>	Suppressor strain	This study
DP-L6260	Δ <i>dacA.5</i>	Suppressor strain	This study
DP-L6261	Δ <i>dacA.6</i>	Suppressor strain	This study
DP-L6262	Δ <i>dacA.7</i>	Suppressor strain	This study
DP-L6263	Δ <i>dacA.8</i>	Suppressor strain	This study
DP-L6264	Δ <i>dacA.9</i>	Suppressor strain	This study
DP-L6265	Δ <i>dacA.10</i>	Suppressor strain	This study
DP-L6266	Δ <i>dacA.11</i>	Suppressor strain	This study
DP-L6267	Δ <i>dacA.12</i>	Suppressor strain	This study
DP-L6268	Δ <i>dacA.13</i>	Suppressor strain	This study
DP-L6269	Δ <i>dacA.14</i>	Suppressor strain	This study
DP-L6270	Δ <i>dacA.15</i>	Suppressor strain	This study
DP-L6271	Δ <i>dacA.16</i>	Suppressor strain	This study
DP-L6272	Δ <i>oppB</i>	In-frame deletion of <i>oppB</i> (<i>Imo2195</i>)	This study
DP-L6273	Δ <i>oppB</i> tRNA ^{Arg} ::pPL2t- <i>oppB</i>	Δ <i>oppB</i> complemented with <i>oppB</i> (<i>Imo2195</i>)	This study
DP-L5936	10403S tRNA ^{Arg} ::pLIV2t- <i>dacA</i>	Wild-type merodiploid for <i>dacA</i> (WT p- <i>dacA</i>)	(Witte et al., 2013)
DP-L6275	Δ <i>dacA-kanR Imo2103/4::himar1</i>	Donor strain for <i>dacA</i> essentiality assay	This study
DP-L6277	Δ <i>dacA-kanR Imo2103/4::himar1</i>	Donor strain for <i>dacA</i> essentiality assay	This study
DP-L6278	Δ <i>dacA-kanR Imo2103/4::himar1</i>	Donor strain for <i>dacA</i> essentiality assay	This study
DP-L6279	Δ <i>dacA-kanR Imo2110::himar1</i>	Donor strain for <i>dacA</i> essentiality assay	This study
DP-L6280	Δ <i>dacA-kanR Imo2110::himar1</i>	Donor strain for <i>dacA</i> essentiality assay	This study
DP-L6281	Δ <i>dacA-kanR Imo2110::himar1</i>	Donor strain for <i>dacA</i> essentiality assay	This study
DP-L6283	<i>dacA^{fl}-kanR Imo2103/4::himar1</i>	Donor strain for <i>dacA</i> essentiality assay	This study
DP-L6284	<i>dacA^{fl}-kanR Imo2103/4::himar1</i>	Donor strain for <i>dacA</i> essentiality assay	This study
DP-L6285	<i>dacA^{fl}-kanR Imo2103/4::himar1</i>	Donor strain for <i>dacA</i> essentiality assay	This study
DP-L6287	<i>dacA^{fl}-kanR Imo2110::himar1</i>	Donor strain for <i>dacA</i> essentiality assay	This study
DP-L6288	<i>dacA^{fl}-kanR Imo2110::himar1</i>	Donor strain for <i>dacA</i> essentiality assay	This study
DP-L6289	<i>dacA^{fl}-kanR Imo2110::himar1</i>	Donor strain for <i>dacA</i> essentiality assay	This study
DP-L6291	<i>relA^{R295S}</i>	<i>relA</i> suppressor allele reconstructed in wild-type	This study
DP-L6292	Δ <i>relA</i>	In-frame deletion of <i>relA</i> (<i>Imo1523</i>)	This study
DP-L5932	Δ <i>dacA</i> tRNA ^{Arg} ::pLIV2t- <i>dacA</i>	Conditional <i>dacA</i> depletion strain (c Δ <i>dacA</i>)	(Witte et al., 2013)
DP-L6294	Δ <i>relAPQ</i>	In-frame deletions of <i>relAPQ</i> (<i>Imo1523</i> , <i>Imo0802</i> , <i>Imo0967</i>)	This study
DP-L6295	Δ <i>relAPQ</i> tRNA ^{Arg} ::pPL2t- <i>relP</i> -term	Δ <i>relAPQ</i> complemented with <i>relP</i> (<i>Imo0802</i>)	This study
DP-L6296	Δ <i>relAPQ</i> tRNA ^{Arg} ::pPL2t- <i>relQ</i> -term	Δ <i>relAPQ</i> complemented with <i>relQ</i> (<i>Imo0967</i>)	This study
DP-L6297	Δ <i>relAPQ</i> tRNA ^{Arg} ::pPL2t- <i>relA</i> -term	Δ <i>relAPQ</i> complemented with <i>relA</i> (<i>Imo0802</i>)	This study
DP-L6298	Δ <i>dacA-kanR</i>	Marked <i>dacA</i> deletion	This study
DP-L6299	Δ <i>dacA-kanR \Delta</i> <i>relAPQ</i>	Marked <i>dacA</i> deletion in Δ <i>relAPQ</i>	This study
DP-L6300	c Δ <i>dacA \Delta</i> <i>relAPQ</i>	Conditional <i>dacA</i> depletion in Δ <i>relAPQ</i>	This study
DP-L6301	Δ <i>relAPQ guaB2 (Imo2758)::himar1</i>	Transposon location <i>LMRG_01938::220</i>	This study
DP-L6302	Δ <i>relAPQ Imo1884::himar1</i>	Transposon location <i>LMRG_01031::319</i>	This study
DP-L6303	Δ <i>relAPQ codY (Imo1280)::himar1</i>	Transposon location <i>LMRG_00730::119</i>	This study
DP-L6304	Δ <i>relAPQ purR (Imo0192)::himar1</i>	Transposon location <i>LMRG_02614::471</i>	This study
DP-L6305	Δ <i>relAPQ anrB (Imo2115)::himar1</i>	Transposon location <i>LMRG_01269::1842</i>	This study
DP-L6307	Δ <i>relAPQ P_{Imo0974}::himar1</i>	Transposon location <i>LMRG_02073::223</i>	This study
DP-L6308	Δ <i>relAPQ Imo0808::himar1</i>	Transposon location <i>LMRG_02789::1593</i>	This study
DP-L6309	Δ <i>relAPQ Imo0218::himar1</i>	Transposon location <i>LMRG_02640::121</i>	This study
DP-L6310	Δ <i>relAPQ P_{spoVG} (P_{Imo0196})::himar1</i>	Transposon location <i>LMRG_02618::144</i>	This study
DP-L6312	Δ <i>relAPQ Imo0948::himar1</i>	Transposon location <i>LMRG_02047::494</i>	This study

DP-L6314	$\Delta relAPQ$ <i>rsbX</i> (<i>Imo0896</i>):: <i>himar1</i>	Transposon location <i>LMRG_02320</i> ::2103	This study
DP-L6315	$\Delta relAPQ$ <i>Imo0767</i> :: <i>himar1</i>	Transposon location <i>LMRG_00455</i> ::222	This study
DP-L6316	$\Delta relAPQ$ <i>Imo1843</i> :: <i>himar1</i>	Transposon location <i>LMRG_00990</i> ::876	This study
DP-L6320	$\Delta relAPQ$ <i>Imo0006/7</i> :: <i>himar1</i>	Transposon location <i>LMRG_02435</i> ::-26	This study
DP-L6321	<i>codY</i> :: <i>spc</i>	Marked deletion of <i>codY</i> (<i>Imo1280</i>)	This study
DP-L6322	$\Delta relAPQ$ <i>codY</i> :: <i>spc</i>	$\Delta relAPQ$ with marked deletion of <i>codY</i>	This study
DP-L6323	$\Delta relAPQ$ $\Delta spoVG$	$\Delta relAPQ$ with in-frame deletion of <i>spoVG1</i> and <i>spoVG2</i>	This study
DP-L6324	$\Delta dacA.MM$	In-frame <i>dacA</i> deletion constructed via allelic exchange in minimal media	This study
DP-L6325	$\Delta dacA$ - <i>kanR.MM1</i>	Marked <i>dacA</i> deletion constructed in minimal media (1)	This study
DP-L6326	$\Delta dacA$ - <i>kanR.MM2</i>	Marked <i>dacA</i> deletion constructed in minimal media (2)	This study

Table 2.3 *L. monocytogenes* strains used in this study

Strain	Plasmid or genotype	Reference
XL1-Blue	Cloning; <i>recA1 endA1 gyrA96 thi-1 hsdR17 supE44 relA1 lac</i> [<i>F'</i> <i>proAB lacI^qZΔM15 Tn10</i> (<i>Tet^r</i>)]	Stratagene
SM10	Conjugation; <i>thi-1 thr-1 leuB6 tonA21 lacY1 supE44 recA λ⁻</i> integrated [<i>RP4-2-Tcr::Mu</i>] <i>aphA⁺</i> (<i>Km^r</i>) <i>Tra⁺</i>	(Shanker and Atkins, 1996)
DP-E6324	pKSV7-oriT	(Camilli et al., 1993)
DP-E6325	pKSV7-oriT -genomic- <i>lox66-dacA-lox71-Imo2119</i>	This study
DP-E6326	pKSV7-oriT - <i>P_{actA}-cre</i> (<i>cre</i> is codon optimized for <i>L. monocytogenes</i>)	This study
DP-E6327	pKSV7-oriT -genomic- <i>lox66-dacA-lox71-kanR-Imo2119</i>	This study
DP-E6328	pKSV7-oriT - $\Delta relA$ (<i>Imo1523</i>)	This study
DP-E6329	pKSV7-oriT - $\Delta relP$ (<i>Imo0802</i>)	This study
DP-E6330	pKSV7-oriT - $\Delta relQ$ (<i>Imo0967</i>)	This study
DP-E6331	pKSV7-oriT - $\Delta codY$::SPC (<i>Imo1280</i>)	This study
DP-E6332	pKSV7-oriT - $\Delta spoVG$ (<i>Imo0196-Imo0197</i>)	This study
DP-E6333	pPL2t, a derivative of pPL2 tetracycline resistant in <i>L. monocytogenes</i>	This study
DP-E6334	pPL2t- <i>relA</i> -term	This study
DP-E6335	pPL2t- <i>relP</i> -term	This study
DP-E6336	pPL2t- <i>relQ</i> -term	This study
DP-E6337	pPL2t- <i>oppB</i>	This study
CF1943	<i>E. coli</i> , W3110	(Xiao et al., 1991)
CF1944	CF1943 but $\Delta relA251$:: <i>kan</i>	(Xiao et al., 1991)

Table 2.4 plasmids and *E. coli* strains used in this study

Table 2.5 Oligonucleotides used in this study

Primer Name	Sequence (5'-3', restriction sites underlined)	Description
<i>dacA</i> ^{fl} -EcoRI-F	gaggaggaattcgtaacaggaccaaacgaatacg	5' Genomic Region (A)
<i>dacA</i> ^{fl} -lox66-R	taccgttcgtataatgtatgctatacgaagttacacttcacctccgtgcc	5' Genomic Region <i>lox66</i> addition (B)
<i>dacA</i> ^{fl} -BamHI-R	gaggagggatcctaccgttcgtataatgtatgctatacgaagttat	5' Genomic Region (B')
<i>dacA</i> ^{fl} -BamHI-F	gaggagggatccatggatcttccaatatgctgatattg	<i>dacA</i> (C)
<i>dacA</i> ^{fl} -lox71-R	ataactcgtataatgtatgctatacgaacgggtatcattcgctttgcctcc	<i>dacA lox71</i> addition (D)
<i>dacA</i> ^{fl} -PstI-R	gaggaggtcgacataactcgtataatgtatgctatacgaacggta	<i>dacA</i> with <i>lox71</i> (D')
<i>dacA</i> ^{fl} -PstI-F	gaggaggtcgacatgatggatcgaattttaaataataaatggt	3' Genomic Region (E)
<i>dacA</i> ^{fl} -Sall-R	gaggagctgcaggtatctgtgcttggttactatctg	3' Genomic Region (F)
<i>dacA</i> -locus-F	gaaacagcggtaatagtagaaata	<i>dacA</i> locus, for deletion screening
<i>dacA</i> -locus-R	ggaggcattttcaaatctgcg	
<i>dacA</i> -F	ggcattttattatcattgcagtcaa	<i>dacA</i> gene, for deletion screening
<i>dacA</i> -R	tccggttgaagataattataattgc	
<i>relA</i> -syn-F	tgaacattagaatatttgcgcc	<i>relA</i> synthase domain sequencing
<i>relA</i> -syn-R	gttaaatgtcaataatcgcgcc	
kanR-Sall-F	gaggaggtcgacaaaatggctaaaatgagaatcacc	Kanamycin resistance marked <i>dacA</i> locus
kanR-Sall-R	gaggaggtcgacctaaaacaattcatccagtaaaatataatattttatt	
Δ <i>relA</i> -5'-Sall-F	gaggaggtcgacggcctaatgcaaaaattggttg	Δ <i>relA</i> (A)
Δ <i>relA</i> -5'-SOE-R	ttagttcattaatcttctattttgtctttcgccattacattc	Δ <i>relA</i> (B)
Δ <i>relA</i> -3'-SOE-F	atggcgaagaacaaaatagaagattaagaactaaaggagtg	Δ <i>relA</i> (C)
Δ <i>relA</i> -3'-PstI-R	gaggagctgcagtcagggtctaaagggg	Δ <i>relA</i> (D)
Δ <i>oppB</i> -5'-Sall-F	gaggaggtcgacacaaaacgtgctggc	Δ <i>oppB</i> (A)
Δ <i>oppB</i> -5'-SOE-R	gccattatttctacctccagactaacgtatatttaaccatctatctctacac	Δ <i>oppB</i> (B)
Δ <i>oppB</i> -3'-SOE-F	gtgtagagatagatggttaaatatacgttagtctggaggtagaaaaaatggc	Δ <i>oppB</i> (C)
Δ <i>oppB</i> -3'-PstI-R	gaggagctgcagttttccattttctcactctc	Δ <i>oppB</i> (D)
Δ <i>codY</i> -5'-SacI-F	gaggagggctcggcggcatgaatcaacc	Δ <i>codY</i> (A)
Δ <i>codY</i> -5'-SOE-R	gctttctagtttttagttattttcaatttttctaataaagtcattattagatcctcc	Δ <i>codY</i> (B)
Δ <i>codY</i> -3'-SOE-F	aaattgaaaaataactaaaaaactagaaaagc	Δ <i>codY</i> (C)
Δ <i>codY</i> -3'-Sall-R	gaggaggtcgacgggtaatgacgcccc	Δ <i>codY</i> (D)
Δ <i>codY</i> -iPCR-EagI-R	gaggagcggccgatcctcctagttattttataaaaatgtgt	<i>codY</i> :: <i>spc</i> iPCR to add EagI site
Δ <i>codY</i> -iPCR-EagI-F	gaggagcggccgaaaaactagaaaagcttctctgga	
<i>spcR</i> -EagI-F	gaggagcggccggtaggaggatatttgaatacatcac	<i>spcR</i> gene
<i>spcR</i> -EagI-R	agaagacggcgttataatttttaactgctatttaaatgattatagttaaatt	
Δ <i>spoVG</i> -5'-KpnI-F	gaggaggtacctatgctagttctgttagtgagcg	Δ <i>spoVG</i> (A)
Δ <i>spoVG</i> -5'-SOE-R	aaattttaaattatcagcagaaacggacacatctgtaatcctcattatctcacc	Δ <i>spoVG</i> (B)
Δ <i>spoVG</i> -3'-SOE-F	ggtgaagataatggagattacagatgtgccgttctgctgaataattaaaatt	Δ <i>spoVG</i> (C)
Δ <i>spoVG</i> -3'-Sall-R	gaggaggtcgacccgcaacgactcatccg	Δ <i>spoVG</i> (D)
<i>relP</i> -Sall-F	gaggaggtcgacacaatttttgctagaataaaaattatct	<i>relP</i> complement
<i>relP</i> -PstI-R	gaggagctgcagttattttctttttatattatcaatttgatc	
<i>relQ</i> -Sall-F	gaggaggtcgactttctgctccttttagttg	<i>relQ</i> complement
<i>relQ</i> -PstI-R	gaggagctgcagttacttattttctttggcactct	
<i>relA</i> -Sall-F	gaggaggtcgacaaaatagactactctattatttagggg	<i>relA</i> complement
<i>relA</i> -PstI-R	gaggagctgcagttagttcataatcttctcactgtatatacg	
<i>oppB</i> -Sall-F	gaggaggtcgacttctcactctaaataaaattcataattca	<i>oppB</i> complement
<i>oppB</i> -EagI-R	gaggagcggccgaaatcttttgcatttttagttct	
Term-SacI-F	gaggagggctcgcataaaaacgaaaggctcagtcgaaagactggccttctgttctgagctcaggag	Transcriptional terminator
Term-SacI-R	ctcctcgagctcaacagataaa	
TN1	gctccaaggagctaaagaggtccctagcgcc	
ARB1	cggggaatttgatcgataaggaatagattttaaattctgctgtattttg	<i>himar1</i> transposon sequencing
TN2	ggccacgctgcgactagtagcnnnnnnnnctct	
ARB2	ggccacgctgcgactagtagc	
TNSEQ	acaataaggataaattgaaactagtagtctcagtgggg	

Chapter 3: c-di-AMP Regulates Osmohomeostasis with Implications for Growth on Rich Medium, Antibiotic Resistance, and Virulence

Summary

Cyclic di-adenosine monophosphate (c-di-AMP) is a conserved nucleotide second messenger that is critical for bacterial growth and resistance to cell wall acting antibiotics. In *Listeria monocytogenes*, the sole diadenylate cyclase, DacA, is essential on rich, but not synthetic media and $\Delta dacA$ mutants are highly sensitive to cefuroxime. In this study, suppressor mutations in the oligopeptide importer (*oppABCDF*), glycine betaine importer (*gbuABC*), and two genes of unknown function (*pstA* and *cbpB*) allowed $\Delta dacA$ mutants to grow in rich media. Oligopeptides were sufficient to inhibit growth of the $\Delta dacA$ mutant and we hypothesized that oligopeptides in rich media may act as osmolytes, similar to glycine betaine, to disrupt intracellular osmotic pressure. Osmotically stabilizing the $\Delta dacA$ mutant with supplemental salt rescued growth on rich media and cefuroxime resistance. Additional suppressor mutations that rescued cefuroxime resistance disrupted acetyl-CoA mediated allosteric activation of pyruvate carboxylase (PycA), an enzyme inhibited by c-di-AMP that provides an essential source of carbon for the TCA cycle. Targeted inactivation of citrate synthase, but not downstream TCA cycle enzymes suppressed $\Delta dacA$ phenotypes. These data suggest that c-di-AMP modulates central metabolism at the pyruvate node to balance production of citrate, with implications for optimal growth, cell wall homeostasis, and virulence.

Introduction

Cyclic diadenosine monophosphate (c-di-AMP) is a prokaryotic signaling molecule and nucleotide second messenger (Corrigan and Gründling, 2013). Production of c-di-AMP from two ATP molecules is catalyzed by diadenylate cyclases that share a common protein domain and are distributed in the genomes of virtually all Gram positive bacteria, a minority of Gram negative bacteria, and some Archeae (Römling, 2008; Witte et al., 2008). c-di-AMP is similar to c-di-GMP, (p)ppGpp, and cAMP, which are synthesized in the cytosol from abundant nucleotide precursors to transduce extracellular stressors into changes in bacterial physiology. However, unlike these related nucleotides the stressors driving production of c-di-AMP are unknown and in multiple bacteria synthesis of c-di-AMP appears constitutive and essential.

Nucleotide second messengers canonically signal through allosteric interactions with proteins and riboswitches. Analysis of previously identified c-di-AMP interacting elements suggests that c-di-AMP is intimately associated with osmoregulation. Systematic screens for proteins that interact with c-di-AMP and analysis of the distribution of a c-di-AMP responsive riboswitch have identified a direct role for c-di-AMP in inhibiting potassium import (Block et al., 2010; Corrigan et al., 2011; Huynh et al., 2016; Nelson et al., 2013; Sureka et al., 2014). Potassium import is the first step in the bacterial response to hyperosmotic shock and a key component of osmoregulation. In addition, c-di-AMP directly inhibits import of carnitine (Huynh et al., 2016). Osmolytes such as carnitine, proline containing peptides, and glycine betaine are termed compatible solutes because import or synthesis of these molecules to high levels can balance extracellular osmotic pressure without interfering with cellular processes (Sleator et al., 2003). In support of these biochemical interactions, mutants in c-di-AMP degrading phosphodiesterase are impaired for growth in both low potassium and high salt environments (Corrigan et al., 2013).

Within the Firmicutes genetic manipulation of c-di-AMP has identified that low c-di-AMP is associated with slowed growth, susceptibility to cell wall acting antibiotics, increased bacteriolysis, and decreased virulence (Corrigan and Gründling, 2013). High c-di-AMP has also been associated with decreased virulence in addition to increased acid resistance and increased resistance to β -lactam antibiotics (Gundlach et al., 2015; Huynh et al., 2015; Rallu et al., 2000). The molecular determinants of these phenotypes were investigated in *Listeria monocytogenes* by affinity purifying proteins from bacterial lysates using c-di-AMP conjugated resin (Sureka et al., 2014). Two phosphodiesterases (PdeA and PgpH), three proteins of unknown function (PstA, CbpA, and CbpB), a transcriptional repressor (NrdR), and an enzyme (PycA) were identified. With the exception of the phosphodiesterases, PstA is the most widely distributed c-di-AMP interacting protein identified. PstA is a small (11.8 kDa), PII-like protein that has been identified and characterized crystallographically in *Bacillus subtilis*, *Staphylococcus aureus*, and *L. monocytogenes* (Campeotto et al., 2014; Choi et al., 2015; Gundlach et al., 2014; Müller et al., 2015). Other PII-like proteins modulate nitrogen metabolism via protein-protein interactions and are inhibited by a cognate small molecule (Ninfa and Jiang, 2005). PstA binds c-di-AMP at high affinity and the protein-protein interaction

PstA may participate in is likely inhibited by c-di-AMP. The *pstA* gene is almost exclusively found neighboring or in an operon with thymidylate kinase and a putative arginine/ornithine/lysine decarboxylase (*yaaO*). Despite a wealth of crystallographic information on PstA, its function remains elusive.

c-di-AMP appears essential in all Firmicutes yet investigated with the exception of *L. monocytogenes*. The sole diadenylate cyclase, *dacA*, could be deleted in conventional media when bacteria harbored suppressor mutations. Although many candidate suppressor mutations were identified, only mutations affecting production of the stringent response second messenger (p)ppGpp were characterized (Whiteley et al., 2015). Decreased c-di-AMP led to increased (p)ppGpp and toxic indirect inactivation of the transcriptional regulator CodY. Whereas (p)ppGpp is essential for growth on synthetic but not rich media, c-di-AMP was identified as only essential for growth in rich media and $\Delta dacA$ mutants constructed on synthetic media do not harbor suppressor mutations. In this report, *L. monocytogenes* $\Delta dacA$ mutants are constructed in synthetic media and additional suppressor mutations are characterized. These data demonstrate that $\Delta dacA$ mutants are unable to regulate intracellular osmotic pressure, which becomes toxic when oligopeptides or cefuroxime are present. C-di-AMP-dependent modulation of the TCA cycle alters osmotic pressure and is important for virulence of *L. monocytogenes*.

Results

Peptides in rich media are selectively toxic in the absence of c-di-AMP

L. monocytogenes encodes only one di-adenylate cyclase capable to producing c-di-AMP, DacA. Previous research demonstrated that *dacA* was conditionally essential for growth in rich but not defined synthetic media. We have extended these observations by constructing Δ *dacA* mutants and other c-di-AMP deficient mutants in a novel *listeria* synthetic medium (LSM, see Table 3.1 for details) that promoted enhanced growth of Δ *dacA* and wild-type and was easily adapted to both liquid culture and nutrient agar. Mutants were constructed in LSM, grown in LSM-culture overnight, and serial dilutions were plated on LSM and the conventional rich medium BHI (Figure 3.1A). Wild-type formed an equivalent number of colonies on LSM vs rich medium while over 10,000-fold fewer colonies were formed on rich medium by the Δ *dacA* mutant (Figure 3.1A and B). The same phenotype was observed for *L. monocytogenes* expressing a catalytically dead *dacA*^{D171A} mutant, which was still able to synthesize DacA but no longer produce c-di-AMP (Figure 3.1B and C)(Rosenberg et al., 2015). Colony formation on rich medium could be rescued by expressing the native diadenylate cyclase *dacA* or the distantly related diadenylate cyclase from *Bacillus subtilis* *disA* (Figure 3.1A and B).

The Δ *dacA* colonies formed when plating on rich media harbored previously identified suppressor mutations (data not shown)(Whiteley et al., 2015). Loss of function mutations in genes encoding the oligo-peptide permease (Opp) were found in over 94% of Δ *dacA* suppressor mutants (Figure 3.1E). The Opp is a five-subunit active importer of 3-8 amino acid oligopeptides consisting of an extracellular solute binding protein (OppA), transmembrane permeases (OppBC), and the possibly redundant ATPases (OppDF)(Figure 3.1D). Deletion of *oppB* enabled the Δ *dacA* mutant to grow in rich media and implicated the substrate of the Opp as toxic to Δ *dacA* (Figure 3.1F). In other organisms the Opp-imported oligopeptides have been described as either nutritive, peptide pheromones important for quorum sensing, or peptide fragments of peptidoglycan (Maqbool et al., 2011). We hypothesized that oligopeptides derived from *L. monocytogenes* would still be synthesized in LSM and that Δ *dacA* is unable to form a colony on rich media due to the abundance of nutritive oligopeptides. By supplementing LSM with nutritive peptides (a tryptic digest of casein) Δ *dacA* was no longer able to form a colony (Figure 3.1F). These data suggest that targets of c-di-AMP affect growth in rich media due to the presence of nutritive oligopeptides.

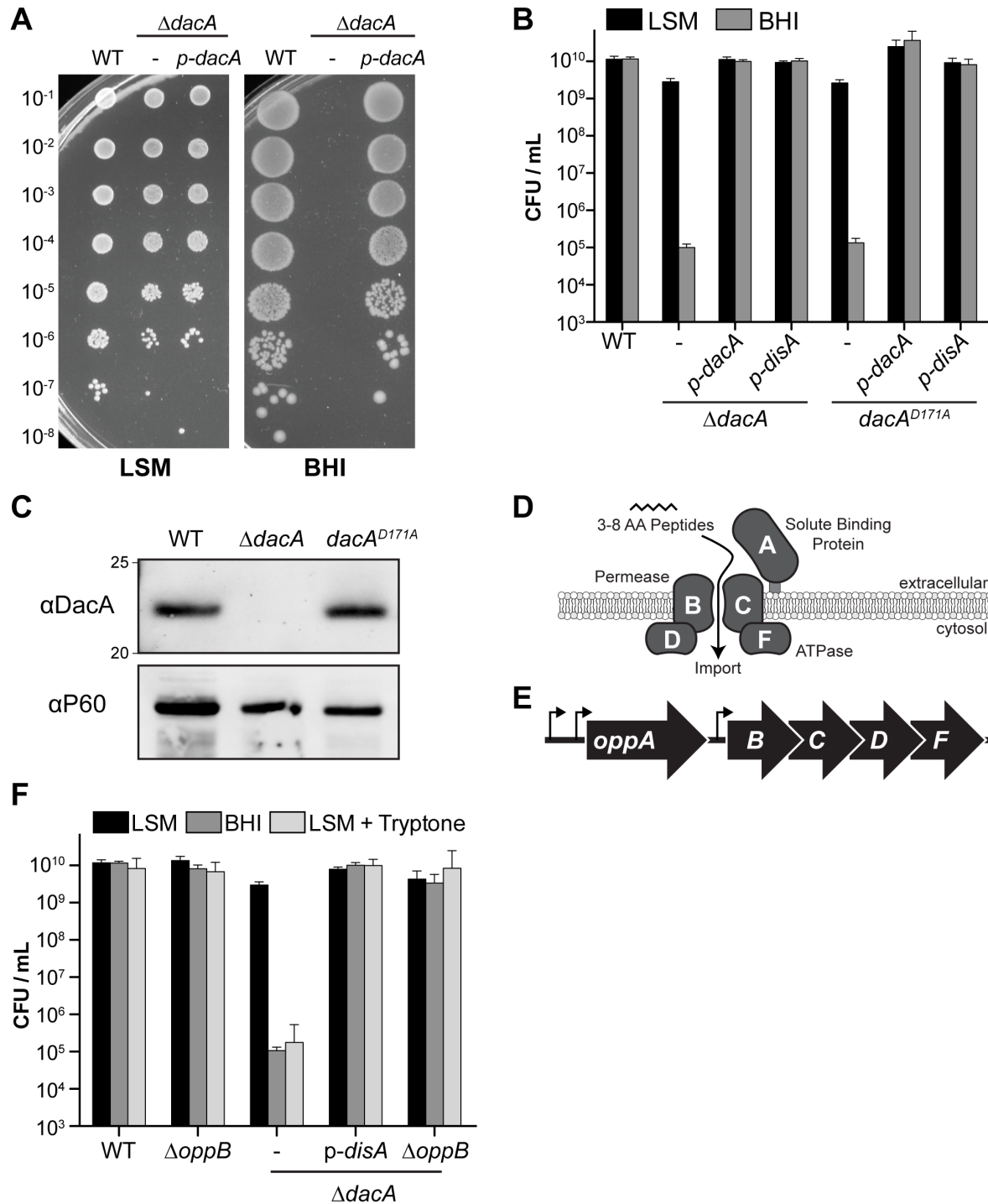


Figure 3.1 Oligopeptides are toxic in the absence of c-di-AMP

(A and B) Mutants constructed and grown overnight in LSM were serially diluted 10-fold in a 96-well plate with PBS then 5 μ L of each dilution was spotted onto either LSM or BHI agar. Images were taken and CFU were enumerated after 48 hrs of incubation at 37 $^{\circ}$ C. (C) Immunoblot of DacA and P60 (loading control) proteins for the strains indicated. Data are representative of three independent experiments. (D and E) Illustration of oligopeptide permease (Opp) protein subunits and operon organization. (F) Enumeration of CFU on indicated media for *L. monocytogenes* strains constructed in LSM. (B and F) Data are mean \pm standard error of the mean (s.e.m) of $n \geq 3$ independent experiments.

c-di-AMP is essential for growth during osmotic stress

After the *opp* locus the most common loss-of-function suppressor mutations were in the *gbuABC* operon, which encodes a glycine betaine importer homologous to *opuAABC* in *B. subtilis* (Figure 3.2A and B). Unlike the *opp* locus, mutations in the *gbuABC* operon were only isolated in $\Delta dacA$ suppressor strains harboring other mutations (Whiteley et al., 2015). However, deleting *gbuABC* or disrupting *gbuC* alone was sufficient to suppress the *dacA* essentiality in rich medium (Figure 3.2C and Figure 3.3). Uptake of compatible osmolytes such as glycine betaine allows bacteria to cope with osmotic stress and modulate the water content and turgor pressure of the cell. Mutations in *gbuABC* are predicted to decrease the internal osmotic pressure of $\Delta dacA$ mutants thus we hypothesized that *dacA* is conditionally essential due to large differences in internal and external osmotic pressure. In support of this hypothesis, addition of NaCl and KCl to rich media restored colony formation of $\Delta dacA$ mutants (Figure 3.2D and E).

In addition to growth in rich media, c-di-AMP also contributes to resistance to cell wall acting antibiotics in *L. monocytogenes* and in a variety of related organisms. In *L. monocytogenes* depletion of *dacA* or deletion of the phosphodiesterase that degrades c-di-AMP (*pdeA*) demonstrated a direct correlation between c-di-AMP and cell wall integrity (Witte et al., 2013). Accordingly, the $\Delta dacA$ and *dacA*^{D171A} mutants displayed significant sensitivity to the β -lactam antibiotic cefuroxime even when grown in LSM, suggesting neither the DacA protein or oligopeptides are not responsible for the cell wall phenotypes (Figure 3.2F). However, the demonstrated effects of osmotic pressure on the growth of $\Delta dacA$ mutants in rich medium led us to speculate that dysregulation of osmotic pressure underlied the cefuroxime sensitivity of the $\Delta dacA$ mutant. Intriguingly, supplementation of LSM with NaCl rescued the sensitivity of the $\Delta dacA$ mutant to cefuroxime but had no effect on wild-type (Figure 3.2G). These data suggest that c-di-AMP modulates bacterial physiology to decrease internal osmotic pressure, which is important for growth on peptides as well as resistance to cell wall acting antibiotics.

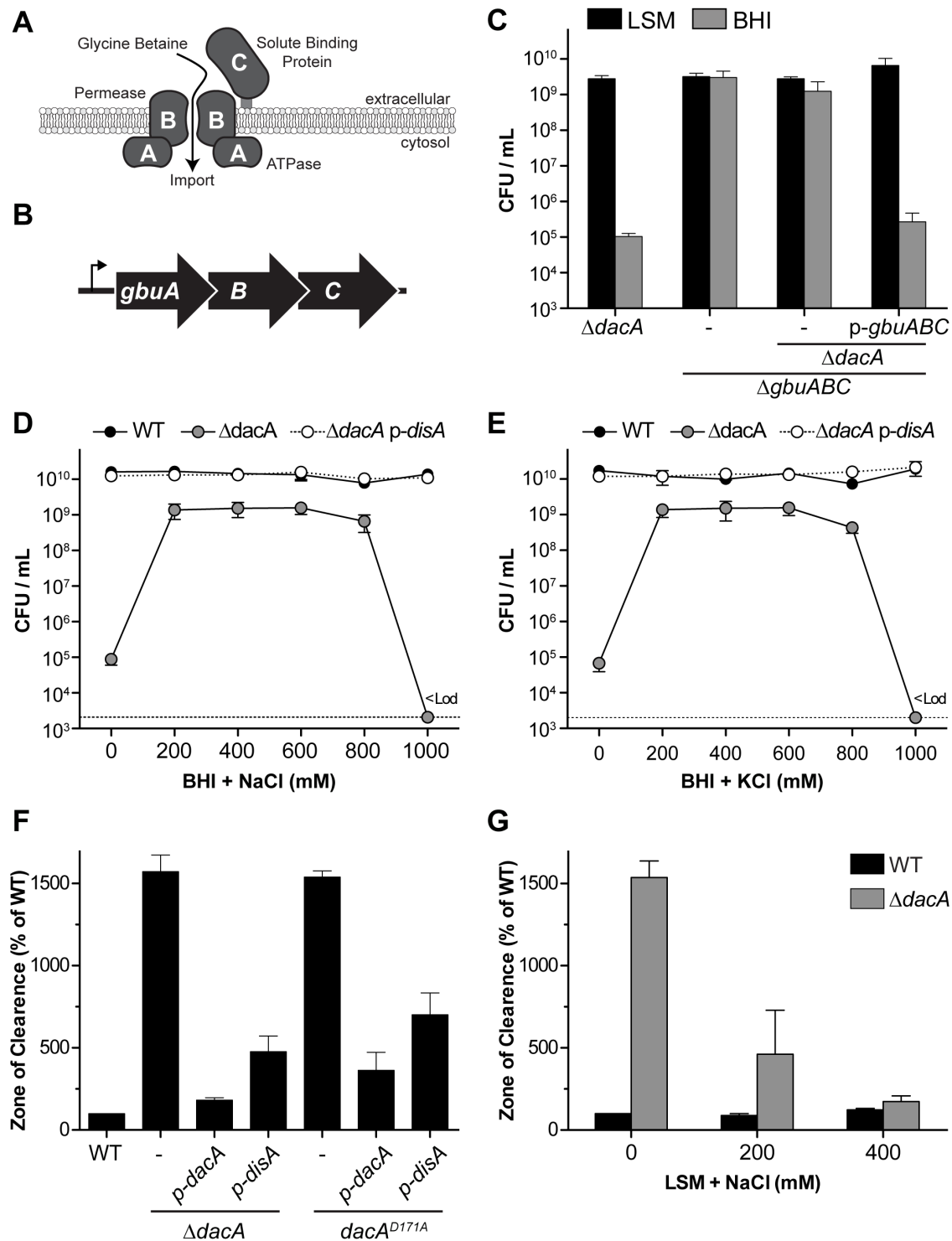


Figure 3.2 $\Delta dacA$ mutants are defective for osmotic homeostasis

(A and B) Illustration of glycine-betaine importer (Gbu) protein subunits and operon organization. (C-E) Enumeration of CFU on indicated media for *L. monocytogenes* strains constructed in LSM. (F) Antibiotic sensitivity measured by disk diffusion of 125 μ g of cefuroxime on LSM-agar for the indicated *L. monocytogenes* strains measured at 48 hrs. (G) Cefuroxime disk diffusion on LSM-agar supplemented with the indicated concentration of NaCl. All data are mean \pm s.e.m. of $n \geq 3$ independent experiments.

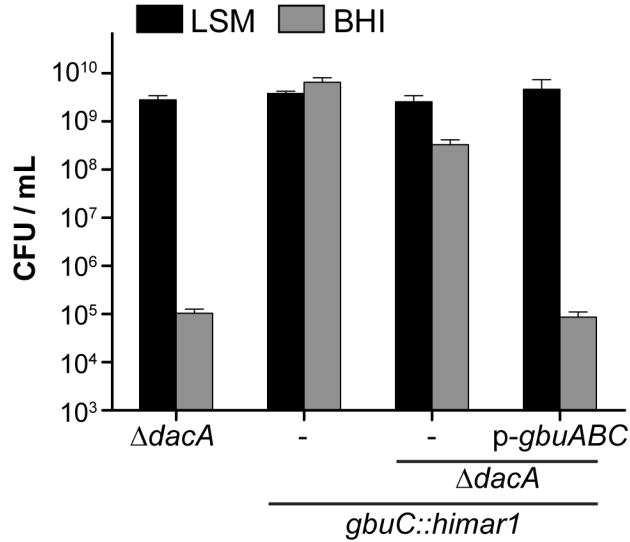


Figure 3.3 Mutations in *gbuC* are sufficient to suppress $\Delta dacA$ growth defects on rich media

Enumeration of CFU on indicated media for *L. monocytogenes* strains constructed in LSM. Data are mean \pm s.e.m of $n \geq 3$ independent experiments.

Characterizing $\Delta dacA$ suppressor mutations

c-di-AMP appeared to alter internal osmotic pressure through a yet unidentified mechanism. Our analysis next aimed to identify mutations that suppressed both growth on rich media and cefuroxime sensitivity. We analyzed the following mutations: $\Delta oppB$, $\Delta gbuABC$, $\Delta pstA$, $\Delta cbpB$, $relA^{R295S}$, and $\Delta pdeA\Delta pgpH$. The first four of these were previously reported as loss-of-function mutations identified in multiple $\Delta dacA$ suppressor strains able to form a colony on rich medium. Point mutations in *relA* also enabled $\Delta dacA$ to form a colony on rich medium. Finally, the $\Delta pde\Delta pgpH$ strain deficient in both identified c-di-AMP hydrolases was interrogated as previous screens may have not identified a suppressive function for these proteins due to their redundancy.

Each previously identified suppressor mutation allowed $\Delta dacA$ mutants to form a colony on rich medium while only $\Delta pdeA\Delta pgpH$ was similar to wild-type (Figure 3.1F, Figure 3.2C, and Figure 3.4A). These phenotypes could be fully complemented in $\Delta gbuABC$ and $\Delta pstA$, partially complemented in $relA^{R295S}$ due to the dominant nature of the mutation (Whiteley et al., 2015), partially complemented in $\Delta cbpB$ (hypothesized to be due to low expression), and not complemented in $\Delta oppB$ due to toxicity to *E. coli* (Figure 3.2C and Figure 3.5). Only the $\Delta pstA$ mutation was capable of suppressing the sensitivity of the $\Delta dacA$ mutant to cefuroxime (Figure 3.4B). This phenotype was complemented by over expressing *pstA* with a C-terminal strep(II)-tag (SII) tag from a neutral locus (Figure 3.4B).

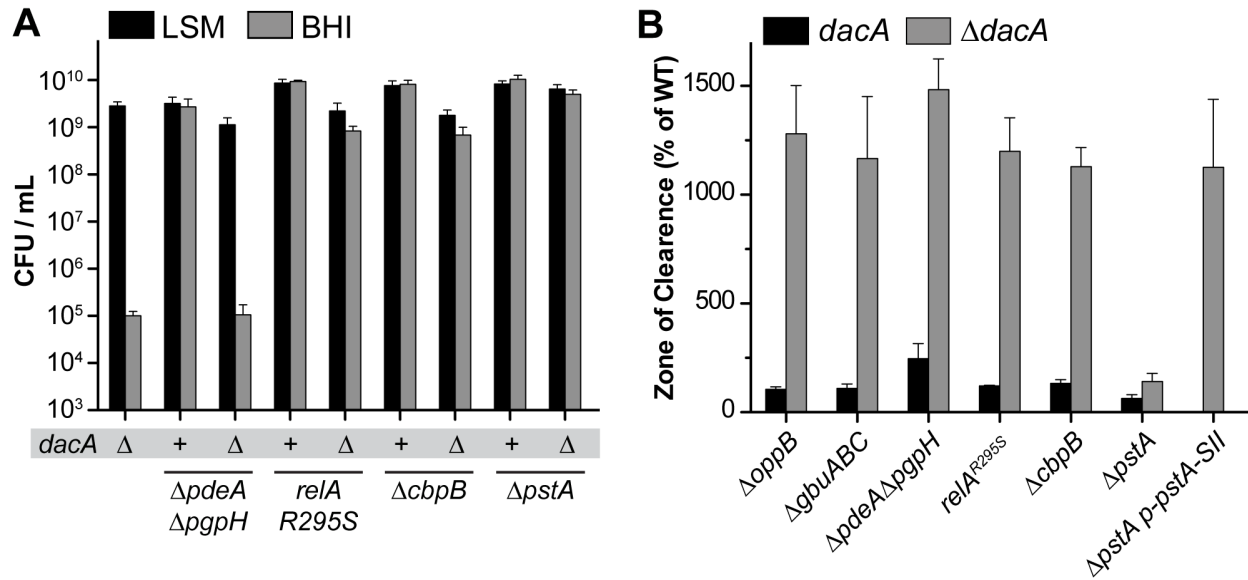


Figure 3.4 Mutations in *pstA* suppress the sensitivity of $\Delta dacA$ to cefuroxime

(A) Enumeration of CFU on indicated media for *L. monocytogenes* strains constructed in LSM. (B) Cefuroxime disk diffusion on LSM-agar of *L. monocytogenes* strains. *dacA* vs. $\Delta dacA$ indicates either a mutation in a wild-type or c-di-AMP deficient background. All data are mean \pm s.e.m of $n \geq 3$ independent experiments.

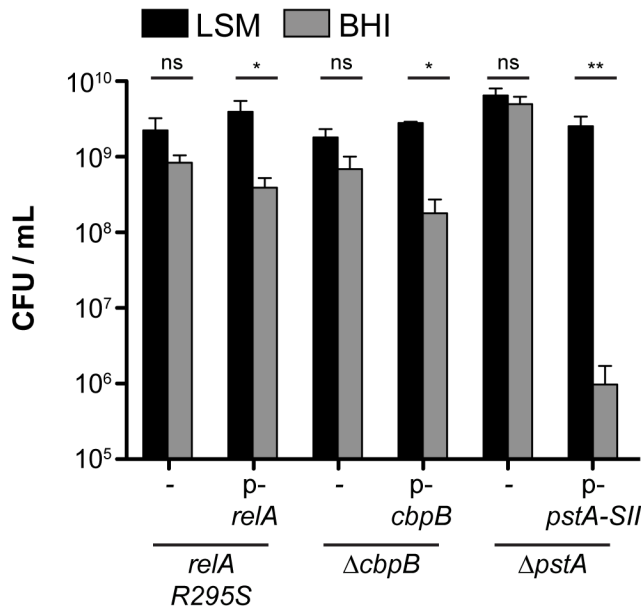


Figure 3.5 Complementation of suppressor mutations

Enumeration of CFU on indicated media for *L. monocytogenes* strains constructed in LSM. Data are mean \pm s.e.m of $n \geq 3$ independent experiments and the p value was calculated using a heteroscedastic Student's t -test; * $p < 0.05$.

PstA protein-protein interactions

PstA appeared to have a central role in $\Delta dacA$ phenotypes and was selected for further characterization. PstA is a PII-like protein, a family of proteins that canonically form protein-protein interactions, which are disassociated upon binding cognate metabolites such as α -ketoglutarate (α KG) and ATP. Crystallographic information suggests that binding of c-di-AMP to trimeric PstA coordinates the “B-loop” of each monomer, decreasing the accessibility of this flexible region to interactions with other proteins (Choi et al., 2015). We hypothesized that in the absence of c-di-AMP, PstA-protein interactions were stabilized which led to the inability to grow in rich media and to resist cefuroxime. Accordingly, we performed SPINE affinity purification of PstA from *L. monocytogenes* and a yeast 2-hybrid to identify PstA interacting proteins (Herzberg et al., 2007).

Affinity tagged *pstA* expressed from the endogenous promoter failed to complement the $\Delta pstA$ mutation and the affinity tag may partially disrupt the activity of the protein (Data not shown). However, the $\Delta pstA$ mutation could be complemented by over-expressing PstA with a C-terminal strep(II)-tag fusion (PstA-SII) indicating this form of the protein retained some biological activity but required increased expression (Figure 3.4A and B). Affinity purifications from lysates of $\Delta dacA \Delta pstA$ *p-pstA-SII* *L. monocytogenes* were compared to purifications from $\Delta dacA$ lysates. We failed to capture any specific PstA interacting proteins without the addition of paraformaldehyde as a cross-linking agent as visualized by SDS-PAGE and silver staining (Figure 3.6 and data not shown). Affinity purifications using crosslinking reagents instead identified an impossibly large set of interacting proteins. While these samples likely contained true PstA interacting proteins it seemed to also include many false positives. 110 Proteins were considered as possible interactors because they were identified in two of the three affinity purifications and not found to non-specifically interact with the resin (in the background purification from lysate that did not express *pstA-SII*)(Table 3.2 and Figure 3.7A).

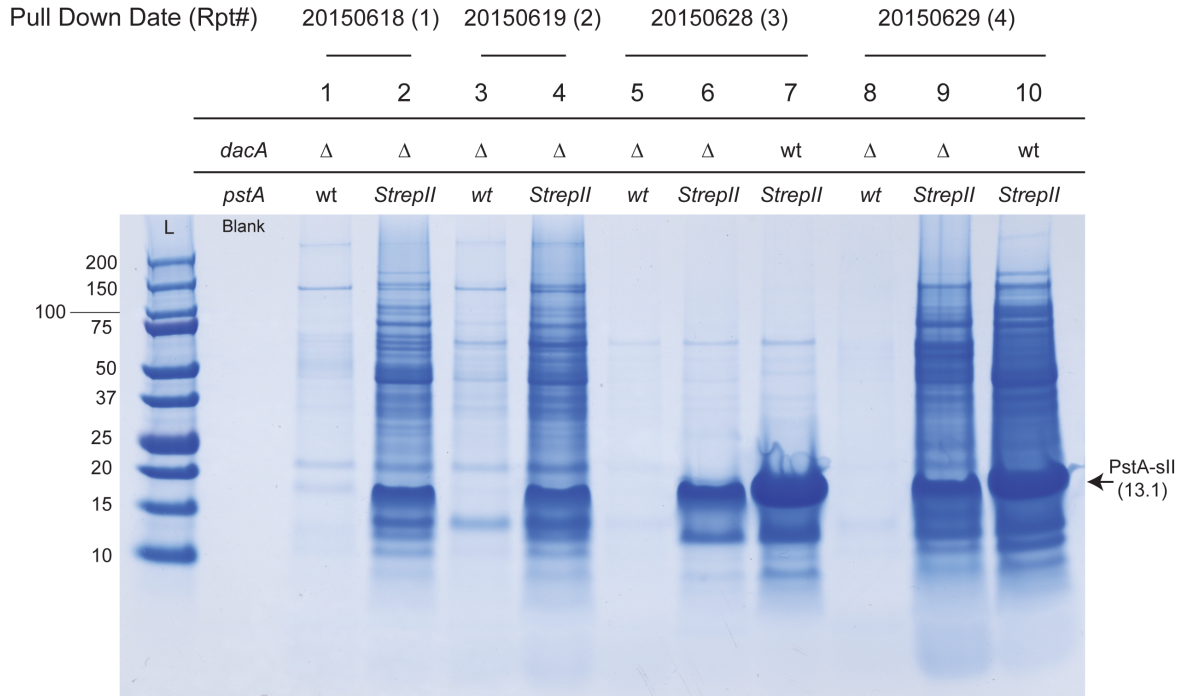


Figure 3.6 Pull-downs of PstA from *L. monocytogenes*

PstA-SII was over-expressed from a neutral locus in the strains indicated and LSM cultures of *L. monocytogenes* was grown to mid-log. In 1 and 2 bacteria were resuspended in PBS and fixed in 0.6% paraformaldehyde for 20 min. In 3 and 4 bacteria were fixed by directly adding 0.4% paraformaldehyde for 20 min. In 5, 6, and 7 bacteria were not fixed. In 8, 9, and 10 bacteria were fixed with resuspended in PBS and fixed with 0.6% paraformaldehyde for 5 minutes. All fixation was stopped with the addition of 0.5 M glycine for 5 minutes. Bacteria were lysed by sonication in TBS pH 7.5+ 10% glycerol and applied to 0.5 mL Streptactin sepharose. Beads were washed with 4x10 mL of TBS pH 7.5 + 10% glycerol, 1mM PMSF, and benzonase and then eluted as per manufacturers instructions with d-Desthiobiotin. Eluates were concentrated by TCA precipitation/acetone wash, resuspendend in LDS buffer, boiled to reverse cross linking, and 90% of the sample was analyzed by SDS-PAGE.

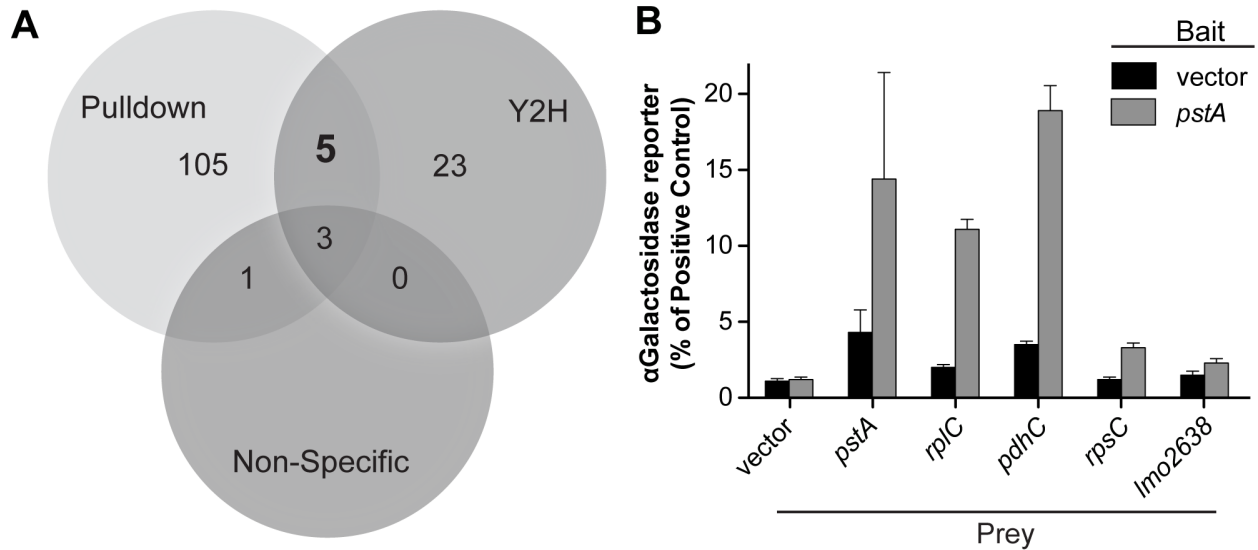


Figure 3.7 PstA protein-protein interactions

(A) Venn diagram of proteins identified by either pull-down (Table 3.2) or yeast 2-hybrid (Table 3.3). See text for details of how specificity was determined. (B) Quantification of the *MEL1* α -galactosidase gene product, a reporter for positive yeast 2-hybrid protein-protein interactions, for the indicated bait and prey. Data are the mean \pm s.e.m. as a proportion of the positive control for four independent y187 cotransformants, each measured three independent times.

The list of candidate interacting proteins was refined by performing a yeast 2-hybrid (Y2H) using Gal4-BD-PstA fusion protein as bait and a prey library of Gal4-AD fused to random, 1kb fragments of *L. monocytogenes* gDNA. The prey library constructed encoded >100,000 unique prey-fusion proteins. 81 proteins activated 2 Y2H reporters and 60 proteins activated all 4 of the reporter genes. Orfs were considered as candidates if they activated at least 2 Y2H reporters and encoded an annotated fusion protein > 10 amino acids in length (Table 3.3). The intersection of the affinity purification and Y2H data sets identified five candidates: pyruvate dehydrogenase (dihydrolipoamide acetyltransferase E2 subunit) (*pdhC*), ribosomal protein L3 (*rplC*), ribosomal protein S3 (*rpsC*), Phenylalanine-tRNA ligase beta subunit (*pheT*), and a predicted NADH dehydrogenase (*Imo2638*). For four of these candidates the Y2H bait-prey interaction was quantified by measuring the α -galactosidase reporter. By comparing prey interactions with either the Gal4-BD or Gal4-BD-PstA fusion protein the specificity of the interaction was demonstrated (Figure 3.7B).

We chose to focus on the interaction between PstA and PdhC, the lipoic acid utilizing E2 subunit of the pyruvate dehydrogenase complex (PDHC). The PDHC is a massive icosahedral protein complex made up of 4 individual proteins (PdhABCD) that form 3 catalytic subunits (E1, E2, and E3) and exceeds 4.5 MDa in related organisms. Pyruvate is decarboxylated by PDHC to acetyl-CoA releasing CO₂ and reducing NAD⁺ to NADH. Despite the robust interaction between PdhC and PstA in the Y2H, we were unable to Co-IP the two proteins or demonstrate a difference in PDHC catalytic activity in the presence of PstA (data not show).

A third orthogonal approach to identifying the PstA interacting protein was undertaken by coating Ni-NTA agarose beads with recombinant 6xhistidine tagged PstA produced in *E. coli*, and then applying lysates from $\Delta dacA \Delta pstA$ *L. monocytogenes*. Proteins that interacted with the PstA-resin were then eluted with 100 μ M c-di-AMP, concentrated, separated by SDS-PAGE, and then identified by in-gel tryptic digest/mass spectrometry. The results (Table 3.4) identified Lmo2638 as the most highly enriched protein identified. Lmo2638 was also identified by Y2H (Table 3.3) and by pull-down (Table 3.2). However, the Lmo2638::himar1 mutation (Whiteley et al., 2015) did not alter *dacA* essentiality nor did the mutation reverse the suppressive nature of the $\Delta pstA$ mutation to $\Delta dacA$. Full length Lmo2638 could not be produced recombinantly (data not shown)(Sureka et al., 2014) and affinity tagged *lmo2638* expressed in *L. monocytogenes* could not be detected by western blot (data not shown).

Acetyl-CoA activation of PycA and is toxic to $\Delta dacA$ mutants

The only mutation identified that suppressed *dacA* essentiality on rich media and sensitivity to β -lactam antibiotics was $\Delta pstA$. However, we were unable to determine any PstA-protein interactions with high confidence. To further understand the mechanism of PstA we searched for mutations that suppressed toxicity of rich media and β -lactam antibiotics in a $\Delta dacA$ mutant merodiploid for *pstA* ($\Delta dacA$ p-*pstA*) (Figure 3.8A). Genome sequencing of 16 suppressor mutants revealed that 15 strains harbored mutations in pyruvate carboxylase (*pycA*)(Table 3.5). PycA converts pyruvate and CO₂ to oxaloacetate using a biotin cofactor and hydrolysis of ATP. In *L. monocytogenes* PycA is the only enzyme capable of producing oxaloacetate due to an incomplete TCA cycle and other metabolic insufficiencies (Figure 3.8B).

PycA is allosterically activated and inhibited by a diverse set of metabolites including inhibition by c-di-AMP. All of the PycA suppressor mutations identified encoded point mutations, which were modeled onto the crystal structure of PycA from *L. monocytogenes* (Figure 3.8D) or homologous residues on the PycA structure from *Staphylococcus aureus* (Figure 3.8E). None of the mutations appeared close to the biotin cofactor or the c-di-AMP binding site (Figure 3.8D). Instead, many of the mutations clustered near the binding site of acetyl-CoA (Figure 3.8E). Two of the mutations, R1051C and R367L, are predicted to directly disrupt two of the four arginine residues that form hydrogen bonds between the phosphates of acetyl-CoA and PycA in a crystal structure from *S. aureus* PycA (Figure 3.8F). In a previous report, mutating one of the other arginine residues in the binding pocket led to an inability of Acetyl-CoA to activate PycA *in vitro* (Xiang and Tong, 2008). Accordingly, R1051C and R367L mutations also resulted in an inability of acetyl-CoA to activate PycA *in vitro* (Figure 3.8G). The two arginine mutations identified were selected from the screen and reconstructed in *L. monocytogenes* by complementing a $\Delta pycA$ strain. PycA protein levels were unaffected in these strains (Figure 3.9A) and when *dacA* was deleted the PycA mutations recapitulated phenotypes from the genetic screen (Figure 3.9B and C). These data suggest a model where PycA is over-active in the absence of c-di-AMP due to activation of the protein by acetyl-CoA, which underlies the $\Delta dacA$ mutant's sensitivity to rich media and β -lactam antibiotics.

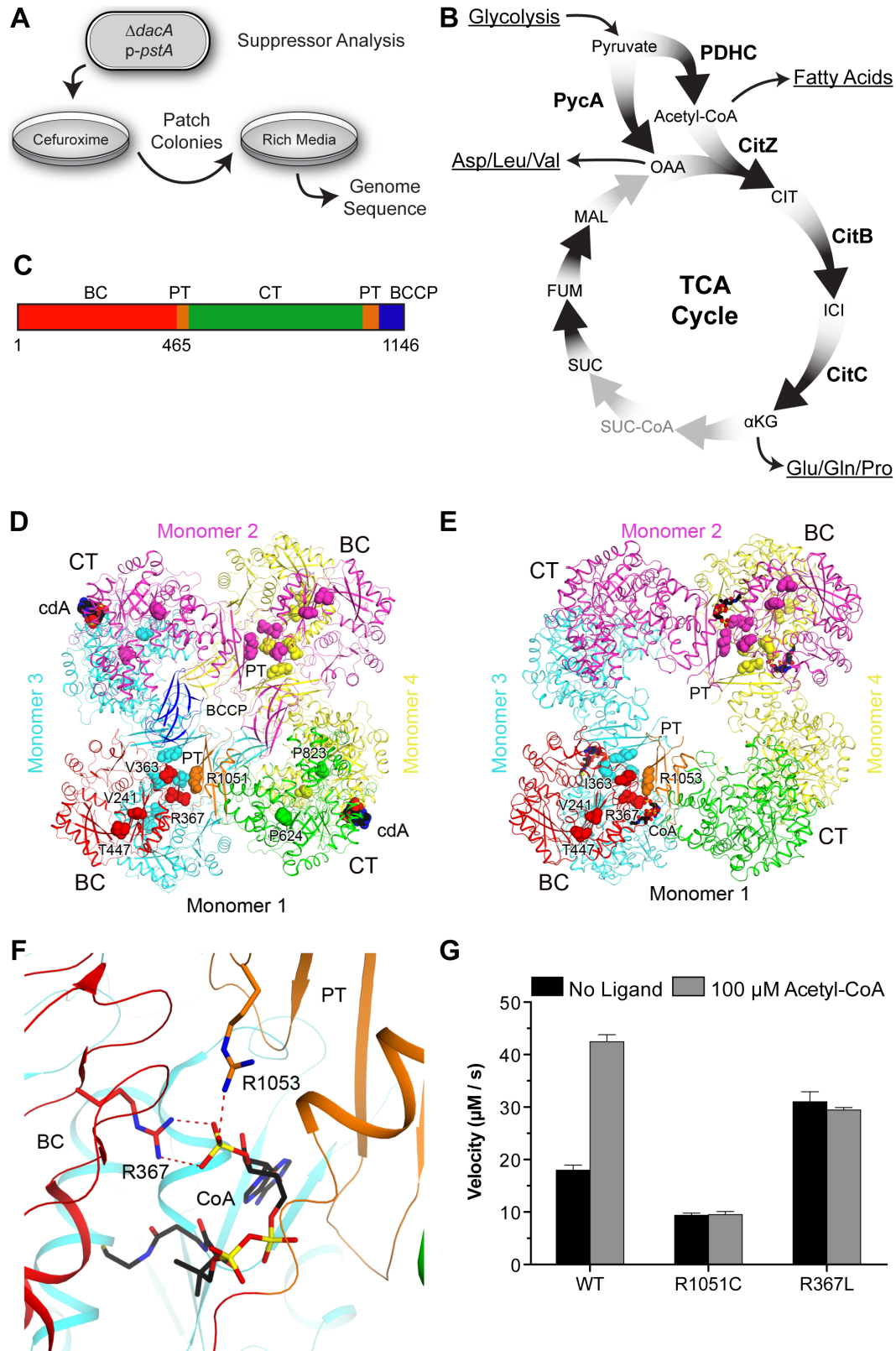


Figure 3.8 Suppressor analysis of cefuroxime resistance in $\Delta dacA$ $p\text{-}pstA$

(A) Illustration of suppressor analysis. (B) Schematic of central metabolism in *L. monocytogenes*. Grey arrows

indicate enzymes not encoded in the genome, bold labels indicate enzyme names, and non-bold labels indicate metabolites. Underlined labels indicate metabolic pathways providing or using precursors/products of the enzymes shown. (C) PycA color-coded protein domains and amino acid addresses showing the biotin carboxylase (BC), PC tetramerization (PT), carboxyltransferase (CT), and biotin carboxyl carrier protein (BCCP) protein domains. (D) Crystal structure of PycA (PDB: 4QSH, (Sureka et al., 2014)) from *L. monocytogenes* with modeled suppressor mutations on all four monomers. Monomer 1 is colored as in (C) and only mutations on this monomer are labeled. The resolved c-di-AMP (cdA) and water molecules (shown in red) are shown and labeled. (E) Crystal structure of PycA homolog from *S. aureus* (PDB: 3HO8, (Yu et al., 2009)) with modeled suppressor mutations at homologous residues on all four monomers. Monomer 1 is colored as in (C) and only mutations on this monomer are labeled. The resolved coenzyme A ligands are also shown. (F) Detailed view of (E) interactions between the homologous arginine residues to R367 and R1051 and coenzyme A, with hydrogen bonds as dashed red lines. (G) Enzymatic activity of PycA alleles in the absence or presence of the allosteric activator acetyl-CoA. Data are the mean \pm s.e.m. of $n \geq 3$ independent experiments.

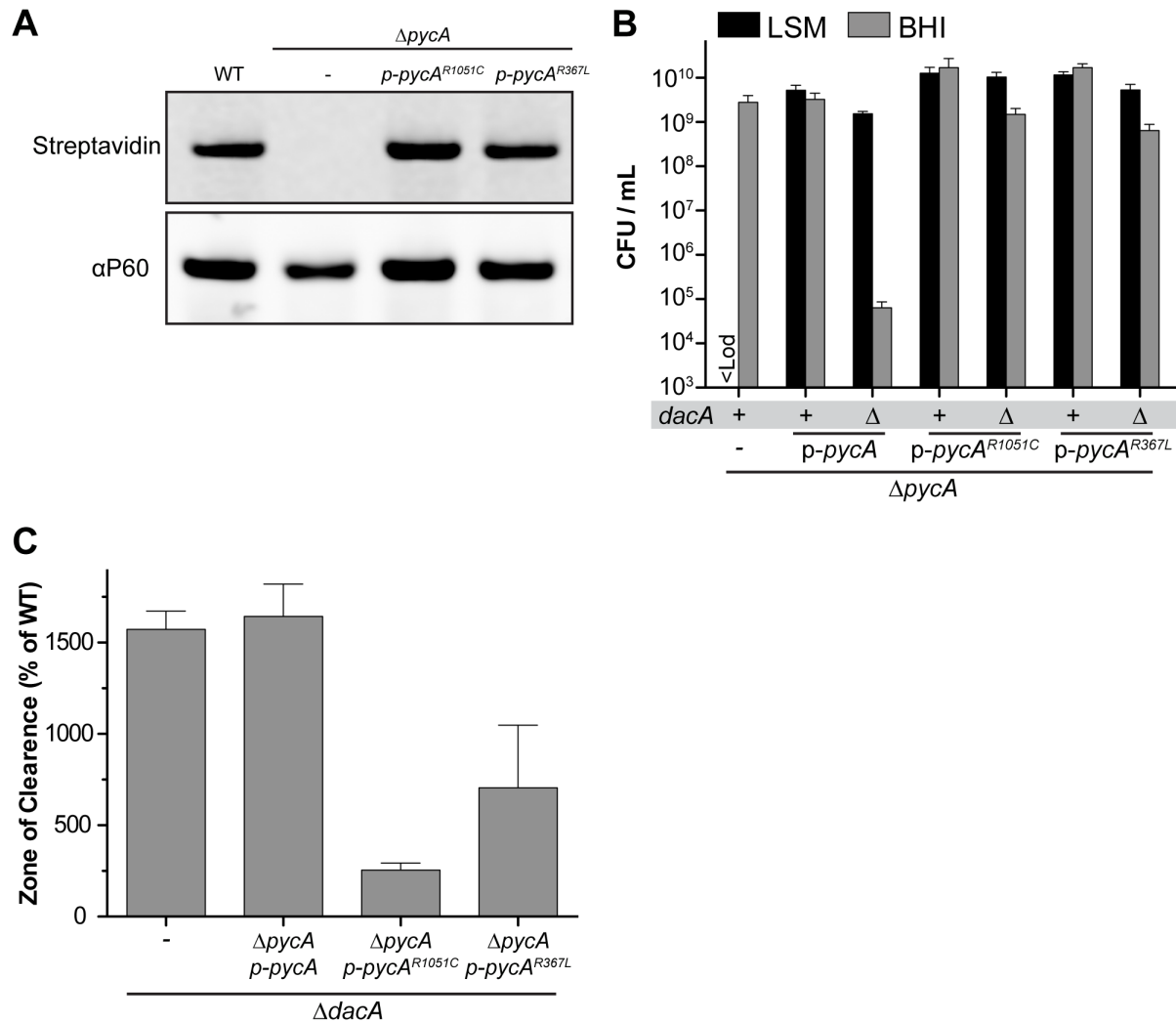


Figure 3.9 Mutations eliminating acetyl-CoA activation of PycA suppress $\Delta dacA$ sensitivity of rich media and cefuroxime

(A) Immunoblot of P60 (loading control) and biotinylated proteins using streptavidin. Data are representative of three independent experiments. (B) Enumeration of CFU on indicated media for *L. monocytogenes* strains constructed in LSM. (C) Cefuroxime disk diffusion on LSM-agar of *L. monocytogenes* strains. (B and C) Data are the mean \pm s.e.m. of $n \geq 3$ independent experiments.

Toxicity of TCA cycle intermediates

c-di-AMP inhibits PycA and upon depletion of the *dacA* gene the increased production of oxaloacetate leads to an accumulation of glutamate/glutamine (Sureka et al., 2014)(Figure 3.8B). Disruption of citrate synthase, the first step of the *L. monocytogenes* TCA cycle is sufficient to abolish the enhanced production of glutamate/glutamine. Glutamate has a well-documented role in osmoprotection and we hypothesized that changes in glutamate levels might underlie the defects of the $\Delta dacA$ mutant for growth in rich media and resistance to cell wall acting antibiotics. In line with this hypothesis, *citZ* mutations suppressed $\Delta dacA$ growth in rich media and resistance to cefuroxime (Figure 3.10A and B). However, mutations in *citB* and *citC*, the next two steps of the TCA cycle (Figure 3.8B), did not phenocopy the *citZ* mutation (Figure 3.10A and B). These results suggest that accumulation of citrate, not products of α KG such as glutamate, are responsible for the observed $\Delta dacA$ phenotypes.

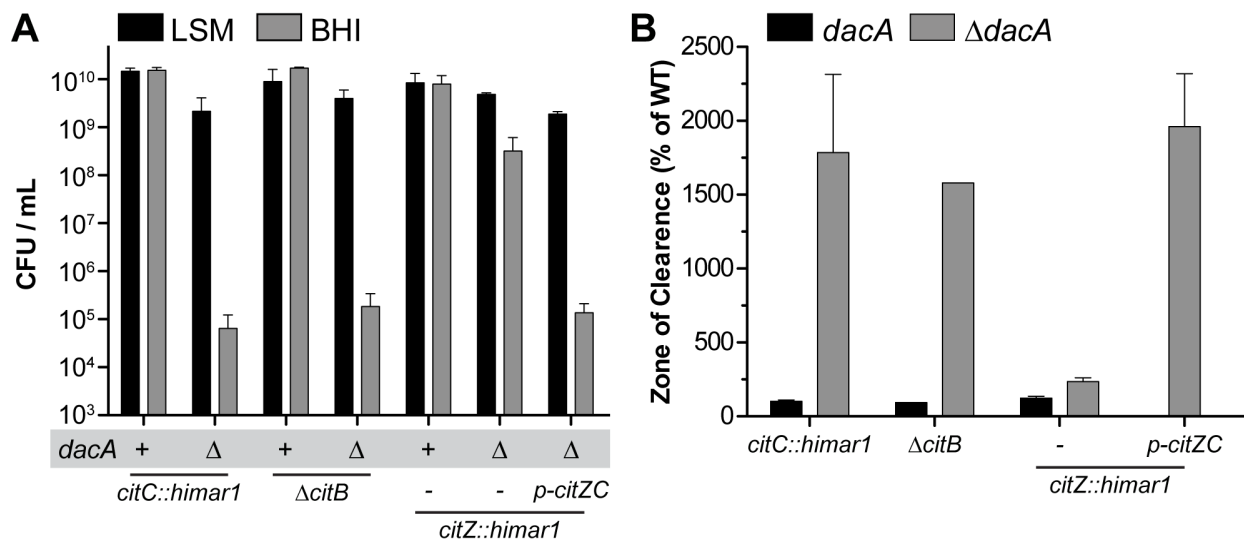


Figure 3.10 TCA cycle intermediates are toxic in the absence of c-di-AMP

(A) Enumeration of CFU on indicated media for *L. monocytogenes* strains constructed in LSM. (B) Cefuroxime disk diffusion on LSM-agar of *L. monocytogenes* strains. *dacA* vs. $\Delta dacA$ indicates either a mutation in a wild-type or c-di-AMP deficient background. All data are mean \pm s.e.m of $n \geq 3$ independent experiments.

$\Delta dacA$ virulence defects

The “pyruvate node” encompassing PDHC and PycA is central to growth of *L. monocytogenes* in both nutrient poor conditions and during growth within a mammalian host (O’Riordan et al., 2003; Schär et al., 2010). Data presented here and published previously have demonstrated that c-di-AMP is a negative regulator of the pyruvate node and decreases flux from pyruvate into the TCA cycle (Sureka et al., 2014). Yet mutants lacking either *pycA*, *dacA*, or only the catalytic activity of DacA are avirulent (Figure 3.11A). We hypothesized that c-di-AMP levels tune PycA to balance allosteric activation by acetyl-CoA during infection. Accordingly, mutations that disrupted PycA activation by acetyl-CoA suppressed the virulence defect of the $\Delta dacA$ mutant (Figure 3.11B).

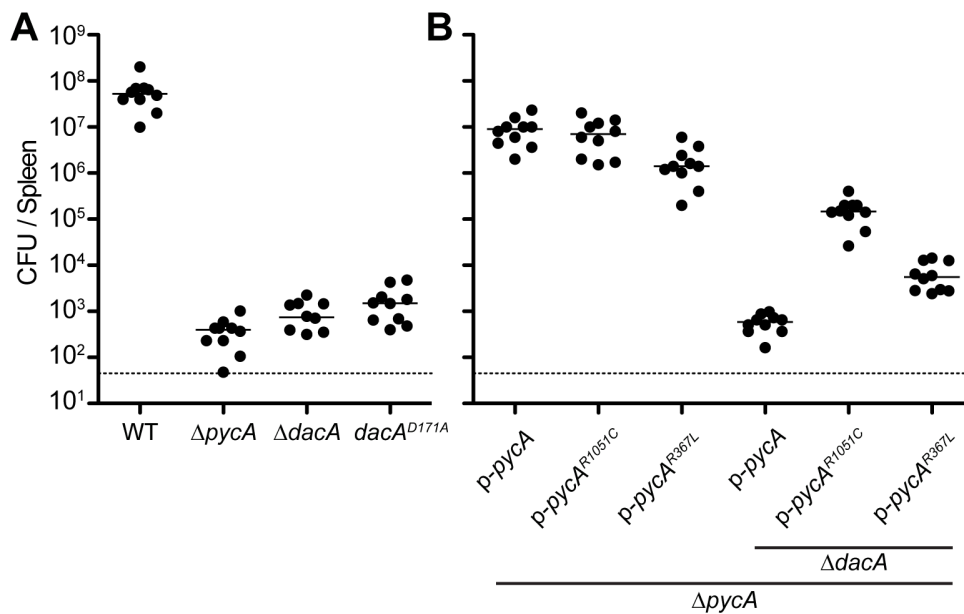


Figure 3.11 *pycA* mutations suppress the $\Delta dacA$ virulence defect

(A and B) CFU recovered at 48hrs from spleens of CD-1 mice infected with 10⁵ CFU of the indicated strains. All data are pooled results from two independent experiments of n = 5 mice.

Table 3.1 Listeria Synthetic Media Recipe

Stock Name	Stock Dil. Factor	Stock Volume (mL)	Ingredient	Final Conc. in M or (µM)	MW (g/mol)	Final Conc. (g/L)	Total in Stock (g)
MOPS (pH 7.5)^a	10	1000	MOPS	0.1000	209.3	20.93	209.3
Glucose	40	1000	Glucose	0.0555	180.2	10	400
Phosphate	100	500	KH ₂ PO ₄	0.0048	136.1	0.656	32.8
			Na ₂ HPO ₄ • 7H ₂ O	0.0115	268.1	3.096	154.8
Magnesium	100	500	MgSO ₄ • 7H ₂ O	0.0017	246.5	0.409	20.45
Micro-Nutrients^b	100	500	Biotin	(2.05)	244.3	0.0005	0.025
			Riboflavin	(1.33)	376.3	0.0005	0.025
			Para-Aminobenzoic Acid	(7.29)	137.1	0.001	0.05
			Lipoic Acid	(0.02)	206.3	0.000005	0.00025
			Niacinamide/Nicotinamide	(8.19)	122.12	0.001	0.05
			D-Pantothenic Acid (hemicalcium)	(4.20)	238.27	0.001	0.05
			Pyridoxal • HCl	(4.91)	203.62	0.001	0.05
			Thiamine • HCl	(2.96)	337.27	0.001	0.05
Minimum Amino Acids^c	50	500	L-Arginine • HCl	0.0005	210	0.1	2.5
			L-Histidine • HCl • H ₂ O	0.0005	209.6	0.1	2.5
			DL-Isoleucine	0.0008	131.17	0.1	2.5
			L-Leucine	0.0008	131.17	0.1	2.5
			DL-Methionine	0.0007	149.21	0.1	2.5
			L-Phenylalanine	0.0006	165.19	0.1	2.5
			L-Tryptophan	0.0005	204.23	0.1	2.5
			DL-Valine	0.0009	117.15	0.1	2.5
Optional "Complete" Amino Acids^d	50	500	Alanine	0.0011	89.09	0.1	2.5
			Asparagine	0.0008	132.12	0.1	2.5
			Aspartic Acid	0.0008	133.1	0.1	2.5
			Glutamic Acid	0.0007	147.13	0.1	2.5
			Glycine	0.0013	75.07	0.1	2.5
			Lysine	0.0007	146.19	0.1	2.5
			Proline	0.0009	115.13	0.1	2.5
			Serine	0.0010	105.09	0.1	2.5
			Threonine	0.0008	119.12	0.1	2.5
			Tyrosine	0.0006	181.19	0.1	2.5
Adenine^e	100	500	Adenine	(18.50)	135.13	0.0025	0.125
Trace Metals	100	500	FeCl ₂ • 4H ₂ O	(5)	198.8	0.00099	0.050
			MnSO ₄ • H ₂ O	(50)	169.0	0.00845	0.423
			ZnSO ₄ • 7H ₂ O	(1)	287.6	0.00029	0.014
			CaCl ₂ • 2H ₂ O	(10)	147.0	0.00147	0.074
			CuSO ₄ • 5H ₂ O	(0.1)	249.7	0.00002	0.001
			CoCl ₂ • 7H ₂ O	(0.1)	281.1	0.00003	0.001
			H ₃ BO ₃	(0.1)	61.8	0.00001	0.0003
			Na ₂ MoO ₄ • 2H ₂ O	(0.1)	242.0	0.00002	0.001
			NaCl	0.008555784	58.44	0.50000	25
			Sodium Citrate (Tri-Sodium Salt)	(100)	294.1	0.02941	1.471
Added Fresh^f			L-Cysteine • 2HCl	(634.44)	157.62	0.1	
			L-Glutamine	(4105.65)	146.14	0.6	

Table 3.1 Listeria Synthetic Media Recipe

Listeria synthetic media (LSM) is made by combining each of the stock solutions based on the appropriate dilution factor in the order that they are listed above. LSM is stable at 2x concentration, which can be used for making media-agar. Filter-sterilize all stock solutions and final LSM. LSM can be made with either the stock of 8 “minimum” amino acids (incomplete or iLSM) or it can be made with the stock of the full 18 amino acids (complete or cLSM). cLSM supports more robust growth of strains but may be inappropriate for some metabolic studies. LSM is stable at 1x for approximately 6 weeks. See notes below for these stocks solutions.

^a Adjust the pH of the MOPS stock solution to 7.5 with approximately 61 ± 2 mL of 10N NaOH.

^b Dissolve all stock components in boiling water prior to filter sterilization.

^c Dissolve the 8 minimum amino acids in hot 0.5N NaOH, this stock is the “minimum amino acid” stock.

^d Dissolve the minimum 8 amino acids plus the addition 10 amino acids in hot 0.5N NaOH, this stock is the “complete amino acid” stock.

^e Dissolve the adenine in 40mL of 0.2N HCl, then dilute to final concentration in water.

^f Add these ingredients fresh to LSM, they cannot be prepared as stock solutions.

Table 3.2 Tryptic Peptides identified by pull-down of PstA

Gene Name	10403S Locus	EGD-e Locus	Protein name	Uniprot Entry	Negative ^a			Positive ^b		
					1	2	3	1	2	3
<i>tuf</i>	LMRG_02198	Imo2653	Elongation factor Tu (EF-Tu)	A0A0H3GG29_LISM4	1	3	0	23	31	15
<i>oppA</i>	LMRG_01636	Imo2196	Peptide/nickel transport system substrate-binding protein	A0A0H3GJB6_LISM4	1	4	0	20	38	0
<i>pycA</i>	LMRG_00534	Imo1072	Pyruvate carboxylase (EC 6.4.1.1)	A0A0H3GJD4_LISM4	19	12	0	13	39	0
<i>rpoC</i>	LMRG_02650	Imo0259	DNA-directed RNA polymerase subunit beta' (RNAP subunit beta') (EC 2.7.7.6)	A0A0H3G8X2_LISM4	0	0	0	9	13	27
<i>pstA</i>	LMRG_02239	Imo2692	Uncharacterized protein	A0A0H3GKU4_LISM4	7	6	4	15	14	16
<i>rpoB</i>	LMRG_02651	Imo0258	DNA-directed RNA polymerase subunit beta (RNAP subunit beta) (EC 2.7.7.6)	A0A0H3GHC0_LISM4	0	0	0	10	17	18
<i>rocG</i>	LMRG_00242	Imo0560	Glutamate dehydrogenase	A0A0H3GI25_LISM4	0	0	0	5	20	19
<i>glnA</i>	LMRG_00749	Imo1299	Glutamine synthetase (EC 6.3.1.2)	A0A0H3GG00_LISM4	0	0	0	20	9	7
<i>glnK</i>	LMRG_01453	Imo1517	Nitrogen regulatory protein P-II	A0A0H3GH23_LISM4	0	0	0	18	6	10
<i>fusA</i>	LMRG_02199	Imo2654	Elongation factor G (EF-G)	A0A0H3GNN6_LISM4	0	0	0	10	15	7
<i>groEL</i>	LMRG_01218	Imo2068	60 kDa chaperonin (GroEL protein) (Protein Cpn60)	A0A0H3GLZ0_LISM4	0	0	0	17	10	5
<i>pflB</i>	LMRG_00858	Imo1406	Formate acetyltransferase	A0A0H3GG91_LISM4	0	0	0	26	1	0
<i>rpsC</i>	LMRG_02170	Imo2626	30S ribosomal protein S3	A0A0H3GJE8_LISM4	0	0	0	6	11	6
<i>dnaK</i>	LMRG_00926	Imo1473	Chaperone protein DnaK (HSP70) (Heat shock 70 kDa protein) (Heat shock protein 70)	DNAK_LISM4	0	0	0	8	9	4
<i>rpoA</i>	LMRG_02150	Imo2606	DNA-directed RNA polymerase subunit alpha (RNAP subunit alpha) (EC 2.7.7.6)	A0A0H3GJC8_LISM4	0	0	0	5	6	8
<i>gap</i>	LMRG_01789	Imo2459	Glyceraldehyde-3-phosphate dehydrogenase (EC 1.2.1.-)	A0A0H3GFI9_LISM4	0	0	0	5	7	6
<i>purB</i>	LMRG_02498	Imo1773	Adenylosuccinate lyase (ASL) (EC 4.3.2.2) (Adenylosuccinase)	A0A0H3GL17_LISM4	0	0	0	12	3	2
<i>hup</i>	LMRG_01081	Imo1934	DNA-binding protein HU-beta	A0A0H3GDE3_LISM4	0	2	0	8	6	3
<i>csxA</i>	LMRG_02289	Imo0866	DEAD-box ATP-dependent RNA helicase CshA (EC 3.6.4.13)	A0A0H3GAJ1_LISM4	0	0	0	7	7	3
<i>rpsD</i>	LMRG_01371	Imo1596	30S ribosomal protein S4	A0A0H3GGL2_LISM4	0	0	0	2	9	5
<i>infC</i>	LMRG_02827	Imo1785	Translation initiation factor IF-3	A0A0H3GH52_LISM4	0	0	0	6	7	2
<i>recA</i>	LMRG_00850	Imo1398	Protein RecA (Recombinase A)	RECA_LISM4	0	0	0	7	6	1
<i>rplN</i>	LMRG_02166	Imo2622	50S ribosomal protein L14	A0A0H3GKP3_LISM4	0	0	0	0	7	5
<i>pdhD</i>	LMRG_00517	Imo1055	Dihydrolipoyl dehydrogenase (EC 1.8.1.4)	A0A0H3GFQ3_LISM4	0	0	0	5	6	1
	LMRG_01069	Imo1922	Uncharacterized protein	A0A0H3GE07_LISM4	0	0	0	5	2	5
<i>ftsH</i>	LMRG_02642	Imo0220	ATP-dependent zinc metalloprotease FtsH (EC 3.4.24.-)	A0A0H3G8Q4_LISM4	0	0	0	3	9	0
<i>pdhC</i>	LMRG_00516	Imo1054	Pyruvate dehydrogenase E2 component	A0A0H3GFB2_LISM4	0	0	0	5	6	0
	LMRG_01114	Imo1967	Uncharacterized protein	A0A0H3GE60_LISM4	0	0	0	8	3	0
	LMRG_00085	Imo0392	UPF0365 protein LMRG_00085	A0A0H3GHN5_LISM4	0	0	0	5	6	0
<i>nrdE</i>	LMRG_01677	Imo2155	Ribonucleoside-diphosphate reductase (EC 1.17.4.1)	A0A0H3GI40_LISM4	0	0	0	4	5	1
<i>cysK</i>	LMRG_02645	Imo0223	Cysteine synthase (EC 2.5.1.47)	A0A0H3G9A7_LISM4	0	0	0	1	6	3
<i>ldh</i>	LMRG_02632	Imo0210	L-lactate dehydrogenase	A0A0H3G8P6_LISM4	0	0	0	4	4	2
<i>sigA</i>	LMRG_00906	Imo1454	RNA polymerase sigma factor SigA	A0A0H3GC51_LISM4	0	0	0	2	4	4
	LMRG_02183	Imo2638	NADH dehydrogenase	A0A0H3GG15_LISM4	0	0	0	2	6	2
<i>uvrA</i>	LMRG_01760	Imo2488	UvrABC system protein A (UvrA protein) (Excinuclease ABC subunit A)	A0A0H3GKC7_LISM4	0	0	0	4	5	0
<i>infB</i>	LMRG_00775	Imo1325	Translation initiation factor IF-2	A0A0H3GGJ4_LISM4	0	0	0	3	4	2
<i>atpD</i>	LMRG_01719	Imo2529	ATP synthase subunit beta (EC 3.6.3.14)	A0A0H3GFR1_LISM4	0	0	0	4	5	0

<i>rny</i>	LMRG_00851	<i>Imo1399</i>	Ribonuclease Y (RNase Y) (EC 3.1.-.-)	RNY_LISM4	0	0	0	4	5	0
<i>rplD</i>	LMRG_02175	<i>Imo2631</i>	50S ribosomal protein L4	A0A0H3GJF3_LISM4	0	0	0	2	4	3
<i>pgdA</i>	LMRG_00107	<i>Imo0415</i>	Peptidoglycan N-acetylglucosamine deacetylase	A0A0H3GDH9_LISM4	0	0	0	8	1	0
	LMRG_01700	<i>Imo2547</i>	Homoserine dehydrogenase (EC 1.1.1.3)	A0A0H3GJ71_LISM4	0	0	0	5	0	3
	LMRG_01691	<i>Imo2556</i>	Fructose-16-bisphosphate aldolase class II	A0A0H3GF41_LISM4	0	0	0	5	2	1
<i>citZ</i>	LMRG_01400	<i>Imo1567</i>	Citrate synthase	A0A0H3GH71_LISM4	0	0	0	2	3	3
<i>oppF</i>	LMRG_01640	<i>Imo2192</i>	Oligopeptide transport ATP-binding protein oppF	A0A0H3GER9_LISM4	0	0	0	0	7	1
<i>lemA</i>	LMRG_02061	<i>Imo0962</i>	LemA protein	A0A0H3GF24_LISM4	0	0	0	4	4	0
<i>clpC</i>	LMRG_02674	<i>Imo0232</i>	ATP-dependent Clp protease ATP-binding subunit ClpC	A0A0H3GCZ0_LISM4	0	0	0	1	0	6
<i>pykA</i>	LMRG_01397	<i>Imo1570</i>	Pyruvate kinase (EC 2.7.1.40)	A0A0H3GCE6_LISM4	0	0	0	5	2	0
	LMRG_01834	<i>Imo2414</i>	FeS assembly protein SufD	A0A0H3GFE5_LISM4	0	0	0	1	5	1
<i>rplA</i>	LMRG_02657	<i>Imo0249</i>	50S ribosomal protein L1	A0A0H3G9H4_LISM4	0	0	0	2	3	2
<i>pdhB</i>	LMRG_00515	<i>Imo1053</i>	Pyruvate dehydrogenase E1 component subunit beta	A0A0H3GB08_LISM4	0	0	0	2	4	1
	LMRG_02558	<i>Imo1711</i>	Aminopeptidase	A0A0H3GKU9_LISM4	0	0	0	5	2	0
	LMRG_01240	<i>Imo2089</i>	Esterase/lipase	A0A0H3GDU3_LISM4	0	0	0	1	4	2
	LMRG_00412	<i>Imo0723</i>	Methyl-accepting chemotaxis protein	A0A0H3GEQ4_LISM4	0	0	0	1	5	1
<i>glyA</i>	LMRG_01708	<i>Imo2539</i>	Serine hydroxymethyltransferase (SHMT) (Serine methylase) (EC 2.1.2.1)	A0A0H3GFS1_LISM4	0	0	0	2	4	0
<i>purH</i>	LMRG_02506	<i>Imo1765</i>	Bifunctional purine biosynthesis protein PurH Enolase (EC 4.2.1.11) (2-phospho-D-glycerate hydro-lyase) (2-phosphoglycerate dehydratase)	A0A0H3GH29_LISM4	0	0	0	3	3	0
<i>eno</i>	LMRG_01793	<i>Imo2455</i>		A0A0H3GN27_LISM4	0	0	0	4	2	0
<i>ccpA</i>	LMRG_01368	<i>Imo1599</i>	Catabolite control protein A Inosine-5'-monophosphate dehydrogenase (IMP dehydrogenase) (IMPD) (IMPDH) (EC 1.1.1.205)	A0A0H3GCH8_LISM4	0	0	0	3	2	1
<i>guaB2</i>	LMRG_01938	<i>Imo2758</i>		A0A0H3GL03_LISM4	0	0	0	2	3	1
<i>pdhA</i>	LMRG_00514	<i>Imo1052</i>	Pyruvate dehydrogenase E1 component	A0A0H3GJB7_LISM4	0	0	0	2	4	0
	LMRG_01907	<i>Imo2790</i>	ParB family chromosome partitioning protein	A0A0H3GGI6_LISM4	0	0	0	4	2	0
<i>rpsQ</i>	LMRG_02167	<i>Imo2623</i>	30S ribosomal protein S17	A0A0H3GFZ9_LISM4	0	0	0	0	5	1
<i>codY</i>	LMRG_00730	<i>Imo1280</i>	GTP-sensing transcriptional pleiotropic repressor CodY	A0A0H3GGF1_LISM4	0	0	0	4	2	0
<i>rplV</i>	LMRG_02171	<i>Imo2627</i>	50S ribosomal protein L22	A0A0H3GKP7_LISM4	0	0	0	2	3	1
	LMRG_00954	<i>Imo1807</i>	3-oxoacyl-[acyl-carrier-protein] reductase	A0A0H3GL80_LISM4	0	0	0	4	2	0
<i>rnj</i>	LMRG_00886	<i>Imo1434</i>	Ribonuclease J (RNase J) (EC 3.1.-.-)	A0A0H3GC32_LISM4	0	0	0	2	2	2
	LMRG_00801	<i>Imo1351</i>	Uncharacterized protein	A0A0H3GCF6_LISM4	0	0	0	3	3	0
			ATP-dependent 6-phosphofructokinase (ATP-PFK) (Phosphofructokinase) (EC 2.7.1.11)	A0A0H3GGK1_LISM4	0	0	0	4	1	0
<i>pfkA</i>	LMRG_01396	<i>Imo1571</i>		A0A0H3GGT0_LISM4	0	0	0	2	3	0
<i>menB</i>	LMRG_01294	<i>Imo1673</i>	1,4-dihydroxy-2-naphthoyl-CoA synthase (DHNA-CoA synthase) (EC 4.1.3.36)	A0A0H3GDI8_LISM4	0	0	0	2	2	1
<i>rplS</i>	LMRG_02811	<i>Imo1787</i>	50S ribosomal protein L19	A0A0H3GID4_LISM4	0	0	0	3	1	1
<i>asnS</i>	LMRG_01043	<i>Imo1896</i>	Asparagine--tRNA ligase (EC 6.1.1.22) (Asparaginyl-tRNA synthetase)	A0A0H3GGV1_LISM4	0	0	0	1	2	2
	LMRG_00888	<i>Imo1436</i>	Aspartokinase (EC 2.7.2.4)	A0A0H3GIQ2_LISM4	0	0	0	2	3	0
<i>ftsZ</i>	LMRG_01181	<i>Imo2032</i>	Cell division protein FtsZ	A0A0H3GCW9_LISM4	0	0	0	2	3	0
	LMRG_01422	<i>Imo1548</i>	Rod shape-determining protein mreB	A0A0H3GHA5_LISM4	0	0	0	3	2	0
	LMRG_01366	<i>Imo1601</i>	Uncharacterized protein	A0A0H3GMC5_LISM4	0	0	0	2	3	0
<i>oppD</i>	LMRG_01639	<i>Imo2193</i>	Peptide/nickel transport system ATP-binding protein	A0A0H3GE77_LISM4	0	0	0	3	1	1
	LMRG_00349	<i>Imo0662</i>	Phosphomethylpyrimidine kinase	A0A0H3GG09_LISM4	0	0	0	1	2	1
<i>rpsJ</i>	LMRG_02177	<i>Imo2633</i>	30S ribosomal protein S10	A0A0H3GHH8_LISM4	0	0	0	3	1	0
<i>rpsB</i>	LMRG_01309	<i>Imo1658</i>	30S ribosomal protein S2							

<i>dnaJ</i>	LMRG_00925	<i>Imo1472</i>	Chaperone protein DnaJ	DNAJ_LISM4	0	0	0	2	1	1
	LMRG_01451	<i>Imo1519</i>	Aspartyl-tRNA synthetase	A0A0H3GKF2_LISM4	0	0	0	1	3	0
<i>tigL</i>	LMRG_00716	<i>Imo1267</i>	Trigger factor (TF) (EC 5.2.1.8) (PPlase)	A0A0H3GJU5_LISM4	0	0	0	2	2	0
	LMRG_00240	<i>Imo0558</i>	6-phosphogluconolactonase	A0A0H3GE90_LISM4	0	0	0	2	2	0
	LMRG_00828	<i>Imo1376</i>	6-phosphogluconate dehydrogenase, decarboxylating (EC 1.1.1.44)	A0A0H3GCI0_LISM4	0	0	0	2	1	0
			Chorismate synthase (CS) (EC 4.2.3.5) (5-enolpyruvylshikimate-3-phosphate phospholyase)	A0A0H3GLH8_LISM4	0	0	0	1	2	0
<i>aroC</i>	LMRG_01075	<i>Imo1928</i>		A0A0H3GGR6_LISM4	0	0	0	2	1	0
<i>tsf</i>	LMRG_01310	<i>Imo1657</i>	Elongation factor Ts (EF-Ts)	A0A0H3GDS8_LISM4	1	1	1	1	1	1
	LMRG_01225	<i>Imo2074</i>	Uncharacterized protein	A0A0H3GG48_LISM4	0	0	0	1	2	0
<i>pheT</i>	LMRG_00668	<i>Imo1222</i>	Phenylalanine--tRNA ligase beta subunit (EC 6.1.1.20)	A0A0H3GN84_LISM4	0	0	0	2	1	0
<i>secA</i>	LMRG_01738	<i>Imo2510</i>	Protein translocase subunit SecA	RS21_LISM4	0	0	0	0	2	1
<i>rpsU</i>	LMRG_00922	<i>Imo1469</i>	30S ribosomal protein S21	A0A0H3GFY0_LISM4	0	0	0	1	2	0
<i>rpsM</i>	LMRG_02152	<i>Imo2608</i>	30S ribosomal protein S13	A0A0H3GCZ5_LISM4	0	0	0	1	2	0
<i>gltX</i>	LMRG_02669	<i>Imo0237</i>	Glutamate--tRNA ligase (EC 6.1.1.17) (Glutamyl-tRNA synthetase)	A0A0H3GPA0_LISM4	0	0	0	2	1	0
	LMRG_01906	<i>Imo2791</i>	Chromosome partitioning protein	A0A0H3GHS6_LISM4	0	0	0	1	2	0
<i>murD</i>	LMRG_01185	<i>Imo2036</i>	UDP-N-acetylmuramoylalanine--D-glutamate ligase (EC 6.3.2.9)	A0A0H3GA40_LISM4	0	0	0	2	1	0
<i>glmS</i>	LMRG_00415	<i>Imo0727</i>	Glutamine--fructose-6-phosphate aminotransferase [isomerizing] (EC 2.6.1.16)	A0A0H3GCL8_LISM4	0	0	0	1	1	1
	LMRG_00875	<i>Imo1423</i>	Uncharacterized protein	A0A0H3GE11_LISM4	0	0	0	1	2	0
	LMRG_01678	<i>Imo2154</i>	Ribonucleoside-diphosphate reductase subunit beta (EC 1.17.4.1)	A0A0H3GKN2_LISM4	0	0	0	2	1	0
<i>rpsK</i>	LMRG_02151	<i>Imo2607</i>	30S ribosomal protein S11	A0A0H3GJH5_LISM4	0	0	0	1	2	0
<i>rpsL</i>	LMRG_02201	<i>Imo2656</i>	30S ribosomal protein S12	A0A0H3GKG1_LISM4	0	0	0	1	1	1
	LMRG_01441	<i>Imo1529</i>	Uncharacterized protein	A0A0H3GFB9_LISM4	0	0	0	0	2	1
<i>rplE</i>	LMRG_02164	<i>Imo2620</i>	50S ribosomal protein L5	A0A0H3GHF1_LISM4	0	0	0	2	1	0
	LMRG_02579	<i>Imo0292</i>	Uncharacterized protein	A0A0H3GH58_LISM4	0	0	0	1	0	1
<i>valS</i>	LMRG_01416	<i>Imo1552</i>	Valine--tRNA ligase (EC 6.1.1.9) (Valyl-tRNA synthetase)	A0A0H3GHB0_LISM4	0	0	0	1	1	0
	LMRG_00982	<i>Imo1835</i>	Carbamoyl-phosphate synthase (glutamine-hydrolyzing) (EC 6.3.5.5)	A0A0H3GD49_LISM4	0	0	0	1	0	1
<i>fnt</i>	LMRG_00970	<i>Imo1823</i>	Methionyl-tRNA formyltransferase (EC 2.1.2.9)	A0A0H3GD60_LISM4	0	0	0	1	1	0
<i>metG</i>	LMRG_02742	<i>Imo0177</i>	Methionine--tRNA ligase (EC 6.1.1.10) (Methionyl-tRNA synthetase)	A0A0H3GH60_LISM4	0	0	0	1	1	0
<i>prs</i>	LMRG_02621	<i>Imo0199</i>	Ribose-phosphate pyrophosphokinase (RPPK) (EC 2.7.6.1)	A0A0H3GFM2_LISM4	0	0	0	1	1	0
<i>uvrB</i>	LMRG_01759	<i>Imo2489</i>	UvrABC system protein B (Protein UvrB) (Excinuclease ABC subunit B)	A0A0H3GKP9_LISM4	0	0	0	0	1	1
<i>rplC</i>	LMRG_02176	<i>Imo2632</i>	50S ribosomal protein L3	A0A0H3GEZ9_LISM4	0	0	0	1	1	0
	LMRG_02030	<i>Imo0931</i>	Lipoate--protein ligase (EC 6.3.1.20)	A0A0H3GGT1_LISM4	0	0	0	1	1	0
	LMRG_00883	<i>Imo1431</i>	Uncharacterized protein	A0A0H3GGE6_LISM4	0	0	0	1	1	0
	LMRG_00944	<i>Imo1491</i>	Ribosome biogenesis GTPase YqeH	A0A0H3GEC3_LISM4	0	0	0	1	1	0
<i>ftsA</i>	LMRG_01182	<i>Imo2033</i>	Cell division protein FtsA	A0A0H3GNA3_LISM4	0	0	0	1	1	0
	LMRG_01723	<i>Imo2525</i>	Rod shape-determining protein MreB	A0A0H3GD11_LISM4	0	0	0	1	1	0
	LMRG_01365	<i>Imo1602</i>	Uncharacterized protein	A0A0H3GFJ9_LISM4	0	0	0	1	0	1
	LMRG_01779	<i>Imo2469</i>	APA family basic amino acid/polyamine antiporter							

Table 3.2 Tryptic Peptides identified by pull-down of PstA

Data correspond to tryptic peptides identified by pull-down of PstA-SII as described and documented in Figure 3.6.

^a Peptides identified from pull-downs of strains that did not express PstA-SII. Peptide counts correspond to lanes from Figure 3.6 where column 1 = lane 1, 2 = lane 3, 3 = lane 8.

b Peptides identified from pull-downs of strains that expressed PstA-SII. Peptide counts correspond to lanes from Figure 3.6 where column 1 = lane 2, 2 = lane 4, 3 = lane 9.

Table 3.3 Orfs interacting with PstA by yeast 2-hybrid

Inventory	Gene Name	10403S Locus	EGD-e Locus	Protein name	UniProt Entry	DDO/X/A Growth ^a	QDO/X/A Growth ^b
yAW005		LMRG_02335	Imo0086	Uncharacterized protein	A0A0H3GKY5_LISM4	Good	Good
yAW062		LMRG_02597	Imo0278	Maltose/maltodextrin transport system ATP-binding protein	A0A0H3G8Z2_LISM4	Good	OK
yAW044		LMRG_00018	Imo0325	Uncharacterized protein	A0A0H3GDN9_LISM4	Good	Good
yAW080		LMRG_00061	Imo0369	Probable transcriptional regulatory protein	A0A0H3GDD6_LISM4	Good	Good
yAW012	<i>aroD</i>	LMRG_00172	Imo0491	3-dehydroquininate dehydratase (3-dehydroquinase) (EC 4.2.1.10)	A0A0H3G9F2_LISM4	Good	Good
yAW057		LMRG_02879	Imo0528	Uncharacterized protein	A0A0H3GE58_LISM4	Poor	Good
yAW046A		LMRG_00212	Imo0530	Uncharacterized protein	A0A0H3GI01_LISM4	Good	Good
yAW006		LMRG_00357	Imo0669	Uncharacterized protein	A0A0H3GIB8_LISM4	Good	None
yAW025	<i>fliM</i>	LMRG_00388	Imo0699	Flagellar motor switch protein	A0A0H3GAL4_LISM4	Good	Good
yAW020		LMRG_00407	Imo0718	Uncharacterized protein	A0A0H3GEP9_LISM4	Good	Good
yAW023		LMRG_02265	Imo0842	Peptidoglycan bound protein	A0A0H3GES0_LISM4	Good	Good
yAW022	<i>liaS</i>	LMRG_02121	Imo1021	Sensor histidine kinase (EC 2.7.13.3)	A0A0H3GBK6_LISM4	Good	Good
yAW027	<i>pdhC</i> ^c	LMRG_00516	Imo1054	Pyruvate dehydrogenase E2 component	A0A0H3GFB2_LISM4	Good	Good
yAW055	<i>pycA</i>	LMRG_00534	Imo1072	Pyruvate carboxylase (EC 6.4.1.1)	A0A0H3GJD4_LISM4	Good	Good
yAW052		LMRG_00663	Imo1217	Aminopeptidase	A0A0H3GG43_LISM4	Good	Good
yAW053	<i>pheT</i> ^c	LMRG_00668	Imo1222	Phenylalanine--tRNA ligase beta subunit (EC 6.1.1.20)	A0A0H3GG48_LISM4	Poor	Good
yAW068		LMRG_00670	Imo1224	Uncharacterized protein	A0A0H3GJQ1_LISM4	Good	OK
yAW030	<i>parC</i>	LMRG_00737	Imo1287	DNA topoisomerase 4 subunit A (EC 5.99.1.3)	A0A0H3GJX6_LISM4	Poor	Good
yAW032		LMRG_00955	Imo1808	Malonyl CoA-acyl carrier protein transacylase (EC 2.3.1.39)	A0A0H3GD36_LISM4	Good	Good
yAW082		LMRG_00998	Imo1851	Carboxyl-terminal processing protease	A0A0H3GI96_LISM4	Good	Good
yAW008	<i>pbuX</i>	LMRG_01031	Imo1884	NCS2 family nucleobase:cation symporter-2	A0A0H3GD98_LISM4	Good	None
yAW003		LMRG_01201	Imo2051	PDZ domain-containing protein	A0A0H3GIS9_LISM4	Good	Good
yAW073		LMRG_01653	Imo2179	Peptidoglycan bound protein	A0A0H3GE32_LISM4	Good	Good
yAW014	<i>oppA</i>	LMRG_01636	Imo2196	Peptide/nickel transport system substrate-binding protein	A0A0H3GJB6_LISM4	Good	Good
yAW067		LMRG_01540	Imo2292	Gp11	A0A0H3GIK8_LISM4	Good	OK
yAW031		LMRG_01743	Imo2505	D-glutamyl-L-m-Dpm peptidase P45	A0A0H3GN80_LISM4	Good	Poor
yAW075	<i>rpsC</i> ^c	LMRG_02170	Imo2626	30S ribosomal protein S3	A0A0H3GJE8_LISM4	Poor	None
yAW011	<i>rplC</i> ^c	LMRG_02176	Imo2632	50S ribosomal protein L3	A0A0H3GKP9_LISM4	Good	Poor
yAW084		LMRG_02183	Imo2638 ^c	NADH dehydrogenase	A0A0H3GG15_LISM4	Good	Poor
yAW013	<i>fusA</i>^d	LMRG_02199	Imo2654	Elongation factor G (EF-G)	A0A0H3GNN6_LISM4	Good	Good
yAW002		LMRG_01855	Imo2843	Uncharacterized protein	A0A0H3GPF0_LISM4	Good	Good

PstA was constructed as a bait fusion protein in a yeast 2-hybrid and screened as per manufacturers instructions (Matchmaker Yeast 2-Hybrid Gold, Clontech). The prey library was constructed from *L. monocytogenes* genomic DNA and consisted of >100,000 unique 1kb fragments. These data are the positive interactions for prey inserts encoding an orf of >10 amino acids in length that activated at least two reporters. Bold face genes were plasmids, containing the identical insert, identified multiple times.

^a Double Drop-out media selecting for bait (-Trp), prey (-Leu) plasmids. Plus the two positive interaction reporters Aureobasidin A resistance and α -galactosidase-dependent blue color development on X- α -gal. Degree of interaction ranges in qualitative analysis from Good > OK > Poor > None.

^b Quadruple Drop-out media selecting as in ^a however with the additional drop outs of (-Ade) and (-His) used as positive interaction reporters.

^c Orfs also identified as specific PstA-SII interactors from pull-downs in Figure 3.6 and Table 3.2.

^d Orf identified with two unique inserts.

Table 3.4 Proteins eluted with c-di-AMP from PstA-resin

Gene Name	10403S Locus	EGD-e Locus	Protein names	Ec ^a	Lm ^b	Elution ^c	Entry name	Other Data Sets ^d
	<i>LMRG_02183</i>	<i>Imo2638</i>	NADH dehydrogenase	0	0	68	A0A0H3GG15_LISM4	Both
<i>rpoC</i>	<i>LMRG_02650</i>	<i>Imo0259</i>	DNA-directed RNA polymerase subunit beta' (RNAP subunit beta') (EC 2.7.7.6)	1	0	24	A0A0H3G8X2_LISM4	Pull-down
	<i>LMRG_00412</i>	<i>Imo0723</i>	Methyl-accepting chemotaxis protein	0	1	23	A0A0H3GEQ4_LISM4	Pull-down
	<i>LMRG_00380</i>	<i>Imo0692</i>	Chemotaxis protein cheA	0	1	23	A0A0H3GEB6_LISM4	
<i>pstA</i>	<i>LMRG_02239</i>	<i>Imo2692</i>	Uncharacterized protein	5	1	16	A0A0H3GKU4_LISM4	Pull-down
<i>ccpA</i>	<i>LMRG_01368</i>	<i>Imo1599</i>	Catabolite control protein A	0	0	13	A0A0H3GCH8_LISM4	Pull-down
<i>ldh</i>	<i>LMRG_02632</i>	<i>Imo0210</i>	L-lactate dehydrogenase (L-LDH) (EC 1.1.1.27)	0	2	11	A0A0H3G8P6_LISM4	Pull-down
<i>cshA</i>	<i>LMRG_02289</i>	<i>Imo0866</i>	DEAD-box ATP-dependent RNA helicase CshA (EC 3.6.4.13)	0	0	11	A0A0H3GAJ1_LISM4	Pull-down
<i>ctaP</i>	<i>LMRG_02384</i>	<i>Imo0135</i>	Peptide/nickel transport system substrate-binding protein	0	1	11	A0A0H3GCP2_LISM4	
	<i>LMRG_01114</i>	<i>Imo1967</i>	Uncharacterized protein	0	0	10	A0A0H3GE60_LISM4	Pull-down
<i>rpsB</i>	<i>LMRG_01309</i>	<i>Imo1658</i>	30S ribosomal protein S2	0	0	9	A0A0H3GHH8_LISM4	Pull-down
<i>rplC</i>	<i>LMRG_02176</i>	<i>Imo2632</i>	50S ribosomal protein L3	0	3	8	A0A0H3GKP9_LISM4	Both
<i>clpP</i>	<i>LMRG_01780</i>	<i>Imo2468</i>	ATP-dependent Clp protease proteolytic subunit (EC 3.4.21.92) (Endopeptidase Clp)	0	0	7	A0A0H3GKA5_LISM4	
	<i>LMRG_01397</i>	<i>Imo1570</i>	Pyruvate kinase (EC 2.7.1.40)	0	0	7	A0A0H3GCE6_LISM4	Pull-down
	<i>LMRG_00840</i>	<i>Imo1388</i>	ABC transport system	0	0	6	A0A0H3GBZ4_LISM4	
	<i>LMRG_01240</i>	<i>Imo2089</i>	Esterase/lipase	0	0	6	A0A0H3GDU3_LISM4	Pull-down
<i>rpsK</i>	<i>LMRG_02151</i>	<i>Imo2607</i>	30S ribosomal protein S11	0	2	6	A0A0H3GKN2_LISM4	Pull-down
	<i>LMRG_02397</i>	<i>Imo0152</i>	Peptide/nickel transport system substrate-binding protein	0	1	6	A0A0H3GH20_LISM4	
<i>rplF</i>	<i>LMRG_02161</i>	<i>Imo2617</i>	50S ribosomal protein L6	0	3	5	A0A0H3GKP0_LISM4	
<i>pplA</i>	<i>LMRG_02182</i>	<i>Imo2637</i>	Pheromone lipoprotein	0	0	5	A0A0H3GKQ3_LISM4	
<i>guaB</i>	<i>LMRG_01938</i>	<i>Imo2758</i>	Inosine-5'-monophosphate dehydrogenase (IMP dehydrogenase)(EC 1.1.1.205)	0	0	5	A0A0H3GL03_LISM4	Pull-down
	<i>LMRG_01330</i>	<i>Imo1636</i>	ABC-2 type transport system ATP-binding protein	0	0	5	A0A0H3GGP8_LISM4	
<i>rpoB</i>	<i>LMRG_02651</i>	<i>Imo0258</i>	DNA-directed RNA polymerase subunit beta (RNAP subunit beta) (EC 2.7.7.6)	2	0	5	A0A0H3GHC0_LISM4	Pull-down
<i>tuf</i>	<i>LMRG_02198</i>	<i>Imo2653</i>	Elongation factor Tu (EF-Tu)	2	1	5	A0A0H3GG29_LISM4	Pull-down
<i>pdhB</i>	<i>LMRG_00515</i>	<i>Imo1053</i>	Pyruvate dehydrogenase E1 component subunit beta	0	1	5	A0A0H3GB08_LISM4	Pull-down
	<i>LMRG_00755</i>	<i>Imo1305</i>	Transketolase (EC 2.2.1.1)	0	0	5	A0A0H3GGH6_LISM4	
<i>sigA</i>	<i>LMRG_00906</i>	<i>Imo1454</i>	RNA polymerase sigma factor SigA	0	0	5	A0A0H3GC51_LISM4	Pull-down
<i>rpsG</i>	<i>LMRG_02200</i>	<i>Imo2655</i>	30S ribosomal protein S7	0	3	4	A0A0H3GFF7_LISM4	
	<i>LMRG_00888</i>	<i>Imo1436</i>	Aspartokinase (EC 2.7.2.4)	0	0	4	A0A0H3GGV1_LISM4	Pull-down
<i>oppD</i>	<i>LMRG_01639</i>	<i>Imo2193</i>	Peptide/nickel transport system ATP-binding protein	0	0	4	A0A0H3GMC5_LISM4	Pull-down
<i>glmS</i>	<i>LMRG_00415</i>	<i>Imo0727</i>	Glutamine--fructose-6-phosphate aminotransferase [isomerizing] (EC 2.6.1.16)	0	0	4	A0A0H3GA40_LISM4	Pull-down
<i>nadK</i>	<i>LMRG_01381</i>	<i>Imo1586</i>	NAD kinase (EC 2.7.1.23) (ATP-dependent NAD kinase)	0	3	3	A0A0H3GGK7_LISM4	
<i>hslU</i>	<i>LMRG_00729</i>	<i>Imo1279</i>	ATP-dependent protease ATPase subunit HslU (Unfoldase HslU)	2	0	3	A0A0H3GFY3_LISM4	
<i>oppF</i>	<i>LMRG_01640</i>	<i>Imo2192</i>	Oligopeptide transport ATP-binding protein oppF	0	0	3	A0A0H3GER9_LISM4	Pull-down
	<i>LMRG_01834</i>	<i>Imo2414</i>	FeS assembly protein SufD	0	0	3	A0A0H3GFE5_LISM4	Pull-down
<i>rpsE</i>	<i>LMRG_02159</i>	<i>Imo2615</i>	30S ribosomal protein S5	0	0	3	A0A0H3GFB3_LISM4	
<i>relA</i>	<i>LMRG_01447</i>	<i>Imo1523</i>	GTP pyrophosphokinase	0	0	3	A0A0H3GCU7_LISM4	
	<i>LMRG_00320</i>	<i>Imo0637</i>	UbiE/COQ5 family methyltransferase	0	4	2	A0A0H3GE50_LISM4	
<i>rplJ</i>	<i>LMRG_02656</i>	<i>Imo0250</i>	50S ribosomal protein L10	2	0	2	A0A0H3GHB6_LISM4	
<i>ilvC</i>	<i>LMRG_01134</i>	<i>Imo1986</i>	Ketol-acid reductoisomerase (EC 1.1.1.86)	0	0	2	A0A0H3GHN3_LISM4	

<i>purR</i>	LMRG_02614	Imo0192	Pur operon repressor	0	0	2	A0A0H3GD74_LISM4	
	LMRG_00085	Imo0392	UPF0365 protein LMRG_00085	0	0	2	A0A0H3GHN5_LISM4	Pull-down
<i>citB</i>	LMRG_01325	Imo1641	Aconitate hydratase (Aconitase) (EC 4.2.1.3)	0	0	2	A0A0H3GGQ1_LISM4	
<i>recA</i>	LMRG_00850	Imo1398	Protein RecA (Recombinase A)	0	0	2	RECA_LISM4	Pull-down
<i>rplD</i>	LMRG_02175	Imo2631	50S ribosomal protein L4	0	0	2	A0A0H3GJF3_LISM4	Pull-down
<i>rpsL</i>	LMRG_02201	Imo2656	30S ribosomal protein S12	0	0	2	A0A0H3GJH5_LISM4	Pull-down
	LMRG_02069	Imo0970	Enoyl-[acyl-carrier-protein] reductase [NADH] (EC 1.3.1.9)	2	0	2	A0A0H3GJ39_LISM4	
	LMRG_01445	Imo1525	Single-stranded-DNA-specific exonuclease	1	0	2	A0A0H3GCA0_LISM4	
<i>dnaK</i>	LMRG_00926	Imo1473	Chaperone protein DnaK (HSP70) (Heat shock 70 kDa protein) (Heat shock protein 70)	0	0	2	DNAK_LISM4	Pull-down
	LMRG_01774	Imo2474	Nucleotide-binding protein	0	0	2	A0A0H3GFK5_LISM4	
<i>psuG</i>	LMRG_01503	Imo2340	Pseudouridine-5'-phosphate glycosidase (PsiMP glycosidase) (EC 4.2.1.70)	0	0	2	A0A0H3GEI7_LISM4	
<i>rplQ</i>	LMRG_02149	Imo2605	50S ribosomal protein L17	0	0	2	A0A0H3GFA2_LISM4	
	LMRG_00545	Imo1083	dTDP-glucose 4,6-dehydratase (EC 4.2.1.46)	0	1	1	A0A0H3GB36_LISM4	
<i>codY</i>	LMRG_00730	Imo1280	GTP-sensing transcriptional pleiotropic repressor CodY	0	0	1	A0A0H3GGF1_LISM4	Pull-down
<i>ispG</i>	LMRG_00893	Imo1441	4-hydroxy-3-methylbut-2-en-1-yl diphosphate synthase (flavodoxin) (EC 1.17.7.3)	0	0	1	A0A0H3GGW0_LISM4	
	LMRG_00104	Imo0412	Uncharacterized protein	0	0	1	A0A0H3G9X7_LISM4	
<i>pgdA</i>	LMRG_00107	Imo0415	Peptidoglycan N-acetylglucosamine deacetylase	0	0	1	A0A0H3GDH9_LISM4	Pull-down
	LMRG_00223	Imo0541	Iron complex transport system substrate-binding protein	0	0	1	A0A0H3G9K0_LISM4	
<i>pycA</i>	LMRG_00534	Imo1072	Pyruvate carboxylase (EC 6.4.1.1)	0	0	1	A0A0H3GJD4_LISM4	Both
	LMRG_00542	Imo1080	Uncharacterized protein	0	0	1	A0A0H3GFS8_LISM4	
	LMRG_00807	Imo1357	Acetyl-CoA carboxylase	0	0	1	A0A0H3GK27_LISM4	
	LMRG_00946	Imo1493	Uncharacterized protein	0	0	1	A0A0H3GCR8_LISM4	
	LMRG_01422	Imo1548	Rod shape-determining protein mreB	0	0	1	A0A0H3GWB9_LISM4	Pull-down
	LMRG_00982	Imo1835	Carbamoyl-phosphate synthase (glutamine-hydrolyzing) (EC 6.3.5.5)	0	0	1	A0A0H3GHW0_LISM4	Pull-down
<i>oppC</i>	LMRG_01638	Imo2194	Peptide/nickel transport system permease	0	0	1	A0A0H3GE46_LISM4	
<i>oppB</i>	LMRG_01637	Imo2195	Peptide/nickel transport system permease	0	0	1	A0A0H3GI75_LISM4	
			Phosphoribosylformylglycinamide synthase subunit PurL (FGAM synthase) (EC 6.3.5.3)	0	0	1	A0A0H3GCX7_LISM4	
<i>purL</i>	LMRG_02502	Imo1769		0	0	1	A0A0H3GFU1_LISM4	
<i>pyrG</i>	LMRG_02710	Imo2559	CTP synthase (EC 6.3.4.2) (CTP synthetase) (UTP--ammonia ligase)	0	0	1	A0A0H3GFC5_LISM4	
<i>rplP</i>	LMRG_02169	Imo2625	50S ribosomal protein L16	0	0	1	A0A0H3GN84_LISM4	Pull-down
<i>secA</i>	LMRG_01738	Imo2510	Protein translocase subunit SecA	0	0	1	A0A0H3GN84_LISM4	Pull-down
<i>tilS</i>	LMRG_02641	Imo0219	tRNA(Ile)-lysidine synthase (EC 6.3.4.19)	0	0	1	A0A0H3GH76_LISM4	
<i>actA</i>	LMRG_02626	Imo0204	Actin-assembly inducing protein ActA	0	0	1	A0A0H3GH64_LISM4	
<i>rplE</i>	LMRG_02164	Imo2620	50S ribosomal protein L5	0	5	0	A0A0H3GFB9_LISM4	Pull-down
<i>rplA</i>	LMRG_02657	Imo0249	50S ribosomal protein L1	0	4	0	A0A0H3G9H4_LISM4	Pull-down
<i>hflX</i>	LMRG_00450	Imo0762	GTPase HflX (GTP-binding protein HflX)	0	3	0	A0A0H3GIL5_LISM4	
	LMRG_02328	Imo0077	Pentapeptide repeats domain-containing protein	0	3	0	A0A0H3GGU4_LISM4	
<i>rpsO</i>	LMRG_00780	Imo1330	30S ribosomal protein S15	0	3	0	A0A0H3GGJ8_LISM4	
<i>rpsS</i>	LMRG_02172	Imo2628	30S ribosomal protein S19	0	3	0	A0A0H3GG04_LISM4	
<i>kdpD</i>	LMRG_02224	Imo2679	Sensor histidine kinase KdpD	0	1	0	A0A0H3GNR9_LISM4	
<i>clpX</i>	LMRG_00718	Imo1268	ATP-dependent Clp protease ATP-binding subunit ClpX	1	0	0	A0A0H3GBK3_LISM4	
	LMRG_01005	Imo1858	Uncharacterized protein	0	3	0	A0A0H3GLB8_LISM4	

	<i>LMRG_02590</i>	<i>Imo0281</i>	Uncharacterized protein	0	2	0	A0A0H3G9K7_LISM4	
<i>rplB</i>	<i>LMRG_02173</i>	<i>Imo2629</i>	50S ribosomal protein L2	0	2	0	A0A0H3GNL3_LISM4	
<i>atpD</i>	<i>LMRG_01719</i>	<i>Imo2529</i>	ATP synthase subunit beta (EC 3.6.3.14)	0	1	0	A0A0H3GFR1_LISM4	Pull-down
	<i>LMRG_02437</i>	<i>Imo0009</i>	Diamine N-acetyltransferase	0	1	0	A0A0H3GGM6_LISM4	
	<i>LMRG_01225</i>	<i>Imo2074</i>	Uncharacterized protein	0	1	0	A0A0H3GDS8_LISM4	Pull-down

Table 3.4 Proteins eluted with c-di-AMP from PstA-resin

PstA was produced in *E. coli* with a C-terminal 6xhistidine tag and then incubated with Ni-NTA resin followed by copious washing. *L. monocytogenes* $\Delta dacA\Delta pstA$ cultures were grown in LSM to mid-log, washed in PBS, and lysed by sonication in TBS pH 7.5 + 10% glycerol, 1mM PMSF, and benzonase. Lysates were applied to resin followed by washing with TBS pH 7.5 + 10% glycerol. Proteins were eluted with wash buffer + 100 μ M c-di-AMP. Eluates were concentrated by TCA precipitation, analyzed by SDS-PAGE, then tryptic digests were analyzed by mass-spectrometry. Bold face orfs indicate this orf was identified in either Table 3.2 or Table 3.3.

^a *E. coli* background. Number of peptides eluted from resin coated in recombinant PstA-His but not exposed to *L. monocytogenes* lysate.

^b *L. monocytogenes* background. Number of peptides eluted from resin exposed to *L. monocytogenes* lysate but not coated in recombinant PstA-His.

^c PstA specific eluate. Number of peptides eluted from resin coated in PstA-His and exposed to *L. monocytogenes* lysate.

^d Pull-down = found in Table 3.2, Both = found in both Table 3.2 and Table 3.3.

Table 3.5 Suppressor mutations identified in $\Delta dacA$ *p-pstA* mutants capable of growing on rich media and resisting cefuroxime

Strain	Genome Coordinates	Reference	Allele ^a	Gene Name	10403S Locus	EGD-e locus	Protein name	Uniprot Entry	Locus amino acid change
BNP21	1081790	T	A	<i>pycA</i>	<i>LMRG_00534</i>	<i>lmo1072</i>	pyruvate carboxylase	A0A0H3GJD4_LISM4	Val241Glu
BNP29	1082155	G	T	<i>pycA</i>	<i>LMRG_00534</i>	<i>lmo1072</i>	pyruvate carboxylase	A0A0H3GJD4_LISM4	Val363Leu
BNP42	1082155	G	T	<i>pycA</i>	<i>LMRG_00534</i>	<i>lmo1072</i>	pyruvate carboxylase	A0A0H3GJD4_LISM4	Val363Leu
BNP31	1082168	G	T	<i>pycA</i>	<i>LMRG_00534</i>	<i>lmo1072</i>	pyruvate carboxylase	A0A0H3GJD4_LISM4	Arg367Leu
BNP36	1082168	G	T	<i>pycA</i>	<i>LMRG_00534</i>	<i>lmo1072</i>	pyruvate carboxylase	A0A0H3GJD4_LISM4	Arg367Leu
BNP36	1272594	C	T						
BNP46	1082408	C	A	<i>pycA</i>	<i>LMRG_00534</i>	<i>lmo1072</i>	pyruvate carboxylase	A0A0H3GJD4_LISM4	Thr447Lys
BNP32	1082408	C	A	<i>pycA</i>	<i>LMRG_00534</i>	<i>lmo1072</i>	pyruvate carboxylase	A0A0H3GJD4_LISM4	Thr447Lys
BNP03	1082939	C	T	<i>pycA</i>	<i>LMRG_00534</i>	<i>lmo1072</i>	pyruvate carboxylase	A0A0H3GJD4_LISM4	Pro624Leu
BNP04	1082939	C	T	<i>pycA</i>	<i>LMRG_00534</i>	<i>lmo1072</i>	pyruvate carboxylase	A0A0H3GJD4_LISM4	Pro624Leu
BNP07	1082939	C	T	<i>pycA</i>	<i>LMRG_00534</i>	<i>lmo1072</i>	pyruvate carboxylase	A0A0H3GJD4_LISM4	Pro624Leu
BNP09	1083536	C	T	<i>pycA</i>	<i>LMRG_00534</i>	<i>lmo1072</i>	pyruvate carboxylase	A0A0H3GJD4_LISM4	Pro823Leu
BNP10	910001	G	A	<i>rsbU</i>	<i>LMRG_02316</i>	<i>lmo0892</i>	Sigma-B regulation protein, phosphatase	A0A0H3GEW1_LISM4	Gly79Ser
BNP10	1083536	C	T	<i>pycA</i>	<i>LMRG_00534</i>	<i>lmo1072</i>	pyruvate carboxylase	A0A0H3GJD4_LISM4	Pro823Leu
BNP11	1083536	C	T	<i>pycA</i>	<i>LMRG_00534</i>	<i>lmo1072</i>	pyruvate carboxylase	A0A0H3GJD4_LISM4	Pro823Leu
BNP18	1084219	C	T	<i>pycA</i>	<i>LMRG_00534</i>	<i>lmo1072</i>	pyruvate carboxylase	A0A0H3GJD4_LISM4	Arg1051Cys
BNP15	1852607	G	T	<i>stp</i>	<i>LMRG_00968</i>	<i>lmo1821</i>	serine/threonine phosphatase	A0A0H3GDQ3_LISM4	His41Asn

Genome sequencing results of suppressor mutants. Some strains harbored identical mutations and it is unclear if these strains were derived from the same parent suppressor mutant or arose independently of one another.

^a Nucleotide variations as compared to the parent strain

Discussion

Despite a detailed structural understanding of PstA and overt phenotypes for the $\Delta pstA$ mutation, we were unable to determine the molecular interactions of PstA using a variety of pull-down and 2-hybrid approaches. Further analysis of the $\Delta pstA$ mutant will hopefully identify if *pstA* affects production of citrate, acetyl-CoA, NADH, or (p)ppGpp. There remains an obvious connection between PstA and Lmo2638, however, technical limitations have left an unclear understanding of how these two might be related. By far the most intuitive interacting partner for PstA is PdhC. PdhC is an integral subunit of the PDHC that produces acetyl-CoA from pyruvate. Given the central role of acetyl-CoA in activating PycA, the simplest model for PstA would be that in the absence of c-di-AMP, PstA activates PdhC. However, this has not been experimentally demonstrated and has proved challenging. The PDHC is a massive complex making an unsuccessful Co-IP likely due to technical limitations. Further, the PDHC enzymatic activity can only be assayed in cell lysates where it is unclear if PstA remains functional and PstA-protein interactions remain intact. By far the largest limitation when working with the PstA orf is that affinity tags seem to affect the function of the protein.

I predict that within Table 3.2, Table 3.3, and Table 3.4 the PstA interacting partner is listed. However, the stability of the interaction may require an unidentified ligand or stimulus. Alternatively, our Co-IPs/pull-downs may have been unsuccessful due to pulling these components down in the absence of a necessary biological input—such as cefuroxime or rich media. The PstA target could be either under-expressed or membrane bound and thus not amenable to conventional pull-downs. Perhaps the least probably but still alternative explanation is that PstA may truly be unique among PII-like proteins and interact with RNA or DNA! Wouldn't that be cool? A further outstanding question is why does *pstA* appear in a hyper conserved operon with thymidylate kinase (*tmk*)? The Tmk protein is essential for production of dTTP and thus replication of DNA and suggests that PstA may be involved with regulation of the cell cycle. However, none of our analyses of PstA binding partners identified Tmk or any orfs in the near vicinity of PstA.

Chapter 4: Glutathione activates virulence gene expression of an intracellular pathogen

The majority of this chapter was published in:

Reniere, M.L., Whiteley, A.T., Hamilton, K.L., John, S.M., Lauer, P., Brennan, R.G., and Portnoy, D.A. Glutathione activates virulence gene expression of an intracellular pathogen. *Nature* **517**, 170–173 (2015).

Summary

Intracellular pathogens are responsible for much of the world-wide morbidity and mortality due to infectious diseases. To successfully colonize their hosts, these pathogens sense their environment and regulate virulence gene expression appropriately. Accordingly, upon entry into mammalian cells, the facultative intracellular bacterial pathogen *Listeria monocytogenes* remodels its transcriptional program by activating the master virulence regulator PrfA (las Heras et al., 2011). It is predicted that PrfA is regulated allosterically via a small molecule activator specific to the host intracellular environment (Ripio et al., 1997b), but even after decades of study, the putative cofactor remains unknown. Here we show that bacterial and host-derived glutathione are required to activate PrfA. In this study a genetic selection led to the identification of a bacterial mutant in glutathione synthase that exhibited reduced virulence gene expression and was attenuated 150-fold in mice. Genome sequencing of suppressor mutants that arose spontaneously *in vivo* revealed a single nucleotide change in *prfA* that locks the protein in the active conformation (PrfA*) and completely bypassed the requirement for glutathione synthase during infection. We hypothesized that glutathione might be the long-sought activator of PrfA, possibly via direct S-glutathionylation of thiol residues. Although the protein thiol groups contributed to PrfA activation *in vivo*, the mechanism was not through covalent interaction with glutathione. Rather, biochemical and genetic studies support a model in which glutathione-dependent PrfA activation is mediated by allosteric binding of glutathione to PrfA. Whereas glutathione and other low molecular weight thiols play important roles in redox homeostasis in all forms of life, here we demonstrate that glutathione represents a critical signaling molecule that activates the virulence of an intracellular pathogen.

Introduction

L. monocytogenes is a Gram positive pathogen of animals and humans that cycles between a saprophytic lifestyle and as an intracellular pathogen that escapes from a vacuole and grows in the cytosol of host cells⁵. The intracellular lifecycle of *L. monocytogenes* has been well characterized and is entirely dependent on the transcription factor PrfA (Chakraborty et al., 1992; Freitag et al., 2009). PrfA directly regulates the transcription of nine virulence factors and is therefore referred to as the master virulence regulator in *L. monocytogenes* (las Heras et al., 2011). In keeping with its central role in pathogenesis, *L. monocytogenes* strains lacking *prfA* are completely avirulent (Chakraborty et al., 1992). PrfA is a member of the cAMP receptor protein (Crp) family of transcription factors, which is characterized by their allosteric regulation via small molecule activators. In *L. monocytogenes* PrfA is exclusively activated in the cytosol of host cells, leading to the assumption that the activating cofactor for PrfA is specific to this compartment. However, the biochemical mechanism by which PrfA detects the intracellular environment is not well understood. The goal of this study was to identify how *L. monocytogenes* recognizes and responds to its intracellular niche: the mammalian cell cytosol.

Results

Genetic selection in macrophages

We devised a genetic selection to isolate bacterial mutants unable to activate virulence genes during intracellular growth. Our strategy took advantage of a *L. monocytogenes* vaccine strain designed to die *in vivo* (Lauer et al., manuscript in preparation). Specifically, *loxP* sites were inserted into the *L. monocytogenes* chromosome flanking the origin of replication (*ori*, Figure 4.1a). Into this background a codon-optimized *cre* recombinase gene was inserted under the control of the *actA* promoter, which is the most exquisitely regulated PrfA-dependent virulence gene in *L. monocytogenes* and is specifically activated in the host cytosol (Moors et al., 1999; Shetron-Rama et al., 2002). The resulting strain grew like wild-type (wt) *in vitro* (Figure 4.1b) where *actA* expression is very low (Moors et al., 1999). However, upon cytosolic access, Cre-mediated recombination of the *loxP* sites resulted in excision of the *ori*, preventing bacterial replication (Figure 4.1c). A transposon library was then generated in this “suicide strain” background. Bone marrow-derived macrophages (BMDM) were infected with the library of transposon mutants and the surviving bacteria recovered.

We identified more than 16 independent insertions in a *L. monocytogenes* gene, previously identified as encoding a bifunctional glutathione synthase (*gshF*) (Gopal et al., 2005), that rescued the death of the suicide strain *in vivo* (Figure 4.1c,d). Glutathione is a tripeptide low molecular weight (LMW) thiol present in all eukaryotes that contain mitochondria and nearly all Gram negative bacteria (Masip et al., 2006). *L. monocytogenes* is one of the few Gram positive bacteria that synthesize glutathione, whereas most utilize alternative LMW thiols such as bacillithiol and mycothiol (Newton et al., 1996; 2009). Glutathione was not required for Cre/*lox* recombination when *cre*

was expressed from a constitutive promoter (data not shown), leading to the hypothesis that glutathione was required specifically for activation of the *actA* promoter.

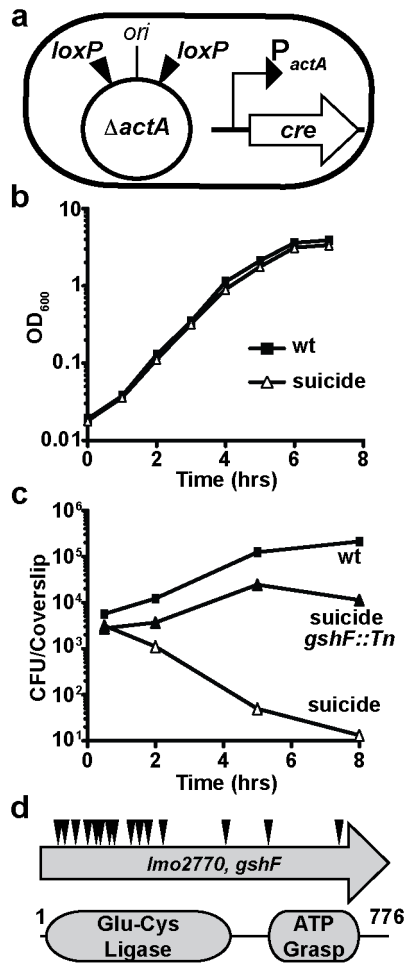


Figure 4.1 Forward genetic selection to identify factors required for virulence gene activation during infection.

a, Schematic of the 'suicide strain' used for genetic selection. See text for description. **b**, Broth growth curve. Data are representative of three independent experiments. OD600, optical density at 600 nm. **c**, BMDM growth curve. Data are a combination of three independent experiments. **d**, Schematic of transposon insertions identified in *gshF* and the conserved protein domains.

Glutathione is required for virulence

To determine the role of *gshF* in *L. monocytogenes*, an in-frame deletion strain was generated by allelic exchange ($\Delta gshF$). Consistent with published work (Gopal et al., 2005), the *gshF*-deficient strain was moderately more sensitive to oxidative stress *in vitro* (Figure 4.2). However, $\Delta gshF$ did not suffer a general loss of fitness, as it exhibited no measurable growth defect *in vitro* (Figure 4.3a) or in BMDM (Figure 4.3b). As expected based on the criteria of the genetic selection, the $\Delta gshF$ mutant expressed lower levels of ActA in cells (Figure 4.3c), formed very small plaques in tissue culture assays that measure cell-to-cell spread (Figure 4.3d), and was greater than 2-logs less virulent in mice (Figure 4.3e). Complementation of $\Delta gshF$ with its native promoter ($\Delta gshF + gshF$) restored wt ActA abundance, wt plaque size, and virulence (Figure 4.3c-e). Since all mammalian cells have high intracellular levels of glutathione (Meister and Anderson, 1983), we assessed the potential contribution of host glutathione using buthionine sulphoximine (BSO). BSO depletes total cellular glutathione levels >98% (Rouzer et al., 1981), but had no effect on bacterial growth during infection (Figure 4.4).

Whereas wt *L. monocytogenes* was unaffected, the $\Delta gshF$ mutant failed to synthesize detectable ActA in the BSO-treated cells (Figure 4.3f). These results demonstrated that the remaining ActA expression in the $\Delta gshF$ mutant was due to imported host glutathione and also established that the phenotypes observed for $\Delta gshF$ were due to a lack of glutathione and not absence of the GshF protein.

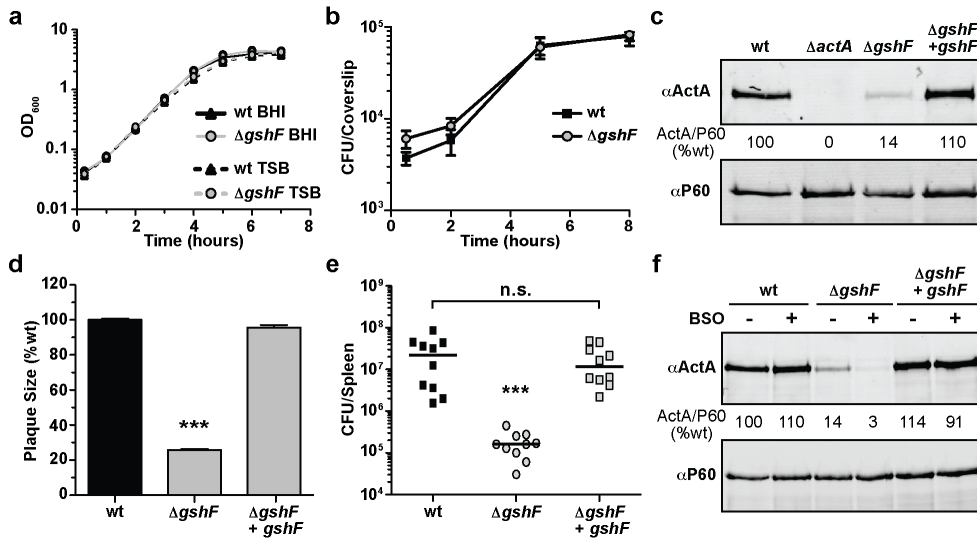
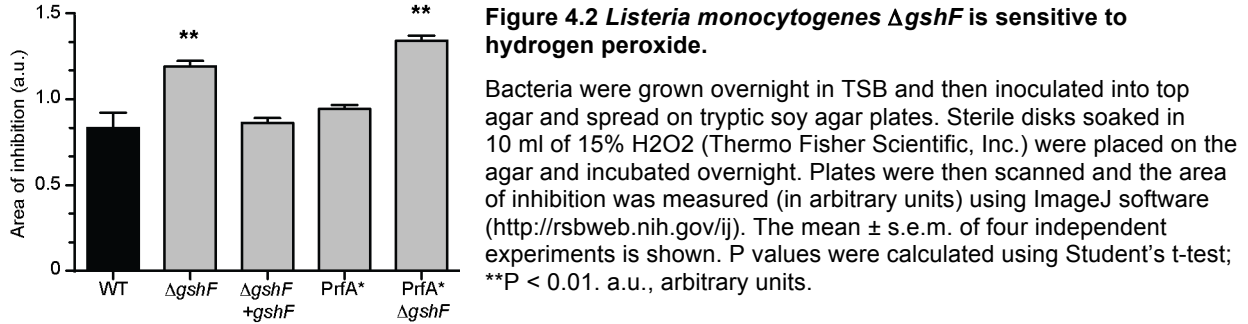


Figure 4.3 *Listeria monocytogenes* $\Delta gshF$ is attenuated *in vivo*.

a, Broth growth curve in brain heart infusion (BHI) or tryptic soy broth (TSB). Data are representative of three independent experiments. **b**, BMDM growth curve. Mean \pm standard error of the mean (s.e.m.) for three independent experiments is shown. **c**, Representative immunoblot of infected BMDMs. Numbers are the mean of four independent experiments and indicate ActA normalized to P60, as a percent of wild-type. **d**, Plaque size. Mean \pm s.e.m. for three independent experiments is shown. **e**, CD-1 mice were infected intravenously and analysed as described in Methods. Data are a combination of two independent experiments, $n = 10$ mice per strain. The median of each group is represented as a horizontal line. **f**, Representative immunoblot of infected BMDMs. Quantification is as described in **c**. In all panels P values were calculated using Student's t-test; ***P < 0.001; NS denotes P > 0.05.

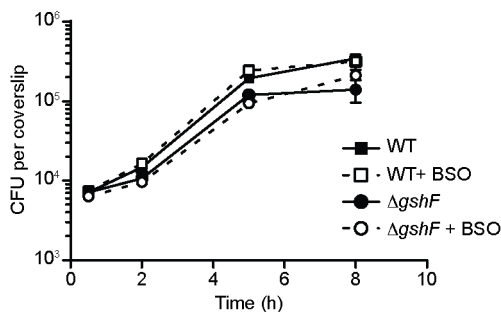


Figure 4.4 BSO does not affect *L. monocytogenes* growth.

BMDM growth curve in which cells were untreated or treated with 2 mM BSO for 16 h before infection and throughout the infection. The mean \pm s.e.m. of three independent experiments is shown.

Isolation of suppressor mutations in vivo

To elucidate the role of glutathione during infection we sought to isolate suppressor mutations. The selective pressure of the host environment was used to select for compensatory mutations in the $\Delta gshF$ background that restored virulence in order to identify functionally interacting genes and/or pathways. Since previous work identified $gshF::Tn$ mutants as hypo-hemolytic (Zemansky et al., 2009), we screened for hyper-hemolytic colonies from the liver homogenates of infected animals on blood agar plates. Two hyper-hemolytic colonies were isolated and genome sequencing identified a single nucleotide polymorphism (SNP) common to both strains and absent from the $\Delta gshF$ parental strain. The SNP encoded a PrfA G145S mutation, which is the most commonly found spontaneous PrfA* allele (Ripio et al., 1997b), so called due to its structural similarity to well-characterized Crp* mutants that are constitutively active in the absence of cofactor (Eiting et al., 2005). The PrfA G145S allele rescued ActA expression and virulence of $\Delta gshF$, confirming the function of this mutation identified by our *in vivo* suppressor analysis (Figure 4.5a-c). This was not specific to *actA*, as transcript levels of two other PrfA-dependent genes were also restored by the PrfA G145S mutation (Figure 4.6). Furthermore, two other previously identified PrfA* alleles (Miner et al., 2008) also rescued the plaque defect of $\Delta gshF$ (Figure 4.5d), indicating that constitutively activating PrfA completely bypassed the requirement for glutathione during infection. Importantly, these data highlighted that $\Delta gshF$ was not attenuated during infection due to a general loss of fitness, but rather, due to a dysregulation of virulence genes.

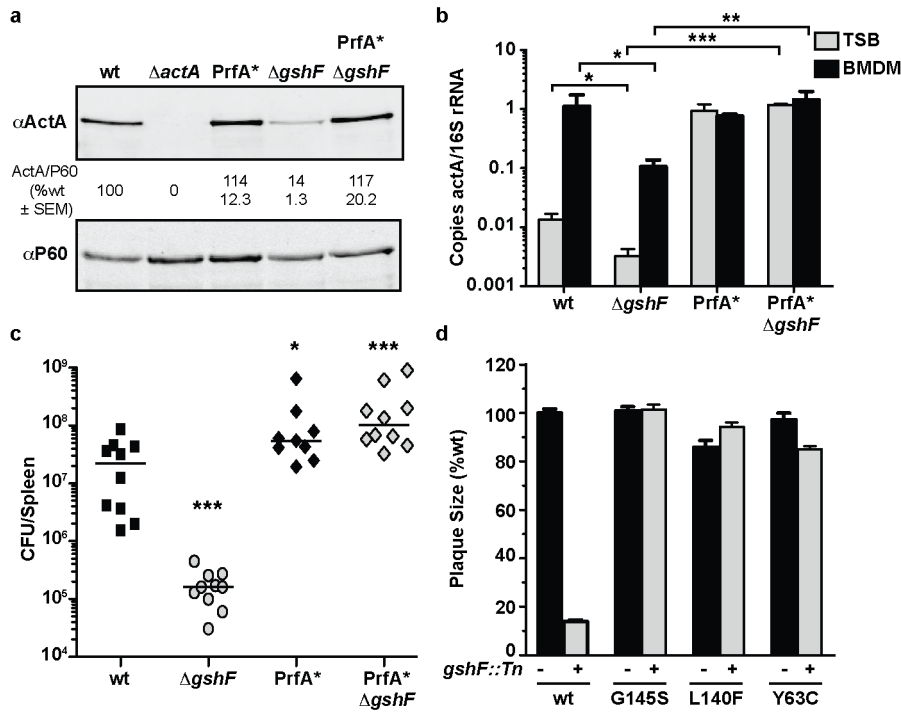


Figure 4.5 PrfA* bypasses the requirement for glutathione during infection.

a, Representative immunoblot of infected BMDMs. Quantification is as described in Figure 4.3. b, Quantitative reverse transcription polymerase chain reaction (RT-PCR) of *actA* transcript abundance. Mean \pm s.e.m. for three independent experiments is shown. c, Mice were infected as described in Figure 4.3. Data are a combination of two independent experiments, $n = 10$ per strain. The median of each group is represented as a horizontal line. d, Plaque size. Mean \pm s.e.m. for three independent experiments is shown. In all panels asterisks denote a significant difference compared to wild-type, unless otherwise indicated, as determined by Student's *t*-test; * $P < 0.05$, ** $P < 0.01$, *** $P < 0.001$.

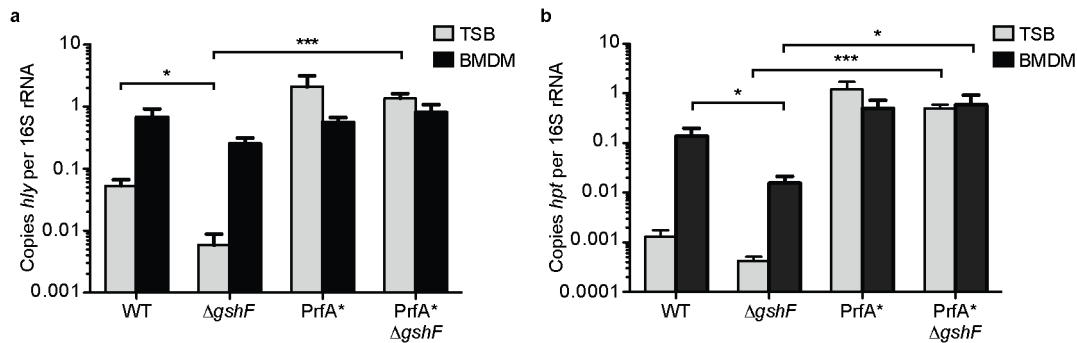


Figure 4.6 The effect of $\Delta gshF$ is not specific to *actA* regulation.

Quantitative RT-PCR of *hly* (a) or *hpt* (b) transcript levels. Bacteria were harvested from TSB at mid-log (grey bars) or 4 h post-infection of BMDMs (black bars). Mean \pm s.e.m. of three independent experiments is shown. *P* values were calculated using Student's *t*-test. * $P < 0.05$; *** $P < 0.001$.

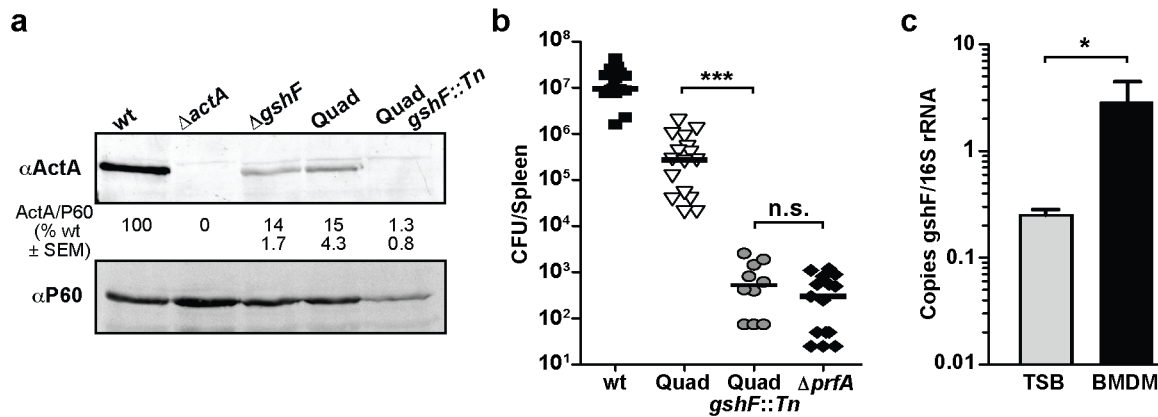


Figure 4.7 Glutathione-dependent PrfA activation is mediated by allosteric binding, not glutathionylation.

a, Representative immunoblot of infected BMDMs. Quantification is as described in Figure 4.3. **b**, Mice were infected as described in Figure 4.3. Data are a combination of at least two independent experiments, $n = 10$ or 16 per strain. The median of each group is represented as a horizontal line. All strains were significantly different from wild-type ($P < 0.001$). **c**, Quantitative RT-PCR of *gshF* transcript abundance. Mean \pm s.e.m. for three independent experiments are shown. In all panels asterisks denote a significant difference compared to wild-type, unless otherwise indicated, as determined by Student's *t*-test; * $P < 0.05$, *** $P < 0.001$; NS denotes $P > 0.05$.

PrfA binds glutathione allosterically

In addition to its role in maintaining redox homeostasis, glutathione can be covalently bonded to protein thiols as a post-translational modification, a process referred to as S-glutathionylation (Dalle-Donne et al., 2009). To determine if glutathionylation of PrfA is required for its activation, we engineered a PrfA protein in which all four cysteine residues were mutated to alanine (referred to as PrfA(C/A)₄). Recombinant PrfA(C/A)₄ bound DNA with an affinity similar to wt *in vitro* (Table 4.1 and Figure 4.8), establishing that these mutations did not disturb the overall structural integrity of the protein. However, the cysteine residues were found to contribute to DNA-binding, as demonstrated by the 35-fold lower affinity of oxidized wt PrfA as compared to reduced (Table 4.1). Although PrfA(C/A)₄ bound DNA *in vitro*, it was less abundant than wt when expressed from the native locus on the chromosome of *L. monocytogenes* (Figure 4.9). Since PrfA is auto-regulated (Mengaud et al., 1991), these data suggested that PrfA(C/A)₄ was less active *in vivo*. Indeed, the PrfA(C/A)₄ strain synthesized less ActA than wt during BMDM infection (Figure 4.7a) and was 30-fold less virulent in mice (Figure 4.7b). Together these results suggested that the cysteine residues of PrfA were dispensable for DNA-binding *in vitro*, as the mutant lacking all cysteine residues (PrfA(C/A)₄) bound DNA with similar affinity as wt (Table 4.1), but were required for activity *in vivo*. If glutathionylation of PrfA were important for its activity, then deleting *gshF* in the PrfA(C/A)₄ background would have no effect. Remarkably, combining the PrfA(C/A)₄ and *gshF::Tn* mutations resulted in a strain that was defective for intracellular growth (Figure 4.10) and completely avirulent in mice (>4-log attenuation, Figure 4.7b).

	DNA-binding affinity ($K_d \pm$ s.e.m.)	
	<i>Phly</i> (nM)	<i>PactA</i> (nM)
Wild-type (oxidized)	888.5 \pm 140.3	ND
Wild-type (reduced)	34.2 \pm 4.9	96.4 \pm 7.3
PrfA(C/A) ₄	32.8 \pm 5.5	124.9 \pm 26.3
PrfA*	40.8 \pm 3.3	45.4 \pm 3.2
	Glutathione-binding affinity ($K_d \pm$ s.e.m.)	
	GSH (mM)	GSSG (mM)
Wild-type	4.37 \pm 1.2	NBD
PrfA(C/A) ₄	4.74 \pm 1.5	NBD

Table 4.1 DNA-binding and glutathione-binding affinities of PrfA

DNA-binding affinity for the *hly* promoter (*Phly*) and the *actA* promoter (*PactA*), as measured by fluorescence anisotropy, and glutathione-binding affinity, as measured by bio-layer interferometry. The affinity of oxidized PrfA to *PactA* was not determined (ND). DNA-binding affinities of PrfA(C/A)₄ and PrfA* were unaffected by oxidation. For oxidized glutathione (GSSG) no measurable binding was detected (NBD).

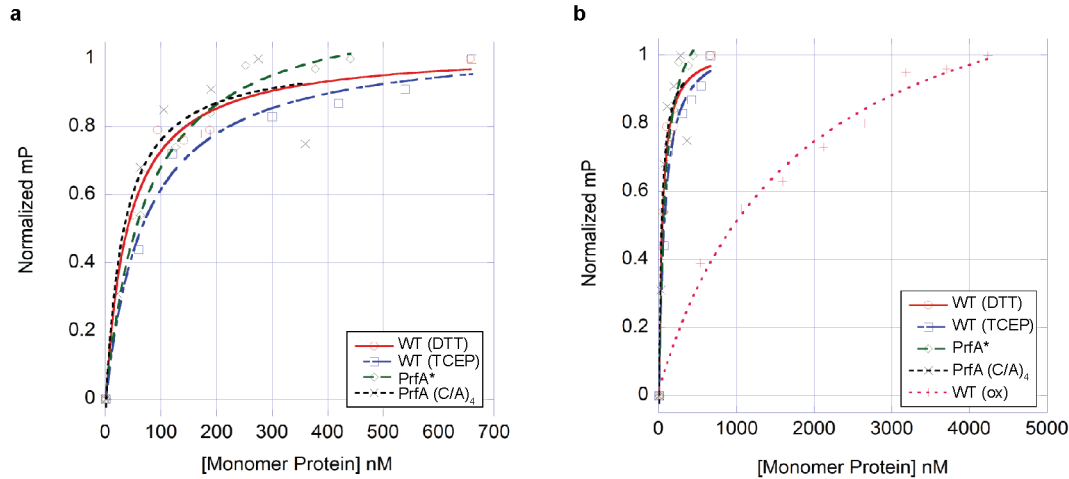


Figure 4.8 Fluorescence polarization binding isotherms.

a. Representative binding isotherms of wild-type PrfA plus DTT (circles), wild-type PrfA plus TCEP (squares), PrfA* (diamonds), and PrfA(C/A)₄ (crosses), to the PrfA box of *Phly*. **b.** Representative binding isotherms of wild-type PrfA plus DTT (circles), wild-type PrfA plus TCEP (squares), PrfA* (diamonds), PrfA(C/A)₄ (crosses), and oxidized wild-type PrfA (plus symbols), to the PrfA box of *Phly*. This plot underscores the very poor binding of oxidized wild-type PrfA to the PrfA box. In both panels the units of millipolarization (mP, y axis) have been normalized to allow the presentation of all binding isotherms on one graph. The protein concentration is shown in terms of protomer on the x axis.

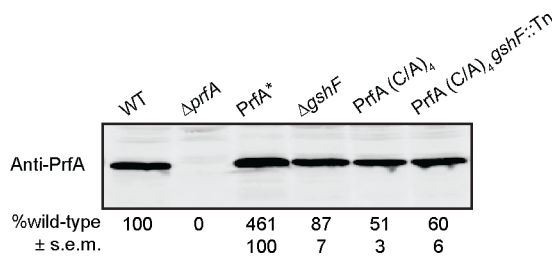


Figure 4.9 PrfA(C/A)₄ expression in *L. monocytogenes* grown in broth.

Immunoblot of PrfA in *L. monocytogenes* lysates harvested at early exponential phase in BHI. Mean \pm s.e.m. of four independent experiments is shown.

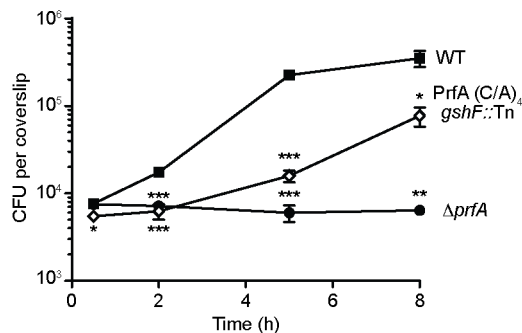


Figure 4.10 The PrfA(C/A)₄ *gshF::Tn* mutant exhibits a significant intracellular growth defect.

The mean \pm s.e.m. of four independent experiments is shown. *P* values were calculated using Student's *t*-test. **P* < 0.05; ***P* < 0.01; ****P* < 0.001.

Although we cannot definitively exclude a role for glutathionylation of PrfA *in vivo*, covalent modification of the protein thiols is not sufficient for PrfA activation, as the PrfA(C/A)₄ mutant is only modestly attenuated during infection (Figure 4.7b). Therefore, we hypothesized that glutathione may be allosterically binding PrfA, analogous to the interaction of cAMP binding to Crp (Kolb et al., 1993). The binding affinity of glutathione for PrfA was measured via bio-layer interferometry. A direct and specific interaction with reduced glutathione (GSH) was detected for both recombinant wild-type and PrfA(C/A)₄ with binding affinities of 4.4 ± 1.2 and 4.7 ± 1.5 mM, respectively, whereas no measurable interaction was found between either protein and oxidized glutathione (GSSG, Figure 4.7c). Although the affinity for reduced glutathione appears to be relatively low, it is well within biologically relevant concentrations of this LMW thiol, as both prokaryotes and eukaryotes have intracellular concentrations of 0.1-10 mM glutathione (Masip et al., 2006). This binding affinity would also allow PrfA to be sensitive to varying concentrations of glutathione, rather than being a simple ON-OFF switch. In support of the hypothesis that glutathione may activate PrfA *in vivo*, *gshF* was transcriptionally up-regulated 10-fold during infection (Figure 4.7c). These data demonstrated that reduced glutathione non-covalently binds PrfA and supported the model that glutathione is the activating cofactor for PrfA.

Discussion

The results of this study clearly demonstrate that both bacterial and host-synthesized glutathione contribute to expression of *L. monocytogenes* virulence factors via allosteric binding of the master virulence regulator PrfA. Unlike Crp, PrfA does not require allosteric activation to bind DNA *in vitro* (Table 4.1). Indeed, the DNA-binding affinity of PrfA was unchanged in the presence of glutathione (data not shown). In this regard PrfA is similar to the phylogenetically more closely related Crp family member NtcA from Cyanobacteria, which also binds DNA in the absence of its cofactor (Valladares et al., 2008). Together, our results suggest a model whereby PrfA activation is a two-step process requiring reduced protein thiols for initial DNA-binding and allosteric binding of glutathione to PrfA for transcription activation (see model in Figure 4.11). Indeed, eliminating both of these steps, as in the PrfA(C/A)₄ *gshF*::*Tn* mutant, resulted in a strain that was as attenuated as a $\Delta prfA$ mutant (Figure 4.7b).

Glutathione is present in the cytosol of all host cells so it is perhaps not surprising that intracellular pathogens import it, as is the case with *Francisella tularensis* (Alkhuder et al., 2009). What is surprising is that *L. monocytogenes* imports glutathione from the host and also synthesizes it. The results of this study suggest that *L. monocytogenes* uses glutathione concentration to regulate its biphasic lifestyle and the switch from saprophyte to pathogen. This may be a reflection of the broad host range of this pathogen and the fact that glutathione is ubiquitous in host cells, making it a reliable signal of the *L. monocytogenes* cytosolic niche. Perhaps other LMW thiols, such as coenzyme A, mycothiol, and bacillithiol play similar activating roles in virulence gene expression in other pathogens.

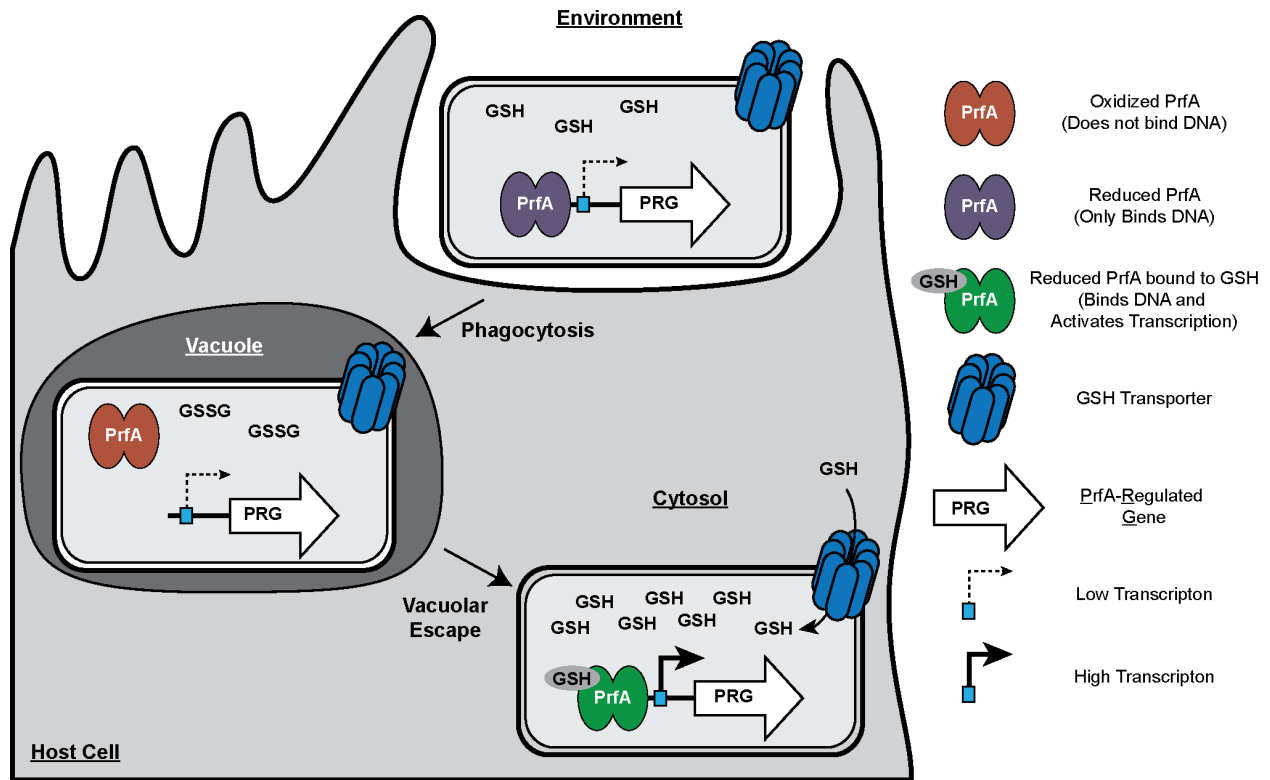


Figure 4.11 Model of glutathione-dependent PrfA activation.

The process of infection or intercellular spread requires that *L. monocytogenes* inhabit an oxidizing vacuole, which may contain both reactive oxygen and nitrogen species. Upon oxidation, glutathione dimerizes to GSSG, which we have demonstrated does not bind PrfA. In addition, PrfA thiols may be reversibly oxidized, temporarily inactivating the protein by inhibiting DNA binding and leading to a downregulation of PrfA-regulated genes (PRG). *Listeria monocytogenes* could then enter the host cytosol, as PrfA activation is dispensable for vacuolar escape *in vivo*. The host cytosol is a highly reducing environment and upon entry into this compartment, all thiols are expected to be in the reduced form. In the absence of glutathione, it is likely that coenzyme A maintains redox homeostasis in the bacterium, as it is the most abundant LMW thiol in *L. monocytogenes*. Reduced glutathione could then bind PrfA and activate transcription of PRG. This two-step activation requirement may explain why the mechanism of PrfA activation has been a mystery for over two decades; the redox changes occurring during transit through a vacuole followed by replication in the highly reducing cytosol have yet to be recapitulated *in vitro*.

Experimental Procedures

Bacterial strains and cell culture.

The *L. monocytogenes* strains used were all in the 10403S background (Table 4.2). Bacteria were cultured in brain heart infusion (BHI) or tryptic soy broth (TSB), as indicated. All media was from Becton Dickinson (New Jersey). For broth growth curves, overnight cultures were diluted 1:100 and OD₆₀₀ was measured at each time point using a spectrophotometer. *gshF* (*Imo2770*) was deleted by allelic exchange using the temperature-sensitive plasmid *pKSV7* (Camilli et al., 1993; Smith and Youngman, 1992). The Δ *gshF* complemented strain was generated by inserting a C-terminal 6xHis-tagged copy of *gshF* with its native promoter into the integration vector *pPL2* (Lauer et al., 2002).

Strain	<i>Escherichia coli</i>	Reference
NF-E1280	BL21(DE3) pET100.prfA	(Miner et al., 2008)
NF-E1281	BL21(DE3) pET100.prfA* (G145S)	(Miner et al., 2008)
DP-E6185	Rosetta pET100.prfA Quad	this work
Strain	<i>Listeria monocytogenes</i>	Reference
10403S	wt	(Bishop and Hinrichs, 1987)
DP-L3078	Δ <i>actA</i>	(Skoble et al., 2000)
DP-L4317	Δ <i>prfA</i>	(Cheng et al., 2005)
NF-L1177	PrfA* (G145S)	(Miner et al., 2008)
BH-3410	suicide	this work
DP-L6187	suicide <i>gshF::Tn</i>	this work
DP-L6188	Δ <i>gshF</i>	this work
DP-L6189	Δ <i>gshF</i> + <i>gshF</i>	this work
DP-L6190	PrfA* (G145S) Δ <i>gshF</i>	this work
DP-L6191	PrfA* (G145S) <i>gshF::Tn</i>	this work
NF-L1166	PrfA* (L140F)	(Miner et al., 2008)
DP-L6192	PrfA* (L140F) <i>gshF::Tn</i>	this work
NF-L1214	PrfA* (Y63C)	(Miner et al., 2008)
DP-L6194	PrfA* (Y63C) <i>gshF::Tn</i>	this work
DP-L6195	PrfA (C/A) ₄	this work
DP-L6196	PrfA (C/A) ₄ <i>gshF::Tn</i>	this work

Table 4.2 *L. monocytogenes* and *E. coli* strains used in this study

Murine L2 fibroblasts were passaged in Dulbecco modified Eagle medium with high glucose (DMEM, Gibco/Invitrogen) supplemented with 1% sodium pyruvate, 1% L-glutamine, and 10% fetal bovine serum (FBS, GemCell) at 37 °C with 5% CO₂. Bone marrow-derived macrophages (BMDM) were cultured in DMEM supplemented with 1% sodium pyruvate, 1% L-glutamine, 20% FBS, and 10% 3T3-MCSF supernatant.

Transposon library generation and genetic selection.

A transposon library was generated in the suicide strain using *himar1 mariner* transposon mutagenesis, as previously described (Zemansky et al., 2009). BMDM were then infected with this library of transposon mutants. Cells were collected at various time points after infection, lysed, and surviving bacteria were plated on BHI agar. Individual colonies were then isolated and used to infect BMDM to confirm the phenotype. To identify the transposon insertion site, colony PCR was performed using primers listed in Table 4.3. A large percentage of the transposon insertion sites were found in the *actA* promoter, *cre*, and each *loxP* site. The fact that we identified multiple

transposon insertions in each *loxP* site, which are less than 40 nucleotides, indicates that the genetic selection approached saturation.

We next screened these mutants by plaque assay and mutants with a plaque size <90% of wt were included. Finally, intracellular growth curves were performed to ensure that the mutants had a defect only in *actA* expression and not in intracellular growth. Greater than 16 independent insertions were identified in *Imo2770* (*gshF*), making it by far the most over-represented hit in the selection.

Primer	Oligonucleotide	Amplicon
MLR#123	CGACATAATATTTGCAGCGAC	<i>actA</i> for qPCR
MLR#124	TGCTTTCAACATTGCTATTAGG	
MLR#133	GACCCTAATCTCCGGAAGC	<i>gshF</i> for qPCR
MLR#134	TACAGAGTCAATCGAGTCCG	
MLR#121	GCGCAACAACTGAAGCAAAG	<i>hly</i> for qPCR
MLR#122	CATTTGCTACTGCATCTCCG	
MLR#125	CTAACGGTCTATCTTCTAAGG	<i>hpt</i> for qPCR
MLR#126	CAATAATAATTGATATAATAGCGG	
MLR#150	ACCCTTGATTTTAGTTGCCAG	16S rRNA for qPCR
MLR#151	TGTGTAGCCCAGGTCATAAG	
MLR#102	GCTTCCAAGGAGCTAAAGAGGTCCCTAGCGCC	Tn PCR Round#1
MLR#103	CGGGGAATTTGTATCGATAAGGAATAGATTTAAAAATTCGCTGT TATTTTG	
MLR#104	GGCCACGCGTCGACTAGTACNNNNNNNNNCTTCT	Tn PCR Round#2
MLR#105	GGCCACGCGTCGACTAGTAC	
MLR#106	ACAATAAGGATAAATTTGAATACTAGTCTCGAGTGGGG	Tn Sequencing
KLH #1	TGAGGCATTAACATTTGTTAACGACGAT	<i>Phly</i> for DNA-binding assays
KLH #2	AACTGATTAACAAATGTTAGAGAAAAC	<i>PactA</i> for DNA-binding assays

Table 4.3 Oligonucleotides used in this study

Intracellular growth curves.

BMDM were harvested as previously described (Sauer et al., 2011) and 3×10^6 cells were plated in 60 mm non-TC treated petri dishes. Cells were infected with an MOI of 0.1 and growth curves were performed as described previously (Portnoy et al., 1988).

Quantitative RT-PCR of bacterial transcripts.

For transcript analysis in broth, bacteria were grown overnight in TSB and subcultured 1:100 into 25 mL TSB. Bacteria were harvested at an OD = 1.0. For transcript analysis during infection, BMDM were plated at a density of 3×10^7 cells in 150 mm TC-treated dishes and infected with an MOI of 10. One hour post-infection the cells were washed and media containing gentamicin (50 μ g/mL) was added. Four hours post-infection the cells were washed and lysed in 0.1% NP-40 containing RNAprotect Bacteria Reagent (Qiagen). Bacteria were harvested by centrifugation.

After harvesting bacteria from either broth or BMDM they were lysed in phenol:chloroform containing 1% SDS by vortexing with 0.1 mm diameter silica/zirconium beads (BioSpec Products Inc.). Nucleic acids were precipitated from the aqueous fraction overnight at -80 °C in ethanol containing 150 mM sodium acetate (pH 5.2). Precipitated nucleic acids were washed with ethanol and treated with TURBO DNase per manufacturer's specifications (Life Technologies Corporation). RNA was again precipitated overnight and then washed in ethanol. RT-PCR was performed with

iScript Reverse Transcriptase (Bio-Rad) and quantitative PCR (qPCR) of resulting cDNA was performed with KAPA SYBR Fast (Kapa Biosystems). Primers used for qPCR are listed in Table 4.3.

Plaque assay

Plaque assays in L2 murine fibroblasts were performed as previously described (Sun et al., 1990). Briefly, bacterial cultures were grown overnight at 30 °C, then washed and diluted 1:10 in sterile PBS. 6-well dishes containing 1.2×10^6 L2 cells per well were infected with *L. monocytogenes* for 1 hour, then washed and overlaid with 3 mL of media containing 0.7% agarose and gentamicin (10 µg/mL) to prevent extracellular growth. After 3 days at 37 °C, an overlay containing gentamicin and neutral red dye (Sigma) was added and stained overnight. The plates were then scanned and analyzed with ImageJ software (Schneider et al., 2012).

Western blots of infected BMDM

BMDM were plated in 12-well dishes at a density of 10^6 cells per well and infected with an MOI of 10. One hour post-infection the cells were washed and media containing gentamicin (50 µg/mL) was added. Where indicated 2 mM buthionine sulfoximine (Santa Cruz Biotechnology) was added to cells 16 hours prior to infection and included throughout the infection. Four hours post-infection the cells were washed and harvested in LDS buffer containing 5% BME. The samples were then boiled and separated by 10% SDS-PAGE. A rabbit polyclonal antibody against the N-terminus of ActA (Lauer et al., 2008) and a mouse monoclonal antibody against P60 (Adipogen) were each used at a dilution of 1:5,000.

Virulence experiments.

Six to eight week old female CD-1 mice (The Jackson Laboratory) were infected intravenously with 1×10^5 colony-forming units (CFU). 48 hours post-infection the mice were euthanized and spleens and livers were harvested, homogenized, and plated for enumeration of bacterial burdens. All animal work was done in accordance with university regulations.

In vivo suppressor analysis.

Female CD-1 mice were infected i.v. with 1×10^7 CFU of $\Delta gshF$ for 72 hours and the livers were harvested, homogenized, and inoculated into broth. New mice were then infected with 1×10^6 CFU of the bacteria from the liver homogenates. 72 hours post-infection the livers were harvested, homogenized and plated on blood agar plates. Two hyper-hemolytic colonies were observed and were chosen for further analysis.

Genome sequencing. *L. monocytogenes* genomic DNA was extracted (MasterPure Kit, Epicentre) and sequenced by Illumina 50SR (library preparation and sequencing performed by UC Berkeley QB3 Genomic Sequencing Laboratory). Sequencing data were aligned to the 10403S reference genome and SNP/InDel/structural variation was determined (CLC Genomics Workbench, CLC bio) for the $\Delta gshF$ parent strain and the two hyper-hemolytic suppressor mutants.

Protein purification and binding analyses.

Recombinant PrfA was purified from *E. coli* BL21(DE3) as previously described (Böckmann et al., 1996). Glutathione binding to the wt or PrfA(C/A)₄ protein was measured by bio-layer interferometry on an Octet RED 384 instrument (Pall ForteBio). The buffer used was PBS, pH 7.3 +/- 2 mM tris(2-carboxyethyl)phosphine (TCEP). Samples or buffer were dispensed into 384-well microtiter plates at a volume of 100 µL per well. Operating temperature was maintained at 26 °C with 1,000 rpm rotary agitation. Ni-NTA biosensor tips (Pall FortéBio) were pre-soaked for 10 minutes with buffer to establish a baseline before protein immobilization. 6xHis-tagged proteins diluted in PBS, pH 7.3 were immobilized onto the biosensors for 8 minutes at a concentration of 35 mg/ml. The immobilization level attained was 7-8 nm. Binding association of the glutathione with biosensor tips was monitored for 30 sec, and subsequent disassociation in buffer was monitored for 30 sec. Glutathione was tested at concentrations of 0.5, 1, 1.5, 2, 3, 4, 5 mM. Reduced glutathione (GSH) was diluted in buffer containing TCEP, while oxidized glutathione (GSSG) was diluted in PBS only. To control for background, association and dissociation of GSH/GSSG was measured with biosensor tips loaded with buffer only and biosensor tips loaded with protein were tested for binding in buffer +/- TCEP. The apparent affinities of glutathione and PrfA were calculated from equilibrium measurements and, when appropriate, global fits of the k_{on} and k_{off} values, yielding similar values. Data are mean and SEM of experiments from four independent protein preparations.

Fluorescence polarization.

A fluorescence-polarization based DNA-binding assay was used to determine the affinities of PrfA, PrfA* and the PrfA(C/A)₄ mutant for the *Phly* and *PactA* promoters. The sequences of the top strands of *Phly* and *PactA* utilized in this study are in Table 4.3. The oligodeoxynucleotides were purchased from IDT (Coralville, Iowa) with a fluorescein label covalently attached to the 5' end. DNA binding was measured in PBS buffer, (11.8 mM Na⁺/K⁺ phosphate, 2.7 mM KCl, 137 mM NaCl) at 25 °C using 5 nM fluoresceinated target dsDNA, and 1 mg poly(dI-dC) as a nonspecific DNA competitor. In some experiments 1 mM TCEP was included to maintain a reducing environment. PrfA was titrated into the DNA until saturation as denoted by no further change in the millipolarization (mP = units of polarization x 10⁻³). The fluoresceinated DNA was excited at 490 nm and its parallel and perpendicular emission intensities measured at 530 nm and converted to units of mP using a Beacon 2000 Variable Temperature Fluorescence Polarization System. Data were plotted and analyzed with the following equation: $mP = \frac{(mP_{bound} - mP_{free})[protein]}{K_d + [protein]} + mP_{free}$, where mP is the millipolarization measured at a given protein concentration, mP_{free} is the initial millipolarization of free fluorescein-labeled DNA, mP_{bound} is the maximum millipolarization of specifically bound DNA, and [protein] is the protein concentration. The generated hyperbolic curves are fit by nonlinear least-squares regression analysis, assuming a bimolecular model such that the K_d values represent the protein concentration at half-maximal ligand binding and plotted by using the graphing program, Kaleidograph. The K_d values are expressed in terms of PrfA dimer binding.

Chapter 5: An *in vivo* selection identifies *Listeria monocytogenes* genes required to sense the intracellular environment and activate virulence factor expression

The majority of this chapter was published in:

Reniere, M. L., Whiteley, A. T. & Portnoy, D. A. An In Vivo Selection Identifies *Listeria monocytogenes* Genes Required to Sense the Intracellular Environment and Activate Virulence Factor Expression. *PLoS Pathog* **12**, e1005741 (2016).

Abstract

Listeria monocytogenes is an environmental saprophyte and facultative intracellular bacterial pathogen with a well-defined life-cycle that involves escape from a phagosome, rapid cytosolic growth, and ActA-dependent cell-to-cell spread, all of which are dependent on the master transcriptional regulator PrfA. The environmental cues that lead to temporal and spatial control of *L. monocytogenes* virulence gene expression are poorly understood. In this study, we took advantage of the robust up-regulation of ActA that occurs intracellularly and expressed Cre recombinase from the *actA* promoter and 5' untranslated region in a strain in which *loxP* sites flanked essential genes, so that activation of *actA* led to bacterial death. Upon screening for transposon mutants that survived intracellularly, six genes were identified as necessary for ActA expression. Strikingly, most of the genes, including *gshF*, *spxA1*, *yjbH*, and *ohrA*, are predicted to play important roles in bacterial redox regulation. The mutants identified in the genetic selection fell into three broad categories: (1) those that failed to reach the cytosolic compartment; (2) mutants that entered the cytosol, but failed to activate the master virulence regulator PrfA; and (3) mutants that entered the cytosol and activated transcription of *actA*, but failed to synthesize it. The identification of mutants defective in vacuolar escape suggests that up-regulation of ActA occurs in the host cytosol and not the vacuole. Moreover, these results provide evidence for two non-redundant cytosolic cues; the first results in allosteric activation of PrfA via increased glutathione levels and transcriptional activation of *actA* while the second results in translational activation of *actA* and requires *yjbH*. Although the precise host cues have not yet been identified, we suggest that intracellular redox stress occurs as a consequence of both host and pathogen remodeling their metabolism upon infection.

Author Summary

Upon recognition of the host, bacterial pathogens activate a genetic virulence program to establish their replicative niche. In this study, we selected for mutants in the model intracellular pathogen *Listeria monocytogenes* that did not up-regulate virulence factors during infection. The screen identified genes involved in sensing the host cell and suggests a model in which expression of virulence factors is spatially and temporally compartmentalized via regulation of transcription and translation. Specifically, results described here indicate two non-redundant host cytosolic cues are sensed by the bacterium in order to activate its virulence program. Future research will illuminate the exact molecular identity of these cytosolic signals. However, the majority of the genes identified are part of the bacterial redox stress response, suggesting that redox changes represent one of the biological cues sensed by *L. monocytogenes* to regulate its virulence program.

Introduction

Intracellular pathogens such as *Plasmodium* spp., *Mycobacterium tuberculosis*, *Salmonella enterica*, *Trypanosoma cruzi*, and *Leishmania* spp. are responsible for an overwhelming amount of morbidity and mortality worldwide. Successful dissemination of many of these pathogens requires complex life cycles that involve survival and replication in environmental or vector niches. To propagate within their hosts, these pathogens establish a variety of unique intracellular niches that are essential for their pathogenesis (Asrat et al., 2014). Although there is considerable understanding of how intracellular pathogens manipulate host cell biology to promote their pathogenesis, less is known about the precise mechanisms by which these pathogens sense their host cell. Such an understanding may lead to targets for therapeutic intervention. In this study we used *Listeria monocytogenes* as a model system for understanding virulence gene regulation of a facultative intracellular bacterium that transitions from extracellular to intracellular growth.

L. monocytogenes is a ubiquitous environmental saprophyte capable of causing severe disease as a foodborne pathogen (Freitag et al., 2009). *L. monocytogenes* is also a model system for studying bacterial adaptation to the host (Hamon et al., 2006). The bacterial virulence program is coordinated with a life cycle that begins upon entry into a mammalian cell either by phagocytosis or bacteria-mediated internalization. To commence intracellular growth, *L. monocytogenes* must first escape from the hostile phagosomal environment by the expression and secretion of a cholesterol-dependent cytolysin, listeriolysin O (LLO) that mediates destruction of the phagosome (Schnupf and Portnoy, 2007). Upon entry into the cytosol, *L. monocytogenes* grows rapidly and expresses an essential determinant of pathogenesis, ActA, an abundant surface protein that mediates host actin polymerization (Kocks et al., 1992; Welch et al., 1998). Appropriate regulation of LLO and ActA is critical for *L. monocytogenes* pathogenesis and transcriptionally coordinated by the master virulence regulator PrfA (Chakraborty et al., 1992).

PrfA is a cAMP receptor protein (Crp) family transcriptional regulator that is absolutely essential for *L. monocytogenes* virulence gene expression and pathogenesis (Scotti et al., 2007). PrfA-mediated gene expression is regulated by PrfA abundance, affinity for target promoters, and activation via cofactor binding (las Heras et al., 2011). PrfA levels are controlled by three promoters. The most proximal promoter contains a site of negative regulation, while the most distal is a PrfA-dependent read-through transcript that is essential for appropriately high levels of intracellular gene expression (Freitag and Portnoy, 1994; Freitag et al., 1993). PrfA binds a palindromic DNA sequence (PrfA-box) and deviations from a consensus sequence result in lower affinity DNA-PrfA interactions (Williams et al., 2000). The affinity of PrfA for DNA determines the degree of transcriptional activation prior to PrfA allosteric activation (Sheehan et al., 1995). For example, the gene encoding LLO (*hly*) has a high affinity PrfA-box and consequently is expressed even during growth in broth when PrfA is not activated. In contrast, the *actA* promoter contains a lower affinity PrfA box and is not expressed during growth in broth (Moors et al., 1999; Shetron-Rama et al., 2002). Upon entry into the host cell cytosol,

PrfA is over-expressed and is activated by a two-step process: first, binding of PrfA to DNA requires reduction of the four PrfA cysteine residues while full transcriptional activation of PrfA requires allosteric binding to glutathione (Reniere et al., 2015). The requirement for glutathione can be bypassed by mutations that lock PrfA in its active conformation (PrfA*) (Ripio et al., 1997b). Strains with PrfA* mutations constitutively express PrfA-activated genes and consequently have growth defects extracellularly, demonstrating the importance of regulating virulence gene expression (Bruno and Freitag, 2010; Vasanthakrishnan et al., 2015). However, even PrfA* strains grown in broth fail to synthesize the amount of ActA observed intracellularly, which is likely attributable to translational control localized to the 5' untranslated region (5' UTR) (Wong et al., 2004). Despite these findings of exquisite gene regulation, little is known about trans-acting factors that affect expression of PrfA or PrfA-activated genes.

In a previous study, a genetic system was designed to select for *L. monocytogenes* mutants that failed to express ActA intracellularly (Reniere et al., 2015). This screen led to the identification of *L. monocytogenes* glutathione synthase (GshF) and glutathione, a tripeptide antioxidant, as the allosteric activator of PrfA. In this study we sought to further understand the host cues that are recognized by intracellular pathogens during infection. We returned to the forward genetic selection and exhaustively screened for additional mutants that failed to express sufficient ActA intracellularly. This selection identified genes required at each stage of the intracellular lifecycle, including: vacuolar escape, PrfA activation, and cell-to-cell spread. These data suggest a model of compartmentalized gene expression, furthering our understanding of the *L. monocytogenes* virulence program.

Results

Genetic Selection in Macrophages

The goal of this study was to identify genes involved in regulation of a principle virulence determinant in *L. monocytogenes*, ActA. A bacterial strain was constructed that failed to replicate upon activation of the *actA* gene, which is specifically up-regulated during cytosolic growth and is essential for pathogenesis. This 'suicide' strain harbored *loxP* sites in the chromosome flanking the origin of replication (*ori*) and several essential genes. Codon-optimized *cre* recombinase was expressed from the *actA* promoter (Figure 5.1A). The suicide strain grew like wild-type in rich media but was unrecoverable after infection of bone marrow-derived macrophages (BMMs). A *himar1* transposon library was then constructed in the suicide strain background and used to infect BMMs. When bacteria were isolated at five hours post-infection (p.i.) nearly all mutants harbored transposon insertions in *cre*, the *actA* promoter driving *cre* expression (*actA1p*), *loxP* sites, and *gshF*, encoding glutathione synthase. To identify additional genes required during infection, colonies were isolated at three and four hours p.i., generating a library of 1,090 transposon mutants from an initial inoculum of >1 million bacteria. Colony PCR excluded strains with transposon insertions in *cre* and *gshF*, resulting in a collection of ~700 strains (Figure 5.1A).

Transposon mutants in the suicide background were screened individually for survival in BMMs, narrowing the list to 300 mutants. Six transposon insertions were identified in *hly* and nine insertions in *prfA*, emphasizing that cytosolic access and PrfA are absolutely required for *actA* activation and subsequent *cre* expression. Saturation of the screen was further demonstrated after identification of 11 insertions in the *actA* promoter driving *cre* and 31 insertions in the *loxP* sites (which are each only 34 nucleotides). The remaining transposon mutations were transduced into a wild-type background and analyzed in a plaque assay, a highly sensitive measure of cell-to-cell spread, which is completely dependent on *actA* expression (Sun et al., 1990). Using a threshold of 85%, 12 mutants were identified that formed plaques significantly smaller than wild-type in L2 murine fibroblasts (Figure 5.2A and Table 5.1). With one exception, the transposon insertions were in open reading frames and likely resulted in loss-of-function mutations. The transposon in the promoter of *Imo2191* (*spxA1*), a gene predicted to be essential in *L. monocytogenes* (Borezee et al., 2000a), resulted in a 10-fold decrease in *spxA1* expression when the bacteria were grown in broth, essentially resulting in a knock-down strain (Figure 5.3). Attempts to make an in-frame deletion of *spxA1* using conventional methods were unsuccessful, consistent with a previous report (Borezee et al., 2000a).

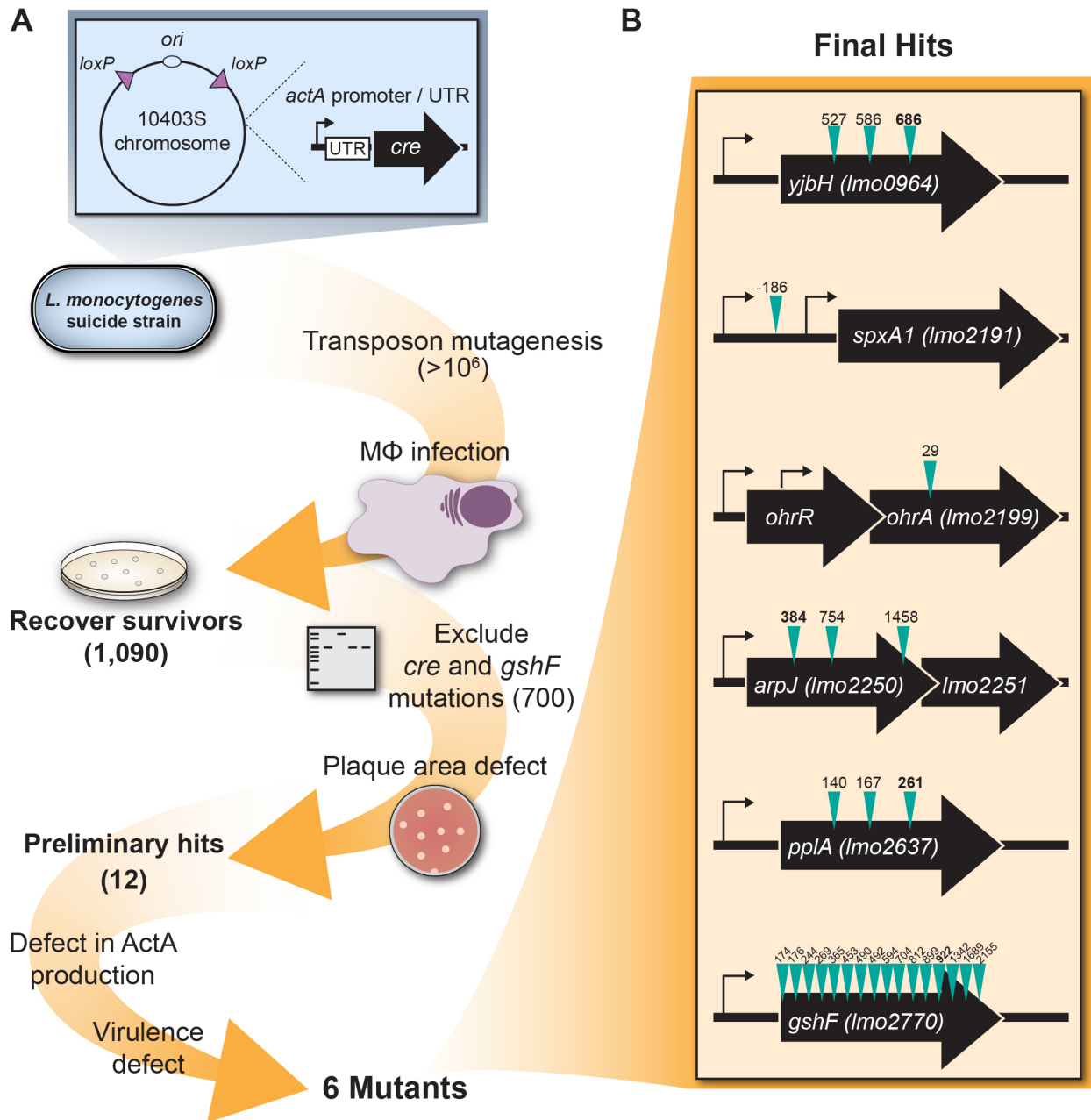


Figure 5.1 Schematic of genetic selection.

(A) Description of the genetic selection. Numbers in parentheses indicate number of mutants remaining after each step. See text for more details. **(B)** Genomic context of the genes identified in the selection. Thin black arrows represent predicted transcription start sites (Wurtzel et al., 2012), teal arrows represent sites of transposon insertions, and numbers above these arrows correspond to mapped transposon locations (nucleotides 3' of the start codon). Bolded numbers denote the transposon insertions used in this study.

Gene ^a	Name	Function	Plaque Size in L2 cells (% wt ± SEM)	Plaque Size in TIB-73 cells (% wt ± SEM)
<i>Imo0441</i>		penicillin-binding protein	71.70 ± 1.60	75.6 ± 3.2
<i>Imo0443</i>		similar to <i>B. subtilis</i> LytR/TagU (LCP family protein)	78.97 ± 1.18	77.8 ± 5.6
<i>Imo0896</i>	<i>rsbX</i>	Indirect regulator of sigma B-dependent gene expression (serine phosphatase)	71.87 ± 0.94	69.6 ± 4.3
<i>Imo0964</i>	<i>yjbH</i>	thiol oxidoreductase	63.56 ± 0.98	53.8 ± 4.3
<i>Imo1566</i>	<i>citC</i>	isocitrate dehydrogenase	82.52 ± 1.25	107.5 ± 5.7
<i>Imo2107</i>		DeoR family transcriptional regulator	84.28 ± 1.36	93.6 ± 6.7
<i>P-Imo2191^b</i>	<i>spxA1</i>	ArsC family transcriptional regulator	75.22 ± 1.52	107.0 ± 4.4
<i>Imo2199</i>	<i>ohrA</i>	hypothetical protein (peroxiredoxin, OsmC/Ohr family)	79.44 ± 1.25	100.6 ± 5.9
<i>Imo2250</i>	<i>arpJ</i>	polar amino acid ABC transporter	47.90 ± 0.82	60.6 ± 2.0
<i>Imo2549</i>	<i>gtcA</i>	wall teichoic acid glycosylation protein	73.98 ± 0.94	83.6 ± 4.5
<i>Imo2637</i>	<i>pplA</i>	conserved lipoprotein	59.00 ± 1.39	77.9 ± 3.6
<i>Imo2770</i>	<i>gshF</i>	glutathione synthase	13.92 ± 0.72	28.4 ± 3.4

Table 5.1 Genes identified in the forward genetic selection.

^a Gene loci based on *L. monocytogenes* EGD-e genome.

^b Transposon insertion in the predicted promoter of *Imo2191*.

As the goal of this selection was to identify mutations that affect ActA expression *in vivo*, we measured ActA abundance during infection of BMMs. Four hours post-infection, cells were lysed and ActA and the constitutively expressed P60 protein were analyzed by immunoblot. Nine strains were found to express less ActA than wild-type after normalizing to P60 abundance (Figure 5.2B). The work-flow of this selection used *cre* expression from the *actA* promoter and plaque area as a criterion for inclusion in the core set of twelve mutants analyzed here. It was therefore unexpected that three mutants (*Imo0441::Tn*, *Imo0443::Tn*, and *citC::Tn*) did not display a defect in ActA abundance during intracellular growth. We hypothesize that these mutations may disrupt elements of bacterial physiology critical to appropriate Cre activity or normal growth.

Virulence

The twelve mutants isolated by the genetic selection were identified based on *in vitro* assays for virulence. While these assays are correlated to *in vivo* outcomes, the importance of these genes to *L. monocytogenes* pathogenesis was confirmed in a murine model of infection. Intravenous infection of mice revealed that four of the mutants displayed no virulence defect (*Imo0441::Tn*, *rsbX::Tn*, *Imo2107::Tn*, and *gtcA::Tn*) while the remaining eight mutants were significantly attenuated (Figure 5.2C). It was surprising that four mutants exhibited impaired plaque formation yet were fully virulent; it is possible that these four mutants are impaired in other aspects of pathogenesis not reflected by changes in CFU during these infection conditions. To determine if the plaque defects in these mutants were due to cell-specific defects evident only in the L2 murine fibroblasts used for plaque assays, cell-to-cell spread defects were also analyzed in TIB-73 cells, a murine hepatocyte cell line (Table 5.1). We observed consistent phenotypes between the plaque defects in TIB-73 cells and L2 cells with the exception of *citC::Tn*, *P-spxA1::Tn*, and *ohrA::Tn*. However, these mutants were significantly attenuated during infection and thus it was unclear why they did not display a plaque defect in TIB-73 cells.

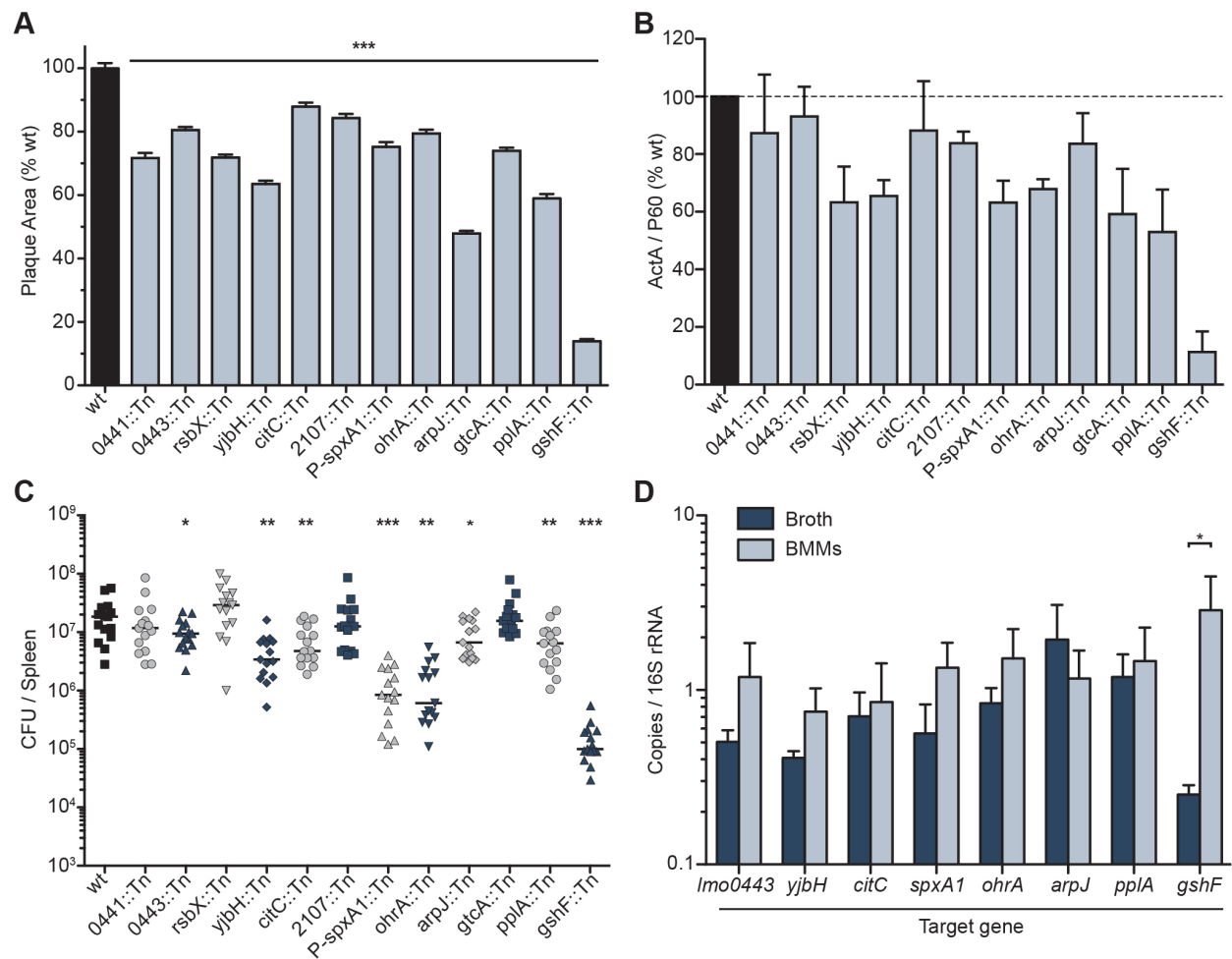


Figure 5.2 Characterization of mutants identified in the genetic selection.

(A) Plaque area as a percentage of wild-type. Data are the mean and error bars indicate the standard error of the mean (s.e.m.) for three independent experiments. p values were calculated using a heteroscedastic Student's t -test and all strains are significantly different from wild-type ($p < 0.001$). (B) Quantification of immunoblots of ActA and P60 during infection. ActA abundance was normalized to P60 abundance and measured as a percentage of wild-type. Data are the mean \pm s.e.m. of at least three independent experiments. (C) Female CD-1 mice were infected with 10^5 colony forming units (CFU) of each mutant. Spleens were harvested 48 hours post-infection and CFU were quantified. The solid lines indicate the median, and data represent three pooled experiments totaling $n=15$ mice per strain. p values were calculated using a heteroscedastic Student's t -test * $p < 0.05$; ** $p < 0.01$; *** $p < 0.001$. (D) Gene expression of target genes measured by quantitative RT-PCR in wild-type *L. monocytogenes* grown in broth compared to expression during infection of BMMs. Data are the mean \pm s.e.m. of at least three independent experiments. p values were calculated using a heteroscedastic Student's t -test * $p < 0.05$.

The specificity of the transposon insertion in seven of the eight attenuated strains was confirmed by expressing the disrupted gene *in trans* and complementing the plaque defect (Figure 5.4). Attempts to complement the *pplA::Tn* plaque defect were unsuccessful. However, *pplA* mutants are difficult to complement and the mutant we identified exhibited phenotypes consistent with published $\Delta pplA$ defects (Xayarath et al., 2015). Other reports have identified genes necessary for virulence of *L. monocytogenes* by comparing changes in gene expression *in vivo* (Chatterjee et al., 2006; Klarsfeld et al., 1994; Toledo-Arana et al., 2009). In our analysis, only *gshF* was differentially transcribed between host cells and rich media (Figure 5.2D). It remains to be

investigated if the activity of these genes is regulated post-transcriptionally in response to the host.

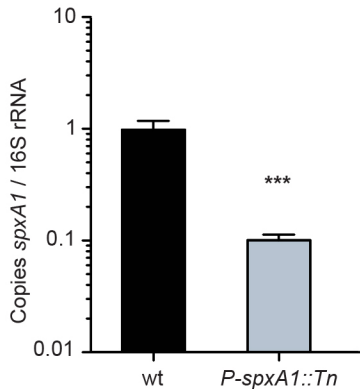
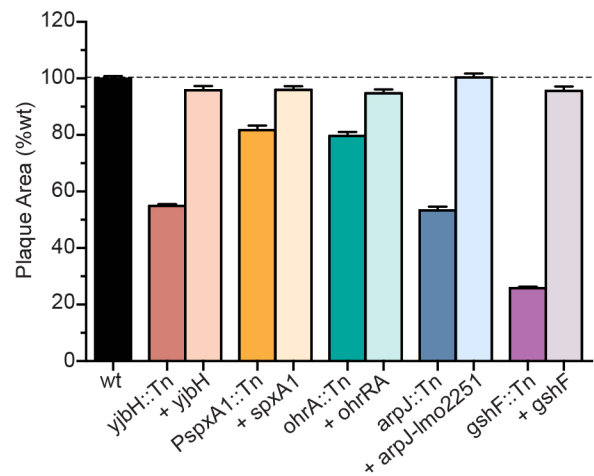


Figure 5.3 Analysis of *P-spxA1::Tn*.

Quantitative RT-PCR of *spxA1* transcript in wild-type compared to *P-spxA1::Tn* grown in broth. Data are the mean \pm s.e.m. of at least three independent experiments and the *p* value was calculated using a heteroscedastic Student's *t*-test; *** *p* < 0.001.

Figure 5.4 Complementation of transposon mutants.

Plaque area as a percentage of wild-type. Data are the mean \pm s.e.m. of at least three independent experiments. Details of each complement strain can be found in the materials and methods.



In this study we focused on the following genes that were required for *actA* expression and pathogenesis (Figure 5.1B). *yjbH* (*Imo0964*) encodes a putative thioredoxin similar to YjbH in *Bacillus subtilis* (57% amino acid similarity) (Larsson et al., 2007). A transposon in *L. monocytogenes yjbH* was previously identified in a screen for mutants defective in LLO production *in vitro* and was found to be attenuated in a competitive infection model (Zemansky et al., 2009). *spxA1* (*Imo2191*) encodes an ArsC family transcriptional regulator similar to the disulfide stress regulator Spx conserved in Firmicutes (83% amino acid identity to *B. subtilis* Spx) (Zuber and Zuber, 2004). The difference in nomenclature is due to the presence of a paralogous gene in *L. monocytogenes* (*Imo2426* or *spxA2*) that is 59% identical to *B. subtilis* Spx while *B. subtilis* encodes only a single *spx*. In *B. subtilis* and *Staphylococcus aureus* YjbH post-translationally regulates Spx (Larsson et al., 2007), although it is not known if this function is conserved in *L. monocytogenes*. *Imo2199* encodes a hypothetical protein with a peroxiredoxin domain and is part of the organic hydroperoxide resistance (Ohr) protein subfamily. It is co-transcribed with *Imo2200*, encoding a MarR family transcriptional regulator which was not required for virulence, suggesting that Lmo2200 may act as a transcriptional repressor (Chatterjee et al., 2006). In *B. subtilis* homologs of Lmo2199 and Lmo2200 are named OhrA (63% amino acid similarity) and OhrR (68%), respectively, and we have adopted this nomenclature for consistency

(Fuangthong et al., 2001). *arpJ* (*Imo2250*) encodes a predicted amino acid ABC transporter permease that was originally identified in a screen for genes with increased intracellular expression (Klarsfeld et al., 1994). However, the data presented here did not show an increase in *arpJ* expression during infection of BMMs. This may be explained by the different growth media and cell types used in the two studies. It is also possible that *arpJ* is autoregulated, as the previous study analyzed *arpJ* expression in an *arpJ* transposon mutant. *pplA* (*Imo2637*) encodes a lipoprotein whose secretion is increased in a PrfA* mutant (Port and Freitag, 2007). The signal sequence of this lipoprotein is processed into a secreted peptide, which is required for vacuolar escape from non-phagocytic cells (Xayarath et al., 2015). Finally, *gshF* (*Imo2770*) encodes the only glutathione synthase in *L. monocytogenes* (Gopal et al., 2005). Glutathione has been demonstrated to be an allosteric activator of PrfA and therefore *gshF* mutants are severely attenuated *in vivo* due to insufficient virulence gene expression (Reniere et al., 2015).

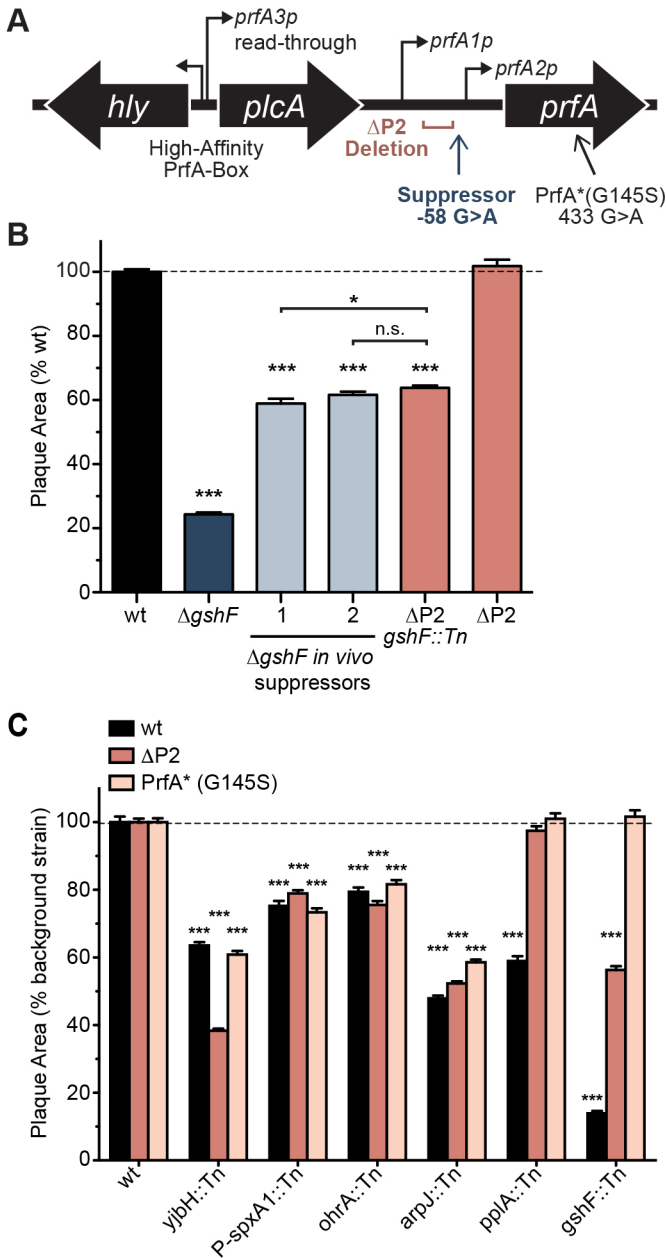


Figure 5.5 *In vivo* suppressor analysis.

(A) Schematic of the *prfA* region. Thin black arrows represent transcription start sites (Freitag and Portnoy, 1994). **(B)** Plaque area as a percentage of wild-type. **(C)** Plaque area as a percentage of the indicated background strain. For panels B and C: data are the mean \pm s.e.m. of at least three independent experiments and *p* values were calculated using a heteroscedastic Student's *t*-test *** *p* < 0.001; n.s. *p* > 0.05.

In vivo suppressor analysis to dissect PrfA abundance versus activation

Given the role of glutathione in activating PrfA, we hypothesized that suppressor mutations of $\Delta gshF$ might illuminate alternative pathways for PrfA activation, potentially involving other genes identified. Accordingly, we screened for mutations that increased the virulence of a $\Delta gshF$ mutant. Mice were serially infected with a high-inoculum of $\Delta gshF$, livers were harvested at 72 hours p.i., homogenized, and diluted to inoculate naive mice. After four successive infections bacteria isolated from infected livers were analyzed by plaque assay. This approach previously identified a mutation in *prfA* that constitutively activates the protein (G145S), known as PrfA*, completely bypassing the

requirement for glutathione during infection (Reniere et al., 2015). The $\Delta gshF$ PrfA* suppressor forms 100% plaque; therefore, for these experiments we selected bacteria that formed intermediate-sized plaques, which were then subjected to genome sequencing. Two suppressor mutants were isolated and found to encode a G>A mutation 58 nucleotides 5' of the *prfA* start codon (Figure 5.5A). This mutation lies within a previously identified site of negative regulation of *prfA*, the so-called "P2 promoter" (*prfA2p*, Figure 5.5A) and deletion of the -35 region of this promoter ($\Delta P2$ mutant) results in a 10-20-fold up-regulation of the *prfA1p*-dependent *prfA* transcript (Freitag and Portnoy, 1994). We hypothesized that the *prfA* -58 G>A mutation also inactivated the P2 promoter and resulted in greater PrfA abundance. Indeed, the $\Delta P2$ *gshF::Tn* double mutant and the $\Delta gshF$ *prfA* -58 G>A suppressor mutants all formed plaques approximately 60% the size of wild-type (Figure 5.5B). These results did not directly implicate any of the other genes identified in our genetic selection, however these findings did highlight the impact of both PrfA abundance and activation during infection.

PrfA expression is controlled by a feed-forward loop in which activated PrfA drives its own transcription (Mengaud et al., 1991). Strains expressing $\Delta P2$ or PrfA* decouple PrfA abundance and activation whereby $\Delta P2$ increases PrfA abundance but still relies on glutathione for PrfA activation; PrfA* increases both the amount and activity of PrfA, independent of glutathione. We next sought to determine if the other mutants identified in the screen affected PrfA abundance or activation by transducing each into *L. monocytogenes* $\Delta P2$ and PrfA* backgrounds and measuring the plaque size in each background (Figure 5.5C). Based on these analyses, mutants fell into three categories. The first category (*yjbH::Tn*, *P-spxA1::Tn*, *ohrA::Tn*, and *arpJ::Tn*) was unaffected by alterations in PrfA expression or activity, indicating that these genes were required down-stream of PrfA. In the second category was *gshF::Tn*, which was partially rescued by $\Delta P2$ and completely rescued by PrfA*, consistent with the demonstrated role for glutathione as the allosteric activator of PrfA. The third category describes *pplA::Tn*, which formed 100% plaques in both the $\Delta P2$ and PrfA* backgrounds. These data suggested that the *pplA* mutant was capable of activating PrfA (because it was rescued by $\Delta P2$) but was deficient in expression of PrfA-dependent genes required early during infection before cytosolic access and glutathione-mediated activation of PrfA.

Vacuolar Escape and Cytosolic Growth

A principle difference between early and late PrfA-dependent genes is that expression of early genes are less dependent on PrfA activation by glutathione (Deshayes et al., 2012). The two early genes are *hly* (encoding LLO) and *plcA*, which share a high-affinity PrfA-box and are transcribed by unactivated PrfA (Böckmann et al., 2000; Deshayes et al., 2012). The $\Delta P2$ mutation results in increased transcription of early genes but does not affect late gene expression, whereas PrfA* increases transcription of both early and late genes. We hypothesized that strains rescued by $\Delta P2$ are specifically deficient in early gene expression. Accordingly, we analyzed early gene expression (LLO production) in broth for each mutant. Several of the mutants were found to secrete less LLO than wild-type (Figure 5.6A). To determine if the defect in LLO production led to impaired phagosomal escape and thus a plaque defect, these mutations were

transduced into a Δhly mutant over-expressing *hly* from a constitutive HyPer promoter (*pH-hly* strain) (Quisel et al., 2001). In this background, efficiency of vacuolar escape should be equivalent in all strains, and indeed, equal LLO secretion was confirmed in broth. Constitutive expression of *hly* rescued the plaque defects of three mutants: *P-spxA1::Tn*, *ohrA::Tn*, and *pplA::Tn* (Figure 5.6B). Interestingly, there was discordance between LLO production in broth and the defect in plaque formation one might predict from an LLO deficiency. For this reason, measuring LLO production in broth may be revealing aspects of bacterial physiology unrelated to LLO production *in vivo*.

The above results suggested that mutations in *P-spxA1*, *ohrA*, and *pplA* resulted in aberrant LLO secretion and/or that these mutants were unable to survive in the harsh environment of the vacuole. Constitutive expression of *hly* would likely overcome either defect. We attempted to segregate these two possibilities by analyzing sensitivity to vacuolar conditions, including reactive oxygen species which *L. monocytogenes* must adapt to in order to survive (Myers et al., 2003). The response of each mutant to peroxide, disulfide stress, and organic hydroperoxide was analyzed by measuring their sensitivity to hydrogen peroxide (H_2O_2), diamide, and cumene hydroperoxide (CHP), respectively. Knock-down of *spxA1* and disruption of *ohrA* or *gshF* significantly increased the sensitivity of *L. monocytogenes* to both peroxide and disulfide stress (Figure 5.6C). In accordance with its annotation and the published role of *ohrA* in *B. subtilis* (Fuangthong et al., 2001), the *ohrA::Tn* mutant was significantly more susceptible to CHP (Figure 5.6C). As these results suggested a role for redox control of virulence genes, we tested the hypothesis that host reactive oxygen or nitrogen species may be sensed by the bacteria during infection to activate *actA*. However, growth of the suicide mutant was not rescued in BMMs lacking inducible nitric oxide synthase (*NOS2^{-/-}*) or NADPH oxidase (*NOX2^{-/-}*) (Figure 5.7). Therefore, *L. monocytogenes* may activate virulence genes in response to multiple redundant host cues or depend on yet unidentified host pathways.

Constitutive production of *hly* restored the majority of the plaque defect for *P-spxA1::Tn* and *ohrA::Tn*, however, it did not restore the plaque to 100% of the parent strain (Figure 5.6B). We hypothesized that these mutants might also be impaired in the ability to grow in the host cytosol, independently from virulence gene expression. All of the mutants identified in the screen grew similarly to wild-type in BMMs with the exception of *P-spxA1::Tn* and *ohrA::Tn* (Figure 5.6D). In fact, *P-spxA1::Tn* and *ohrA::Tn* were also the only mutants that exhibited growth defects in rich media (Figure 5.6E). These pleiotropic growth defects and sensitivity to redox stress are likely why *pH-hly* was only partially able to complement the plaque defect of these mutants (Figure 5.6B).

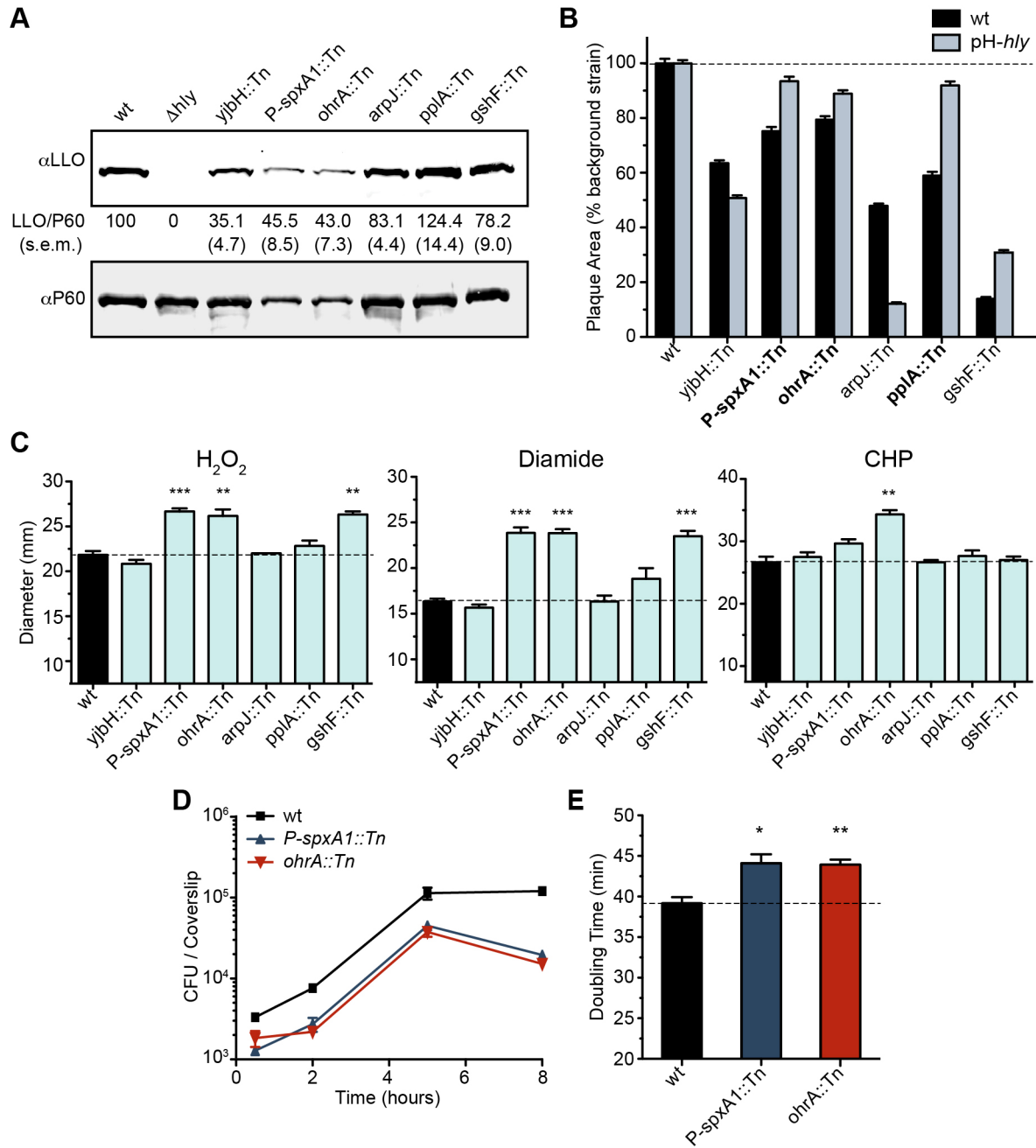


Figure 5.6 Mutants impaired for vacuolar escape.

(A) Representative immunoblots of the secreted proteins LLO and P60. LLO abundance was normalized to P60 abundance and measured as a percentage of wild-type. Data are the mean \pm s.e.m. of at least three independent experiments. (B) Plaque area as a percentage of the indicated background strain. The mutants that were rescued by *pH-hly* are in bold. Data are the mean \pm s.e.m. of at least three independent experiments. (C) Sensitivity of mutants to hydrogen peroxide (5% v/v), diamide (1 M), and cumene hydroperoxide (CHP, 80% v/v) as measured by growth inhibition in a disk diffusion assay. Dotted line corresponds to the wild-type diameter for comparison. The disks were 7.5 mm in diameter. Data are the mean \pm s.e.m. of at least three independent experiments and *p* values were calculated using a heteroscedastic Student's *t*-test ** *p* < 0.01; *** *p* < 0.001. (D) BMM growth curve. Data indicate the mean and s.e.m. of three technical replicates and are representative of three independent experiments. (E) Log phase doubling time of mutants grown shaking in broth. Data are the mean \pm s.e.m. of at least three independent experiments. *p* values were calculated using a heteroscedastic Student's *t*-test * *p* < 0.05; ** *p* < 0.01.

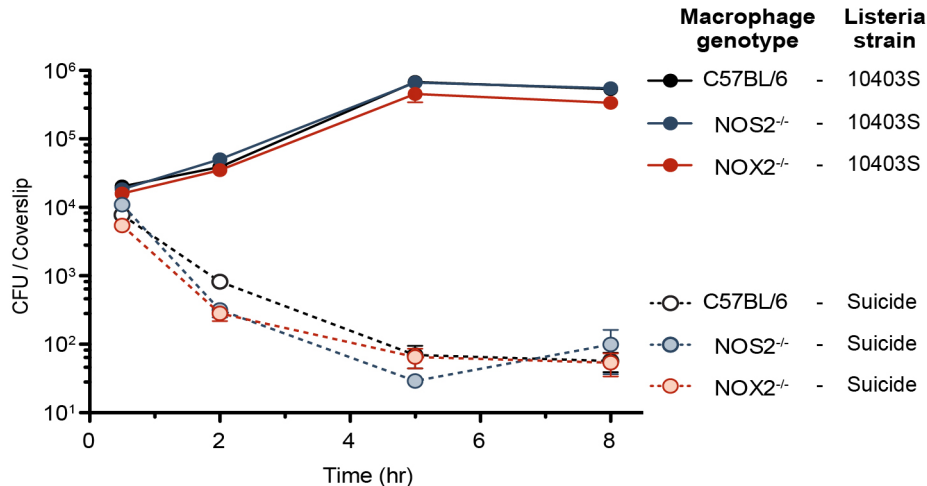


Figure 5.7 Growth curve in NOS2^{-/-} and NOX2^{-/-} BMMs.

Data indicate the mean \pm s.e.m. of data pooled from two independent experiments, each containing three technical replicates.

YjbH is necessary for *ActA* translation

Previous work clearly demonstrated that glutathione was essential for transcriptional activation of virulence genes (Reniere et al., 2015). In order to assess which factors might be independent of glutathione-dependent transcriptional activation, we combined each transposon with an in-frame $\Delta gshF$ mutation. The only mutation not epistatic to *gshF* was *yjbH::Tn*, which produced an additive plaque defect (Figure 5.8A). Further, *yjbH::Tn* was not rescued by constitutive activation of *hly* (Figure 5.6B) or *prfA* (Figure 5.5C). Together, these data suggested that *yjbH* was required for *actA* expression post-transcriptionally. Indeed, transcript levels of *actA* were identical in BMMs infected with wild-type or the $\Delta yjbH$ mutant (Figure 5.8B). It is intriguing that *arpJ::Tn* was epistatic to *gshF*, yet not rescued by constitutive activation of PrfA, indicating that *arpJ* may contribute to glutathione-dependent transcriptional activation of *actA* through an unknown mechanism.

The *actA* gene is preceded by 149 nucleotides of untranslated mRNA (Figure 5.8C) which is important for sufficient ActA expression (Wong et al., 2004). A strain was constructed in which ActA was expressed independent of PrfA by expressing the entire *actA* transcript (including the 5' UTR) under the control of the constitutive HyPer promoter in a strain deleted for *actA* (*pH-actA* Strain, Figure 5.8D). ActA protein abundance was then analyzed by immunoblot. In this background, ActA abundance was equivalent among all strains when the bacteria were grown in broth (Figure 5.8E). However, during infection of BMMs, disruption of *yjbH* resulted in significant impairment in ActA abundance (Figure 5.8F), indicating a failure to translationally activate *actA*. Given that disrupting *yjbH* rescued the death of the suicide strain in which *cre* was expressed under *actA1p* and the 5' UTR, these data indicate a genetic interaction between *yjbH* and the 5' UTR of *actA*. To further support this genetic interaction we engineered a fluorescent strain of *L. monocytogenes* in which *rfp* was expressed under the *actA1p* promoter and 5' UTR (*actA1p-rfp*, Figure 5.8G). During infection of BMMs the $\Delta yjbH$ *actA1p-rfp* strain exhibited significantly less fluorescence than wild-type *actA1p-rfp* (Figure 5.8H). Unfortunately, we were unable to interrogate the effect of a *yjbH* mutation on ActA abundance in the absence of its 5' UTR due to an inability to

detect ActA when the 5' UTR was deleted, consistent with this region being critical for ActA expression (Wong et al., 2004).

A drawback to *pH-actA* is that although ActA is over-expressed in broth, this strain still elaborates much less ActA *in vivo* and fails to form a plaque (Figure 5.8E and F). To analyze the role of translational activation during infection, the *actA* gene and 5' UTR were moved to a neutral locus within the *L. monocytogenes* chromosome (Lauer et al., 2002). In this strain, *actA* was expressed only from the PrfA-dependent *actA1p* proximal promoter, eliminating read-through transcription from the distal *actA2p* promoter (Figure 5.8C). This strain was called *actA1p* and was only mildly impaired in plaque formation and virulence (Figure 5.8I and J). However, *actA1p yjbH::Tn* was unable to form a plaque (Figure 5.8I). The importance of *actA* translational activation was further underscored by a 3-log defect for *actA1p yjbH::Tn* in the livers of infected mice (Figure 5.8J). These data revealed a critical role for *yjbH* in *actA* activation that was less apparent in the wild-type background due to redundant PrfA-dependent promoters.

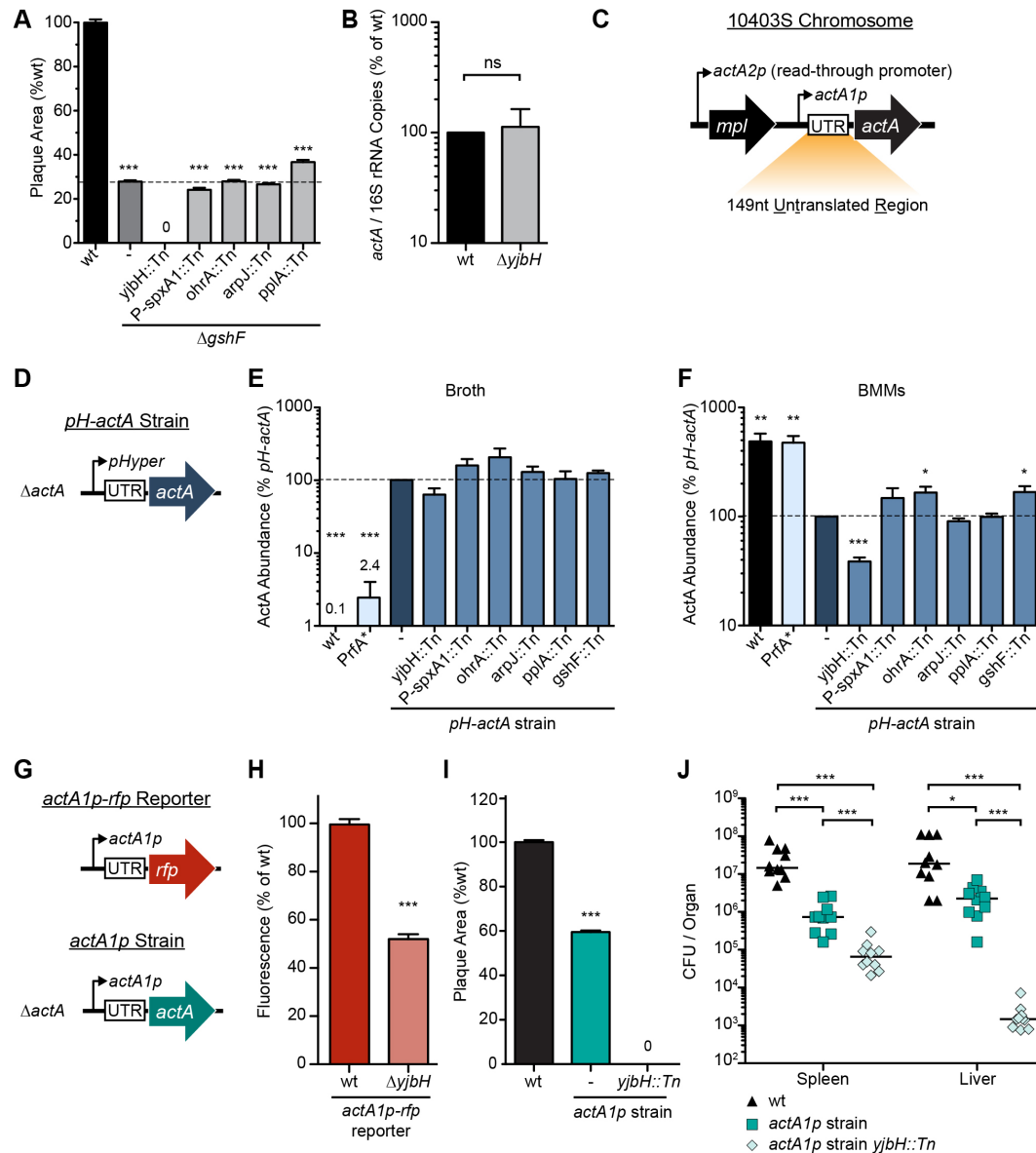


Figure 5.8 Post-transcriptional activation of ActA.

(A) Plaque area as a percentage of wild-type. (B) qPCR of *L. monocytogenes* transcripts during BMM infection. For panels A and B, data are the mean \pm s.e.m. of at least three independent experiments. (C) Schematic of the *actA* region in the chromosome. Thin black arrows represent predicted transcription start sites (Shetron-Rama et al., 2002). (D) Schematic of the constitutive *pH-actA* strain. (E) *In vitro* abundance of ActA normalized to P60 was measured by immunoblot and plotted as a percentage of the *pH-actA* strain during broth growth. Data are the mean \pm s.e.m. of at least three independent experiments. (F) Abundance of ActA normalized to P60 was measured during BMM infection by immunoblot and plotted as a percentage of the *pH-actA* strain four hours post-infection of BMMs. Data are the mean \pm s.e.m. of at least three independent experiments. (G) Schematic of the *actA1p-rfp* reporter strain and the *actA1p* strain. (H) RFP fluorescence six hours post-infection of BMMs with the *actA1p-rfp* reporter strains. Data are the mean \pm s.e.m. of at least three independent experiments. (I) Plaque area as a percentage of wild-type. Data are the mean \pm s.e.m. of at least three independent experiments. (J) Female CD-1 mice were infected with 10^5 CFU of each mutant. Spleens and livers were harvested 48 hours post-infection and CFU were quantified. The solid lines indicate the median, and data represent two pooled experiments totaling $n=10$ mice per strain. In all panels, *p* values were calculated using a heteroscedastic Student's *t*-test * $p < 0.05$; ** $p < 0.01$; *** $p < 0.001$; ns (not significant) $p > 0.05$.

Discussion

In this study, rather than search for novel virulence factors or genes up-regulated *in vivo*, we screened for genes required for activation of an essential determinant of *L. monocytogenes* pathogenesis (*ActA*) that is up-regulated over 200-fold during intracellular growth. Mutants identified in the genetic selection fell into three broad categories: (1) those that failed to reach the cytosolic compartment; (2) mutants that entered the cytosol, but failed to activate the master virulence transcriptional regulator PrfA; and (3) mutants that entered the cytosol and activated transcription of *actA*, but failed to synthesize it (Figure 5.9). This approach highlighted how expression of virulence factors is spatially and temporally compartmentalized via regulation of transcription and translation during infection. One of the most striking findings of this study was that the majority of genes identified in the selection encode proteins predicted to control bacterial redox regulation, suggesting that redox changes represent one of the biological cues sensed by *L. monocytogenes* to regulate its virulence program. Redox stress during infection can arise from endogenous by-products of bacterial metabolism and exogenously derived factors generated by the host. However, it remains to be discovered whether the redox stress that may trigger virulence gene expression is produced by the host, the bacteria, or both.

YjbH, Spx, OhrA, and GshF have defined roles in maintaining redox homeostasis in the presence of disulfide and organic peroxide stresses in Firmicutes. In *B. subtilis* OhrA is a peroxiredoxin required during organic hydroperoxide stress (Fuangthong et al., 2001). In *S. aureus* and *B. subtilis* YjbH interacts with Spx to regulate the abundance and activity of Spx (Larsson et al., 2007). Specifically, YjbH-bound Spx is recognized by the ClpXP protease and is degraded so that Spx concentrations are low under steady-state conditions (Garg et al., 2009; Kommineni et al., 2011). During disulfide stress the YjbH:Spx interaction is disrupted by intramolecular disulfide bonds in both proteins that result in reduced proteolysis of Spx. *B. subtilis* Spx represses transcription of 176 genes and activates transcription of 106 genes (Nakano et al., 2003), the majority of which are required to adapt to redox stress, including genes for production of the low-molecular weight (LMW) thiol utilized by *B. subtilis*, bacillithiol (Gaballa et al., 2013). *L. monocytogenes* *spxA1* cannot be deleted and its regulon has not yet been characterized (Borezee et al., 2000a). Similarly, in *Streptococcus pneumoniae* simultaneous deletion of both *spxA1* and *spxA2* paralogues is lethal (Turlan et al., 2009), supporting the notion that the Spx regulon(s) may contain essential genes in some Firmicutes.

Mutants exhibiting the most severe virulence phenotypes contained insertions in *gshF*, which encodes the sole *L. monocytogenes* glutathione synthase (Gopal et al., 2005). Glutathione is a tripeptide LMW thiol antioxidant present at millimolar concentrations that contributes to maintaining a reducing environment in both bacterial and host cells (Masip et al., 2006). Not surprisingly, *L. monocytogenes* Δ *gshF* mutants are more sensitive to redox stressors such as hydrogen peroxide and diamide and are 200-fold less virulent in mice, indicating that bacterially-derived glutathione is essential for pathogenesis (Reniere et al., 2015). However, Δ *gshF* mutants are fully virulent in *L. monocytogenes* harboring *prfA** mutations that lock PrfA in its constitutively active

conformation. Therefore, the primary role of GshF-derived glutathione during infection is to activate virulence gene expression via PrfA activation, although we cannot rule out a contribution of imported host-derived glutathione (Reniere et al., 2015). Indeed, host-derived glutathione activates virulence gene expression in *Burkholderia pseudomallei* (Wong et al., 2015). In the case of *L. monocytogenes*, *gshF* is transcriptionally up-regulated 10-fold during intracellular growth, suggesting the existence of an unidentified cue, likely redox-related, that stimulates glutathione production.

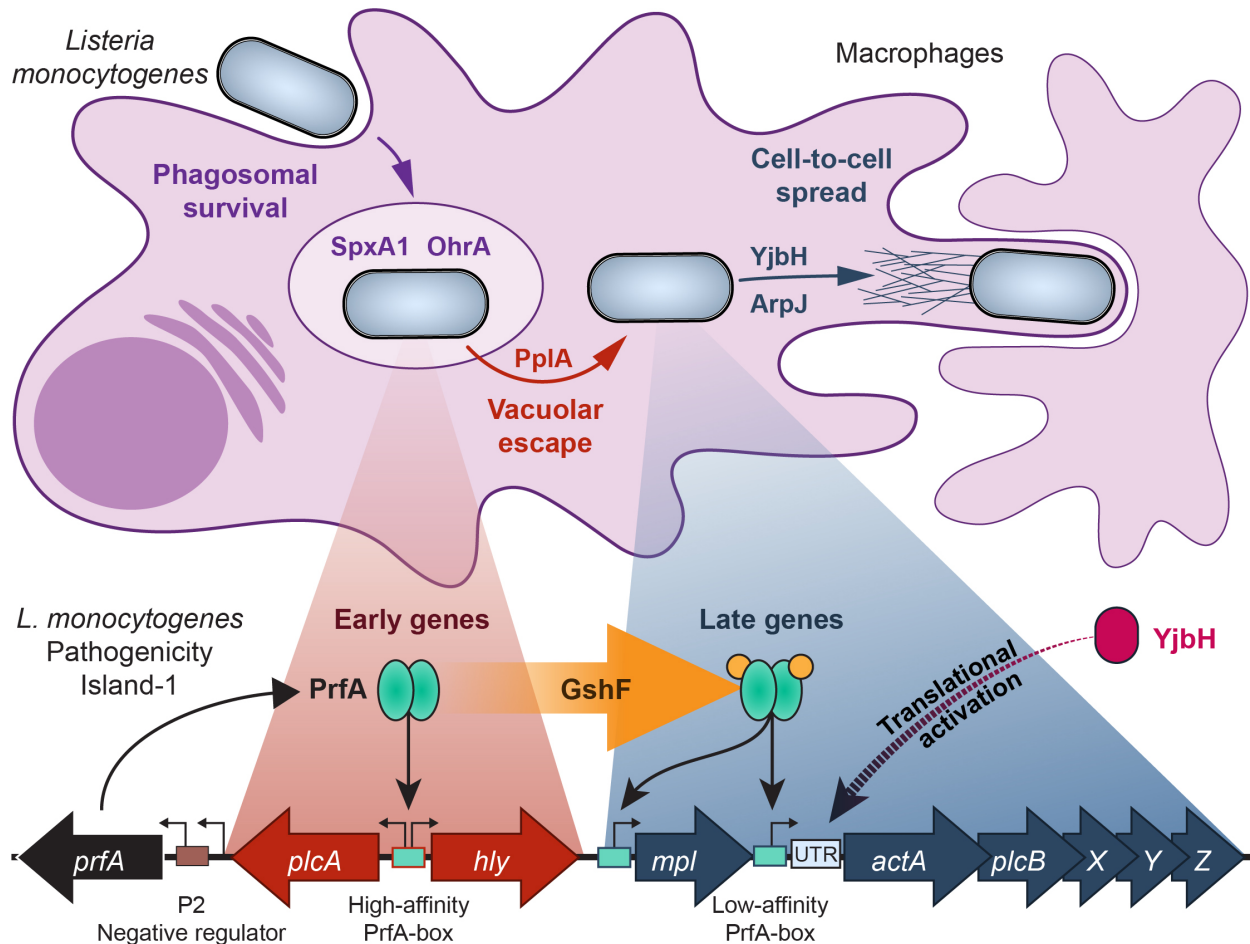


Figure 5.9 Model of genes identified in this genetic selection and where in the *L. monocytogenes* life cycle they are required.

Once phagocytosed by a host macrophage, *L. monocytogenes* (light blue rods) requires the gene products of *spxA1* and *ohrA* to survive in the phagosome. By a mechanism that is not yet understood, *PplA* is required for vacuolar escape in non-phagocytic cells. *YjbH* and *ArpJ* are then required for cell-to-cell spread. The *L. monocytogenes* Pathogenicity Island-1 is pictured below. Early genes (depicted in red) are those with high-affinity PrfA boxes that do not require active PrfA (teal) for transcription. Late genes (depicted in blue) are those with relatively low-affinity PrfA boxes that require activated PrfA to be transcribed and these are required later during infection, in the host cytosol. The transition from unactivated to activated PrfA requires glutathione (orange circles), which is synthesized by *GshF*. *YjbH* (magenta) is then required for translational activation of *actA*, although the mechanism is not yet understood. See text for more details, model is not drawn to scale.

The identification of many redox-related bacterial factors in this genetic selection led to our working model that specific redox changes during infection are sensed by the

bacteria as a mechanism to identify their intracellular location and activate virulence genes appropriately. Redox stress during infection could arise from host-derived antimicrobial factors. For example, the host generates antibacterial factors that assault invading pathogens with redox stresses, including: reactive oxygen species (ROS), reactive electrophilic species (RES) such as methylglyoxal, and reactive nitrogen species (RNS) such as nitric oxide and peroxyxynitrite (Myers et al., 2003). Interestingly, these redox stresses from the host are spatially compartmentalized. RNS and ROS are produced in the phagosome and once in the host cytosol, *L. monocytogenes* is confronted with RES and mitochondrial-derived ROS (Myers et al., 2003). It is possible that the bacterial response to the redox stressors is also compartmentalized, requiring specific factors in the vacuole (such as *spxA1* and *ohrA*) and host cytosol (such as *yjbH*).

Eliminating host nitric oxide synthase (NOS2) or NADPH oxidase did not rescue growth of the suicide mutant (S3 Fig). NOS2-generated nitric oxide is required for efficient *L. monocytogenes* cell-to-cell spread during infection, although this is due to the nitric oxide-mediated delay of phagolysosome maturation and not a direct effect on the bacteria (Cole et al., 2012). Together, these data suggest that a combination of host factors are likely required to activate *actA* during infection.

Alternatively, the source of redox stress may come from bacterial metabolism via ROS generated from incomplete reduction of oxygen during aerobic respiration (Hassett and Cohen, 1989). Carbon source and phosphate abundance also affect the production of ROS and methylglyoxal (Booth et al., 2003; Joseph and Goebel, 2007). PrfA activity has been demonstrated to be sensitive to available carbon sources (Freitag et al., 2009). Growth on plant-derived beta-glucoside sugars in the environment, such as cellobiose, represses PrfA activation, whereas growth on host-derived sugars such as glucose-1-phosphate stimulates PrfA-dependent gene expression (las Heras et al., 2011; Ripio et al., 1997a). Therefore, entry of *L. monocytogenes* into the host cytosol results in a remodeling of carbon metabolism that may be linked to virulence gene regulation. Glycerol is the principle carbon source used by *L. monocytogenes* intracellularly and growth on glycerol is a well-described stimulant of methylglyoxal production (Booth, 2005; Eisenreich et al., 2010; Eylert et al., 2008; Kistler and Lin, 1971). In *B. subtilis*, methylglyoxal stress stimulates the Spx regulon and production of bacillithiol, a low molecular weight thiol used by *B. subtilis* to detoxify methylglyoxal (Chandrangsu et al., 2014). Thus, the 10-fold increase in *gshF* transcript levels in *L. monocytogenes* may correspond to increased methylglyoxal production during infection, which would further link metabolism of an alternative carbon source to virulence. Coupling of metabolism to virulence gene regulation may allow the system to remain OFF in the environment while remaining poised to turn ON upon entering a host. Considering our finding of multiple redox factors that are required for proper virulence gene expression, we speculate that changes in carbon metabolism could alter the endogenous levels of ROS and RES produced, thus affecting PrfA activation and leading to the “sugar-mediated repression” observed previously (las Heras et al., 2011).

Appropriate up-regulation of *actA* at the translational level is understood to require its 5' UTR, although the mechanism remains unknown (Wong et al., 2004). The data reported

here further emphasize the sensitivity of *actA* translation to the environment in which *L. monocytogenes* is growing. In broth, the PrfA* strain elaborated 2.4% the amount of ActA protein as compared to constitutively expressed *actA* (Figure 5.8E), and increased 200-fold during infection (Figure 5.8F), despite the fact that transcript levels of *actA* are equivalent in both growth conditions (Reniere et al., 2015). These data emphasize the importance of the translational control of this virulence factor. Importantly, *yjbH* was required for the increased abundance of ActA protein during infection. In wild-type *L. monocytogenes*, multiple PrfA-dependent promoters may compensate for loss of translational activation; however, when *actA* was isolated under its most proximal promoter, disruption of *yjbH* resulted in an attenuation of over 3-logs in the livers of infected animals (Figure 5.8J). It seems unlikely that the thioredoxin YjbH activates translation of *actA* via direct binding to the 5' UTR. However, YjbH may indirectly activate translation via interaction with another factor(s) or modulation of a small-molecule signal produced by the host.

PrfA-dependent transcription and activation are regulated redundantly at multiple levels, including: a temperature-sensitive riboswitch (Johansson et al., 2002), allosteric activation by glutathione (Reniere et al., 2015), multiple read-through transcripts (Camilli et al., 1993; Freitag et al., 1993), positive and negative promoter elements (Freitag and Portnoy, 1994), and yet to be fully characterized translational control. The complexity of *actA* activation is likely the result of selective pressure to respond appropriately to host-derived cues. This study investigated the virulence defects associated with failure to up-regulate virulence genes; however, over-production or inappropriate regulation of virulence factors extracellularly also results in a competitive disadvantage for *L. monocytogenes* (Bruno and Freitag, 2010; Vasanthakrishnan et al., 2015). How *L. monocytogenes* and other intracellular pathogens regulate virulence gene expression is central to understanding their pathogenesis. Results reported here suggest that redox cues are a mechanism by which intracellular pathogens recognize the host and represents an exciting new area of further investigation.

Experimental Procedures

Ethics Statement

This study was carried out in strict accordance with the recommendations in the Guide for the Care and Use of Laboratory Animals of the National Institutes of Health. All protocols were reviewed and approved by the Animal Care and Use Committee at the University of California, Berkeley (AUP-2016-05-8811).

Bacterial Culture and Strains

All *L. monocytogenes* strains are a derivative of wild-type 10403S (Bécavin et al., 2014; Bishop and Hinrichs, 1987) and were cultivated in Brain Heart Infusion (BHI, Difco), shaking at 37 °C unless otherwise stated. All *E. coli* strains were cultivated shaking in LB (Miller) at 37 °C. Antibiotics (purchased from Sigma) were used at the following concentrations: carbenicillin (100 µg/mL), streptomycin (200 µg/mL), chloramphenicol (7.5 µg/mL for *L. monocytogenes* and 10 µg/mL for *E. coli*), erythromycin (1 µg/mL), and tetracycline (2 µg/mL). All *E. coli* strains are listed in Table 5.2 and all *L. monocytogenes* strains are listed in Table 5.3. Bacterial broth growth curves were performed as previously described (Witte et al., 2013). The suicide strain was a gift from Peter Lauer and Bill Hanson (Aduro Biotech); details of its construction are reported elsewhere (Reniere et al., 2015). Briefly, *loxP* sites were inserted on either side of the origin of replication by allelic exchange into a $\Delta actA\Delta inlB$ strain of *L. monocytogenes*. A transcriptional fusion of *cre* with *actA* that included the *actA1p* promoter, 5' UTR, and ribosomal binding site of *actA*, was inserted adjacent to a *loxP* site.

Strain	Description	Reference
XL1-Blue	For vector construction	Stratagene
SM10	For trans-conjugation	(Simon et al., 1983)
DP-E6333	XL1-Blue pPL2t	(Whiteley et al., 2015)
DP-E6415	SM10 pPL2t.P _{hyper} -hly	(Mitchell et al., 2015)
DP-E6416	SM10 pPL2t.P _{hyper} -actA	This study
DP-E6475	SM10 pPL2.yjbH.His	This study
DP-E6476	XL1 pPL2.spxA1.His	This study
DP-E6477	SM10 pPL2t.ohrRA (LMRG_01632-LMRG_01633)	This study
DP-E6478	SM10 pPL2t.arpJ (LMRG_01581-LMRG_01580)	This study
DP-E6479	SM10 pPL2.gshF.His	(Reniere et al., 2015)
DP-E6510	SM10 pPL2.actA1p-TagRFP (<i>actA1p-rfp</i> reporter)	(Zeldovich et al., 2011)

Table 5.2 *Escherichia coli* Strains.

Strain	Description	Reference
10403S	wt	(Bécavin et al., 2014)
DP-L6186	'suicide strain' (BH-3410)	(Reniere et al., 2015)
DP-L6419	<i>lmo0441::Tn</i>	This study
DP-L6420	<i>lmo0443::Tn</i>	This study
DP-L6421	<i>rsbX::Tn, (lmo0896)</i>	This study
DP-L6422	<i>yjbH::Tn, (lmo0964)</i>	This study
DP-L6423	<i>citC::Tn, (lmo1566)</i>	This study
DP-L6424	<i>lmo2107::Tn</i>	This study
DP-L6425	<i>P-spxA1::Tn, (lmo2191)</i>	This study
DP-L6426	<i>ohrA::Tn (lmo2199)</i>	This study
DP-L6427	<i>arpJ::Tn, (lmo2250)</i>	This study
DP-L6428	<i>gtcA::Tn, (lmo2549)</i>	This study
DP-L6429	<i>pplA::Tn, (lmo2637)</i>	This study
DP-L6430	<i>gshF::Tn, (lmo2770)</i>	This study
DP-L6188	Δ <i>gshF</i>	(Reniere et al., 2015)
DP-L1866	Δ <i>prfA2p</i> -35 (Δ P2 strain)	(Freitag and Portnoy, 1994)
DP-L5451	PrfA* (G145S)	(Miner et al., 2008)
DP-L6431	DP-L1866 + <i>yjbH::Tn</i>	This study
DP-L6432	DP-L1866 + <i>P-spxA1::Tn</i>	This study
DP-L6433	DP-L1866 + <i>ohrA::Tn</i>	This study
DP-L6434	DP-L1866 + <i>arpJ::Tn</i>	This study
DP-L6435	DP-L1866 + <i>pplA::Tn</i>	This study
DP-L6436	DP-L1866 + <i>gshF::Tn</i>	This study
DP-L6437	PrfA* <i>yjbH::Tn</i>	This study
DP-L6438	PrfA* <i>P-spxA1::Tn</i>	This study
DP-L6439	PrfA* <i>ohrA::Tn</i>	This study
DP-L6440	PrfA* <i>arpJ::Tn</i>	This study
DP-L6441	PrfA* <i>pplA::Tn</i>	This study
DP-L6191	PrfA* <i>gshF::Tn</i>	This study
DP-L4511	Δ <i>hly</i> pPL2.P _{hyper} - <i>hly</i> (pH- <i>hly</i> strain)	(Shen and Higgins, 2005)
DP-L6442	DP-L4511 + <i>yjbH::Tn</i>	This study
DP-L6443	DP-L4511 + <i>P-spxA1::Tn</i>	This study
DP-L6444	DP-L4511 + <i>ohrA::Tn</i>	This study
DP-L6445	DP-L4511 + <i>arpJ::Tn</i>	This study
DP-L6446	DP-L4511 + <i>pplA::Tn</i>	This study
DP-L6447	DP-L4511 + <i>gshF::Tn</i>	This study
DP-L6448	Δ <i>gshF yjbH::Tn</i>	This study
DP-L6449	Δ <i>gshF P-spxA1::Tn</i>	This study
DP-L6450	Δ <i>gshF ohrA::Tn</i>	This study
DP-L6451	Δ <i>gshF arpJ::Tn</i>	This study
DP-L6452	Δ <i>gshF pplA::Tn</i>	This study
DP-L6418	Δ <i>actA</i> pPL2t.P _{hyper} - <i>actA</i> (pH- <i>actA</i> strain)	This study
DP-L6453	DP-L6418 + <i>yjbH::Tn</i>	This study
DP-L6454	DP-L6418 + <i>P-spxA1::Tn</i>	This study
DP-L6455	DP-L6418 + <i>ohrA::Tn</i>	This study
DP-L6456	DP-L6418 + <i>arpJ::Tn</i>	This study
DP-L6457	DP-L6418 + <i>pplA::Tn</i>	This study
DP-L6458	DP-L6418 + <i>gshF::Tn</i>	This study
DP-L4077	Δ <i>actA</i> pPL1. <i>actA1p-actA</i> (<i>actA1p</i> strain)	(Lauer et al., 2002)
DP-L6459	DP-L4077 + <i>yjbH::Tn</i>	This study
DP-L6460	DP-L4077 + <i>P-spxA1::Tn</i>	This study
DP-L6461	DP-L4077 + <i>ohrA::Tn</i>	This study
DP-L6462	DP-L4077 + <i>arpJ::Tn</i>	This study
DP-L6463	DP-L4077 + <i>pplA::Tn</i>	This study
DP-L6464	DP-L4077 + <i>gshF::Tn</i>	This study
DP-L6189	Δ <i>gshF</i> pPL2. <i>gshF.His</i>	(Reniere et al., 2015)
DP-L6480	<i>yjbH::Tn</i> pPL2. <i>yjbH.His</i>	This study
DP-L6481	<i>P-spxA1::Tn</i> pPL2. <i>spx.His</i>	This study
DP-L6482	<i>arpJ::Tn</i> pPL2. <i>arpJ</i> region	This study
DP-L6483	<i>ohrA::Tn</i> pPL2. <i>ohrRA</i>	This study
DP-L6507	Δ <i>yjbH</i>	This study
DP-L6508	pPL2. <i>actA1p-TagRFP</i>	This study
DP-L6509	Δ <i>yjbH</i> pPL2. <i>actA1p-TagRFP</i>	This study

Table 5.3 *Listeria monocytogenes* Strains.

Knock-in of pPL2 derivative plasmids was performed by standard methods (Lauer et al., 2002). Briefly, constructed pPL2 plasmids were transformed into chemically competent SM10 *E. coli*, selecting on chloramphenicol. Donor SM10 and recipient *L. monocytogenes* were mixed at a 1:1 ratio on a non-selective BHI plate at 37 °C for 4-24 hours, then trans-conjugation was selected for by plating bacteria on BHI containing streptomycin plus either chloramphenicol (pPL2), erythromycin (pPL2e), or tetracycline (pPL2t). Single colonies were re-streaked for purifying selection onto BHI containing the same antibiotics as used after trans-conjugation.

In-frame deletions of genes was accomplished by allelic exchange using pKSV7-oriT and conventional methods (Camilli et al., 1993). Briefly, the constructed knock-out plasmid was transformed into SM10 *E. coli*, recovered on LB containing carbenicillin, and trans-conjugated into *L. monocytogenes* by mixing the donor SM10 and recipient *L. monocytogenes* at a 1:1 ratio on a non-selective BHI plate for 4-24 hours at 30 °C, the permissive temperature for pKSV7-oriT to replicate in Gram-positive organisms. Trans-conjugation was selected on BHI containing both streptomycin and chloramphenicol at 30 °C. After isolation of a single colony of *L. monocytogenes* containing pKSV7-oriT at 30 °C, bacteria were grown at 42 °C on BHI agar containing both streptomycin and chloramphenicol to select for chromosomal integration. Colonies were re-streaked onto selective media at 42 °C two additional times for purifying selection and integrated pKSV7-oriT. This strain was then serially passaged at 30 °C to enrich for excision and loss of pKSV7-oriT. Mutants that lost pKSV7-oriT were identified by sensitivity to chloramphenicol using indirect patch-plating methods. Finally, allelic exchange was confirmed by PCR and, when necessary, Sanger DNA sequencing.

Himar1 Mutagenesis and Transposon Junction Sequencing

Preparation of electro-competent *L. monocytogenes* and *himar1* transposon mutagenesis were performed as previously described (Zemansky et al., 2009), generating a transposon mutant library that was not fully characterized previously (Reniere et al., 2015). Transposon junctions were mapped as previously described (Whiteley et al., 2015). The position of each *himar1* transposon refers to the distance of the insertion site, 3' of the first nucleotide of each gene. Transposons were mapped to the 10403S genome, however, for continuity of nomenclature the EGD-e loci names have been used. For reference: *Imo0441* (LMRG_00133), *Imo0443* (LMRG_00135), *rsbX* is *Imo0896* (LMRG_02320), *yjbH* is *Imo0964* (LMRG_02063), *citC* is *Imo1566* (LMRG_01401), *Imo2107* is (LMRG_01261), *spxA1* is *Imo2191* (LMRG_01641), *ohrA* is *Imo2199* (LMRG_01633), *arpJ* is *Imo2250* (LMRG_01581), *gtcA* is *Imo2549* (LMRG_01698), *pplA* is *Imo2637* (LMRG_02182), *gshF* is *Imo2770* (LMRG_01925).

Generalized transduction

Transposons in the chromosome were introduced into different genetic backgrounds by generalized transduction using the phage U153, as previously described (Hodgson, 2000; Zemansky et al., 2009). Briefly, a transducing lysate was generated by lysogenizing approximately 10⁹ CFU of *L. monocytogenes* transposon donor with

approximately 10^7 PFU of phage in 3-4 mL of 0.7% LB Agar containing MgSO_4 and CaCl_2 (10 mM each) on LB agar and incubated overnight at 30 °C. Phage was soaked out of the agar by incubating with 5 mL of TM buffer (10 mM Tris, pH 7.5 and 10 mM MgSO_4) for 8-24 hours and these recovered phage stocks were filter sterilized. With the newly generated transducing lysate, 10^8 *L. monocytogenes* recipients were lysogenized with 10^7 PFU of lysate, incubated at 30 °C for 30 min in LB containing MgSO_4 and CaCl_2 (10 mM each), and then plated on selective BHI agar at 37 °C. When transducing the *himar1* transposon using erythromycin selection, colonies appeared after two days. These colonies were purified by re-streaking transductants for single colonies and verified by sequencing the transposon junction. U153 phage stocks were propagated using *L. monocytogenes* strain SLCC-5762.

Cloning and Plasmid Construction

Knock-in plasmids were constructed as previously described using primers listed in Table 5.4 and reagents are from New England Biolabs, unless otherwise specified (Whiteley et al., 2015). Briefly, vectors for complementing *yjbH* and *spxA1* were constructed by amplifying each gene along with its predicted native promoters using a reverse primer that appended a DNA sequence encoding a six histidine affinity tag at the C-terminus. These DNA fragments and pPL2 (Lauer et al., 2002) were then digested with KpnI and BamHI and ligated using Quick Ligase, according to manufacturer's instructions. The *arpJ* and *ohrA* complement vectors were constructed by amplifying their entire predicted operon and predicted native promoter (*arpJ*: LMRG_01581-LMRG_01580, *ohrA*: LMRG_01632-LMRG_01633) without addition of affinity tags. The DNA fragment was combined with linearized pPL2t harboring a transcriptional terminator (Whiteley et al., 2015) and assembled using In-Fusion Cloning (Clontech) or Gibson Assembly Ultra (Synthetic Genomics). The pPL2t-*P_{hyper}-actA* vector was constructed by amplifying both 5' UTR and CDS of *actA* (LMRG_02626), and combining the DNA fragment with linearized pPL2t harboring a modified *P_{spac-hy}* (*P_{hyper}*) (Quisel et al., 2001) sequence: "aattgtgagcgcctcacaattttgcaaaaagttgtgactttatctacaaggtgtggcataatgtgtGTAATTGTGAGC GCTCACAATT", inserted via gBLOCK (IDT), and a transcriptional terminator for assembly using In-Fusion Cloning (Clontech).

Target Gene	Forward Primer Sequence ^a	Reverse Primer Sequence ^a
16S rRNA	accctgattttagttgccag	tgtagccagggtcataag
<i>actA</i>	cgacataaatattgcagcgcac	tgcttcaacattgctattag
<i>lmo0443</i>	gggtagttgcagttataggt	tcaagctgtctgatcgcc
<i>yjbH</i>	cgatccagcttgtagtact	gcggctttgactgcaagac
<i>citC</i>	ggcattcgttcaactaacggt	cgattctatgctaccttcta
<i>spxA1</i>	gccgaaaagctcgtgcatg	ccatcctcagtcatacgaag
<i>ohrA</i>	ggtgaagttcattcgccaga	cagttgctgttactgtgctc
<i>arpJ</i>	ggttcagaagtagittccct	gtggaacccttcggcattgc
<i>pplA</i>	cgacgacaaaagctggaaaag	gattgattttaactaaagaatcg
<i>gshF</i>	gaccctaactcaccggaagc	tacagagtcactcagatccg
pPL2. <i>yjbH</i> .His	ggccggtaccgatacttttagcaaaaagaca	ggccggatccttaatgatgatgatgatgatgtaagttccgatgattccag
pPL2. <i>spxA1</i> .His	ggccggtaccgaaaacatcaatcagagttaaatt	ggccggatccttaatgatgatgatgatgatggttaaccatttttgccctca
pPL2t. <i>arpJ</i> (LMRG_01581-LMRG_01580)	gctggtaccgggcccctaactgttagagccttgctatg	ccagcttgccggccgctataatagctcctttttctataagtc
pPL2t. <i>P_{hyper}-actA</i>	gtaattgtgagcgcctcaaatctgcagaattcatgaatattttcttatattagctaattaagaag	gaattgtggatggctccagcttgcggccgcttaattattttcttaattgaataattttgataaacgc
pPL2t. <i>ohrRA</i> (LMRG_01632-LMRG_01633)	agggaaacaaaagctggtaccggcctaaatataatcaaaagccttac	gtggatggctccagcttgcggccgcttggccgtaaacgcag
pKSV7. <i>ΔyjbH</i> 5' homology	GAGGAGggtaccggttagaaaaagaagcttggagg	taaatttgggtaacatttctatcacctgattttcaaattc
pKSV7. <i>ΔyjbH</i> 3' homology	atgattaacaaaatttaTACATCGGAAACTTATAAaaaagaagcaccattcctg	gaggagctgcagcaccaaaagtagagtttaagcc

Table 5.4 Oligonucleotide Primers Used in this Study

^a Oligonucleotide primers listed 5'-3', underline indicates restriction endonuclease site or complementary overhang for Gibson Assembly.

The *pKSV7-oriT-ΔyjbH* vector was constructed according to methods previously described (Whiteley et al., 2015). Briefly, the vector was constructed by sequentially amplifying ~1 kb of homology flanking the *yjbH* coding region using primers in Table 5.4. These two fragments were joined by sequence overlap extension PCR, which included the coding region for the first six and last six amino acids of YjbH. The final PCR fragment and *pKSV7-oriT* were digested with KpnI and PstI (rSAP was also included for the vector) and ligated using Quick Ligase. The ligation product was transformed into XL1 Blue *E. coli* and transformants were screened by PCR for the presence of the insert, followed by Sanger sequencing confirmation.

Plaque Assay

The plaque assay was carried out by conventional methods (Durack et al., 2014; Sun et al., 1990). Briefly, L2 fibroblasts (generated previously from L929 cells (Sturman and Takemoto, 1972) and provided as a generous gift from Susan Weiss in 1988, as detailed in Sun et al. (Sun et al., 1990)) or TIB-73 hepatocytes (ATCC TIB-73) were maintained in high-glucose DMEM medium plus 10% FBS (Hyclone), 2 mM L-glutamine (Gibco), and 1 mM sodium pyruvate (Gibco). Cells were plated at 1.2×10^6 cells per well in a six-well dish and infected the next day at an MOI of 300 with *L. monocytogenes* grown overnight at 30 °C, stationary. The infection was allowed to proceed for one hour before the wells were washed twice with PBS and 3 mL of medium plus 0.7% agarose and 10 μg/mL gentamicin was overlaid. At 48 hours post-infection the plaques were stained with 2 mL of medium plus 0.7% agarose, 10 μg/mL gentamicin, and 25 μL/mL neutral red (Sigma). The plaques were then imaged at 72 hours post-infection. Plaque area was quantified using ImageJ software (Schneider et al., 2012). Each experiment

represented an average of the area of at least five plaques per strain as a proportion to wild-type plaques in that experiment. Data are representative of at least three experiments.

Macrophage Growth Curves

Macrophage growth curves were performed as previously described (Mitchell et al., 2015; Portnoy et al., 1988). Briefly, bone marrow-derived macrophages (BMMs) were derived from bone marrow of C57BL/6 mice purchased from The Jackson Laboratory and were cultivated/differentiated in high-glucose DMEM medium containing CSF (from mouse CSF-1-producing 3T3 cells), 20% FBS (Hyclone), 2 mM L-glutamine (Gibco), 1 mM sodium pyruvate (Gibco), and 14 mM 2-mercaptoethanol (BME, Gibco). BMMs were derived as previously described and plated in 60 mm non-TC treated dishes that contained 14 TC-treated coverslips at 3×10^6 cells per dish. These dishes were then infected at an MOI of 0.1 for 30 minutes, washed twice with PBS prior to replacing media, and gentamicin was added at 50 $\mu\text{g}/\text{mL}$ one hour post-infection. Three coverslips were removed from each dish at 0.5, 2, 5, and 8 hours post-infection and added to 5 mL of sterile water. Coverslips were rigorously mixed prior to plating on LB agar. Each graph is representative of three experiments and each data point represents the average of three coverslips.

Virulence assays and in vivo suppressor analysis

To analyze virulence, female CD-1 mice were infected intravenously (i.v.) via the tail vein using 200 μL of sterile PBS containing 10^5 CFU of each *L. monocytogenes* strain as previously described (Archer et al., 2014). The infection was allowed to progress for 48 hours, at which point animals were euthanized and the spleens and livers were harvested. Organs were homogenized in 0.1% NP-40 and serial dilutions were plated on LB agar containing streptomycin. Graphs represent pooled data from at least two experiments of greater than four mice each. Groups were statistically compared using a heteroscedastic Student's *t-test*.

In vivo suppressors were identified similarly to previously described methods (Reniere et al., 2015). Briefly, CD-1 mice were infected i.v. with 1×10^7 CFU of ΔgshF for 72 hours and the livers were harvested, homogenized, and 100 μL was inoculated into broth. Naïve mice were then infected with these liver homogenate cultures. After four successive infections bacteria isolated from infected livers were analyzed via plaque assay and two strains with intermediate plaque phenotype were selected for genome sequencing.

Genome Sequencing

Genomic DNA was isolated from *L. monocytogenes* using the MasterPure Gram-Positive DNA Purification Kit (Epicentre) according to the manufacturer's instructions. Genome sequencing and DNA library preparation was performed as previously described (Whiteley et al., 2015) at the Vincent J. Coates Genomics Sequencing Laboratory at UC Berkeley. Data was assembled and aligned to the 10403S reference genome (GenBank: GCA_000168695.2) demonstrating >50x coverage. SNP/InDel/structural variation was determined as compared to the ΔgshF parent strain using CLC Genomics Workbench (CLC bio).

Immunoblots

All immunoblotting was performed as previously described (Reniere et al., 2015). Briefly, for bacteria grown in broth, overnight cultures were diluted 1:10 into BHI, incubated for five hours at 37 °C, shaking, then the bacteria were separated from the supernatant by centrifugation. For secreted proteins, the supernatant was treated with 10% v/v TCA for one hour on ice to precipitate all proteins. The protein pellet was washed twice with ice- cold acetone, followed by vacuum drying. The proteins were dissolved in LDS buffer (Invitrogen) containing 5% BME using a volume that normalized for OD₆₀₀ of harvested bacteria, boiled for 20 minutes, and separated by SDS-PAGE. For surface associated proteins, bacteria were suspended in 150 µL of LDS buffer containing 5% BME, boiled for 20 minutes, and proteins separated by SDS-PAGE.

Immunoblots of bacteria grown intracellularly within infected BMMs used 12-well dishes with BMMs at a density of 10⁶ cells per well and infected with an MOI of 10. One hour post-infection the cells were washed and media containing gentamicin (50 µg/mL) was added. Four hours post-infection the cells were washed twice with PBS and harvested in 150 µL LDS buffer containing 5% BME. The samples were then boiled and separated by SDS-PAGE. Primary antibodies were each used at a dilution of 1:5,000, including: rabbit polyclonal antibody against the N-terminus of ActA (Lauer et al., 2008), rabbit polyclonal antibody against LLO, and a mouse monoclonal antibody against P60 (Adipogen). P60 is a constitutively expressed bacterial protein used as a loading control (Köhler et al., 1991). All immunoblots were visualized and quantified using Odyssey Imager and appropriate secondary antibodies from the manufacturer according to the manufacturer's instructions.

Quantitative RT-PCR of bacterial transcripts

Transcript analysis in broth was performed as previously described (Burke et al., 2014). Briefly, bacteria were grown overnight in BHI and subcultured 1:100 into 25 mL BHI. Bacteria were harvested at an OD₆₀₀ = 1.0. Transcript analysis during infection was analyzed as previously described (Reniere et al., 2015). Briefly, BMMs were plated at a density of 3 x 10⁷ cells in 150 mm TC-treated dishes and infected with an MOI of 10. One hour post-infection the cells were washed and media containing gentamicin (50 µg/mL) was added. Four hours post-infection the cells were washed with PBS and lysed in 5 mL of 0.1% NP-40. After collecting the lysate, the dishes were then washed in RNeasy Protect Bacteria Reagent (Qiagen), which was combined with the lysate. Bacteria were isolated by centrifugation. Bacteria harvested from either broth or BMMs were lysed in phenol:chloroform containing 1% SDS by vortexing with 0.1 mm diameter silica/zirconium beads (BioSpec Products Inc.). Nucleic acids were precipitated from the aqueous fraction overnight at -80 °C in ethanol containing 150 mM sodium acetate (pH 5.2). Precipitated nucleic acids were washed with ethanol and treated with TURBO DNase per manufacturer's specifications (Life Technologies Corporation). RNA was again precipitated overnight and then washed in ethanol. RT-PCR was performed with iScript Reverse Transcriptase (Bio-Rad) and quantitative PCR (qPCR) of resulting cDNA was performed with KAPA SYBR Fast (Kapa Biosystems). Primers used for qPCR are listed in Table 5.4.

Disk diffusions

Disk diffusions were performed similarly to previously described methods (Rae et al., 2011). Briefly, approximately 3×10^7 CFU from overnight cultures of bacteria were immobilized using 4 mL of molten (55 °C) top-agar (0.8% NaCl and 0.8% bacto-agar) spread evenly on tryptic soy agar plates. After the agar cooled, Whatman paper disks soaked in 5 μ L of 5% hydrogen peroxide, 1 M diamide solution, or 80% cumene hydroperoxide solution were placed on top of the bacteria-agar. The zone of inhibition was measured after 18-20 hours of incubation at 37 °C.

actA1p-rfp Fluorescence Measurements in BMMs

BMMs were differentiated and cultivated as described for BMM growth curves. Cells were plated at 5×10^5 cells per well in a 24-well dish in media without antibiotics. The following day BMMs were infected at an MOI of 5 with *L. monocytogenes* mutants that had been incubated at 30 °C without shaking. After 30 minutes cells were washed once with PBS and fresh media containing gentamicin (50 μ g/mL) was added. Six hours post infection media was removed from each well, the cells were washed with 1 mL of PBS, and 0.5 mL of PBS was replaced for each well. RFP fluorescence was measured using a plate reader (Infinite M1000 PRO, TECAN) with 555 nm excitation, 584 nm emission, and 5 nm band filters. Each well was interrogated 64 times on an 8 X 8 grid and the edge reads were excluded. Data were normalized by subtracting baseline fluorescence of wild-type (without RFP) infected cells and plotting data as a percentage of wild-type expressing *actA1p-rfp*. Each experiment represents three infected wells per *L. monocytogenes* genotype and data are representative of three pooled independent experiments.

Chapter 6: Concluding Thoughts and Unanswered Questions

Data presented here focused on the phenotypic consequences of decreased intracellular c-di-AMP, nucleotide receptor proteins, and the basics of why c-di-AMP is a PAMP. Our work on c-di-AMP was inspired by the host innate immune system. Innate immune detection of c-di-AMP implies that this nucleotide is critical to the physiology of bacteria and led us to explore a truly fundamental aspect of microbiology. The second portion of this dissertation focused on how the intracellular pathogen *L. monocytogenes* recognizes the host cytosol. In many ways understanding the signal transduction leading to virulence gene upregulation is analogous to innate immune detection. It is likely that the bacterium has identified conserved host associated molecular patterns (HAMPS) unique to the mammalian cytosol.

c-di-AMP

Through bacterial genetics, ablation of either the phosphodiesterases responsible for c-di-AMP degradation or the diadenylate cyclases responsible for c-di-AMP synthesis has demonstrated common phenotypes associated with c-di-AMP signaling. However, the most outstanding question in the field remains: How and when are c-di-AMP levels regulated? Other bacterial signaling nucleotides such as (p)ppGpp, cAMP, and c-di-GMP are synthesized upon induction or stimulus by some stress and quickly degraded thereafter. In contrast, c-di-AMP appears to be synthesized during all stages of growth analyzed, and in many bacteria, appears to be essential. Is c-di-AMP truly governed by a different paradigm for a second messenger or are we missing something? Intuitively, the continual turnover of ATP into c-di-AMP would appear energy-intensive and wasteful (although the c-di-AMP pool is estimated to be <1% of the ATP pool). Could it be that growth in rich media itself a stress? Understanding the regulation of c-di-AMP, and particularly identifying a condition in which c-di-AMP is not synthesized, will undoubtedly lead to a more complete and unifying theory of its function in bacteria.

So far, only one diadenylate cyclase protein domain has been identified but it would be surprising if alternative diadenylate cyclases didn't exist. Recently, degenerate GGDEF domain-containing proteins that were predicted to synthesize c-di-GMP were identified that synthesize cyclic AMP-GMP (Kellenberger et al., 2015; Nelson et al., 2015). Thus, not only may there be alternative diadenylate cyclases but the protein domain responsible for synthesizing c-di-AMP, the DisA_N domain (Pfam: PF02457) (Witte et al., 2008), may synthesize other molecules in some organisms. The DisA_N domain appears modular and the architectures of the protein domains that are paired with DisA_N allow classification of distinct DAC categories. Three representative DAC categories make up 98.7% of DisA_N-containing proteins: DisA, DacB (a.k.a. YojJ and CdaS), and DacA (a.k.a. YbbP and CdaA) (Corrigan and Gründling, 2013). Organisms such as *B. subtilis* encode DisA, DacB and DacA, *L. monocytogenes* and *S. aureus* encode only DacA, and most Actinobacteria (such as *M. tuberculosis*) only encode DisA. The distribution of these DAC proteins is paradoxical and an unanswered question is whether c-di-AMP produced from different DAC proteins within a single organism signal through the same receptors or if the spatial localization of each DAC confines its signaling capability.

DisA is an octameric diadenylate cyclase that binds DNA and scans the chromosome for damage in the form of lesions and stalled replication forks (Witte et al., 2008). Upon encountering DNA damage, the active sites of the DisA monomers are pulled apart and continual synthesis of c-di-AMP is halted (Bejerano-Sagie et al., 2006; Witte et al., 2008). This constitutive activity is unique among second messenger systems and is, on its face, energetically paradoxical: Why would c-di-AMP signaling evolve to be “ON” until the stimulus is encountered? Considering that DisA is estimated to be present at 465 monomers per *B. subtilis* cell (Muntel et al., 2014), could a reduction in c-di-AMP synthesis by the loss of one functional DisA complex change nucleotide levels enough to initiate a DNA damage response or halt sporulation? This question will likely be answered through understanding why DisA-GFP fusions are observed as a single foci rather than multiple independent octomers (Bejerano-Sagie et al., 2006). It is conceivable that individual DisA complexes form a larger signaling apparatus to coordinate c-di-AMP synthesis as a whole.

DacB homologs make up 5.5% of DisA_N containing proteins identified and is involved in synthesizing c-di-AMP during sporulation in *B. subtilis* (Corrigan and Gründling, 2013; Mehne et al., 2013). Unlike DisA and DacA, DacB appears to be “OFF” in its native state due to an auto-inhibitory protein domain. Mutations in this domain lead to enhanced c-di-AMP synthesis and it is hypothesized that this domain serves as a sensor for initiation of c-di-AMP synthesis (Mehne et al., 2013). DacB appears to be exclusive to endospore-forming bacteria; therefore, identification of the sensory input for DacB may help to identify novel stimuli necessary for sporulation initiation. Interestingly, in *B. subtilis* DacB synthesis might be able to overcome the block in sporulation of the *disA* mutant, suggesting that there may be times when DNA damage is tolerated during sporulation.

DacA homologs are the most widely distributed DAC, comprising over 69.1% of DisA_N containing proteins identified (Corrigan and Gründling, 2013). Depletion of DacA results in severe sensitivity to beta-lactam antibiotics, slowed growth, and an inability to grow in rich medium (Commichau et al., 2015). It appears that DacA is the “cell wall DAC” but it remains unclear how DacA is regulated during cell wall stress and how c-di-AMP contributes to cell wall homeostasis. DacA is almost exclusively encoded in an operon with *dacR* (a.k.a. *cdaR* and *ybbR*), a protein encoding a predicted N-terminal transmembrane domain and extracellular repeats of the YbbR protein domain. The two proteins were shown to physically interact through their transmembrane domains, thus connecting DacA activity to extracellular signals sensed by DacR (Rismondo et al., 2015). From these data it has been hypothesized that DacR transduces the state of the cell wall into appropriate activity of DacA. In *B. subtilis* and *L. monocytogenes* DacR activates and inhibits DacA, respectively (Mehne et al., 2013; Rismondo et al., 2015), revealing unexpectedly opposite results despite the relative similarities between species. It is unclear why the consequences of physical protein-protein interaction may not be conserved between species. Furthermore, the molecular cue that DacR detects remains unknown. Structural analysis of the YbbR protein domain shows similarity to ribosomal proteins, which interact with both rRNA and peptides (Barb et al., 2011). The

ability of structural homologs of YbbR to interact with carbohydrates and peptides may suggest that DacR may directly interact with the peptidoglycan to sense the “health” of the cell wall.

DacA is further regulated by glucosamine-6-phosphate mutase (GlmM) the third gene conserved in virtually all *dacA* operons. GlmM is an essential enzyme for cell wall synthesis and in *Lactococcus lactis* and *B. subtilis*, GlmM directly interacts with DacA (Mehne et al., 2013; Zhu et al., 2016). Intuitively, one might hypothesize that depletion of DacA leads to cell wall defects due to a loss of the DacA-GlmM interaction; however, data presented here show that simply mutating the active site of DacA is sufficient to render *L. monocytogenes* sensitive to cefuroxime. Further, DacA defects could be complemented with over expression of DisA, a DAC that is not predicted to interact with GlmM. Instead, GlmM was shown to inhibit DacA, though reciprocal regulation of GlmM by DacA is still a formal and untested possibility (Zhu et al., 2016).

c-di-AMP is emerging as a regulator of osmotic stress in a wide variety of organisms. There now exist multiple c-di-AMP-interacting proteins that participate in osmotic homeostasis, such as potassium importers (Corrigan et al., 2013) and carnitine importers (Huynh et al., 2016). In data presented here, osmo-homeostasis underlies the sensitivity of the *L. monocytogenes* $\Delta dacA$ mutant to cefuroxime, representing a previously unappreciated role of osmotic pressure in sensitivity to cell-wall-acting antibiotics. It would appear that the cell wall/c-di-AMP connection is really just a product of osmotic stress. However, in *L. lactis* there is evidence for a signaling loop between cell wall precursor biosynthesis and c-di-AMP, as observed by a direct correlation between c-di-AMP levels and UDP-N-acetylglucosamine (Zhu et al., 2016). Is c-di-AMP regulating *both* cell wall biosynthesis and cellular osmotic pressure to resist cell wall targeting antibiotics? It is a formal possibility that alterations in bacterial osmotic pressure feedback on peptidoglycan synthesis to balance the cell wall with turgor pressure. A simpler, alternative hypothesis is that c-di-AMP is inhibiting an intracellular protein that synthesizes peptidoglycan precursors downstream of UDP-N-acetylglucosamine production.

A unique way to identify the mysterious c-di-AMP-protein interaction responsible for regulation of peptidoglycan biosynthesis might be to look at the genomic distribution of the c-di-AMP-interacting yuaA/ydaO riboswitch. *L. monocytogenes* does not encode the identified c-di-AMP riboswitch, however in other organisms the yuaA/ydaO riboswitch precedes a diverse range of genes, many of which are annotated as cell wall-degrading enzymes, potassium importers, amino acid transporters, and osmolyte importers (Block et al., 2010; Nelson et al., 2013). Through a spectacular feat of evolution, c-di-AMP has converged to regulate the same protein elements in different species by alternative biochemical mechanisms! In *S. aureus* the KtrA potassium importer is directly inhibited by c-di-AMP at the protein level (Corrigan et al., 2013; Kim et al., 2015). However, in *B. subtilis* KtrA translation is inhibited via the c-di-AMP-responsive riboswitch (Nelson et al., 2013). By mining the dataset of genes regulated by the yuaA/ydaO riboswitch, novel c-di-AMP-interacting proteins might be identified in organisms that are not predicted to encode a c-di-AMP-responsive riboswitch. To this end, the yuaA/ydaO riboswitch

regulates expression of an oligopeptide permease in *Thermoanaerobacter tengcongensis* and given the genetic association between Opp and c-di-AMP in *L. monocytogenes* presented here, there may be a direct and more general role for c-di-AMP regulating the Opp transporter (Block et al., 2010).

Although a diverse array of pathogens are predicted to synthesize c-di-AMP, there is only evidence of c-di-AMP secretion from *L. monocytogenes* (Woodward et al., 2010), *M. tuberculosis* (Dey et al., 2015; Yang et al., 2014), and *Chlamydia tracomatis* (Barker et al., 2013). In *L. monocytogenes* the transporters responsible for c-di-AMP secretion have been identified and despite homologs existing in related Firmicutes, c-di-AMP secretion has not been reported (Crimmins et al., 2008; Kaplan Zeevi et al., 2013). Secretion, therefore, may represent a specific adaptation by *L. monocytogenes* to intracellular growth: either to manipulate the immune system, control intracellular c-di-AMP levels, or alter the function of extracellular c-di-AMP-binding proteins. Control of c-di-AMP levels via secretion of the molecule would be unprecedented for nucleotide second messengers, although secretion is plausibly the fastest method to lower intracellular nucleotide concentration. Alternatively, secretion of c-di-AMP may simply be promiscuous and a reflection of changes in intracellular concentrations of nucleotide. Although there are none yet identified, the existence of an extracellular c-di-AMP binding proteins would imply a functional role for c-di-AMP secretion. There is some support for this hypothesis from one report, where extracellular c-di-AMP alters the sensitivity of *L. monocytogenes* to vancomycin (Kaplan Zeevi et al., 2013).

The definition of a PAMP is at times nebulous and was first hypothesized in 1989 with the example of lipopolysaccharide from Gram negative bacteria (Janeway, 1989). A PAMP can be described as non-self (not made by mammals), conserved, critical to function and physiology of the pathogen, and detected by a cognate pattern recognition receptor. Ultimately, it remains to be determined if c-di-AMP is a true PAMP that the immune system detects to generate an antibacterial response. STING knock-out mice are not more susceptible to any bacterial infections yet identified, however, pathogens like *L. monocytogenes* may simply be capable of avoiding the antimicrobial implications of STING signaling. Evolution of STING in metazoan hosts might provide clues to these remaining questions. Ancestral STING detects bacterial cyclic di-nucleotides and STING homologs may predate the acquisition of cGAS homologs (Kranzusch et al., 2015), suggesting that at least in a common ancestor, STING signaling was important for detection of bacteria. However, within the human population, alleles of STING that are less responsive to bacterial di-nucleotides have emerged and may suggest that sensing bacterial cyclic dinucleotides in humans is counterproductive to immunity (Diner et al., 2013), which would be consistent with data from the mouse model of *L. monocytogenes* infection (Archer et al., 2014; Auerbuch et al., 2004). A more complete molecular understanding of STING signaling, especially in regard to detection of non-pathogens, will undoubtedly help answer these questions.

Virulence Gene regulation

L. monocytogenes is an ideal model pathogen, in part due to an extremely well-characterized lifecycle that is facilitated by virulence factors required at each step. These virulence factors, such as LLO for escape from the vacuole and ActA for spreading cell-to-cell, have been identified yet considerably less is known about their regulation. The second half of this dissertation employed a forward genetic selection for bacteria unable to up-regulate *actA*, and allowed the screening of a large library of mutants for defective *in vivo* gene expression. We then took two different approaches to understand the multitude of mutations identified. The first (and conventional) approach was to focus on the most prominent hit from the screen. Findings on how *gshF* is regulated and the role of glutathione during infection provide a molecular mechanism for how *L. monocytogenes* activates PrfA and transitions virulence gene expression from “early” to “late” PrfA-boxes. The second body of work included in this dissertation experimented with an alternative analysis method. Rather than selecting an individual mutant from the screen to focus on in detail, we took a broad approach and classified each mutant into a category that corresponded to its particular block in virulence. This approach highlighted how virulence factor expression is spatially compartmentalized via regulation of transcription and translation during infection. We hope that by analyzing each mutant agnostic to its molecular mechanism we have captured a dimension of forward genetics that can be lost by concentrating on only the most prominent result of a screen.

Ultimately the large and unanswered question posed by the exquisitely specific location for induction of ActA in the cell is “what does the bacterium sense in the mammalian cytosol that triggers ActA expression?”. ActA is induced in kangaroo cells (Theriot et al., 1994), mouse cells (Reniere et al., 2015), zebra fish (Levraud et al., 2009), and insect cells (Mansfield et al., 2003), providing evidence that the molecular cues that trigger virulence gene expression in *L. monocytogenes* are evolutionarily ancient. Results from the forward genetic selection for mutants that are unable to upregulate ActA led us to hypothesize that there are two distinct molecular inputs to virulence gene expression in *L. monocytogenes*. The first HAMP provides cue-1 and activates PrfA via glutathione and *gshF*, the second HAMP provide cue-2 and activates the 5' UTR of *actA* and requires *yjbH*.

Cue-1 triggers 10-fold increased expression of *gshF*, increasing glutathione levels and activating PrfA. Although the affinity of PrfA for glutathione *in vitro* appears very low, it is well within biologically relevant concentrations. In a $\Delta gshF$ mutant, host glutathione can activate PrfA but host glutathione is not required to activate virulence genes in wild type organisms, nor is host glutathione sufficient for virulence gene induction. The paradox we are presented with is: if *L. monocytogenes* can sense host glutathione, why would it encode its own glutathione synthase that is required for infection? I hypothesize that a long time ago, in a galaxy far, far away, an ancestor of *L. monocytogenes* evolved to sense host glutathione directly and did not encode a glutathione synthase. This organism may have instead synthesized bacillithiol, another low molecular weight thiol that performs an analogous role to glutathione but is not predicted to activate PrfA.

Close relatives of *L. monocytogenes* such as *B. subtilis* and *S. aureus* encode bacillithiol synthesis genes, suggesting that present day *L. monocytogenes* has likely lost the ability to synthesize bacillithiol (Lee et al., 2007). Responding to host glutathione might have been ideal for our ancestral and hypothetical organism. However, if the *L. monocytogenes* ancestor acquired glutathione synthase, the system could be simplified. Regulating the *gshF* gene may have allowed *L. monocytogenes* to sense a new HAMP (cue-1) and by decreasing the affinity of PrfA for glutathione and increasing glutathione production, bacillithiol could be replaced. Further support for this model is found in the metabolism of *L. monocytogenes* whose incomplete TCA cycle makes synthesis of malate, a building block for bacillithiol, challenging (Fuchs et al., 2012).

Cue-2 activates the 5' UTR of the *actA* RNA to increase translation. Previous characterization of the 5' UTR of *actA* established that this region was important for adequate production of ActA during infection (Wong et al., 2004). However, it was unknown if this RNA region was responsive to stimuli *in vivo* or solely acted as an enhancer. Data presented here demonstrate a sensory role for the 5' UTR that is dependent on YjbH. In the simplest model the *actA* UTR might be a riboswitch like element that binds a small molecule. Interaction of the small molecule with the 5' UTR might then alter the accessibility of the ribosomal binding site and activate *actA* for translation. YjbH might be necessary to produce the small molecule or to process the HAMP into the active Cue-2 compound. These data may also broadly implicate the 5' UTRs of other virulence genes as having a sensory capacity. For example, the 5' UTR of *hly* is required for virulence of *L. monocytogenes* post-transcriptionally (Shen and Higgins, 2005); could this UTR also be a riboswitch like element?

Chapter 7: Literature Cited

Abranches, J., Martinez, A.R., Kajfasz, J.K., Chávez, V., Garsin, D.A., and Lemos, J.A. (2009). The molecular alarmone (p)ppGpp mediates stress responses, vancomycin tolerance, and virulence in *Enterococcus faecalis*. *J Bacteriol* *191*, 2248–2256.

Alkhuder, K., Meibom, K.L., Dubail, I., Dupuis, M., and Charbit, A. (2009). Glutathione provides a source of cysteine essential for intracellular multiplication of *Francisella tularensis*. *PLoS Pathog* *5*, e1000284.

Archer, K.A., Durack, J., and Portnoy, D.A. (2014). STING-Dependent Type I IFN Production Inhibits Cell-Mediated Immunity to *Listeria monocytogenes*. *PLoS Pathog* *10*, e1003861.

Asrat, S., de Jesús, D.A., Hempstead, A.D., Ramabhadran, V., and Isberg, R.R. (2014). Bacterial Pathogen Manipulation of Host Membrane Trafficking. *Annu. Rev. Cell Dev. Biol.* *30*, 79–109.

Auerbuch, V., Brockstedt, D.G., Meyer-Morse, N., O'Riordan, M., and Portnoy, D.A. (2004). Mice lacking the type I interferon receptor are resistant to *Listeria monocytogenes*. *J Exp Med* *200*, 527–533.

Barb, A.W., Cort, J.R., Seetharaman, J., Lew, S., Lee, H.-W., Acton, T., Xiao, R., Kennedy, M.A., Tong, L., Montelione, G.T., et al. (2011). Structures of domains I and IV from YbbR are representative of a widely distributed protein family. *Protein Sci.* *20*, 396–405.

Barker, J.R., Barker, J.R., Koestler, B.J., Koestler, B.J., Carpenter, V.K., Carpenter, V.K., Burdette, D.L., Burdette, D.L., Waters, C.M., Waters, C.M., et al. (2013). STING-dependent recognition of cyclic di-AMP mediates type I interferon responses during *Chlamydia trachomatis* infection. *MBio* *4*, e00018–13.

Bejano-Sagie, M., Oppenheimer-Shaan, Y., Berlatzky, I., Rouvinski, A., Meyerovich, M., and Ben-Yehuda, S. (2006). A checkpoint protein that scans the chromosome for damage at the start of sporulation in *Bacillus subtilis*. *Cell* *125*, 679–690.

Bennett, H.J., Pearce, D.M., Glenn, S., Taylor, C.M., Kuhn, M., Sonenshein, A.L., Andrew, P.W., and Roberts, I.S. (2007). Characterization of *relA* and *codY* mutants of *Listeria monocytogenes*: identification of the CodY regulon and its role in virulence. *Mol Microbiol* *63*, 1453–1467.

Bécavin, C., Bouchier, C., Lechat, P., Archambaud, C., Creno, S., Gouin, E., Wu, Z., Kühbacher, A., Brisse, S., Pucciarelli, M.G., et al. (2014). Comparison of widely used *Listeria monocytogenes* strains EGD, 10403S, and EGD-e highlights genomic variations underlying differences in pathogenicity. *MBio* *5*, e00969–14.

Bishop, D.K., and Hinrichs, D.J. (1987). Adoptive transfer of immunity to *Listeria*

monocytogenes. The influence of in vitro stimulation on lymphocyte subset requirements. *J Immunol* 139, 2005–2009.

Block, K.F., Hammond, M.C., and Breaker, R.R. (2010). Evidence for widespread gene control function by the *ydaO* riboswitch candidate. *J Bacteriol* 192, 3983–3989.

Booth, I.R., Ferguson, G.P., Miller, S., Li, C., Gunasekera, B., and Kinghorn, S. (2003). Bacterial production of methylglyoxal: a survival strategy or death by misadventure? *Biochem. Soc. Trans.* 31, 1406–1408.

Booth, I.R. (2005). Glycerol and Methylglyoxal Metabolism. *EcoSal Plus* 1.

Borezee, E., Msadek, T., Durant, L., and Berche, P. (2000a). Identification in *Listeria monocytogenes* of *MecA*, a homologue of the *Bacillus subtilis* competence regulatory protein. *J Bacteriol* 182, 5931–5934.

Borezee, E., Pellegrini, E., and Berche, P. (2000b). *OppA* of *Listeria monocytogenes*, an oligopeptide-binding protein required for bacterial growth at low temperature and involved in intracellular survival. *Infect Immun* 68, 7069–7077.

Böckmann, R., Dickneite, C., Goebel, W., and Bohne, J. (2000). *PrfA* mediates specific binding of RNA polymerase of *Listeria monocytogenes* to *PrfA*-dependent virulence gene promoters resulting in a transcriptionally active complex. *Mol. Microbiol.* 36, 487–497.

Böckmann, R., Dickneite, C., Middendorf, B., Goebel, W., and Sokolovic, Z. (1996). Specific binding of the *Listeria monocytogenes* transcriptional regulator *PrfA* to target sequences requires additional factor(s) and is influenced by iron. *Mol Microbiol* 22, 643–653.

Brinsmade, S.R., Alexander, E.L., Livny, J., Stettner, A.I., Segrè, D., Rhee, K.Y., and Sonenshein, A.L. (2014). Hierarchical expression of genes controlled by the *Bacillus subtilis* global regulatory protein *CodY*. 111, 8227–8232.

Bruno, J.C., and Freitag, N.E. (2010). Constitutive activation of *PrfA* tilts the balance of *Listeria monocytogenes* fitness towards life within the host versus environmental survival. *PLoS ONE* 5, e15138.

Burdette, D.L., Monroe, K.M., Sotelo-Troha, K., Iwig, J.S., Eckert, B., Hyodo, M., Hayakawa, Y., and Vance, R.E. (2011). *STING* is a direct innate immune sensor of cyclic di-GMP. *Nature* 478, 515–518.

Burke, T.P., Loukitcheva, A., Zemansky, J., Wheeler, R., Boneca, I.G., and Portnoy, D.A. (2014). *Listeria monocytogenes* is resistant to lysozyme through the regulation, not the acquisition, of cell wall-modifying enzymes. *J Bacteriol* 196, 3756–3767.

Camilli, A., Beattie, D.T., and Mekalanos, J.J. (1994). Use of genetic recombination as a reporter of gene expression. *Proceedings of the National Academy of Sciences* 91,

2634–2638.

Camilli, A., Tilney, L.G., and Portnoy, D.A. (1993). Dual roles of *plcA* in *Listeria monocytogenes* pathogenesis. *Mol Microbiol* *8*, 143–157.

Campeotto, I., Zhang, Y., Mladenov, M.G., Freemont, P.S., and Gründling, A. (2014). Complex Structure and Biochemical Characterization of the *Staphylococcus aureus* cyclic di-AMP binding Protein PstA, the Founding Member of a New Signal Transduction Protein Family. *Journal of Biological Chemistry* *290*, 2888–2901.

Chakraborty, T., Leimeister-Wächter, M., Domann, E., Hartl, M., Goebel, W., Nichterlein, T., and Notermans, S. (1992). Coordinate regulation of virulence genes in *Listeria monocytogenes* requires the product of the *prfA* gene. *J Bacteriol* *174*, 568–574.

Chandrangsu, P., Dusi, R., Hamilton, C.J., and Helmann, J.D. (2014). Methylglyoxal resistance in *Bacillus subtilis*: contributions of bacillithiol-dependent and independent pathways. *Mol Microbiol* *91*, 706–715.

Chatterjee, S.S., Hossain, H., Otten, S., Kuenne, C., Kuchmina, K., Machata, S., Domann, E., Chakraborty, T., and Hain, T. (2006). Intracellular gene expression profile of *Listeria monocytogenes*. *Infect Immun* *74*, 1323–1338.

Chaudhuri, R.R., Allen, A.G., Owen, P.J., Shalom, G., Stone, K., Harrison, M., Burgis, T.A., Lockyer, M., Garcia-Lara, J., Foster, S.J., et al. (2009). Comprehensive identification of essential *Staphylococcus aureus* genes using Transposon-Mediated Differential Hybridisation (TMDH). *BMC Genomics* *10*, 291.

Cheng, L.W., Viala, J.P.M., Stuurman, N., Wiedemann, U., Vale, R.D., and Portnoy, D.A. (2005). Use of RNA interference in *Drosophila* S2 cells to identify host pathways controlling compartmentalization of an intracellular pathogen. *102*, 13646–13651.

Cheng, X., Zheng, X., Zhou, X., Zeng, J., Ren, Z., Xu, X., Cheng, L., Li, M., Li, J., and Li, Y. (2016). Regulation of oxidative response and extracellular polysaccharide synthesis by a diadenylate cyclase in *Streptococcus mutans*. *Environmental Microbiology* *18*, 904–922.

Chiang, S.L., Mekalanos, J.J., and Holden, D.W. (1999). In vivo genetic analysis of bacterial virulence. *Annu. Rev. Microbiol.* *53*, 129–154.

Chico-Calero, I., Suárez, M., González-Zorn, B., Scotti, M., Slaghuis, J., Goebel, W., Vázquez-Boland, J.A., European *Listeria* Genome Consortium (2002). Hpt, a bacterial homolog of the microsomal glucose- 6-phosphate translocase, mediates rapid intracellular proliferation in *Listeria*. *99*, 431–436.

Choi, P.H., Sureka, K., Woodward, J.J., and Tong, L. (2015). Molecular basis for the recognition of cyclic-di-AMP by PstA, a PII-like signal transduction protein. *4*, 361–374.

- Cole, C., Thomas, S., Filak, H., Henson, P.M., and Lenz, L.L. (2012). Nitric Oxide Increases Susceptibility of Toll-like Receptor-Activated Macrophages to Spreading *Listeria monocytogenes*. *Immunity* 36, 807–820.
- Commichau, F.M., Dickmanns, A., Gundlach, J., Ficner, R., and Stülke, J. (2015). A jack of all trades: the multiple roles of the unique essential second messenger cyclic di-AMP. *Mol Microbiol* 97, 189–n/a.
- Corrigan, R.M., and Gründling, A. (2013). Cyclic di-AMP: another second messenger enters the fray. *Nat Rev Micro* 11, 513–524.
- Corrigan, R.M., Abbott, J.C., Burhenne, H., Kaeffer, V., and Gründling, A. (2011). c-di-AMP is a new second messenger in *Staphylococcus aureus* with a role in controlling cell size and envelope stress. *PLoS Pathog* 7, e1002217.
- Corrigan, R.M., Bowman, L., Willis, A.R., Kaeffer, V., and Gründling, A. (2015). Crosstalk between two Nucleotide-Signaling Pathways in *Staphylococcus aureus*. *Journal of Biological Chemistry* 290, 5826–5839.
- Corrigan, R.M., Campeotto, I., Jeganathan, T., Roelofs, K.G., Lee, V.T., and Gründling, A. (2013). Systematic identification of conserved bacterial c-di-AMP receptor proteins. *110*, 9084–9089.
- Cossart, P. (2011). Illuminating the landscape of host-pathogen interactions with the bacterium *Listeria monocytogenes*. *108*, 19484–19491.
- Crimmins, G.T., Herskovits, A.A., Rehder, K., Sivick, K.E., Lauer, P., Dubensky, T.W., and Portnoy, D.A. (2008). *Listeria monocytogenes* multidrug resistance transporters activate a cytosolic surveillance pathway of innate immunity. *105*, 10191–10196.
- Dalebroux, Z.D., and Swanson, M.S. (2012). ppGpp: magic beyond RNA polymerase. *Nat Rev Micro* 10, 203–212.
- Dalle-Donne, I., Rossi, R., Colombo, G., Giustarini, D., and Milzani, A. (2009). Protein S-glutathionylation: a regulatory device from bacteria to humans. *Trends in Biochemical Sciences* 34, 85–96.
- Danilchanka, O., and Mekalanos, J.J. (2013). Cyclic dinucleotides and the innate immune response. *Cell* 154, 962–970.
- Deshayes, C., Bielecka, M.K., Cain, R.J., Scotti, M., las Heras, de, A., Pietras, Z., Luisi, B.F., Núñez Miguel, R., and Vázquez-Boland, J.A. (2012). Allosteric mutants show that PrfA activation is dispensable for vacuole escape but required for efficient spread and *Listeria* survival in vivo. *Molecular Microbiology* 85, 461–477.
- Dey, B., Dey, R.J., Cheung, L.S., Pokkali, S., Guo, H., Lee, J.-H., and Bishai, W.R. (2015). A bacterial cyclic dinucleotide activates the cytosolic surveillance pathway and mediates innate resistance to tuberculosis. *Nat Med* 21, 1–8.

Diner, E.J., Burdette, D.L., Wilson, S.C., Monroe, K.M., Kellenberger, C.A., Hyodo, M., Hayakawa, Y., Hammond, M.C., and Vance, R.E. (2013). The Innate Immune DNA Sensor cGAS Produces a Noncanonical Cyclic Dinucleotide that Activates Human STING. *Cell Reports* 3, 1355–1361.

Durack, J., Burke, T.P., and Portnoy, D.A. (2014). A *prl* mutation in *SecY* suppresses secretion and virulence defects of *Listeria monocytogenes* *secA2* mutants. *J Bacteriol* 197, 932–942.

Eisenreich, W., Dandekar, T., Heesemann, J., and Goebel, W. (2010). Carbon metabolism of intracellular bacterial pathogens and possible links to virulence. *Nat Rev Micro* 8, 401–412.

Eiting, M., Hagelüken, G., Schubert, W.-D., and Heinz, D.W. (2005). The mutation G145S in *PrfA*, a key virulence regulator of *Listeria monocytogenes*, increases DNA-binding affinity by stabilizing the HTH motif. *Molecular Microbiology* 56, 433–446.

Epstein, W. (2003). The roles and regulation of potassium in bacteria. *Prog. Nucleic Acid Res. Mol. Biol.* 75, 293–320.

Eylert, E., Schär, J., Mertins, S., Stoll, R., Bacher, A., Goebel, W., and Eisenreich, W. (2008). Carbon metabolism of *Listeria monocytogenes* growing inside macrophages. *Mol Microbiol* 69, 1008–1017.

Freitag, N.E., and Portnoy, D.A. (1994). Dual promoters of the *Listeria monocytogenes* *prfA* transcriptional activator appear essential *in vitro* but are redundant *in vivo*. *Molecular Microbiology* 12, 845–853.

Freitag, N.E., Rong, L., and Portnoy, D.A. (1993). Regulation of the *prfA* transcriptional activator of *Listeria monocytogenes*: multiple promoter elements contribute to intracellular growth and cell-to-cell spread. *Infect Immun* 61, 2537–2544.

Freitag, N.E., Port, G.C., and Miner, M.D. (2009). *Listeria monocytogenes* - from saprophyte to intracellular pathogen. *Nat Rev Micro* 7, 623–628.

French, C.T., Lao, P., Loraine, A.E., Matthews, B.T., Yu, H., and Dybvig, K. (2008). Large-scale transposon mutagenesis of *Mycoplasma pulmonis*. *Mol Microbiol* 69, 67–76.

Fuangthong, M., Atichartpongkul, S., Mongkolsuk, S., and Helmann, J.D. (2001). *OhrR* is a repressor of *ohrA*, a key organic hydroperoxide resistance determinant in *Bacillus subtilis*. *J Bacteriol* 183, 4134–4141.

Fuchs, T.M., Eisenreich, W., Kern, T., and Dandekar, T. (2012). Toward a Systemic Understanding of *Listeria monocytogenes* Metabolism during Infection. *Front Microbiol* 3, 23.

Gaballa, A., Gaballa, A., Antelmann, H., Antelmann, H., Hamilton, C.J., Hamilton, C.J.,

- Helmann, J.D., and Helmann, J.D. (2013). Regulation of *Bacillus subtilis* bacillithiol biosynthesis operons by Spx. *Microbiology* *159*, 2025–2035.
- Garg, S.K., Garg, S.K., Kommineni, S., Kommineni, S., Henslee, L., Henslee, L., Zhang, Y., Zhang, Y., Zuber, P., and Zuber, P. (2009). The YjbH protein of *Bacillus subtilis* enhances ClpXP-catalyzed proteolysis of Spx. *J Bacteriol* *191*, 1268–1277.
- Gawronski, J.D., Wong, S.M.S., Giannoukos, G., Ward, D.V., and Akerley, B.J. (2009). Tracking insertion mutants within libraries by deep sequencing and a genome-wide screen for *Haemophilus* genes required in the lung. *106*, 16422–16427.
- Geiger, T., and Wolz, C. (2013). Intersection of the stringent response and the CodY regulon in low GC Gram-positive bacteria. *Int. J. Med. Microbiol.* *304*, 150–155.
- Geiger, T., Kästle, B., Gratani, F.L., Goerke, C., and Wolz, C. (2014). Two Small (p)ppGpp Synthases in *Staphylococcus aureus* Mediate Tolerance against Cell Envelope Stress Conditions. *J Bacteriol* *196*, 894–902.
- Glass, J.I., Assad-Garcia, N., Alperovich, N., Yooseph, S., Lewis, M.R., Maruf, M., Hutchison, C.A., Smith, H.O., and Venter, J.C. (2006). Essential genes of a minimal bacterium. *103*, 425–430.
- Goodman, A.L., McNulty, N.P., Zhao, Y., Leip, D., Mitra, R.D., Lozupone, C.A., Knight, R., and Gordon, J.I. (2009). Identifying genetic determinants needed to establish a human gut symbiont in its habitat. *Cell Host Microbe* *6*, 279–289.
- Gopal, S., Borovok, I., Ofer, A., Yanku, M., Cohen, G., Goebel, W., Kreft, J., and Aharonowitz, Y. (2005). A multidomain fusion protein in *Listeria monocytogenes* catalyzes the two primary activities for glutathione biosynthesis. *J Bacteriol* *187*, 3839–3847.
- Gundlach, J., Dickmanns, A., Schröder-Tittmann, K., Neumann, P., Kaesler, J., Kampf, J., Herzberg, C., Hammer, E., Schwede, F., Kaefer, V., et al. (2014). Identification, characterization and structure analysis of the c-di-AMP binding PII-like signal transduction protein DarA. *Journal of Biological Chemistry* *290*, 3069–3080.
- Gundlach, J., Mehne, F.M.P., Herzberg, C., Kampf, J., Valerius, O., Kaefer, V., and Stülke, J. (2015). An Essential Poison: Synthesis and Degradation of Cyclic Di-AMP in *Bacillus subtilis*. *J Bacteriol* *197*, 3265–3274.
- Hamon, M., Bierne, H., and Cossart, P. (2006). *Listeria monocytogenes*: a multifaceted model. *Nat Rev Micro* *4*, 423–434.
- Hassett, D.J., and Cohen, M.S. (1989). Bacterial adaptation to oxidative stress: implications for pathogenesis and interaction with phagocytic cells. *Faseb J.* *3*, 2574–2582.
- Hengge, R. (2009). Principles of c-di-GMP signalling in bacteria. *Nat Rev Micro* *7*, 263–

273.

Hensel, M., Shea, J.E., Gleeson, C., Jones, M.D., Dalton, E., and Holden, D.W. (1995). Simultaneous identification of bacterial virulence genes by negative selection. *Science* **269**, 400–403.

Herzberg, C., Weidinger, L.A.F., Dörrbecker, B., Hübner, S., Stülke, J., and Commichau, F.M. (2007). SPINE: a method for the rapid detection and analysis of protein-protein interactions in vivo. *Proteomics* **7**, 4032–4035.

Hodgson, D.A. (2000). Generalized transduction of serotype 1/2 and serotype 4b strains of *Listeria monocytogenes*. *Mol Microbiol* **35**, 312–323.

Hogg, T., Mechold, U., Malke, H., Cashel, M., and Hilgenfeld, R. (2004). Conformational antagonism between opposing active sites in a bifunctional RelA/SpoT homolog modulates (p)ppGpp metabolism during the stringent response. *Cell* **117**, 57–68.

Huynh, T.N., Choi, P.H., Sureka, K., Ledvina, H.E., Campillo, J., Tong, L., and Woodward, J.J. (2016). Cyclic di-AMP targets the cystathionine beta-synthase domain of the osmolyte transporter OpuC. *Molecular Microbiology*.

Huynh, T.N., Luo, S., Pensinger, D., Sauer, J.-D., Tong, L., and Woodward, J.J. (2015). An HD-domain phosphodiesterase mediates cooperative hydrolysis of c-di-AMP to affect bacterial growth and virulence. *112*, E747–E756.

Janeway, C.A. (1989). Approaching the asymptote? Evolution and revolution in immunology. *Cold Spring Harb. Symp. Quant. Biol.* **54 Pt 1**, 1–13.

Johansson, J., Mandin, P., Renzoni, A., Chiaruttini, C., Springer, M., and Cossart, P. (2002). An RNA thermosensor controls expression of virulence genes in *Listeria monocytogenes*. *Cell* **110**, 551–561.

Joseph, B., and Goebel, W. (2007). Life of *Listeria monocytogenes* in the host cells' cytosol. *Microbes Infect* **9**, 1188–1195.

Jutras, B.L., Chenail, A.M., Rowland, C.L., Carroll, D., Miller, M.C., Bykowski, T., and Stevenson, B. (2013). Eubacterial SpoVG homologs constitute a new family of site-specific DNA-binding proteins. *PLoS ONE* **8**, e66683.

Kamegaya, T., Kuroda, K., and Hayakawa, Y. (2011). Identification of a *Streptococcus pyogenes* SF370 gene involved in production of c-di-AMP. *Nagoya J Med Sci* **73**, 49–57.

Kaplan Zeevi, M., Shafir, N.S., Shaham, S., Friedman, S., Sigal, N., Nir-Paz, R., Boneca, I.G., and Herskovits, A.A. (2013). *Listeria monocytogenes* multidrug resistance transporters and cyclic di-AMP, which contribute to type I interferon induction, play a role in cell wall stress. *J Bacteriol* **195**, 5250–5261.

- Kellenberger, C.A., Wilson, S.C., Hickey, S.F., Gonzalez, T.L., Su, Y., Hallberg, Z.F., Brewer, T.F., Iavarone, A.T., Carlson, H.K., Hsieh, Y.-F., et al. (2015). GEMM-I riboswitches from *Geobacter* sense the bacterial second messenger cyclic AMP-GMP. *Proc. Natl. Acad. Sci. U.S.A.* *112*, 5383–5388.
- Kim, H., Youn, S.-J., Kim, S.O., Ko, J., Lee, J.-O., and Choi, B.-S. (2015). Structural Studies of Potassium Transport Protein KtrA Regulator of Conductance of K⁺ (RCK) C Domain in Complex with Cyclic Diadenosine Monophosphate (c-di-AMP). *J Biol Chem* *290*, 16393–16402.
- Kistler, W.S., and Lin, E.C. (1971). Lethal synthesis of methylglyoxal by *Escherichia coli* during unregulated glycerol metabolism. *J Bacteriol* *108*, 137–144.
- Klarsfeld, A.D., Goossens, P.L., and Cossart, P. (1994). Five *Listeria monocytogenes* genes preferentially expressed in infected mammalian cells: *plcA*, *purH*, *purD*, *pyrE* and an arginine ABC transporter gene, *arpJ*. *Mol Microbiol* *13*, 585–597.
- Kline, B.C., McKay, S.L., Tang, W.W., and Portnoy, D.A. (2015). The *Listeria monocytogenes* hibernation-promoting factor is required for the formation of 100S ribosomes, optimal fitness, and pathogenesis. *J Bacteriol* *197*, 581–591.
- Kocks, C., Guin, E., Tabouret, M., Berche, P., Ohayon, H., and Cossart, P. (1992). *L. monocytogenes*-induced actin assembly requires the *actA* gene product, a surface protein. *Cell* *68*, 521–531.
- Kolb, A., Busby, S., Buc, H., Buc, I.I., Garges, S., and Adhya, S. (1993). Transcriptional Regulation by cAMP and its Receptor Protein. *62*, 749–797.
- Kommineni, S., Kommineni, S., Garg, S.K., Garg, S.K., Chan, C.M., Chan, C.M., Zuber, P., and Zuber, P. (2011). YjbH-Enhanced Proteolysis of Spx by ClpXP in *Bacillus subtilis* Is Inhibited by the Small Protein YirB (YuzO). *J Bacteriol* *193*, 2133–2140.
- Köhler, S., Bubert, A., Vogel, M., and Goebel, W. (1991). Expression of the *iap* gene coding for protein p60 of *Listeria monocytogenes* is controlled on the posttranscriptional level. *J Bacteriol* *173*, 4668–4674.
- Kranzusch, P.J., Wilson, S.C., Lee, A.S.Y., Berger, J.M., Doudna, J.A., and Vance, R.E. (2015). Ancient Origin of cGAS-STING Reveals Mechanism of Universal 2',3' cGAMP Signaling. *Mol Cell* *59*, 891–903.
- Kriel, A., Bittner, A.N., Kim, S.H., Liu, K., Tehranchi, A.K., Zou, W.Y., Rendon, S., Chen, R., Tu, B.P., and Wang, J.D. (2012). Direct regulation of GTP homeostasis by (p)ppGpp: a critical component of viability and stress resistance. *Mol Cell* *48*, 231–241.
- Kriel, A., Brinsmade, S.R., Tse, J.L., Tehranchi, A.K., Bittner, A.N., Sonenshein, A.L., and Wang, J.D. (2014). GTP dysregulation in *Bacillus subtilis* cells lacking (p)ppGpp results in phenotypic amino acid auxotrophy and failure to adapt to nutrient downshift and regulate biosynthesis genes. *J Bacteriol* *196*, 189–201.

Langridge, G.C., Phan, M.-D., Turner, D.J., Perkins, T.T., Parts, L., Haase, J., Charles, I., Maskell, D.J., Peters, S.E., Dougan, G., et al. (2009). Simultaneous assay of every *Salmonella* Typhi gene using one million transposon mutants. *Genome Res.* *19*, 2308–2316.

Larsson, J.T., Rogstam, A., and Wachenfeldt, von, C. (2007). YjbH is a novel negative effector of the disulphide stress regulator, Spx, in *Bacillus subtilis*. *Mol Microbiol* *66*, 669–684.

las Heras, de, A., Cain, R.J., Bielecka, M.K., and Vázquez-Boland, J.A. (2011). Regulation of *Listeria* virulence: PrfA master and commander. *Curr Opin Microbiol* *14*, 118–127.

Las Peñas, De, A., Connolly, L., and Gross, C.A. (1997). SigmaE is an essential sigma factor in *Escherichia coli*. *J Bacteriol* *179*, 6862–6864.

Lauer, P., Hanson, B., Lemmens, E.E., Liu, W., LUCKETT, W.S., Leong, M.L., Allen, H.E., Skoble, J., Bahjat, K.S., Freitag, N.E., et al. (2008). Constitutive Activation of the PrfA Regulon Enhances the Potency of Vaccines Based on Live-Attenuated and Killed but Metabolically Active *Listeria monocytogenes* Strains. *Infect Immun* *76*, 3742–3753.

Lauer, P., Chow, M.Y.N., Loessner, M.J., Portnoy, D.A., and Calendar, R. (2002). Construction, characterization, and use of two *Listeria monocytogenes* site-specific phage integration vectors. *J Bacteriol* *184*, 4177–4186.

Lee, J.-W., Soonsanga, S., and Helmann, J.D. (2007). A complex thiolate switch regulates the *Bacillus subtilis* organic peroxide sensor OhrR. *Proceedings of the National Academy of Sciences* *104*, 8743–8748.

Lemos, J.A., Lin, V.K., Nascimento, M.M., Abranches, J., and Burne, R.A. (2007). Three gene products govern (p)ppGpp production by *Streptococcus mutans*. *Mol Microbiol* *65*, 1568–1581.

Levraud, J.-P., Disson, O., Kissa, K., Bonne, I., Cossart, P., Herbomel, P., and Lecuit, M. (2009). Real-time observation of *Listeria monocytogenes*-phagocyte interactions in living zebrafish larvae. *Infect Immun* *77*, 3651–3660.

Liu, S., Bayles, D.O., Mason, T.M., and Wilkinson, B.J. (2006). A cold-sensitive *Listeria monocytogenes* mutant has a transposon insertion in a gene encoding a putative membrane protein and shows altered (p)ppGpp levels. *Appl Environ Microbiol* *72*, 3955–3959.

Lobel, L., Sigal, N., Borovok, I., Belitsky, B.R., Sonenshein, A.L., and Herskovits, A.A. (2015). The metabolic regulator CodY links *Listeria monocytogenes* metabolism to virulence by directly activating the virulence regulatory gene prfA. *Mol Microbiol* *95*, 624–644.

Lobel, L., Sigal, N., Borovok, I., Ruppin, E., and Herskovits, A.A. (2012). Integrative

genomic analysis identifies isoleucine and CodY as regulators of *Listeria monocytogenes* virulence. *PLoS Genet.* 8, e1002887.

Luo, Y., and Helmann, J.D. (2012). Analysis of the role of *Bacillus subtilis* $\sigma(M)$ in β -lactam resistance reveals an essential role for c-di-AMP in peptidoglycan homeostasis. *Mol Microbiol* 83, 623–639.

Mansfield, B.E., Dionne, M.S., Schneider, D.S., and Freitag, N.E. (2003). Exploration of host-pathogen interactions using *Listeria monocytogenes* and *Drosophila melanogaster*. *Cellular Microbiology* 5, 901–911.

Manzanillo, P.S., Shiloh, M.U., Portnoy, D.A., and Cox, J.S. (2012). *Mycobacterium tuberculosis* activates the DNA-dependent cytosolic surveillance pathway within macrophages. *Cell Host Microbe* 11, 469–480.

Maqbool, A., Levdikov, V.M., Blagova, E.V., Hervé, M., Horler, R.S.P., Wilkinson, A.J., and Thomas, G.H. (2011). Compensating stereochemical changes allow murein tripeptide to be accommodated in a conventional peptide-binding protein. *Journal of Biological Chemistry* 286, 31512–31521.

Masip, L., Veeravalli, K., and Georgiou, G. (2006). The Many Faces of Glutathione in Bacteria. *Antioxid. Redox Signal.* 8, 753–762.

Matsuno, K., and Sonenshein, A.L. (1999). Role of SpoVG in asymmetric septation in *Bacillus subtilis*. *J Bacteriol* 181, 3392–3401.

McLaggan, D., Logan, T.M., Lynn, D.G., and Epstein, W. (1990). Involvement of gamma-glutamyl peptides in osmoadaptation of *Escherichia coli*. *J Bacteriol* 172, 3631–3636.

McLaggan, D., Naprstek, J., Buurman, E.T., and Epstein, W. (1994). Interdependence of K⁺ and glutamate accumulation during osmotic adaptation of *Escherichia coli*. *J Biol Chem* 269, 1911–1917.

Mechold, U., Cashel, M., Steiner, K., Gentry, D., and Malke, H. (1996). Functional analysis of a *relA/spoT* gene homolog from *Streptococcus equisimilis*. *J Bacteriol* 178, 1401–1411.

Mehne, F.M.P., Gunka, K., Eilers, H., Herzberg, C., Kaefer, V., and Stülke, J. (2013). Cyclic di-AMP homeostasis in *Bacillus subtilis*: both lack and high level accumulation of the nucleotide are detrimental for cell growth. *J Biol Chem* 288, 2004–2017.

Meier, S., Goerke, C., Wolz, C., Seidl, K., Homerova, D., Schulthess, B., Kormanec, J., Berger-Bächi, B., and Bischoff, M. (2007). *sigmaB* and the *sigmaB*-dependent *arlRS* and *yabJ-spoVG* loci affect capsule formation in *Staphylococcus aureus*. *Infect Immun* 75, 4562–4571.

Meister, A., and Anderson, M.E. (1983). Glutathione. *Annu. Rev. Biochem.* 52, 711–

760.

Mengaud, J., Dramsi, S., Gouin, E., Vázquez-Boland, J.A., Milon, G., and Cossart, P. (1991). Pleiotropic control of *Listeria monocytogenes* virulence factors by a gene that is autoregulated. *Molecular Microbiology* 5, 2273–2283.

Miner, M., Port, G., and Freitag, N. (2007). Regulation of *Listeria monocytogenes* virulence genes. *Listeria Monocytogenes: Pathogenesis and Host Response* 139–158.

Miner, M.D., Port, G.C., and Freitag, N.E. (2008). Functional impact of mutational activation on the *Listeria monocytogenes* central virulence regulator PrfA. *Microbiology (Reading, Engl)* 154, 3579–3589.

Mitchell, G., Ge, L., Huang, Q., Chen, C., Kianian, S., Roberts, M.F., Schekman, R., and Portnoy, D.A. (2015). Avoidance of autophagy mediated by PlcA or ActA is required for *Listeria monocytogenes* growth in macrophages. *Infect Immun* 83, 2175–2184.

Monk, I.R., Gahan, C.G.M., and Hill, C. (2008). Tools for functional postgenomic analysis of *listeria monocytogenes*. *Appl Environ Microbiol* 74, 3921–3934.

Moors, M.A., Levitt, B., Youngman, P., and Portnoy, D.A. (1999). Expression of listeriolysin O and ActA by intracellular and extracellular *Listeria monocytogenes*. *Infect Immun* 67, 131–139.

Muntel, J., Fromion, V., Goelzer, A., Maass, S., Mader, U., Buttner, K., Hecker, M., and Becher, D. (2014). Comprehensive absolute quantification of the cytosolic proteome of *Bacillus subtilis* by data independent, parallel fragmentation in liquid chromatography-mass spectrometry. *Molecular & Cellular Proteomics* 13, 1008–1019. - PubMed - NCBI.

Müller, M., Hopfner, K.-P., and Witte, G. (2015). c-di-AMP recognition by *Staphylococcus aureus* PstA. *FEBS Lett.* 589, 45–51.

Myers, J.T., Tsang, A.W., and Swanson, J.A. (2003). Localized reactive oxygen and nitrogen intermediates inhibit escape of *Listeria monocytogenes* from vacuoles in activated macrophages. *J Immunol* 171, 5447–5453.

Nakano, S., Nakano, S., Nakano, M.M., Nakano, M.M., Zhang, Y., Zhang, Y., Leelakriangsak, M., Leelakriangsak, M., Zuber, P., and Zuber, P. (2003). A regulatory protein that interferes with activator-stimulated transcription in bacteria. *Proceedings of the National Academy of Sciences* 100, 4233–4238.

Nanamiya, H., Kasai, K., Nozawa, A., Yun, C.-S., Narisawa, T., Murakami, K., Natori, Y., Kawamura, F., and Tozawa, Y. (2008). Identification and functional analysis of novel (p)ppGpp synthetase genes in *Bacillus subtilis*. *Mol Microbiol* 67, 291–304.

Nelson, J.W., Sudarsan, N., Furukawa, K., Weinberg, Z., Wang, J.X., and Breaker, R.R. (2013). Riboswitches in eubacteria sense the second messenger c-di-AMP. *Nat. Chem. Biol.* 9, 834–839.

- Nelson, J.W., Sudarsan, N., Phillips, G.E., Stav, S., Lünse, C.E., McCown, P.J., and Breaker, R.R. (2015). Control of bacterial exoelectrogenesis by c-AMP-GMP. *112*, 201419264–5394.
- Newton, G.L., Arnold, K., Price, M.S., Sherrill, C., Delcardayre, S.B., Aharonowitz, Y., Cohen, G., Davies, J., Fahey, R.C., and Davis, C. (1996). Distribution of thiols in microorganisms: mycothiol is a major thiol in most actinomycetes. *J Bacteriol* *178*, 1990–1995.
- Newton, G.L., Rawat, M., Rawat, M., La Clair, J.J., Jothivasan, V.K., Jothivasan, V.K., Budiarto, T., Hamilton, C.J., Claiborne, A., Helmann, J.D., et al. (2009). Bacillithiol is an antioxidant thiol produced in Bacilli. *Nat. Chem. Biol.* *5*, 625–627.
- Ninfa, A.J., and Jiang, P. (2005). PII signal transduction proteins: sensors of alpha-ketoglutarate that regulate nitrogen metabolism. *Curr Opin Microbiol* *8*, 168–173.
- O’Riordan, M., Moors, M.A., and Portnoy, D.A. (2003). *Listeria* intracellular growth and virulence require host-derived lipoic acid. *Science* *302*, 462–464.
- O’Riordan, M., Yi, C.H., Gonzales, R., Lee, K.-D., and Portnoy, D.A. (2002). Innate recognition of bacteria by a macrophage cytosolic surveillance pathway. *Proceedings of the National Academy of Sciences* *99*, 13861–13866.
- Oberdoerffer, P., Otipoby, K.L., Maruyama, M., and Rajewsky, K. (2003). Unidirectional Cre-mediated genetic inversion in mice using the mutant loxP pair lox66/lox71. *Nucleic Acids Research* *31*, e140–e140.
- Phan-Thanh, L., and Gormon, T. (1997). A chemically defined minimal medium for the optimal culture of *Listeria*. *Int. J. Food Microbiol.* *35*, 91–95.
- Port, G.C., and Freitag, N.E. (2007). Identification of novel *Listeria monocytogenes* secreted virulence factors following mutational activation of the central virulence regulator, PrfA. *Infect Immun* *75*, 5886–5897.
- Portnoy, D.A., Chakraborty, T., Goebel, W., and Cossart, P. (1992). Molecular determinants of *Listeria monocytogenes* pathogenesis. *Infect Immun* *60*, 1263–1267.
- Portnoy, D.A., Jacks, P.S., and Hinrichs, D.J. (1988). Role of hemolysin for the intracellular growth of *Listeria monocytogenes*. *J Exp Med* *167*, 1459–1471.
- Portnoy, D.A. (2005). Manipulation of innate immunity by bacterial pathogens. *Curr Opin Immunol* *17*, 25–28.
- Quisel, J.D., Burkholder, W.F., and Grossman, A.D. (2001). In vivo effects of sporulation kinases on mutant Spo0A proteins in *Bacillus subtilis*. *J Bacteriol* *183*, 6573–6578.
- Rae, C.S., Geissler, A., Adamson, P.C., and Portnoy, D.A. (2011). Mutations of the *Listeria monocytogenes* peptidoglycan N-deacetylase and O-acetylase result in

enhanced lysozyme sensitivity, bacteriolysis, and hyperinduction of innate immune pathways. *Infect Immun* 79, 3596–3606.

Rallu, F., Gruss, A., Ehrlich, S.D., and Maguin, E. (2000). Acid- and multistress-resistant mutants of *Lactococcus lactis* : identification of intracellular stress signals. *Mol Microbiol* 35, 517–528.

Rao, F., Ji, Q., Soehano, I., and Liang, Z.-X. (2011). Unusual heme-binding PAS domain from YybT family proteins. *J Bacteriol* 193, 1543–1551.

Rao, F., See, R.Y., Zhang, D., Toh, D.C., Ji, Q., and Liang, Z.-X. (2010). YybT is a signaling protein that contains a cyclic dinucleotide phosphodiesterase domain and a GGDEF domain with ATPase activity. *J Biol Chem* 285, 473–482.

Reniere, M.L., Whiteley, A.T., Hamilton, K.L., John, S.M., Lauer, P., Brennan, R.G., and Portnoy, D.A. (2015). Glutathione activates virulence gene expression of an intracellular pathogen. *Nature* 517, 170–173.

Ripio, M.T., Brehm, K., Lara, M., Suárez, M., and Vázquez-Boland, J.A. (1997a). Glucose-1-phosphate utilization by *Listeria monocytogenes* is PrfA dependent and coordinately expressed with virulence factors. *J Bacteriol* 179, 7174–7180.

Ripio, M.T., Domínguez-Bernal, G., Lara, M., Suárez, M., and Vázquez-Boland, J.A. (1997b). A Gly145Ser substitution in the transcriptional activator PrfA causes constitutive overexpression of virulence factors in *Listeria monocytogenes*. *J Bacteriol* 179, 1533–1540.

Rismondo, J., Gibhardt, J., Rosenberg, J., Kaefer, V., Halbedel, S., and Commichau, F.M. (2015). Phenotypes associated with the essential diadenylate cyclase CdaA and its potential regulator CdaR in the human pathogen *Listeria monocytogenes*. *J Bacteriol* 198, JB.00845–15–426.

Rosenberg, J., Dickmanns, A., Neumann, P., Gunka, K., Arens, J., Kaefer, V., Stülke, J., Ficner, R., and Commichau, F.M. (2015). Structural and biochemical analysis of the essential diadenylate cyclase CdaA from *Listeria monocytogenes*. *Journal of Biological Chemistry* 290, jbc.M114.630418–jbc.M114.636606.

Rouzer, C.A., Scott, W.A., Griffith, O.W., Hamill, A.L., and Cohn, Z.A. (1981). Depletion of glutathione selectively inhibits synthesis of leukotriene C by macrophages. *Proceedings of the National Academy of Sciences* 78, 2532–2536.

Römling, U. (2008). Great times for small molecules: c-di-AMP, a second messenger candidate in Bacteria and Archaea. *Sci Signal* 1, pe39–pe39.

Sassetti, C.M., Boyd, D.H., and Rubin, E.J. (2001). Comprehensive identification of conditionally essential genes in mycobacteria. *Proceedings of the National Academy of Sciences* 98, 12712–12717.

Sauer, J.-D., Sotelo-Troha, K., Moltke, von, J., Monroe, K.M., Rae, C.S., Brubaker, S.W., Hyodo, M., Hayakawa, Y., Woodward, J.J., Portnoy, D.A., et al. (2011). The N-ethyl-N-nitrosourea-induced Goldenticket mouse mutant reveals an essential function of Sting in the in vivo interferon response to *Listeria monocytogenes* and cyclic dinucleotides. *Infect Immun* 79, 688–694.

Sauer, J.-D., Witte, C.E., Zemansky, J., Hanson, B., Lauer, P., and Portnoy, D.A. (2010). *Listeria monocytogenes* Triggers AIM2-Mediated Pyroptosis upon Infrequent Bacteriolysis in the Macrophage Cytosol. *Cell Host Microbe* 7, 412–419.

Schär, J., Stoll, R., Schauer, K., Loeffler, D.I.M., Eylert, E., Joseph, B., Eisenreich, W., Fuchs, T.M., and Goebel, W. (2010). Pyruvate carboxylase plays a crucial role in carbon metabolism of extra- and intracellularly replicating *Listeria monocytogenes*. *J Bacteriol* 192, 1774–1784.

Schneider, C.A., Rasband, W.S., and Eliceiri, K.W. (2012). NIH Image to ImageJ: 25 years of image analysis. *Nat Methods* 9, 671–675.

Schnupf, P., and Portnoy, D.A. (2007). Listeriolysin O: a phagosome-specific lysin. *Microbes Infect* 9, 1176–1187.

Scotti, M., Monzó, H.J., Lacharme-Lora, L., Lewis, D.A., and Vázquez-Boland, J.A. (2007). The PrfA virulence regulon. *Microbes Infect* 9, 1196–1207.

Shanker, R., and Atkins, W.M. (1996). Luciferase-Dependent, Cytochrome P-450-Catalyzed Dehalogenation in Genetically Engineered *Pseudomonas*. *Biotechnol. Prog.* 12, 474–479.

Sheehan, B., Klarsfeld, A., Msadek, T., and Cossart, P. (1995). Differential activation of virulence gene expression by PrfA, the *Listeria monocytogenes* virulence regulator. *J Bacteriol* 177, 6469–6476.

Shen, A., and Higgins, D.E. (2005). The 5' untranslated region-mediated enhancement of intracellular listeriolysin O production is required for *Listeria monocytogenes* pathogenicity. *Molecular Microbiology* 57, 1460–1473.

Shetron-Rama, L.M., Marquis, H., Bouwer, H.G.A., and Freitag, N.E. (2002). Intracellular induction of *Listeria monocytogenes* actA expression. *Infect Immun* 70, 1087–1096.

Simon, R., Priefer, U., and Puhler, A. (1983). A Broad Host Range Mobilization System for In Vivo Genetic Engineering: Transposon Mutagenesis in Gram Negative Bacteria. *Nat. Biotechnol.* 1, 784–791.

Skoble, J., Portnoy, D.A., and Welch, M.D. (2000). Three regions within ActA promote Arp2/3 complex-mediated actin nucleation and *Listeria monocytogenes* motility. *J Cell Biol* 150, 527–538.

- Sleator, R.D., Gahan, C.G.M., and Hill, C. (2003). A postgenomic appraisal of osmotolerance in *Listeria monocytogenes*. *Appl Environ Microbiol* 69, 1–9.
- Smith, K., and Youngman, P. (1992). Use of a new integrational vector to investigate compartment-specific expression of the *Bacillus subtilis* spoIIIM gene. *Biochimie* 74, 705–711.
- Somerville, G.A., and Proctor, R.A. (2009). At the crossroads of bacterial metabolism and virulence factor synthesis in *Staphylococci*. *Microbiol. Mol. Biol. Rev.* 73, 233–248.
- Sonenshein, A.L. (2007). Control of key metabolic intersections in *Bacillus subtilis*. *Nat Rev Micro* 5, 917–927.
- Song, J.-H., Ko, K.S., Lee, J.-Y., Baek, J.Y., Oh, W.S., Yoon, H.S., Jeong, J.-Y., and Chun, J. (2005). Identification of essential genes in *Streptococcus pneumoniae* by allelic replacement mutagenesis. *Mol. Cells* 19, 365–374.
- Sternberg, N., and Hamilton, D. (1981). Bacteriophage P1 site-specific recombination. I. Recombination between loxP sites. *J Mol Biol* 150, 467–486.
- Sturman, L.S., and Takemoto, K.K. (1972). Enhanced growth of a murine coronavirus in transformed mouse cells. *Infect Immun* 6, 501–507.
- Sun, A.N., Camilli, A., and Portnoy, D.A. (1990). Isolation of *Listeria monocytogenes* small-plaque mutants defective for intracellular growth and cell-to-cell spread. *Infect Immun* 58, 3770–3778.
- Sun, L., Wu, J., Du, F., Chen, X., and Chen, Z.J. (2012). Cyclic GMP-AMP Synthase Is a Cytosolic DNA Sensor That Activates the Type I Interferon Pathway. *Science* 339, 786–791.
- Sureka, K., Choi, P.H., Precit, M., Delince, M., Pensinger, D.A., Huynh, T.N., Jurado, A.R., Goo, Y.A., Sadilek, M., Iavarone, A.T., et al. (2014). The Cyclic Dinucleotide c-di-AMP Is an Allosteric Regulator of Metabolic Enzyme Function. *Cell* 158, 1389–1401.
- Tadmor, K., Pozniak, Y., Burg Golani, T., Lobel, L., Brenner, M., Sigal, N., and Herskovits, A.A. (2014). *Listeria monocytogenes* MDR transporters are involved in LTA synthesis and triggering of innate immunity during infection. *Front Cell Infect Microbiol* 4, 16.
- Tagami, K., Nanamiya, H., Kazo, Y., Maehashi, M., Suzuki, S., Namba, E., Hoshiya, M., Hanai, R., Tozawa, Y., Morimoto, T., et al. (2012). Expression of a small (p)ppGpp synthetase, YwaC, in the (p)ppGpp(0) mutant of *Bacillus subtilis* triggers YvyD-dependent dimerization of ribosome. *Microbiologyopen* 1, 115–134.
- Tang, Q., Luo, Y., Zheng, C., Yin, K., Ali, M.K., Li, X., and He, J. (2015). Functional Analysis of a c-di-AMP-specific Phosphodiesterase MsPDE from *Mycobacterium smegmatis*. *Int. J. Biol. Sci.* 11, 813–824.

Taylor, C.M., Beresford, M., Epton, H.A.S., Sigee, D.C., Shama, G., Andrew, P.W., and Roberts, I.S. (2002). *Listeria monocytogenes* relA and hpt mutants are impaired in surface-attached growth and virulence. *J Bacteriol* 184, 621–628.

Taylor, R.K., Miller, V.L., Furlong, D.B., and Mekalanos, J.J. (1987). Use of phoA gene fusions to identify a pilus colonization factor coordinately regulated with cholera toxin. *J Bacteriol* 84, 2833–2837.

Teng, F., Murray, B.E., and Weinstock, G.M. (1998). Conjugal transfer of plasmid DNA from *Escherichia coli* to enterococci: a method to make insertion mutations. *Plasmid* 39, 182–186.

Theriot, J.A., Rosenblatt, J., Portnoy, D.A., Goldschmidt-Clermont, P.J., and Mitchison, T.J. (1994). Involvement of profilin in the actin-based motility of *L. monocytogenes* in cells and in cell-free extracts. *Cell* 76, 505–517.

Tilney, L.G., and Portnoy, D.A. (1989). Actin filaments and the growth, movement, and spread of the intracellular bacterial parasite, *Listeria monocytogenes*. *J Cell Biol* 109, 1597–1608.

Toledo-Arana, A., Dussurget, O., Nikitas, G., Sesto, N., Guet-Revillet, H., Balestrino, D., Loh, E., Gripenland, J., Tiensuu, T., Vaitkevicius, K., et al. (2009). The *Listeria* transcriptional landscape from saprophytism to virulence. *Nature* 459, 950–956.

Trinchieri, G. (2010). Type I interferon: friend or foe? *J Exp Med* 207, 2053–2063.

Tsai, H.-N., and Hodgson, D.A. (2003). Development of a synthetic minimal medium for *Listeria monocytogenes*. *Appl Environ Microbiol* 69, 6943–6945.

Turlan, C., Prudhomme, M., Fichant, G., Martin, B., and Gutierrez, C. (2009). SpxA1, a novel transcriptional regulator involved in X-state (competence) development in *Streptococcus pneumoniae*. *Mol. Microbiol.* 73, 492–506.

Valladares, A., Flores, E., and Herrero, A. (2008). Transcription activation by NtcA and 2-oxoglutarate of three genes involved in heterocyst differentiation in the cyanobacterium *Anabaena* sp. strain PCC 7120. *J Bacteriol* 190, 6126–6133.

van Opijnen, T., Bodi, K.L., and Camilli, A. (2009). Tn-seq: high-throughput parallel sequencing for fitness and genetic interaction studies in microorganisms. *Nat Methods* 6, 767–772.

Vance, R.E., Isberg, R.R., and Portnoy, D.A. (2009). Patterns of pathogenesis: discrimination of pathogenic and nonpathogenic microbes by the innate immune system. *Cell Host Microbe* 6, 10–21.

Vasanthakrishnan, R.B., las Heras, de, A., Scotti, M., Deshayes, C., Colegrave, N., and Vázquez-Boland, J.A. (2015). PrfA regulation offsets the cost of *Listeria* virulence outside the host. *Environmental Microbiology* 17, 4566–n/a.

Vázquez-Boland, J.A., Kuhn, M., Berche, P., Chakraborty, T., Domínguez-Bernal, G., Goebel, W., González-Zorn, B., Wehland, J., and Kreft, J. (2001). *Listeria* pathogenesis and molecular virulence determinants. *Clin. Microbiol. Rev.* *14*, 584–640.

Wang, J.D., Sanders, G.M., and Grossman, A.D. (2007). Nutritional control of elongation of DNA replication by (p)ppGpp. *Cell* *128*, 865–875.

Welch, M.D., Rosenblatt, J., Skoble, J., Portnoy, D.A., and Mitchison, T.J. (1998). Interaction of human Arp2/3 complex and the *Listeria monocytogenes* ActA protein in actin filament nucleation. *Science* *281*, 105–108.

Welch, M. (2007). Actin-based motility and cell-to-cell spread of *Listeria monocytogenes*. *Listeria Monocytogenes: Pathogenesis and Host Response* 197–223.

Whiteley, A.T., Pollock, A.J., and Portnoy, D.A. (2015). The PAMP c-di-AMP Is Essential for *Listeria monocytogenes* Growth in Rich but Not Minimal Media due to a Toxic Increase in (p)ppGpp. *Cell Host Microbe* *17*, 788–798.

Williams, J.R., Thayyullathil, C., and Freitag, N.E. (2000). Sequence variations within PrfA DNA binding sites and effects on *Listeria monocytogenes* virulence gene expression. *J Bacteriol* *182*, 837–841.

Winter, S.E., Lopez, C.A., and Bäumlner, A.J. (2013). The dynamics of gut-associated microbial communities during inflammation. *EMBO Rep.* *14*, 319–327.

Winter, S.E., Thiennimitr, P., Winter, M.G., Butler, B.P., Huseby, D.L., Crawford, R.W., Russell, J.M., Bevins, C.L., Adams, L.G., Tsolis, R.M., et al. (2010). Gut inflammation provides a respiratory electron acceptor for *Salmonella*. *Nature* *467*, 426–429.

Witte, C.E., Whiteley, A.T., Burke, T.P., Sauer, J.-D., Portnoy, D.A., and Woodward, J.J. (2013). Cyclic di-AMP is critical for *Listeria monocytogenes* growth, cell wall homeostasis, and establishment of infection. *MBio* *4*, e00282–13–13.

Witte, G., Hartung, S., Büttner, K., and Hopfner, K.-P. (2008). Structural biochemistry of a bacterial checkpoint protein reveals diadenylate cyclase activity regulated by DNA recombination intermediates. *Mol Cell* *30*, 167–178.

Wong, J., Chen, Y., and Gan, Y.-H. (2015). Host Cytosolic Glutathione Sensing by a Membrane Histidine Kinase Activates the Type VI Secretion System in an Intracellular Bacterium. *Cell Host Microbe* *18*, 1–12.

Wong, K.K.Y., Bouwer, H.G.A., and Freitag, N.E. (2004). Evidence implicating the 5' untranslated region of *Listeria monocytogenes* actA in the regulation of bacterial actin-based motility. *Cellular Microbiology* *6*, 155–166.

Woodward, J.J., Iavarone, A.T., and Portnoy, D.A. (2010). c-di-AMP secreted by intracellular *Listeria monocytogenes* activates a host type I interferon response. *Science* *328*, 1703–1705.

Wu, J., Sun, L., Chen, X., Du, F., Shi, H., Chen, C., and Chen, Z.J. (2012). Cyclic GMP-AMP Is an Endogenous Second Messenger in Innate Immune Signaling by Cytosolic DNA. *Science* 339, 826–830.

Wurtzel, O., Sesto, N., Mellin, J.R., Karunker, I., Edelheit, S., Bécavin, C., Archambaud, C., Cossart, P., and Sorek, R. (2012). Comparative transcriptomics of pathogenic and non-pathogenic *Listeria* species. *Mol. Syst. Biol.* 8, 583.

Xayarath, B., Alonzo, F., and Freitag, N.E. (2015). Identification of a Peptide-Pheromone that Enhances *Listeria monocytogenes* Escape from Host Cell Vacuoles. *PLoS Pathog* 11, e1004707.

Xiang, S., and Tong, L. (2008). Crystal structures of human and *Staphylococcus aureus* pyruvate carboxylase and molecular insights into the carboxyltransfer reaction. *Nat Struct Mol Biol* 15, 295–302.

Xiao, H., Kalman, M., Ikehara, K., Zemel, S., Glaser, G., and Cashel, M. (1991). Residual guanosine 3',5'-bispyrophosphate synthetic activity of *relA* null mutants can be eliminated by *spoT* null mutations. *J Biol Chem* 266, 5980–5990.

Yang, J., Bai, Y., Zhang, Y., Gabrielle, V.D., Jin, L., and Bai, G. (2014). Deletion of the cyclic di-AMP phosphodiesterase gene (*cnpB*) in *Mycobacterium tuberculosis* leads to reduced virulence in a mouse model of infection. *Mol Microbiol* 93, 65–79.

Yu, L.P.C., Xiang, S., Lasso, G., Gil, D., Valle, M., and Tong, L. (2009). A symmetrical tetramer for *S. aureus* pyruvate carboxylase in complex with coenzyme A. *Structure* 17, 823–832.

Zeldovich, V.B., Robbins, J.R., Kapidzic, M., Lauer, P., and Bakardjiev, A.I. (2011). Invasive extravillous trophoblasts restrict intracellular growth and spread of *Listeria monocytogenes*. *PLoS Pathog* 7, e1002005.

Zemansky, J., Kline, B.C., Woodward, J.J., Leber, J.H., Marquis, H., and Portnoy, D.A. (2009). Development of a mariner-based transposon and identification of *Listeria monocytogenes* determinants, including the peptidyl-prolyl isomerase PrsA2, that contribute to its hemolytic phenotype. *J Bacteriol* 191, 3950–3964.

Zhang, L., and He, Z.-G. (2013). Radiation-sensitive gene A (*RadA*) targets DisA, DNA integrity scanning protein A, to negatively affect its cyclic-di-AMP synthesis activity in *Mycobacterium smegmatis*. *Journal of Biological Chemistry* 288, 22426–22436.

Zhu, Y., Pham, T.H., Nhiep, T.H.N., Vu, N.M.T., Marcellin, E., Chakraborti, A., Wang, Y., Waanders, J., Lo, R., Huston, W.M., et al. (2016). Cyclic-di-AMP synthesis by the diadenylate cyclase *CdaA* is modulated by the peptidoglycan biosynthesis enzyme *GlmM* in *Lactococcus lactis*. *Mol. Microbiol.* 99, 1015–1027.

Zuber, P., and Zuber, P. (2004). Spx-RNA Polymerase Interaction and Global Transcriptional Control during Oxidative Stress. *J Bacteriol* 186, 1911–1918.